X-507-67-281

NASA TMX- 63180

ANALYSIS
OF THE
APOLLO REENTRY RADAR

JAMES R. MOORE
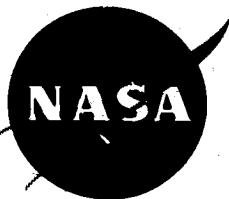
JUNE 1967

GODDARD SPACE FLIGHT CENTER ──
GREENBELT, MARYLAND

N 68-23733

ANALYSIS OF THE APOLLO REENTRY RADAR

By

James R. Moore
Mission Analysis Office

N68 23733

June 1967

GODDARD SPACE FLIGHT CENTER
Greenbelt, Maryland

CONTENTS

LIST OF ILLUSTRATIONS

LIST OF ILLUSTRATIONS (Continued)

LIST OF ILLUSTRATIONS (Continued)

LIST OF ILLUSTRATIONS (Continued)

LIST OF ILLUSTRATIONS (Continued)

LIST OF ILLUSTRATIONS (Continued)

LIST OF ILLUSTRATIONS (Continued)

ANALYSIS OF THE APOLLO REENTRY RADAR

James R. Moore
Mission Analysis Office

SUMMARY

In this report a more exacting analysis of the performance of the Apollo acquisition and tracking radar has been made. The coverage of the radar has been expanded to include all possible trajectories which do not exceed 16 g deceleration during the reentry phase. Most of the entering trajectories which develop more than 16 g will also be acquired and tracked.

Radar station positions, relative to the entry point and the projected pre-reentry ground track, have been ascertained for optimum radar performance. It is shown that a single position, 603 nautical miles from entry and on the projected ground track is suitable for the acquisition of all the specified trajectories. Trajectories representative of the extreme acquisition conditions have been developed, and the probability of detection of a spacecraft in these trajectories has been presented.

A station location at a down range distance greater than 603 nautical miles is more suitable and more desirable for trajectories entering at entry angles more shallow than the deepest possible entry angles. Further down range station positions have an advantage in extended tracking capability and longer communication and data coverage.

Optimum down range station location have been derived for entry angles within the specified range of entry angles. The probability of detection for extreme limit trajectories have been found for the radar positioned at these stations.

The derogatory influence of network tracking errors and ship navigation errors on the performance of the radar have been examined. Under normal network operating conditions, these errors

do not appreciably degrade the performance of the radar. In view of the number of ground stations and the back up facilities at each station it is reasonable to expect normal network performance.

The placement of the ship in the position for optimum performance of the radar should be given careful consideration in planning and in the execution of the mission. At least two acquisition messages, in addition to those planned for the network, should be prepared for the ship.

It is important that the ship to network communications be sufficiently adequate to ensure the prompt delivery of the acquisition messages to the ship.

ANALYSIS OF THE APOLLO REENTRY RADAR

James R. Moore
Mission Analysis Office

INTRODUCTION

The possible use of active surface based Radar for the acquisition of the spacecraft during the reentry phase of the Apollo mission has been discussed in a previous paper[1] entitled, "Apollo Entry Radar Acquisition Study," GSFC Report X-513-65-225, dated May 28, 1965 (Reference 1). In that report it was pointed out that a tracking station or ship equipped with a suitable pulse radar, would entertain a very high probability of detection during any normal Apollo reentry mission, if the station were properly located relative to the reentry point of the mission trajectory.

The study mentioned in the foregoing, was intended to establish the feasibility of active surface based radar for the acquisition of the spacecraft during the reentry phase. Since the publication of that report, the study has been extended with intent to establish the operational procedures which would yield optimum radar performance and the characteristics of the radar under these conditions.

Many additional trajectories have been analyzed for the purpose of evaluating the performance of the acquisition radar against missions with maximum tolerable deviation from the mean normal trajectory. The tolerable deviation from the normal reentry trajectory is physically limited by the detrimental effects of excessive accelerative loading and by the failure of the spacecraft to effectively capture in the earth's atmosphere.

It is also desired to provide in this report information pertinent to the optimum positioning of the radar relative to the entry point, the orientation of the radar, and other operational data which will be of assistance in the utilization of such an acquisition radar.

In the preparation of this report, it has been necessary to utilize information derived in many other studies made at GSFC and at other NASA centers or collaborating industrial enterprises. Many of the contributing and supporting technical papers are listed in the references.

1

I.   INITIAL CONDITIONS

The trajectory pursued by the Apollo Command Module, subsequent to the reentry point, is governed by the velocity vector at the entry point and the bank angle program of the Module during the reentry period (Reference 2, 3, & 4).

The velocity vector at entry is established by conditions which prevail prior to the entry point. The magnitude of the velocity at the 400,000 ft altitude level can be considered constant, or practically so, for all lunar return trajectories. The horizontal projection of the velocity vector at the entry point will be considered the horizontal reference axis for these studies.

The entry angle is defined as the vertical angle between the local horizontal and the velocity vector at the point of entry. A negative entry angle is associated with a velocity having a downward component.

The predicted location of the entry point and the magnitude of the entry angle are ascertained from tracking data taken during the trans-earth phase of the missions.

A typical trans-earth trajectory is illustrated in Figure 1. A sample trans-earth trajectory has been computed for mid-corridor reentry by a "Quick-Look" program developed by contract from the Mission Analysis Office, (Reference 5). Pertinent characteristics of this trajectory have been presented herein. The elevation of the spacecraft above the surface of the earth is given in Figure 2 as a function of time from reentry. Figure 3 is a plot of the velocity in orbit as a function of time from reentry.

The accuracy with which the initial conditions for the reentry phase are known depends upon the errors which prevail at the end of the trans-earth phase of the missions. The errors at the end of the trans-earth phase are the errors which result from inaccuracies in the tracking equipment accrued during the trans-earth phase and projected to the point of entry. A mathematical method for the evaluation of the trans-earth trajectory tracking errors, and for projecting the resulting errors to a predicted position in the trajectory has been developed by contract from the Mission Analysis Office (Reference 6). This program has been applied to the sample Apollo trajectory utilizing the tracking procedures and equipment currently being installed in ground tracking network for the Apollo mission.

The errors which may exist at the initiation of the reentry phase, or at the termination of the trans-earth phase, have been computed for three trans-earth trajectories. The first trajectory is a normal trajectory having terminal

conditions representative of mid corridor reentry conditions. The sample trajectory has a return time of about 100 hours. The second error analysis is made on the same trajectory in which an unannounced velocity change of 100 ft per second is injected at about 20 hours after entering the earth's influence. The velocity increment is incorporated in the program by increasing the "a priori" knowledge of the one sigma velocity error by 100 feet per second at the point at which the error is injected. This infers that no information relative to the velocity change is communicated to the tracking stations.

In the third error analysis, a second error is injected into the trajectory of the second study. The second velocity change has a magnitude of 10 feet per second, and is injected ten hours prior to the time of entry. The second ΔV is inserted in the program in the same manner as was done in the case of the first velocity change.

These midcourse velocity changes are in accordance with the latest information obtained from Mr. M. P. Frank of the Mission Analysis Branch at Manned Spacecraft Center (MSC). They represent the most severe applications of the ΔV which is being budgeted in the current design of the Apollo trans-earth phase. Simulator tests at MSC indicate that in the manned trajectory much smaller velocity corrections will be required.

It must also be assumed that midcourse velocity corrections are made in such a manner as to bring the actual entry point nearer to the nominal entry point. These velocity changes can move the entry point to a position beyond the range capability of the reentry ship if incorrectly applied.

Figure 4 is a plot of the down range error in the predicted position of the entry point. In Figure 4, one curve is the error for the trajectory with no mid-course velocity change. The other curve is for a trajectory with a velocity change of 100 feet per second introduced 68 hours prior to entry. The curves are continued in Figure 4a, where the dashed line is for the trajectory without velocity change, the dotted line is the trajectory with the 100 foot per second change at 68 hours prior to entry, and the solid line is a trajectory with a 10 foot per second velocity change at 10 hours prior to entry.

Similar curves have been prepared for the predicted error in cross range position as a function of time from entry as shown in Figures 5 and 5a and for the error in the predicted entrance angle as shown in Figures 6 and 6a.

The error in the predicted time of arrival at the entry point is assumed to be equal to the error in the time of arrival at the trajectory perigee, since there is little displacement between the entry point and the perigee. Figures 7 and 7a display the error in time of arrival at the entry point.

The error in cross range velocity predicted to the point of entry is shown in Figure 8 for the last 10 hours of the trans-earth flight.

Figures 4 through 8 may be utilized to ascertain the initial conditions for the reentry trajectory provided the time for communicating the computed reentry information to the tracking ship is known. According to existing plans, only a few seconds will be required for the transmission from the tracking stations to the computation centers at MSC and Goddard and for the computation of the predicted reentry conditions. It remains necessary to communicate the predicted information from the network to the reentry ship.

The message required for the predicted data is not complex and does not require high speed or broad band transmission. In its most elementary form, it may contain the latitude and longitude of the predicted reentry point, the predicted entry angle, the predicted time of entry, and the predicted ground track. However, unless this information is communicated to the tracking ship with certainty comparable with the desired acquisition certainty (99.9+%), there will be a degradation in the expected performance of the system. The amount of degradation can be computed from the information and techniques utilized in the preparations of this report, but is considered outside the scope of the present writing. For this report it will be assumed that the final predicted data will be available to the ship with a certainty of 99.9% within 5 minutes after network tracking data is taken.

Based upon the foregoing analysis, final predictions will be computed from data taken by the network 30 minutes prior to entry. These predictions will be contained in the 25-minute acquisition message as now planned. There is also a 5-minute acquisition message which will contain more exact information; however, it is not considered advisable to place great confidence in the communication of this message in time for incorporation in the acquisition plan. Table I is a summary of the errors which may prevail at the initiation of the reentry phase.

Table I
Initial Errors

Altitude at Entry	400,000 ft
Time of Last Tracking Data	30 min. before entry
Error in Entry Angle (3 sigma)	±0.025 degrees
Down Range Position Error (3 sigma)	±12.0 n. mi.
Cross Range Position Error (3 sigma)	±1.71 n. mi.
Error in Arrival Time at Entry (3 sigma)	±1.2 sec
Error in Cross Range Velocity (3 sigma)	±24 ft/sec

II. OPERATIONAL FEATURES OF REENTRY

The trajectory pursued by the Command Module, after the reentry point has been reached, is governed by two factors. First the entry angle which is established by conditions which prevail during the trans-earth phase and second the attitude of the Command Module as represented by the roll or bank angle. The latter is under the control of onboard personnel or computing equipment.

Under normal conditions the bank angle will be adjusted so as to develop and maintain a comfortable deceleration during the reentry phase, or as nearly so as is feasible. However, under abnormal or emergency situations which can happen and consequently must be considered, the trajectory followed may be quite different.

After passing the nominal point of entry (400,000 ft attitude) the Apollo Command Module is subject to increasing aerodynamic forces. At an elevation of about 300,000 feet, the ion sheath surrounding the spacecraft becomes opaque to electromagnetic radiation in the data transmission frequency range. Also, at about this time the forces due to lift and drag become quite significant.

Thus, when the spacecraft becomes most maneuverable, the normal system for observation and tracking is blind. Depending on how the vehicle is rolled, it may or may not shed the ion sheath until the immediate proximity of the recovery area. There are many possible trajectories of relatively short duration which have excellent deceleration characteristics, and which do not come out of blackout until in the vicinity of the recovery area. These trajectories also experience a minimum of heating in the Command Module.

The intent and purpose of the active pulse radar is to acquire the Command Module prior to or during the blackout period, and to track the Module during the highly maneuverable portion of the trajectory associated with the region of high aerodynamic forces.

If the Module pursues a short trajectory, and reaches a recovery area within radar range of the ship, the radar should pinpoint the recovery area. If a longer trajectory is selected, the radar should track the Module during the blackout phase and accumulate sufficient tracking information to bring other tracking equipment on the target, or to minimize the region in which the recovery phase may take place.

Acquisition is accomplished by positioning a radar searched volume in an area which must be traversed by the Command Module. The searched volume must contain all possible trajectories for a sufficient period of time to ensure detection by the radar.

The use of a fixed search pattern during the acquisition phase has been done to reduce operational complexity. This is in concurrence with the recommendations of Dr. F. O. Vonbun and is consistant with the field experience of the author.

To escape acquisition, the CM must either pass through the upper portion of the searched volume at such a range or speed as to escape detection, (this is called the upper limit), or it must pass under the lower surface of the searched volume (this is called the lower limit), or it must pass out a side at such range and speed as to preclude detection (this is called the side limit).

The searched volume must be of such size and so positioned as to make the escape from detection virtually impossible for any of the specified trajectory conditions.

If the inclusion of the trajectory in the searched volume were the only criterion for the position of the search volume, the problem would be easily solved by bringing the searched volume to the proximity of the entry point. Unfortunately, there are a number of other factors which must also be considered. These are discussed in the following paragraphs.

Tracking experience has shown that during the build-up of the ionic sheath, the radar target presented by the sheath may fluctuate or become extremely small. Dr. J. Marini (Reference 8) from the Mission Analysis Office has examined the available data from radar targets displaying this effect, and tentatively conclude that attenuation is initiated at the onset of blackout, or at an elevation of about 280,000 feet for reentry trajectories at the C-band frequency, and that the attenuation continues until there is a further decrease of 10,000 feet in altitude. Thus, to avoid this attenuation region, the radar search volume should not include the portion of the trajectory lying between an elevation of 280,000 feet altitude and 270,000 feet altitude. The down range distance from entry at which the initial attenuation region terminates is given in Figure 8 for C-band radar.

It is also desired that telemetry data be taken from the spacecraft after the termination of the S-band blackout (References 9 & 10). In order to have as much time for data as is possible, the ship should be stationed as far down range as is possible, consistent with the requirement for the acquisition of minimum range trajectories.

In order to minimize the recovery area for spacecraft that travel beyond the radar horizon of the ship, tracking should be continued through the initial region of high maneuverability and as far down range as possible. This also

specifies a ship position as far down range as possible consistent with the minimum range trajectory acquisition requirement.

The radar target presented by the spacecraft approaches 0.2 sq meters when observed from the apex end of the conical surface. To avoid skin tracking against the apex end of command module, the tracking station should be located down range as far as possible. Thus, it is intended that the region of blackout will be near termination when the Module passes down range of the ship, and beacon tracking will become available to replace skin tracking when the radar target size is small.

It should be observed that, except for re-acquisition where the radar range should never exceed 75 nautical miles, the radar will be operating in the process of tracking rather than acquiring the spacecraft when the spacecraft is presenting a small target area. The radar tracking range should be considerably greater than the acquisition range, and, should future tests establish the desirability, the tracking range can be increased by incorporating memory in the receiving channels.

One other operational feature should be given consideration in the planning of the ship position. This concerns the fact that mechanical motion of the antenna does not permit good tracking within ten degrees of the zenith. Thus, to reduce the necessity of re-acquisition, the probability of a zenith pass over the ship should be held low.

The foregoing operational features dictate a ship location down range of the entry point, at a maximum distance which can be tolerated by the acquisition search pattern. Since the dispersion pattern is symmetrical about the projected pre-reentry ground track, or very nearly so, and since the search patterns are symmetrical about its mid azimuth center line, optimum coincidence between the dispersion pattern and the search pattern is obtained when the ship is on the projected pre-reentry ground track. A slight deviation from the ground track may be advisable to reduce the possibility of a zenith passover the ship.

In the initial phase of the study, the trajectory and entry point will be considered fixed in the nominal position. The effect of errors and displacements from the nominal situation will be examined later.

Figure 10 depicts the horizontal projection of the trajectory and radar search pattern as proposed herewith. The vertical projection of the initial tracking deployment is illustrated in Figure 11.

It now remains to select the optimum down range distance for the ship position to ensure the desired confidence of detection.

7

III. INTRODUCTORY TRAJECTORY ANALYSIS

At the initial part of the reentry phase, the Command Module enters the dense atmosphere and is subject to aerodynamic forces. The maneuverability of the spacecraft depends on the altitude, the orientation of the lift force, and the lift to drag ratio (L/D).

The aerodynamic forces which cause deceleration and heating are directly proportional to the density of the atmosphere and the square of the velocity relative to the atmosphere. Thus, to avoid excessive forces on the spacecraft or the personnel aboard, penetration to the denser atmosphere must be avoided until the velocity has been sufficiently reduced.

In order to ensure survival in the spacecraft, the usable trajectory is constrained by the peak aerodynamic forces to which the spacecraft may be subjected. The structural limit on the spacecraft is 20 g. Centrifuge tests have indicated the personnel may survive when subjected to equally high forces, however, their ability to execute normal logical performance ceases at a much lower level of force.

In the preparation of this report, high acquisition probability will be established up to a force level of 16 g. This is consistent with the recommendations of Claud Graves of Manned Spacecraft Center and Dr. F. O. Vonbun of the Mission Analysis Office. It is considered quite unlikely that decelerations of more than 16 g and less than 20 g will be experienced in practice. Furthermore, only a few such trajectories would pass undetected, and those which are not observed have a very confined region of possible splash down. In case of no detection, this particular area should be searched first by the recovery forces.

For the computation in this report, a lift to drag ratio of 0.4 has been used. At present, estimates for the possible range of L/D for the Command Module extend from 0.28 to 0.42. The value selected is near the maximum end of the range, since lower values will lessen maneuverability in the acquisition region and increase rather than decrease detection probability.

As an introduction to the study of reentry trajectories, a number of trajectories in which the bank angle, or roll, is maintained constant during the reentry phase, have been examined. Thus, for the purpose of study, one variable is fixed.

The trajectories were developed by a simulation program called "Missile and Satellite Systems Program," prepared by A. J. Dennison and J.F. Butler, February 1962, (Reference 11). For trajectories involving guidance, this program was modified by M. P. Frank at MSC, Houston.

The dash-dot lines in Figure 12 are the vertical projection of trajectories having an entrance angle of -7.51 degrees. Bank angles of 0°, 45°, 60°, and 90° have been selected for presentation.

The plot for 0° bank angle (lift vector up) shows that the Command Module penetrates the atmosphere to an altitude of 171,000 feet before the downward motion is arrested. The lift force continues to push the Module upward and out of the atmosphere. The Module then pursues a ballistic trajectory to a second atmospheric entry point further down range.

The Module is subject to a maximum deceleration force of about 9.7 g at the point of deepest penetration into the atmosphere.

For larger bank angles, the Module penetrates deeper into the atmosphere and is subjected to higher deceleration force before "bouncing." Also, it does not bounce as high or as far as in the case of the 0° bank angle.

In the proximity of 72° bank angle, the bounce disappears, and the spacecraft continues downward into the dense atmosphere with very high deceleration forces.

Similar vertical projections for reentry trajectories of constant bank angle are plotted in Figure 13 for an entrance angle of -6.80°. This projections are similar to the projections for the -7.53° entrance angle except that, for the same bank angle, they do not penetrate the atmosphere as deeply before "bouncing."

Figure 14, the vertical projection for fixed bank angle trajectories with entrance angle of 60° shows even more shallow penetration than the curves of Figure 13.

Figure 15, similar vertical projection for an entrance angle of -5.53° shows the presence of a "bounce" at bank angles in the proximity of 90°.

Horizontal projections for reentry trajectories of constant bank angle and with an entry angle of -7.51° are shown in Figure 16. Trajectories with shallow bank angles have little deviation from the projected pre-entry ground track. The horizontal dispersion increases up to the bank angle of ±90°. Maximum lateral dispersion is developed at a bank angle of 90° for a fixed bank angle trajectory. Greater lateral dispersion may be obtained by a variable bank angle which will be discussed later.

Figure 17 is a similar plot for trajectories with an entrance angle of -6.80°. Here again, the maximum dispersion is at a bank angle of 90 degrees, but like in the vertical projection, the dispersion takes place further down range than in the similar plot for an entrance angle of -7.51°.

Horizontal projections for trajectories of constant bank angles are given in Figure 18 for an entrance angle of -6.00° and in Figure 19 for an entrance angle of -5.53°. It can be seen that at shallows entrance angles, lateral dispersions does not reach proportions comparable to deep entrance angles until much greater down range distances have been traveled.

The velocities of the spacecraft relative to the surface of the earth are given for trajectories of constant bank angle in Figures 20 through 23. Figure 20 is for an entrance angle of -7.51°, Figure 21 is for an entrance angle of -6.80°, Figure 22 is for an entrance angle of -6.00°, and Figure 23 is for an entrance angle of -5.53°. It is important to note that for deep entry angles, the velocity decreases rapidly during the initial plunge into the atmosphere, and that for shallow entry angles the spacecraft travels at near entry speed until it sinks into the dense atmosphere at further down range distances.

It should be observed that the fixed bank angle trajectories are for study only and are not intended as suggested practice. A number of normal reentry trajectories have been computed and are shown as solid and dotted lines on Figures 12 through 19. The solid line represents normal trajectories with a range of 1500 nautical miles. The dotted lines represent normal trajectories with a range of 2500 nautical miles.

The velocity of the spacecraft in these normal trajectories is given in Figure 24. The deceleration forces experienced in a normal trajectory are plotted in Figure 28.

The decelerations experienced during the acquisition area of the reentry phase are plotted in Figure 25 for entry angles of -7.51°, and constant bank angles. Minimum initial accelerations are experienced with zero bank angle. For larger bank angles, the deceleration forces increase until capsule destructive levels are reached at bank angles slightly less than 90°.

In Figure 25, the area under the curve is the integral of the acceleration times incremental time. Thus, the area represents the change in velocity accrued during the time interval. The zero launch angle curve has a minimum area under the curve, consequently, the change in velocity during the initial plunge is a minimum for zero bank angle. This means that the CM emerges from the initial lunge with higher velocity in a zero bank angle trajectory than

10

for any trajectory with other than zero bank angle. Also, the zero bank angle trajectory represents the minimum time of flight to any down range distance in the initial reentry phase. It will give the maximum "skip out" distance prior to the second atmospheric entrance and is subject to a minimum of lateral deviation prior to the second atmospheric entry.

Since the energy which is not dissipated during the initial plunge must be dissipated later in the trajectory (if the spacecraft is to be captured in the atmosphere), the zero bank angle entry leaves the maximum energy to be dissipated in the second entry and subsequent portion of the reentry phase.

Figure 26 is a plot of the decelerations in the acquisition portion of the reentry phase for trajectories with an entry angle of $-6.80°$. These curves are quite similar to those of Figure 25. It can be seen that the maximum deceleration, for any given bank angle is less for the $-6.80°$ entry angle than for the $-7.51°$ entry angle. Also, the peak deceleration is reached at a slightly greater time from entry. The change in velocity during the initial entry phase is greater for the deeper entry angle, as is more clearly shown by a comparison of Figure 20 and Figure 21.

The decelerations on the CM during the acquisition portion of the reentry phase are given in Figure 27 for fixed bank angles and for an entry angle of $-5.53°$. By comparison with Figures 25 and 27, it can be seen that the energy dissipated in the initial plunge from an entry angle of $-5.53°$ has decreased considerably under that dissipated from an entry angle of $-7.51°$ for bank angles up to about $90°$. In the proximity of a $90°$ fixed bank angle, the skip out begins to disappear, and the initial plunge merges with the final entry to give continuous high level drag during the reentry phase.

As the bank angle is increased above $90°$, the dip in the deceleration curve disappears and the initial deceleration load grows in magnitude until all energy is absorbed in the initial plunge. Physically, the down directed lift vector forces the module into more dense atmosphere at high velocity resulting in extremely high drag forces until all energy is dissipated.

For entry angles much more shallow than $-5.53°$, it is necessary that a negative lift, (roll angle in excess of $90°$) be employed during the initial part of the reentry trajectory to ensure capture in the atmosphere or to prevent an excessive skip out period.

As has been stated, a number of trajectories with constant roll angle have been examined. The maximum decelerations experienced during the acquisition phase of these trajectories are summarized in Figure 29. For deep entry angles

these maximum decelerations take place during the initial plunge into the atmosphere. For shallow entry angles, maximum deceleration is experienced when the CM is pulled into the dense atmosphere by the negative lift force further down range.

A distortion in the curve for entry angle equal to -5.53° is found in the region between bank angle 85° and bank angle 100°. This distortion may be explained with the assistance of Figure 27. When the bank angle is held at 85° or less, there is a region of deceleration in the acquisition area, and another deceleration down range at the point of second entry. As the bank angle is increased above 85°, the two periods of deceleration came nearer together as shown for the curve for 90° bank angle. At this bank angle, the influence of the second deceleration will be observed in the conduct of the spacecraft in the acquisiting phase.

As the bank angle is further increased, the two decelerations merge into a single maximum, as indicated in the curve for a 97° bank angle. In Figure 29, the dotted line on the curve for the -5.53° entry angle represents the far down range peak deceleration value.

In Figure 30, the deceleration experienced during an initial pull-up at zero bank angle is given as a function of the entry angle. As indicated in Figure 30, zero bank angle represents the condition of minimum deceleration during the initial pull up. Thus, values taken from Figure 30 represent the minimum deceleration which could be developed for a given entry angle, or conversely, it represents the maximum numerical value of the entry angle which may be used for a given peak deceleration.

The start and termination of the first blackout region has been marked on Figures 12 through 15 and on some of the other curves in this report. These blackout boundary conditions have been computed from information contained in Reference 9. The curves in Figure 31 are computed from Reference 9 and are presented here for the convenience of the reader. With reference to Figure 31, the CM is in the blackout region for a given communication frequency when a plot of its altitude and velocity falls beneath the curve designated for that frequency on the graph.

In view of the requirement for tracking after acquisition, the radar must be stationed down range of the entry point with the search pattern facing up range toward the approaching spacecraft. Thus, after acquisition the spacecraft must first approach the proximity of the ship, pass over, and proceed down range until obscured by the horizon.

In the initial phase of this study, the entry point will be considered fixed at the nominal position. Later, the effect of errors will be incorporated. Also, the ship will be stationed on the projection of the pre-reentry ground track for the initial computations, and the effect of displacement from the projected ground track will be examined later. Figure 10 depicts the horizontal projection of a trajectory and the horizontal projection of the radar search pattern as envisioned in the initial part of the analyses. Figure 11 is a vertical projection of a reentry trajectory and the vertical projection of the radar search pattern.

IV. BOUNDARY CONDITIONS

The tracking network will provide knowledge of the trans-earth trajectory. Based upon this knowledge, the reentry ship will be stationed in the most suitable position for acquiring and tracking any possible surviving reentry trajectory. The ship station must be such that, with proper radar orientation, all possible reentry trajectories which fall within the prescribed limitations will be acquired and tracked.

It is not assumed that any knowledge of the spacecraft bank angle, during the reentry phase, is available to the tracking radar. Furthermore, it is expected that the high deceleration loading which will develop during the reentry phase will place severe handicaps on both the personnel and equipment in the spacecraft. The possibility that optimum performance will not be realized during the reentry phase is being given full consideration. Consequently, the radar should pinpoint the splash down position for any trajectory which terminates within the radar range of the ship, and should minimize the search area for those trajectories will terminate beyond the radar range.

As has been previously indicated, failure to acquire can happen only if the spacecraft passes above the upper limit, below the lower limit or outside the side limits. In the following, the location of the limits will be defined for a maximum deceleration of 16 g, and for a lift to drag ratio of 0.4.

UPPER LIMIT

The study of the fixed bank angle trajectories shows that, in the region of acquisition, the highest trajectory is achieved at zero bank angle. The zero bank angle trajectory is also the trajectory having the highest velocity in the acquisition region. Thus, the zero bank angle trajectory represents the most difficult acquisition situation in the upper limit. Upper limit trajectories are plotted as the upper curve in Figures 32 through 38.

LOWER LIMIT

The lower limit trajectory is not as easily generated. In order to establish the trajectory of minimum altitude, the spacecraft must be brought to maximum allowable deceleration and held at this level until the spacecraft passes under the radar search pattern.

High deceleration is introduced most rapidly by maintaining a full negative lift (180°) bank angle. However, if there is a limit on the maximum allowable deceleration, the lift force must be made positive (less than 90°) in time to avoid excess deceleration in the dense lower atmosphere. If full negative lift is to be applied for as long as possible, a full positive lift force (0° bank angle) must be used to prevent overrun.

Figure 39 shows the effect of rotating from 180° bank angle to 0° bank angle at intervals of 30 to 40 seconds after reentry. Thus, if a maximum deceleration of 16 g is allowed at an entry angle of -8.50°, the bank angle must be rotated from 180° to 0° at 38 seconds after entry. It will be observed that peak deceleration of 16 g is not reached until 59.5 seconds after entry even through the rotation was executed at 38 seconds after entry.

Figure 40 and Figure 41 are composite graphs developed from numerous computed trajectories. Figure 40 shows the peak deceleration which will be developed as a function of the time at which the lift force is rotated from full negative to full positive. Figure 41 shows the time after entry at which this deceleration is reached.

Figure 42, which shows the time at which the lift force reversal must take place for a maximum deceleration of 16 g, is derived by striking a horizontal line at the 16 g level on Figure 40. Similarly, the minimum time from entry at which 16 g can be developed, without exceeding the 16 g maximum, is given in Figure 43.

With reference to Figure 39 it can be seen that if the lift vector is held at 0° after reaching maximum deceleration, the deceleration rapidly decays to a lower value. To obtain maximum reduction in velocity and altitude in a minimum time, it is desired that the deceleration force be held at the specified upper limit until the trajectory passes under the radar search pattern. Figure 44 shows the influence of the bank angle orientation after peak deceleration on the deceleration value subsequent to the peak. As can be seen, a bank angle of about 96° would result in a long period of sustained relatively constant deceleration for the illustrated situation.

14

A second rotation of the bank angle for sustained deceleration level, similar to that described above, has been applied, following the development of peak deceleration, in each of the "minimum time specified deceleration" trajectories. Sample values of sustained deceleration are shown in Figures 45 through 47 for entry angles distributed over the possible range of utility. The vertical mark on these curves represents the position of the spacecraft when acquisition should be completed. It can be seen that the deceleration is held essentially constant out to the point of detection.

It is recognized that by continuously varying the bank angle during the post peak deceleration region, a more constant level of deceleration may be maintained. This complication is not considered necessary for a sufficiently accurate solution of the existing problem in this report.

In summary, the lower limit trajectory as generated in this report consists of three stages. First, the CM is forced down into the dense atmosphere as quickly as possible by a full negative lifting force. Second, the downward motion is arrested at the specified maximum deceleration level by a full upward lifting force. Third, the bank angle is set to a value which will maintain the deceleration level at or near the peak value until the acquisition region has been passed.

Lower limit trajectories have been computed for entry angles through the possible range of utility. The vertical projection of these low limit trajectories are plotted as the lower curve in Figures 32 through 38.

SIDE LIMIT

To prevent high detection probability by escape through the side of the search pattern, the spacecraft must execute lateral acceleration as early as possible in the reentry phase and at the same time keep the velocity as high as possible. In order to develop lateral thrust, the spacecraft must seek the denser atmosphere. This in turn, reduces the speed of the spacecraft so that more time becomes available for acquisition.

Although an analytical solution to the limiting side escape trajectory is considered possible, the present solutions were obtained by the "cut & try" procedure.

It has been found that the trajectory development which imposed most severe horizontal beam width requirement for deep entry angles does not apply to shallow entry angle trajectories.

15

An examination of many multiple bank angle trajectories for deep entry angles led to the conclusion that maximum horizontal deviation is developed at minimum down range distance and at minimum reduction in velocity by holding the bank angle at the angle which develops the specified maximum deceleration force until that maximum is attained, and then rolling the bank angle to a value slightly greater than 90°.

The bank angle which gives the desired peak deceleration can be found from Figure 29. The sustained bank angle which will give a maximum deceleration of 16 g is given in Figure 48, which is derived from Figure 29. The time, after entry, at which the maximum deceleration is developed for sustained bank angles, is given in Figure 49.

Thus, for deep entry angles, the side limit trajectories for 16 g maximum are developed as follows: The bank angle is set at entry according to the entry angle as given in Figure 48. This bank angle is held until the maximum deceleration is reached at the time given in Figure 49. The bank angle is then set to a value in the proximity of 100° where a high sustained acceleration load is maintained for a period of time.

This development for side limit trajectories is suitable between entry angles of -8.50° and -6.00°. Sample trajectories of this kind are shown in Figures 50 through 54.

For shallow entry angles between -4.75° and -6.00° it has been found that a bank angle with negative lift is needed in the initial part of the reentry trajectory. At an entry angle of -5.53°, an initial bank angle of 120° has proven most evasive. At 106 seconds after entry the bank angle was rotated to 90°.

For an entry angle of -5.00°, the initial bank angle for most evasive side motion is 160°. The bank angle is rotated to 90° after 162 seconds of the reentry phase.

The horizontal projection of the side limit trajectory for an entry angle of -5.53° is shown in Figure 55, and for an entry angle of -5.00° in Figure 56.

In summary, the side limit trajectories have been selected by a "cut and try" procedure employing up to three values of bank angle for one reentry trajectory. It is admittedly possible that slightly more evasive trajectories could be developed by continuous variation of the bank angle. With this in mind, a conservative appraisal of the probability of detection has been taken when evaluating the side limit trajectories.

V. RADAR CHARACTERISTICS

The limiting trajectories discussed in the previous section have been accurately plotted to scale on a flat rigid surface. The vertical projections are referenced to an arc of circle, scaled to the radius of the earth, as indicated in Figure 57. Figure 57 is a picture of the actual plot which, due to its large size cannot be included herewith. The horizontal projection, scaled to the same size as the vertical projection is also shown in Figure 57. The photograph shows only a few of the trajectories which have been plotted and studied.

When all the limiting trajectories have been plotted on the composite figure, the areas which must be searched for acquisition may be defined for any down range distance from the entry point. The area may be specified as containing all possible trajectories of less than 16 g deceleration, or it may contain only those 16 g trajectories with a limited range of entry angles. The spacecraft must remain within the searched volume long enough to insure detection. Thus, a considerable length of any specified trajectory must be within the space searched by the radar.

In this report, the detection range of the radar will be considered as the range at which there is a 50% probability of detection on the specified target [1,12] during one search raster. The target size, as given in Reference 1, is one square meter minimum when the spacecraft is approaching the radar. Initial acquisition is intended with the spacecraft approaching the radar, with the radar stationed as far down range as practical.

It has been stated that a region of unstable target size prevails at the onset of ionization. This region terminates near an altitude of 270,000 feet. To avoid this unfavorable target region, the search area should be positioned down range of the termination. The maximum range from entry for the termination of the absorption region may be found from the upper limit curves in Figures 34 through 40. The maximum distance of the termination from entry is plotted in Figure 9 as a function of the entry angle. This distance is the minimum distance of the radar search volume from the entry point.

Further technical analyses here and at RCA have verified the state of the art capability to achieve the radar range as specified in Reference 1. The raster size utilized in the study in Reference 1 was 23° wide by 6° high. The time allowed for the completion of one search raster was 5 seconds. The traverse of the raster was accomplished by mechanical sweep in the horizontal and by a combination of mechanical and electronic sweep in the vertical.

In this report the deceleration force allowed on the spacecraft is 16 g in contrast to the 10 g maximum in Reference 1. As a result, trajectories which plunge more rapidly to a low level must be acquired. This requires that the radar be advanced to a much shorter distance from the entry point than was originally proposed. (It will be shown that a down range distance of about 603 nautical miles is more suitable than the 850 nautical miles which was optimum for 10 g trajectories.) It has been found that, with the radar near to the entry point, a more suitable vertical coverage is obtained with an eight degree vertical search pattern. Also, the requirement for the horizontal coverage has been reduced.

In Appendix A it is shown that a search pattern 8° high by 15.0° wide may be obtained, employing the same beam traverse velocities and angular acceleration as in the previous 6° by 23° pattern, in a search time of 5 seconds previously specified. Since the same scan velocity and beam overlay is employed, the probability of detection is the same in either pattern. Also, since the same peak and average velocity is used, and the same angular accelerations are needed, the scanning equipment will be satisfactory for either pattern.

In this study an 8° by 15° search raster will be utilized. The 281 nautical mile range for a 50% probability of detection in a 5-second raster search period is still valid on a one square meter target. The overall false target rate is taken as 10^{-8}.

The elevation of the center line of the search pattern will be taken as 8° in this report. Since the vertical coverage is now 8°, the lower edge of the search pattern will be 4° above the horizon, as it was when the search pattern was 6° high with the center line at 7° above the horizon.

If the elevation of the search pattern could be dropped to 7°, essentially the same acquisition probabilities would be obtained with the ship stationed 30 nautical miles further down range. The further down range position is advantageous, but the lower edge of the search pattern would be reduced to three degrees above the horizon. Since the lower elevation could increase the probability of false target return, it is not considered advisable to utilize the 7° elevation until field tests have been made to establish the false target rate is acceptable at this elevation.

The selection of the 5 second search period for a raster has been based upon several factors:

First, the raster seach should be made as fast as possible to provide reasonable uniformity of detection probability over the raster. Since the target

is moving relative to the radar, and since detection probability is dependent upon range, the search should be completed quickly for uniformity of detection probability. For example, if a single 20 second raster were used, the probability of detection would be 90% for the portion of the raster search first, and 99.99+% for the areas searched last. With four 5 second rasters, the probability of detection is 99.99% over the entire surface of the raster. (For example it is assumed that the target remains in the beam for 20 seconds at an average velocity of 4.7 nautical miles per second in the direction of the radar.)

Second, the search rate is limited by the time required for the radar pulse to return from maximum range, and by the physical rate of beam motion. The ideal solution would involve complete electronic sweep but the cost in money and time is excessive and such a development would involve excessive developmental risk for this application. A compromise using mechanical horizontal sweep with a combination mechanical-electronic vertical sweep will give the necessary speed and involves the least development and modification of existing equipment.

A third factor, the ability of the target to inadvertently evade a slow scan, due to its own motion suggests a reasonably fast raster search.

The choice of the 5 second raster search period appears to be very good at this time, although in practice considerable deviation can be tolerated. Any change in the raster search period will influence the probability of detection as given herein.

Angular motion applied to the radar beam during the transit time of the radar pulse (from radar to target and return) effectively reduces the area of the beam at the half power level. This reduction in beam coverage must be considered in planning the raster configuration and scan rates. The effect of angular motion on the radar beam is shown in Figure 58. It can be seen that the beam may be moved as much as 20% of the radius during the pulse transit time without appreciable detrimental effect on the beam coverage.

After the initial detection, it is necessary to stop the search antenna and return to the target region. To ensure acquisition, the entire region of possible target position must be researched at a relatively slow scan rate. The slow scan rate is required to facilitate final stoppage and "lock on", and to provide high pulse density for positive (very high probability of detection) re-dection. To minimize the second stage search area, the beam must be returned to the point of initial contact as quickly as possible.

Two-and-one-half seconds has been allowed for the second acquisition phase. With the specified false target rate, there is one chance in five that the second

phase of the acquisition procedure will be invoked a false target during the entire mission.

The final acquisition phase will include a program for transfer of control of the radar servamechanism to simultaneous lobe information for tracking. In case of failure to acquire, the radar should be automatically returned to the search mode.

An acquisition routine is given in Appendix B which may be investigated for use with the acquisition radar.

VI. PROBABILITY OF DETECTION COMPUTATION METHODS

An analogue method has been devised for the computation of the probability of detection during the reentry phase of the Apollo Mission. In the most recent version, computations are made in the following sequence.

(a) The plan and elevation projections of the reentry trajectory are plotted accurately on a flat rigid surface (Masonite). The plot is made as large as practical for office work (36" x 60") and traces are drawn with five line pens. The scale used is 100,000 feet to the inch and the accuracy goal is 1/100 inch, or 1000 feet. Figure 57 is a photograph of this plot.

(b) The velocity of the vehicle is plotted as a function of position along the trajectory for each trajectory. (Examples are shown in Figures 20 through 24.)

(c) An overlay is drawn representing the vertical projection of the radar search pattern. The probability of detection is specified at 50% at a range of 281 nautical miles (References 1, 13, 14 & 15). Since the target area is fixed at one square meter, the probability of detection may be computed as a function of the range from the radar. Arcs are drawn on the radar beam at ranges corresponding to specific values for probability of detection.

These probabilities of detection arcs represent the range at which the particular probability of detection will be achieved provided the target is at, or inside, of that range for a search period of 5 seconds. Figure 59 is a picture of the vertical projection overlay.

(d) A similar overlay for the horizontal projection of the radar beam, with probability of detection arcs, has been prepared. Figure 60 is a picture of this overlay. The circle around the radar station represents the blind area

caused by the maximum elevation of 80° specified for an azimuth-elevation mount. The radius of the circle is computed on the assumption that the altitude at the station is usually less than 300,000 feet, but for deep entry angles and for distances in excess of 650 nautical miles down range higher altitudes may develop. Should this situation arise, a slightly larger blind circle should be used.

(e) To complete the computation, a third overlay is needed. This overlay shows the distance traveled during a 5 second search period at any velocity. Figure 61 is a picture of the velocity distance overlay.

The procedure by which these charts and overlays are utilized to ascertain detection probability is discussed in the following. First, take the condition in which the desired ship position lies on the projected pre-reentry ground track.

(a) The horizontal and vertical projection are carefully plotted on the chart pictured in Figure 57. If a group of trajectories, such as all trajectories with an entrance angle of 8.5° and having less than 16 g decelerative force, are to be examined for tolerance, only the extreme projections (upper limit, lower limit, and side limit) need be plotted, if they can be established. In the case of the side limit, it may be necessary to examine many possible trajectories to establish which is the limiting trajectory.

(b) The vertical radar pattern overlay is placed over the vertical projection on the trajectory chart. The apex of the pattern is placed at the desired station location and the pattern is elevated to the desired elevation with the assistance of the elevation scale on the chart.

(c) The horizontal radar search pattern overlay is placed over the horizontal projection trajectory chart. When the radar is stationed on the projection of the pre-reentry ground track, the horizontal projection will be centered on the pre-reentry ground track, since dispersion to the left or right may be expected to be symmetrical about the pre-reentry ground track.

(d) The points at which the trajectory enters and leaves the search pattern are observed for both the vertical and horizontal overlays. The minimum distance between either point of entrance and either point of exit represents the track time in the search pattern. To be in the pattern, the trajectory must be in both projections simultaneously. The mean distance from the trajectory reentry point to the section of the trajectory in search pattern can be read from the distance scale on the trajectory charts.

21

(e) The mean velocity during the radar observation period can be ascertained from the trajectory velocity curves as represented in Figures 20 through 24. Usually, there is not much change in velocity during the time that the target is in the radar search pattern. A conservative mean should be taken favoring the higher velocity side of mean.

(f) A horizontal line at the level of the mean velocity is drawn parallel to the velocity lines on the velocity overlay, pictured in Figure 61. The velocity line is divided into five equal segments by the orthogonal (nearly so) time lines on the chart. Each segment represents the distance traveled in 5 seconds at the lead of the velocity line. The velocity overlay is placed on top of the search pattern overly in such a manner that this velocity line coincides as nearly as possible with the trajectory, and time line on the extreme right-hand side is located at the point where the trajectory passes out of the search pattern. The segments of line in the velocity chart now represent 5 second intervals along the trajectory, in reverse order, starting at the point of exit from the search pattern. The segment on the velocity line, nearest the exit point, represents the last 5 second search prior to exit from the search pattern. The CM is within 5 seconds of exit during this period. The time line of the left side of this segment is the greatest distance from the radar during the search last period. The probability of detection at any position in the last search raster will be equal to or better than the probability of detection associated with this range. Thus, the probability of detection at this point may be conservatively taken as the probability of detection during the last 5 second search period. The probability of detection associated with this point may be read directly from the scale on the search raster pattern. The last 5 second search period is called Nth search period.

Similarly, the next up range segment on the velocity line marks the next to the last 5 second search period. The probability of detection for the next to the last, (N-1)th, 5 second search period may be found at the time line on the left-hand side of this segment, etc.

The probability of detection for the entire pass is the statistical sum of the detection probability in the individual 5 second intervals. The overall probability of detection is usually very high for the trajectories and ship stations under discussion. A better understanding of the situation is provided by plotting the probability of detection for each 5 second search period, individually as will be done in the report.

If it has been found necessary or desirable to station the radar off the projection of the pre-reentry ground track, the foregoing procedure is subject to some modifications.

22

From the offset radar position, the search pattern intercept with the trajectory envelope in the horizontal projection is no longer symmetrical about the axis of the search pattern. It is necessary to select the proper search pattern orientation relative to the projected ground track to yield the optimum probability of detection over the full range of possible trajectories.

The selection of the optimum azimuth offset angle usually involves the "cut and try" process with due consideration given to the desire for multiple search periods in situations where the edge of the search pattern and the trajectory are tangent.

Scales are provided on the horizontal projection of the radar search pattern to show the angle between the trajectories and the search pattern axis. In practice, the offset horizontal angle would be added to (or subtracted from) the orientation of the projected trajectory ground track to obtain the azimuth angle of the radar search pattern.

An exact representation of the vertical projection of the search pattern would involve functions of the elevation angle; the offset angle and the curvature of the earth. However, an approximate solution can be obtained for small offset angles by moving the origin of the pattern overlay down range to a virtual station position on the projection of the pre-reentry ground track. The down range displacement is such as to maintain the proper projected distance between the radar and the search area.

This approximation should not be used for offset distances greater than 100 nautical miles. Arcs are drawn on the vertical projection of the search pattern to indicate the virtual ship position for given offset distances.

The curvature of the earth will cause a tilt in the search raster when the origin is offset from the projected pre-reentry ground track. This may be partially corrected by adding (or subtracting) the earth offset angle to the stabilized inertial reference angle. The earth offset angle is the distance of offset divided by the radius of the earth. Since only small offset distances should be considered, this complication should be avoided in practice. In fact, it is an argument in favor of avoiding offset radar positions.

As was previously stated, the requirement for accuracy necessitated plots of the trajectories and radar search patterns which were too large to be included in this report. The vertical and horizontal trajectory projections which have been included are reduced to an appropriate scale and size. Dr. F. O. Vonbun has proposed a coordinate conversion system by which the radar search pattern can be constructed in the scale of the included trajectory projections. A vertical

search pattern plot, utilizing this coordinate conversion system is shown in Figure 62 for a search pattern with an elevation angle of seven degrees and in Figure 63 for a search pattern with an elevation of eight degrees. A horizontal plot is shown in Figure 64.

Overlays taken from Figures 62 through 64 are included in a pocket in this report. These overlays may be used with the vertical and horizontal trajectory projections in the report to indicate the pattern coverage. The overlays are not usable over the picture of the projections, shown in Figure 57.

VII. PROBABILITY OF DETECTION

Utilizing the procedures outlined in the foregoing, the probability of detection has been ascertained for numerous trajectories and radar positions.

The normal reentry, as pictured in Figures 12 and 24 in the solid and dotted lines, is of interest. It is anticipated that this type of reentry will be characteristic of many future Apollo class missions.

The probability of detection for the normal Apollo reentry trajectory under control of the onboard guidance system is given in Figures 65 through 68 for radar position on the projected ground track of the pre-reentry trajectory.

When the radar is positioned off the projected ground track it is necessary to orient the axis of the search pattern relative to the ground track at an angle that will give optimum performance. The angle between the projected ground track and the horizontal axis of the search pattern, as shown in Figure 69, is called the offset angle.

The optimum offset angle will place the effective centroid of the radar search pattern over the centroid of the envelope of possible trajectories.

The optimum offset angle, plotted in Figure 70, has been found by graphical analysis, and is used in the following studies unless otherwise specified.

Figures 71 through 74 give the probability of detection for the normal 2500 nautical mile trajectory when the radar station is offset 50 nautical miles from the projected ground track. Similar information is given in Figures 75 through 78 for an offset distance of 100 nautical miles.

The normal reentry trajectory is assumed to proceed along the pre-reentry ground track to a designated recovery area, also located on or near the projected

ground track. It is assumed that in the normal reentry the onboard guidance system will keep the spacecraft within a distance of plus or minus ten miles lateral displacement from the designated course.

Although theoretically a detection probability of 100% is never reached, any probability of detection factor greater than 99.99% is referred to as 100% probability in this report.

It will be noted that there is a deterioration in detection probability with increase offset, even for normal trajectories. It is therefore recommended that, in general, offset should be avoided if possible.

A single station and offset angle could be selected for overall best performance on the projected ground track, or for any specified offset. However, the basic purpose of the acquisition radar is to acquire and track any reentering spacecraft which is not subject to more than 16 g deceleration. In fact, most trajectories involving greater than 16 g decelerations will also be acquired. The selection of the optimum station location must involve all possible trajectory which may be developed from the known entry conditions.

There are reasons for stationing the radar as far as possible down range from the entry point (post blackout data reception, communications, etc.). The maximum down range radar placement is usually limited by the acquisition of the low limit trajectory, which has been previously discussed (exceptions are very shallow entry angles). When the foregoing probability of detection analyses is applied to the low limit trajectories, shown in Figures 32 through 38, the maximum down range station distance can be ascertained for a given search pattern and search pattern elevation. Figure 79 is a plot of the maximum down range station distance for acquiring trajectories with a maximum deceleration of 16 g and with a 15° by 8° search pattern elevated 8° above the horizon (this is the low limit constraint). Also plotted in Figure 79 is the minimum down range distance between the entry point and the radar as found by adding the nominal radar range, 281 nautical miles, to the absorption terminal as given in Figure 9.

With reference to Figure 30, it can be seen that the deepest entry angle that can be used without exceeding 16 g deceleration is -8.93°. Thus, with reference to Figure 79, the maximum down range station position which will allow acquisition of all 16 g trajectories is 603 nautical miles. With reference to the same figure, this range corresponds to the minimum down range station position for an entry angle of -4.95°.

According to Reference 16, Volume I, Reentry Guidance for Apollo, by Raymond Morth, R-532, an entry trajectory with an entry angle of -4.75° is

possible. This means that, from a station at 603 nautical miles down range of the entry point may have the first 27 nautical miles of the search pattern in radar attenuation for extremely shallow entry angles. Even so, the 4.75° trajectory would still be exposed to two and a fraction 5 second search periods, one at 98% probability of detection and the other at 99.99% probability of detection. Although the two search period situation is not desirable, the overall probability of detection is adequate. If it is desired to cover all 16 g trajectories from a single station, the most efficient location is on the projection of the pre-reentry ground track at a distance of 603 nautical miles from the entry point. Figure 80 lists the probability of detection for limiting condition trajectories as seen from the optimum single station location similar curves for a station at the same range and with a lateral displacement of 50 nautical miles are shown in Figure 81. All other trajectories, of no greater than 16 g maximum deceleration will entertain a probability of detection equal to or better than those shown in these figures.

The operational plan involving a single ship position for all entry conditions is very good from the standpoint of operational simiplicity. However, the information obtained from the spacecraft entering with shallow entry angles is far from optimum with the station so near the entry point.

With the radar stationed at 603 nautical miles from entry, communications blackout can extend beyond the radar range after the spacecraft has passed down range of the radar. In fact, blackout could extend to the down range radar horizon from this station.

To alleviate the down range deficiencies of the single position operational plan, a second ship may be used for tracking communications and data recording at a position further down range. The second ship, which is assumed to be without an acquisition radar, must rely on trajectory predictions from the first reentry ship to enable acquisition. It is estimated that the second ship should be stationed at about 400 nautical miles down range from the first reentry ship. Reliable communication facilities would be required between the two ships.

Another operational precodure may be employed to improve down range information obtained from the reentry ship. This procedure involves positioning the radar at a distance from the entry point which is a function of the entry angle. An examination of the trajectory charts shows that the vertical dispersion for an entry angle of -8.50° at a range of 460 nautical miles from entry is about the same as the dispersion for an entry angle of -5.00° at a range of 940 nautical miles. For the above down range distances, the horizontal dispersion for the -5.00° entry angle is even less than the horizontal dispersion for the -8.50° entry angle. For optimum down range information transfer the radar ship

should be stationed as far down range as is possible for a given entry angle. Thus, the upper curve in Figure 79, which gives the maximum down range station position for given entry angles would represent optimum ship distance from the entry point for post entry communication and data transfer. The probability of detection for a ship stationed according to the upper curve in Figure 79 is given in Figures 82 through 85.

It can be seen that the slope of the upper curve in Figure 79 is quite steep on the region of shallow entry angles. This means that the ship positions would be very sensitive to entry angle value and also the range of possible ship positions would be in excess of 600 nautical miles.

Since the down range extent of blackout will terminate at a distance less than 1100 nautical for most trajectories, a maximum down range station location of 900 nautical miles is considered satisfactory for data and communication. In view of this, the recommended ship locations for general use are shown in Figure 86.

The range of entry angles which may be covered under most severe trajectory conditions is shown in Figure 87 for the ship locations given in Figure 86. The dotted line on the minimum curve indicates that some absorption may be experienced in that region, but that the probability of detection is still satisfactory although some part of the coverage may be blanked out.

The probability of detection for the most severe trajectories designated for the ship positions as given in Figure 86, are shown in Figures 88 through 91 for a ship station on the projected ground track. The probability of detection for similar trajectories, with the ship stationed 50 nautical miles from the ground track are shown in Figure 92 through 95.

A ship stationed according to the curve in Figure 86 will have a satisfactory acquisition performance on any and all entering trajectories which have an entry angle equal to or more shallow than that specified by the curve in Figure 86.

It may be noted that trajectories from very shallow entry angles do not really have a side limit for these station positions. These trajectories are unable to develop sufficient lateral motion, in the distance traveled before acquisition, to reach the side of the pattern before passing out through the top of the pattern.

Also, the limitation on acquisition of trajectories of given entry angles as shown in Figures 86 applies only to the most evasive trajectories which may be executed without exceeding the 16 g deceleration factor. The limit does not apply to trajectories which do not take the most effective evasive maneuver.

Examples of the foregoing are shown in Figure 96. From a station located 618 nautical miles down range from entry, adequate acquisition is possible on a trajectory which an entry angle of –10.0° and a constant bank angle of 0°, or on a trajectory entering at –7.51° with a constant bank angle of 90°. The former trajectory would develop a deceleration of 22 g and the latter a deceleration of 25 g.

The probability of detection analysis thus far has been based upon a lift to drag ratio of 0.4. At the present time the exact value of the L/D is not known, but it will be within the range of 0.28 to 0.42. The most probable value is taken to be 0.35.

The value of 0.4 was taken in the analysis since it is near the high end of the possible range of values, and presents the more difficult acquisition task.

For comparison, the upper and lower limit trajectories for 16 g maximum deceleration are plotted in Figures 97 and 98. The deepest possible entry angles have been used for a trajectory with an L/D of 0.4 in Figure 97 and for a trajectory with an L/D of 0.3 in Figure 98. The deep entry angle trajectory represents the condition where the L/D will be most influential on the detection probability.

The upper limit trajectory is represented by the constant zero bank angle trajectory for both values of L/D. The deceleration for the –8.90° entry angle at an L/D of 0.4 is 16.13 g.

The lower limit trajectory is represented by a zero bank angle to 58 seconds after entry, and a 100° bank angle from 58 seconds to splash down for the L/D of 0.4. The lower limit trajectory for the L/D of 0.3 is found to have a bank angle of 0° from entry to 61 seconds after entry, followed by a bank angle of 100° to splash down.

By comparison of Figures 99 and 100, it can be seen that the 0.4 L/D trajectory is higher in the upper limit and lower in the lower limit than the trajectory with an L/D of 0.3. From a given down range position, the trajectory with an L/D of 0.3 travels further in the radar search pattern than the trajectory with an L/D of 0.4.

In the upper limit the velocity during the transit of the search pattern is higher for the 0.4 L/D trajectory than for the 0.3 L/D trajectory. Thus, in the upper limit, the probability of detection will be greater in the case of the 0.3 L/D trajectory than in the case of the 0.4 L/D trajectory.

In the lower limit, the trajectory for the 0.3 L/D value is in the radar search pattern a much greater distance than the trajectory with the 0.4 L/D value. However, this advantage is slightly offset by the fact that the velocity during observation is higher for the trajectory of 0.3 L/D than in the case of the trajectory of 0.4 L/D.

For a station position at 603 nautical miles from entry, the probability of detection is better on the 0.3 L/D trajectory than on the 0.4 L/D trajectory.

An analysis has also been made on trajectories with an entry angle of -6.00°. Similar results were obtained. In the limiting conditions, the trajectory computed for an L/D of 0.3 subjected the spacecraft to a higher probability of detection than a similar trajectory with 0.4 L/D. For the -6.00° entry angle the station position was 735 nautical miles down range.

In view of the foregoing, it is reasonable to assume that the performance of the acquisition radar, over the range of probable lift to drag ratio rations values, will be essentially equal to or better than that found for the 0.4 L/D value used in the analysis.

VIII. EFFECT OF TRACKING AND INSTRUMENTATION ERRORS

The computations thus far have been based upon nominal entry conditions. In the discussion of initial conditions it was shown that there may be some differences between the actual and the predicted entry conditions. The effect of these deviations are discussed in the following.

The component of positional error of the entry point in the direction of the ground track as seen by the tracking network is given in Figure 4 and 4a. As may be expected, the error decreases as the time to entry is reduced. Present plans for C-band acquisition messages include a message at five minutes prior to predicted acquisition and a message at 25 minutes predicted acquisition. The time required for tracking information to be communicated to the computation center, and for the computation of the predictions to be completed may be as little as three minutes or as much as five minutes.

With good communication facilities, the acquisition message is transmitted to the station within a few seconds. Thus, the five minute acquisition message is based on data taken slightly less than ten minutes prior to entry (entry is about one to two minutes before predicted acquisition, see Figure 98). The 25 minute acquisition message will be based on data taken 30 minutes prior to entry.

The final movement of the ship will be based on the 25 minute acquisition message. From Figure 4a, the down range positional error at 30 minutes prior to entry is two nautical miles. Here it is assumed that the maximum ten feet/second velocity change has been made at the most detrimental time, that is, ten hours prior to reentry.

The two mile error is a one sigma value, and since a better than 99.9% overall detection probability is desired, at three sigma value of six nautical miles will be used.

In addition to other navigation equipment, the reentry ships are expected to have a good inertial navigation system, and an ARN-9 satellite navigation system. Thus equipped, it is extremely unlikely that the ship positional error will be as great at 1.4 nautical miles. The statistical sum of the relative positional error in the projected ground track direction is 6.16 nautical miles at 30 minutes prior to entry.

If the positional error is along the projected ground track in the up range direction, the ship may be stationed nearer to the entry point for compensation, and the probability of detection on all specified possible trajectories is essentially unchanged. In the extreme conditions, a few nautical miles of post blackout data or tracking may be lost as a result of this movement.

If the error is in the down range direction and the ship is stationed by the no error analysis, a few additional low limit trajectories will come under surveillance with essentially no change on other trajectories.

The question now arises as to how much penalty should be leveled against the vast majority of probable trajectories to benefit an extremely few possible trajectories in an extremely unlikely situation. It might be advisable to station the ship two or three miles nearer the entry point than is indicated by the no error analysis shown in Figure 86 if it is desired to acquire the same extreme low limit trajectories.

The cross range error, as seen by the tracking network, for the predicted position of the reentry point is shown in Figures 5 and 5a. The one sigma value at 30 minutes prior to entry is 0.55 nautical miles for the curve which includes the 10 hour pre-reentry velocity change. The three sigma value of this error is 1.65 nautical miles.

The ship's position error of 1.4 nautical miles (3σ) will increase the relative position of the entry point in the cross range direction to 2.17 nautical miles (3σ).

There are two other factors which influence the width of the trajectory dispersion in the horizontal plane. The error in orientation of the search pattern is less than 6 minutes of arc (3σ). At a range of 281 nautical miles, this error produces a lateral displacement of 0.6 nautical miles. Also there may be an error of up to 24 feet per second (3σ) in the cross range velocity as predicted thirty minutes prior to entry, as shown in Figure 8. The travel time between the entry point and the search area may be as much as 125 seconds. Thus, a positional error of 3000 feet or 0.5 nautical miles (3σ) may result at the initiation of search.

The total cross range error is the statistical sum of the foregoing components or 2.31 nautical miles (3σ).

The cross range errors are symmetrical about the projected pre-reentry ground track and do not suggest a lateral displacement of the acquisition radar. They do, however, broaden the width of the horizontal dispersion pattern, and will cause a slight decrease in probability of detection in the case of trajectories whose traverse in the search pattern are limited by the side exit. Figure 97 is an example of the decrease in detection probability caused by a lateral error of 2.31 nautical miles. The influence of cross range error is included in the study by shifting the horizontal projection of the search pattern 2.31 nautical miles from the ground track in the unfavorable direction.

The errors in the predicted entry angle is shown in Figure 6 and 6a. On the curve which includes the 10 hours pre-reentry velocity change, the error in entry angle is $\pm 0.005°$ at 30 minutes prior to entry. The performance of the acquisition radar is quite insensitive to an error in entry angle of this magnitude. No modification of the operational procedures are needed to compensate for this error.

The time of arrival of the spacecraft at the acquisition area is quite important to the radar operation personnel. The error in time of arrival at the predicted entry point is given in Figure 7 and 7a. The three sigma value is insignificant in comparison to the variation in time of arrival which will result from the variation in possible post entry trajectories. The maximum and minimum travel time between the entry point and the search pattern is given in Figure 98 for the trajectories which reach the search pattern at that station location. These values are based on a pattern elevation of 8°, and will change with the elevation angle (maximum travel time will be decreased with reduced elevation angle).

In summary of the tracking errors, it does not appear that the derogatory effect of these errors is sufficient to warrent much consideration. Only in the

31

situation where the ship is placed as far down range as possible to acquire a specified low limit trajectory, it would be desirable to reduce the computed down range distance by a few miles (no more than six) to ensure that any low limit trajectory of specified deceleration does not escape detection.

These conclusions are based upon the assumption that the tracking network is operating at normal performance level.

IX. SHIP MOVEMENT

Since the velocity of the reentry ship is 15 knots under normal conditions, and may be as low as 10 knots under such adverse conditions as would permit recovery operations, the desired location of the radar must be known well in advance of reentry. Also, special trajectory computations and special messages will be needed to supply the entry ship with the necessary positional information.

A procedure by which the ship can be properly stationed is given in the following. It is not intended to represent the procedure as optimum, it very likely is not. It is, however, desired to establish the possibility of utilizing available information for accomplishing the fact.

If a message is prepared at 20 hours prior to entry, the ship could be directed to a spot which is within 133 nautical miles along the ground track and within 5.3 nautical miles cross range of the predicted entry point (all values 3σ, see Figures 4 and 5). Here it is assumed that the position of the reentry ship will be taken into consideration in planning any change in reentry conditions. It is quite likely that the most critical aspect in the reentry operation is the entry angle. A change in the transearth velocity to improve the entry angle will effect a change in the place of entry.

With reference to Figure 5, the entry angle is known to an accuracy of 0.4° (3σ) 20 hours prior to entry, and the desirability of a modification in entry angle should be known at that time. The effect of any anticipated change in entry point position as a result of the modification to the entry angle should be incorporated in the instruction for ship movement at the 20 hour message, and in all other acquisition messages.

A second message is prepared at 10 hours from entry. This message will be made on data taken before the 10 hour velocity correction is made. The information available at 10 hours prior to entry involves a predicted entry error of 17.4 nautical miles (3σ) in the direction of the ground track and one error of 0.75 nautical miles (3σ) cross range.

The errors listed in Figures 4a, 5a, 6a, and 7a are tracking errors with no knowledge of the magnitude or direction of the velocity change introduced at the 10 hour pre-reentry velocity correction.

To properly station the ship, it is necessary to take advantage of the knowledge of the velocity increment made at the 10 hour correction.

The error in the predicted entry point based upon the ten hour correction will include the error in establishing the predicted entry point and the error introduced by the inaccuracy in generating the desired change in velocity. It is assumed that no appreciable error in introduced by the process of computation.

A perturbation method has been used to establish the positional error at entry due to the error in the velocity increment at 10 hours before entry. A normal trans earth trajectory has been generated by the Quick-Look Program used in the Mission Analysis Office (Reference 5). This trajectory has a mid-corridor entry angle of $-6.256°$. After the initial run of the trajectory, another run was prepared in which a velocity change of ten feet per second was inserted 10 hours prior to entry. The velocity increment was in the direction of the velocity vector.

The program was then run again with a velocity change of similar magnitude inserted at 10 hours prior to entry, but with the increment in the direction negative of the velocity vector.

Other similar runs were made with the incremental velocity inserted normal to the velocity vector. Two of these were in the plane of the earth's surface and the other two were in the plane of the velocity vector and the earth radius vector.

The displacement of the entry point relative to the undisturbed trajectory were observed for each run. The results are shown in Figure 101 for the increment in the direction of the velocity vector, in Figure 102 for the increment in the plane of the earth's surface, and normal to the velocity vector, and in Figure 103 for the increment in the plane of the velocity vector and the earth radius vector and normal to the velocity vector.

Since this study is concerned with a small velocity increment, representative of the error in the velocity change, the rate of change in position per unit change in velocity is taken as the tangent to the curve at the undisturbed value. It should be observed that the 10 feet per second velocity change can result in a gross movement of both the down range position of the entry point and the value of the entry angle. It is assumed that in planning the velocity correction, no correction will be specified which would result in an impossible ship position.

The error which may exist in the velocity increment was obtained from Mr. F. H. Beardsley at Manned Spacecraft Center, Houston, Texas. According to Mr. Beardsley, the change in velocity can be controlled and measured to an accuracy of ±0.1 feet per second, 3σ value.

Two of the velocity errors contribute to displacement along the ground track. The error component along the velocity vector may contribute 0.1 feet per second times the slope of Figure 101, or 0.775 nautical miles. The error in the velocity increment normal to the direction of the velocity vector and in the plane of the velocity vector and the earth radius vector can contribute as much as 0.1 times the slope of Figure 103, or 3.00 nautical miles. Since the error in the velocity increment is a 3σ statistical error, these displacements add statistically to give a 3σ displacement of 3.1 nautical miles.

The displacements due to the error in the velocity increment statistically augment the predicted tracking error of 17.4 nautical miles as shown in Figure 4a, to give a total 3σ ambiguity of 17.7 nautical miles in the predicted position of entry point along the ground track.

A similar procedure, utilizing the information from Figure 5a and from Figure 102 gives a 3σ ambiguity of 0.76 nautical miles in the predicted position of the entry point and in the direction normal to the ground track. The total 3σ ambiguity in the predicted position of the entry point as observed at 10 hours prior to entry is 17.8 nautical miles.

The ship was within 133 nautical miles of the desired position at the start of the 10 hour pre-entry period. Computations made for the 10 hour message place the ship within 17.7 nautical miles of the desired station. Thus, if it is desired to reach this predicted station one hour prior to entry, a maximum distance of 115 nautical miles may be traveled in 9 hours. This calls for a ship speed of 12.8 knots.

For any reentry trajectory approximately a normal reentry, this position is quite adequate. As shown by Figures 65 through 68 and Figure 97, an 18 nautical miles displacement of the ship position along the ground track, or a 0.76 nautical mile displacement normal to the ground track will have little or no effect on the probability of detection for the normal reentry trajectory.

To insure acquisition of extreme trajectories, a more exacting procedure may be desired. Repeated messages one at one hour prior to entry and the second at 30 minutes prior to entry can station the ship within six nautical miles (3σ) of the desired down range position. The off track displacement of a small fraction of a mile is negligible.

34

A second procedure, which substitutes antenna pointing for ship motion may be utilized in place of or in addition to the final phase of ship motion. By comparison of Figures 79 and 86 it can be seen that, if the recommended ship positions are used, full coverage is obtained for any specified entry angle more shallow than $-7.00°$ even though the ship position may be off by 15 nautical miles. To cover the low limit for entry angles deeper than $-7.00°$, the elevation angle of the search pattern may be depressed. The decrement in elevation angle to compensate for excessive down range distance when acquiring low limit trajectories is given in Figure 104.

Likewise, lateral displacement from the ground track in excess of five nautical miles should be compensated by an azimuth angle correction. The recommended azimuth angle correction for small lateral displacement is given in Figure 105. The offset angle for large lateral displacement has been shown in Figure 70.

ACKNOWLEDGEMENTS

REFERENCES

1. Moore, J. R., "Apollo Entry Radar Acquisition Study, GSFC, May 28, 1965.

2. Chapman, D. R., "An Approximate Analytical Method for Studying Entry Into Planetary Atmospheres, " Ames Research Center, 1959.

3. Bryant, J. P., and Frank, M. P., "An Automatic Long Range Guidance System for a Vehicle Entering at Parabolic Velocity, " Martin Co., June 1962.

4. Frank, M. P., "Detailed Mission Planning Considerations and Constraints, " MSC Internal Note No. 66-FM-134, November 10, 1966.

5. Philco Corporation, "Quick Look Mission Analysis Program, " Report WDL-TR-2217, January 1964.

6. Philco Corporation, "User's Manual for Mark II Error Propagation Program, " contract NAS5-9700, February 15, 1966.

7. Vonbun, F. O., "Reentry Tracking for Apollo, " GSFC, March 1964.

8. Marini, J. W., "On the Decrease of Radar Cross Section of the Apollo Command Module due to Reentry Effects, " GSFC, June 1967.

9. Lehnert, R., and Rosenbaum, B., "Plasma Effects on Apollo Reentry Communications, " NASA TN D-2732, March 1965.

10. Burton, John, "Communications Blackout Regions for Lunar Returns Using the AS-504 Reentry Guidance, " MSC Internal Note 66-FM-142 November 25, 1966.

11. Dennison, A. J., and Butler, J. F., "Missile and Satellite System Program for the IBM 7090, " General Electric 61-SD-170, February 1962.

12. Daniels, R. L., "Final Report on Plasma Reentry Studies, " North American Aviation Inc., SID63-746, July 5, 1963.

13. Nolen, J. C., and Lacis, J. G., and Smith, J. J., "Sequential Detection with Application to Radar, " February 14, 1964.

14. Blake, L. V., "A Guide to Basic Pulse-Radar Maximum-Range Calculations," Part I, Naval Research Laboratory, December 28, 1962.

15. Marcum, J. I., "A Statistical Theory of Target Detection by Pulsed Radar," Project Rand RM-754, December 1, 1947.

16. Morth, Raymond, "Reentry Guidance for Apollo," Massachusetts Institute of Technology, R-532 Volume I, January 1966.

Fig. 1

TRAJECTORY
PRIOR TO
REENTRY

LONG RANGE TRACKING STATIONS (2)

RECOVERY AREA

REENTRY POINT
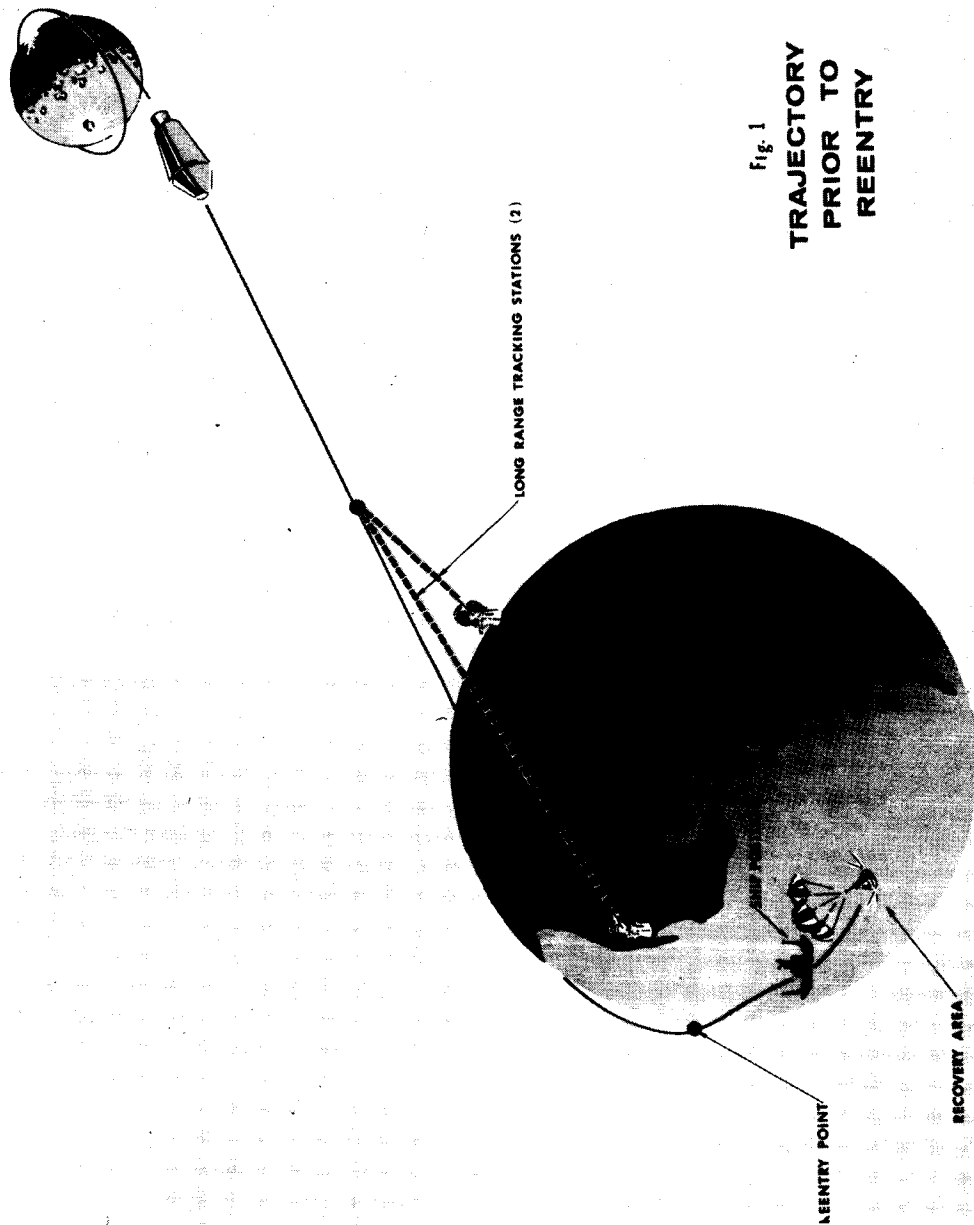
Figure 1. Trajectory Prior to Reentry

41
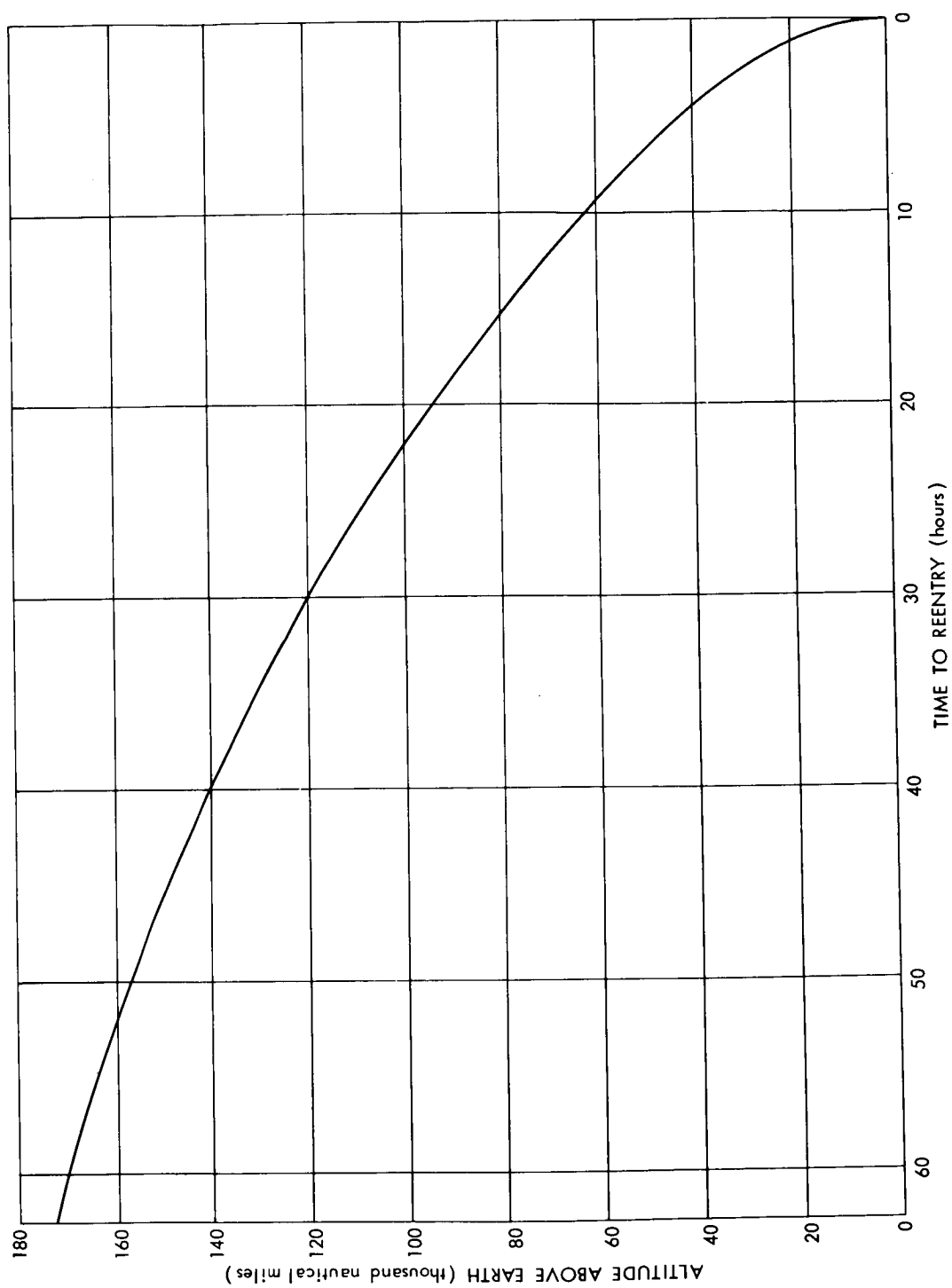
Figure 2. Altitude of Spacecraft in Typical Pre-Reentry Trajectory

42
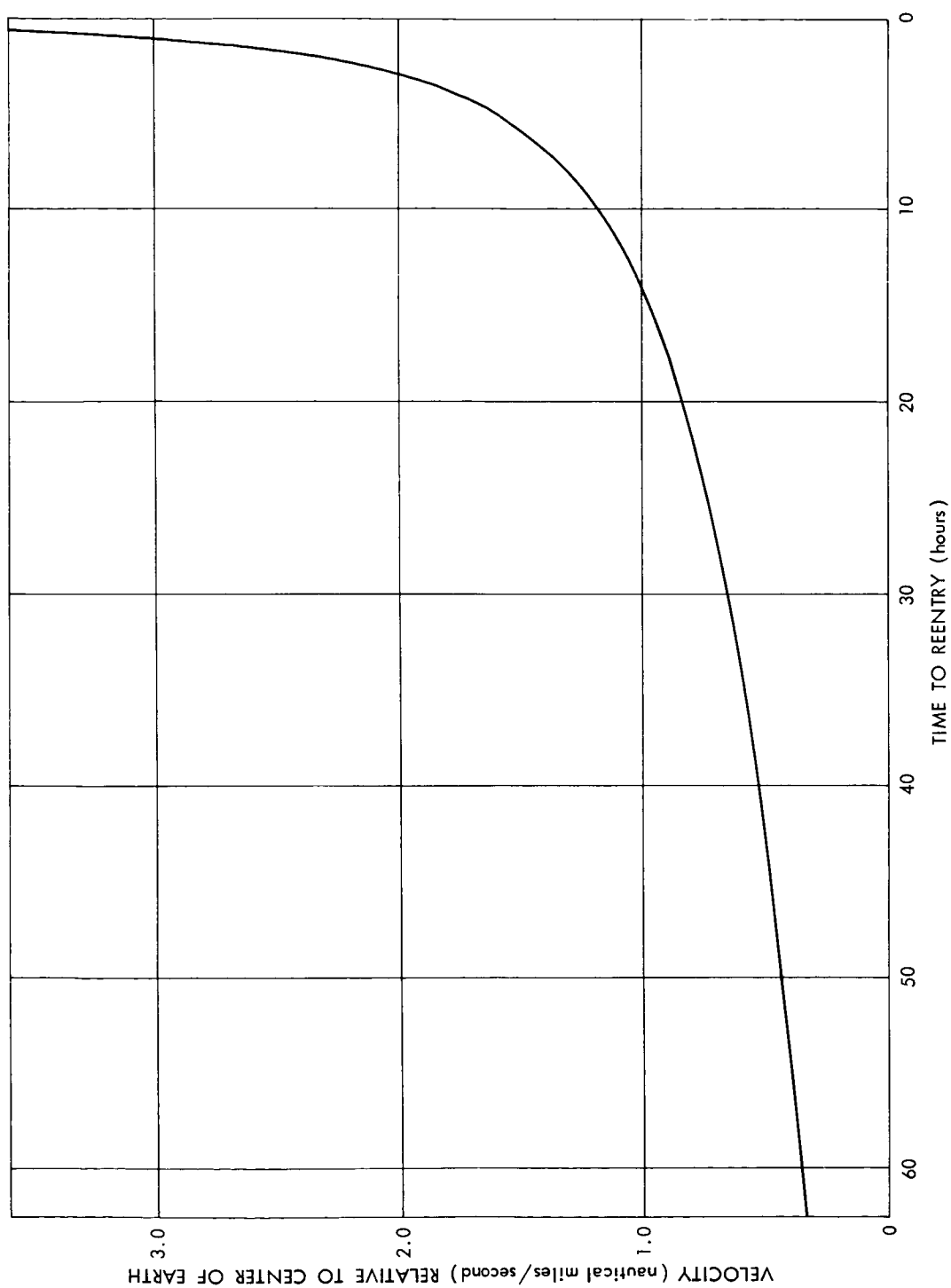
Figure 3. Velocity of Spacecraft in Typical Pre-Reentry Trajectory

43
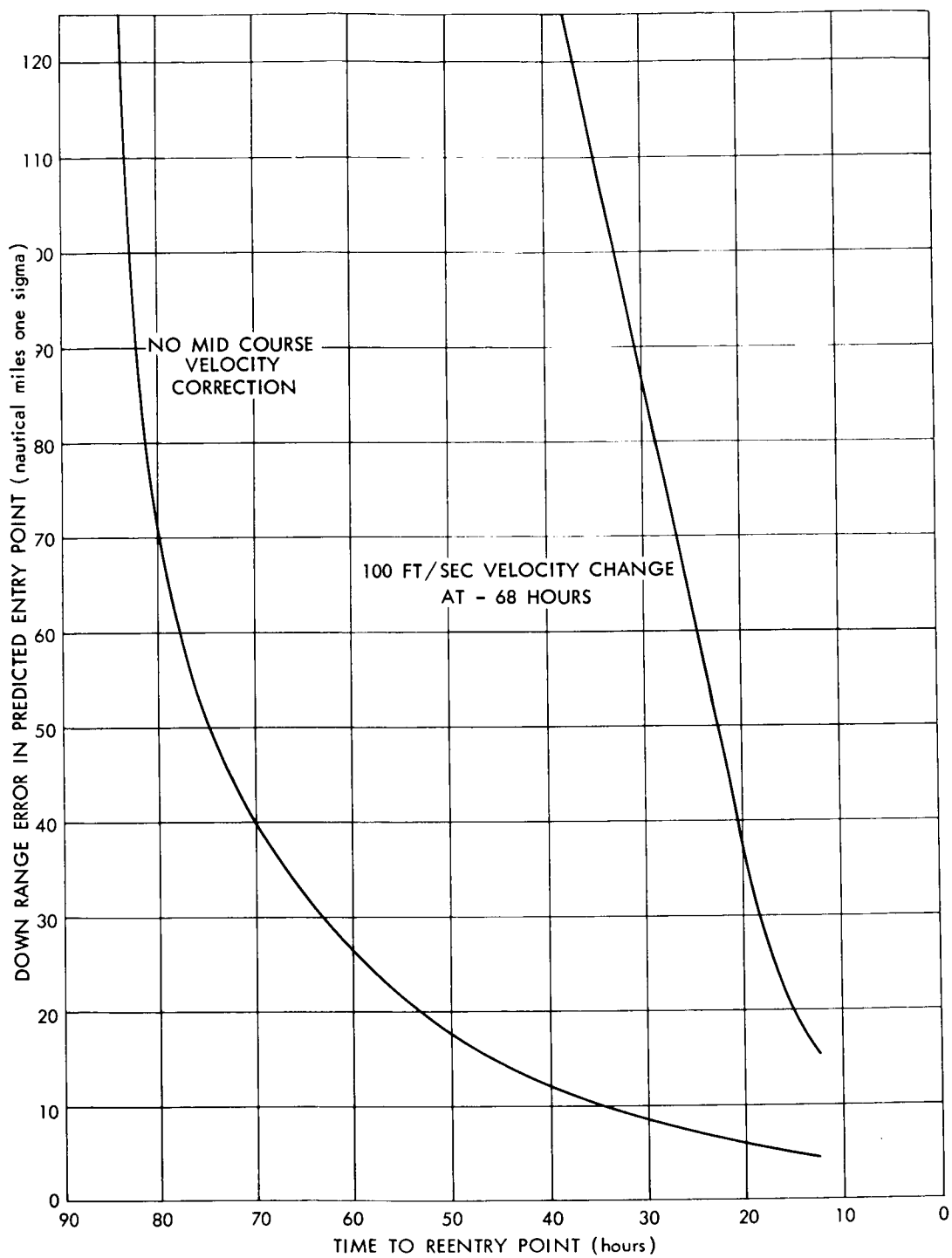
Figure 4. Error in Predicted Entry Point Component in Down Range Direction
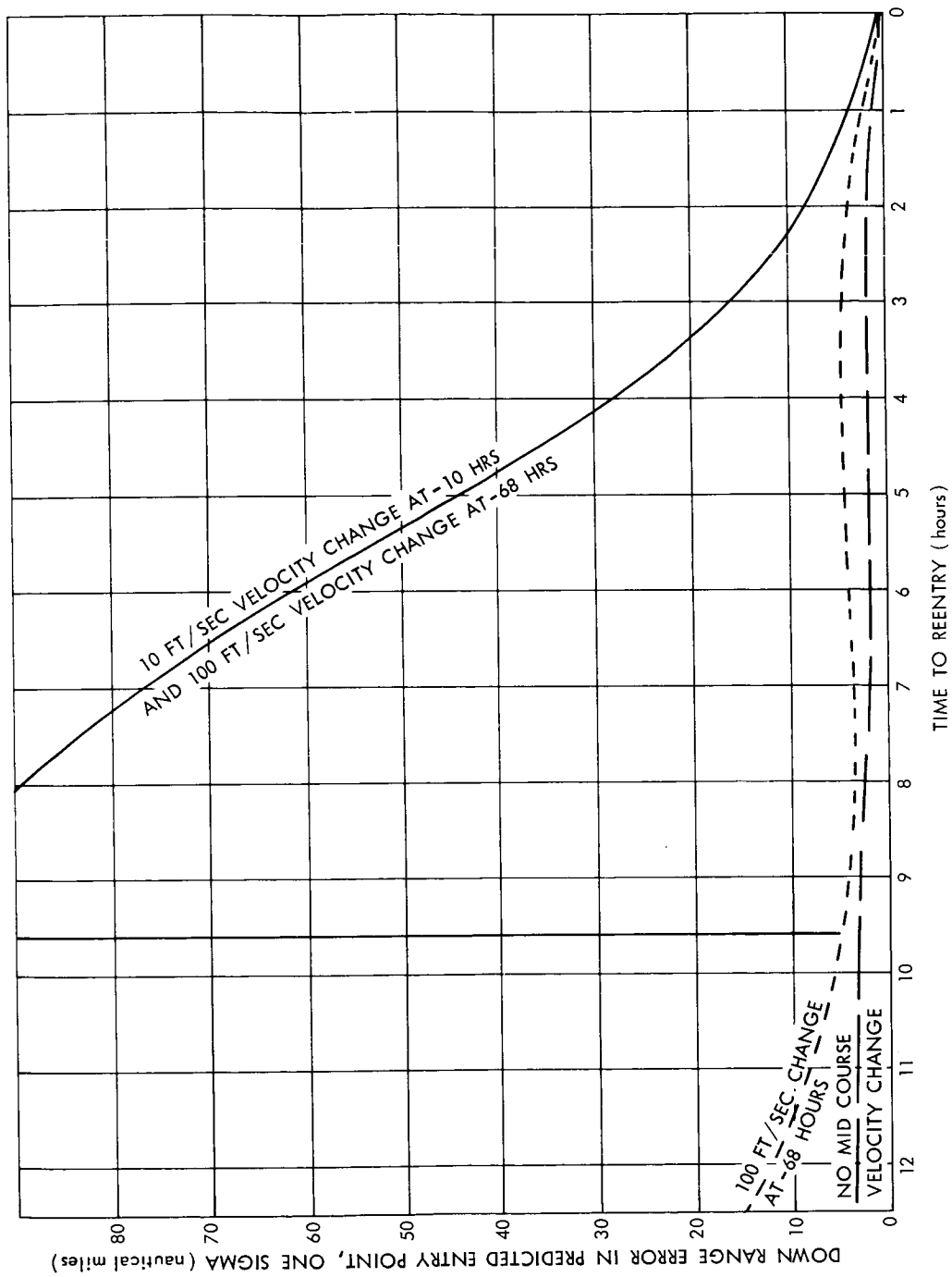
Figure 4a. Error in Predicted Entry Point Component in Down Range Direction
(Continued from Figure 4)
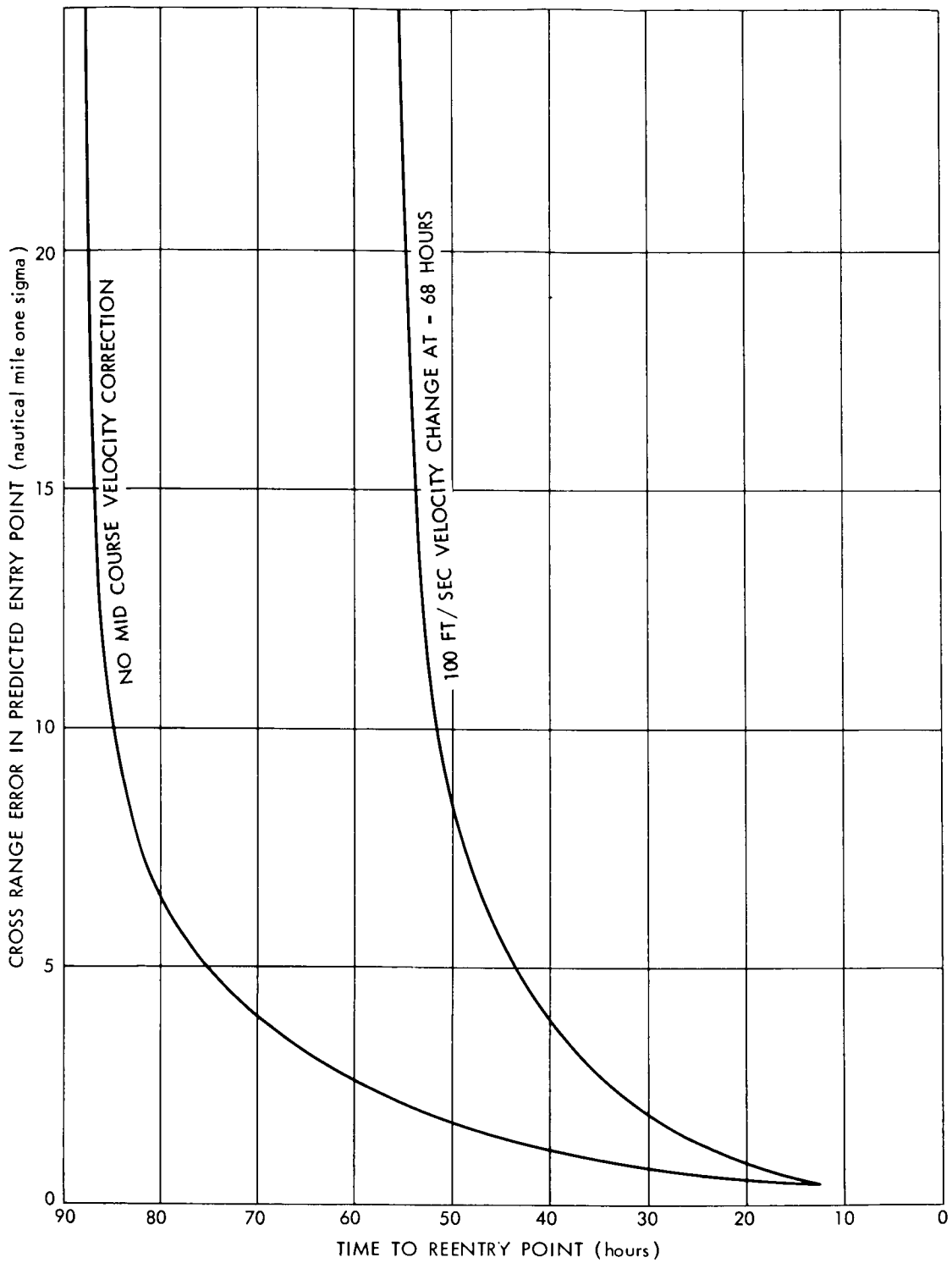
Figure 5. Error in Predicted Entry Point Cross Range Component
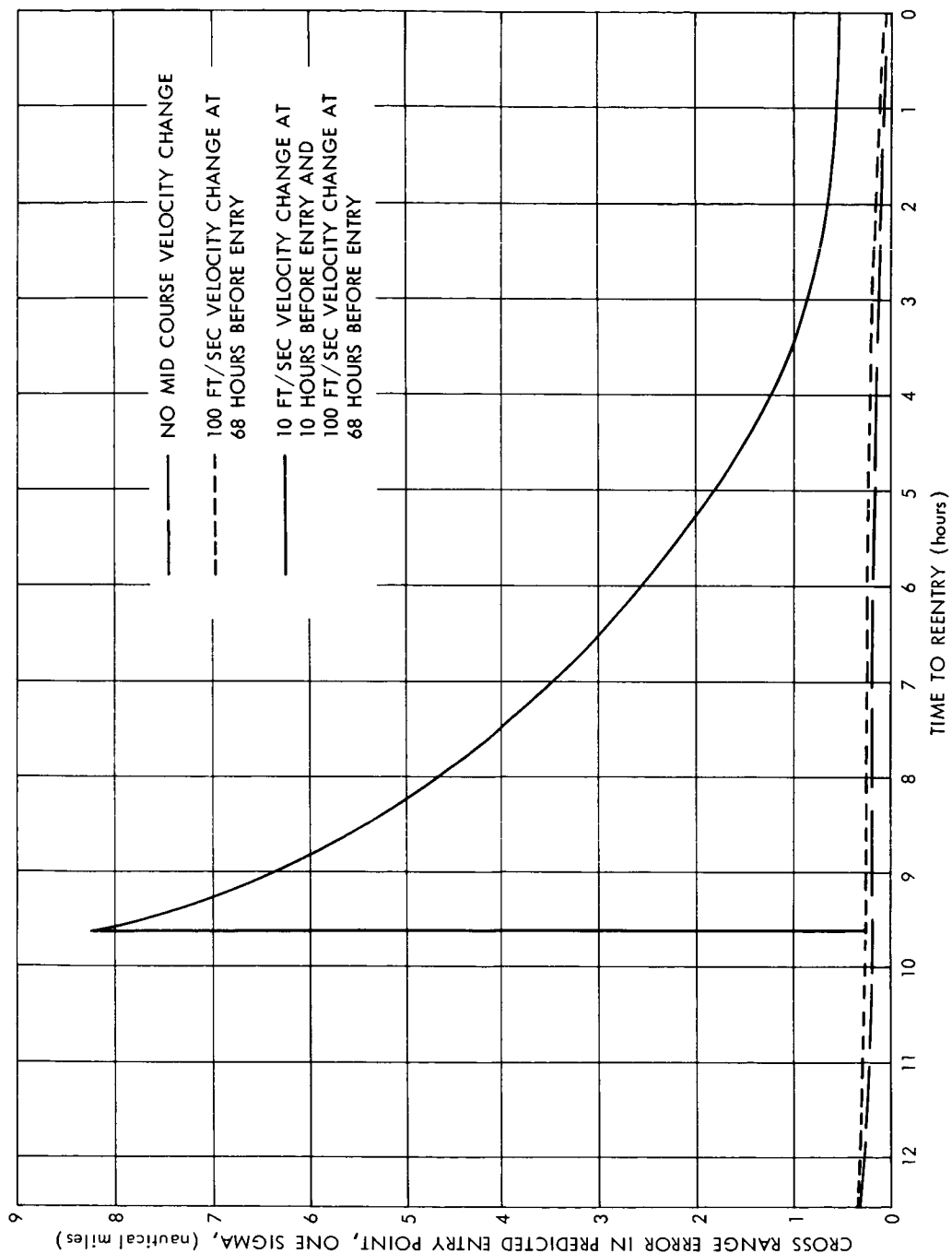
Figure 5a. Error in Predicted Entry Point Cross Range Component (Continued from Figure 5)

47
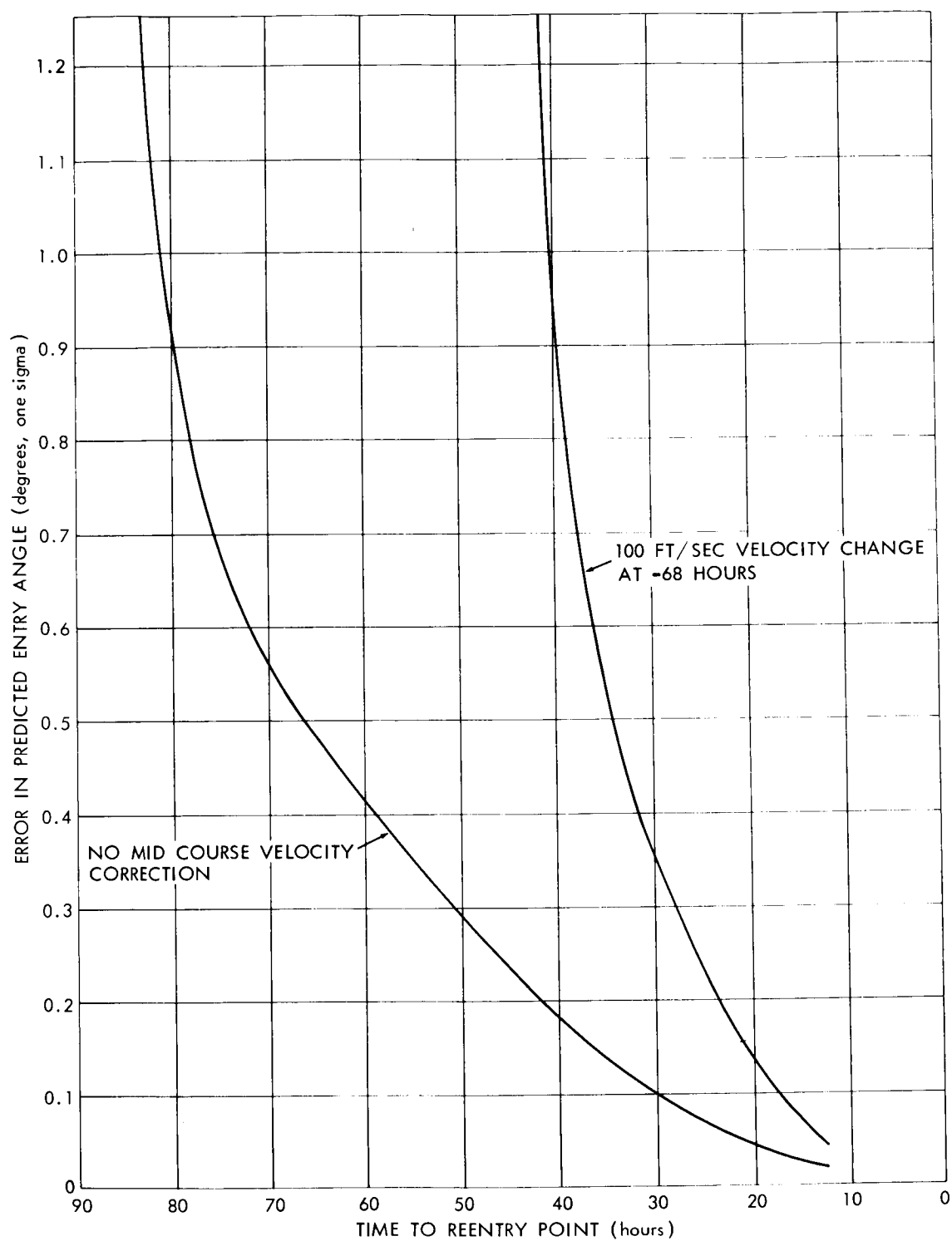
Figure 6. Error in Predicted Entry Angle
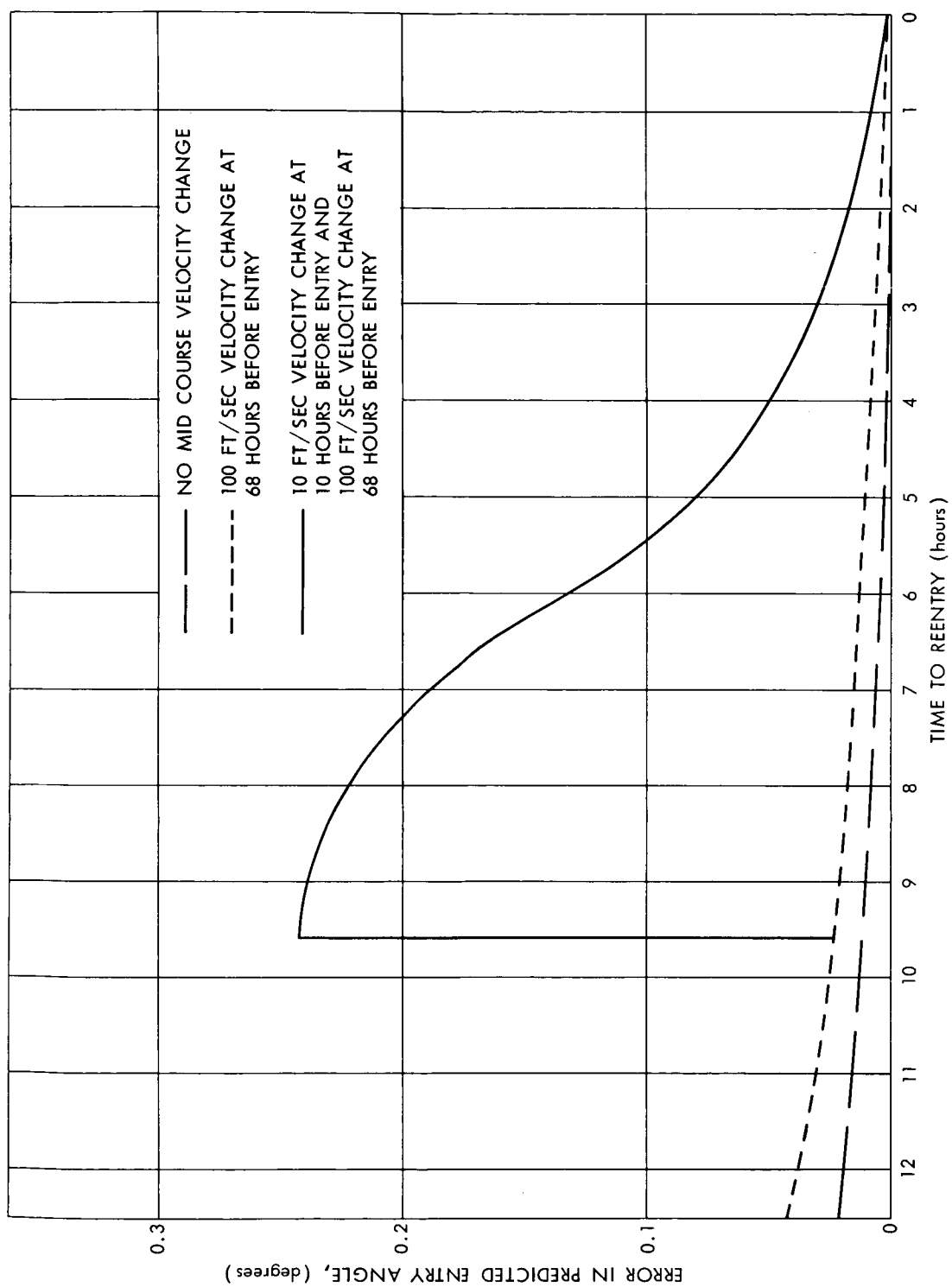
Figure 6a. Error in Predicted Entry Angle (Continued from Figure 6)

The legend on the figure reads:

— NO MID COURSE VELOCITY CHANGE

--- 100 FT/SEC VELOCITY CHANGE AT 68 HOURS BEFORE ENTRY

— 10 FT/SEC VELOCITY CHANGE AT 10 HOURS BEFORE ENTRY AND 100 FT/SEC VELOCITY CHANGE AT 68 HOURS BEFORE ENTRY

Y-axis: ERROR IN PREDICTED ENTRY ANGLE, (degrees)

X-axis: TIME TO REENTRY (hours)

49
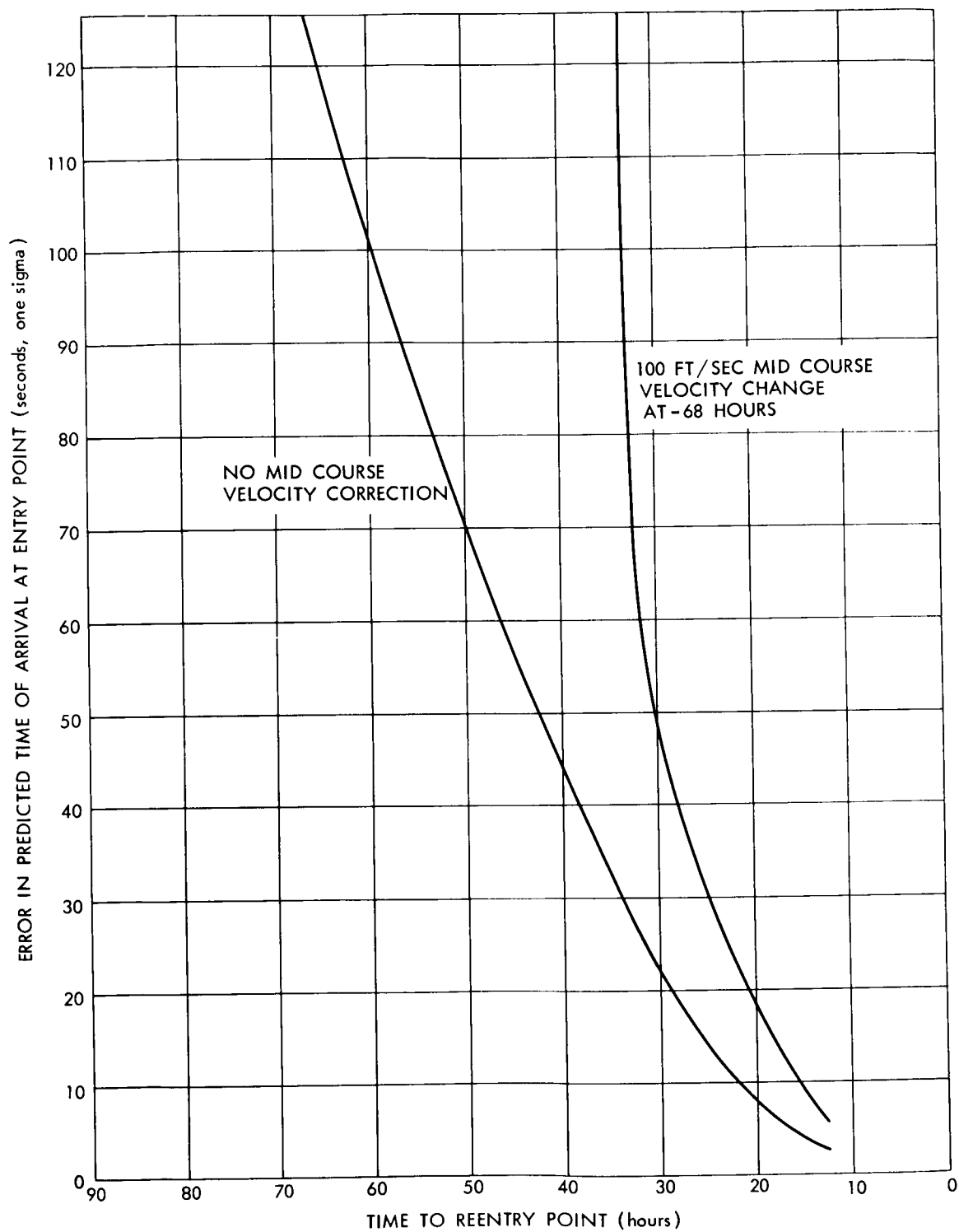
Figure 7. Error in Predicted Time of Arrival at Entry Point

50
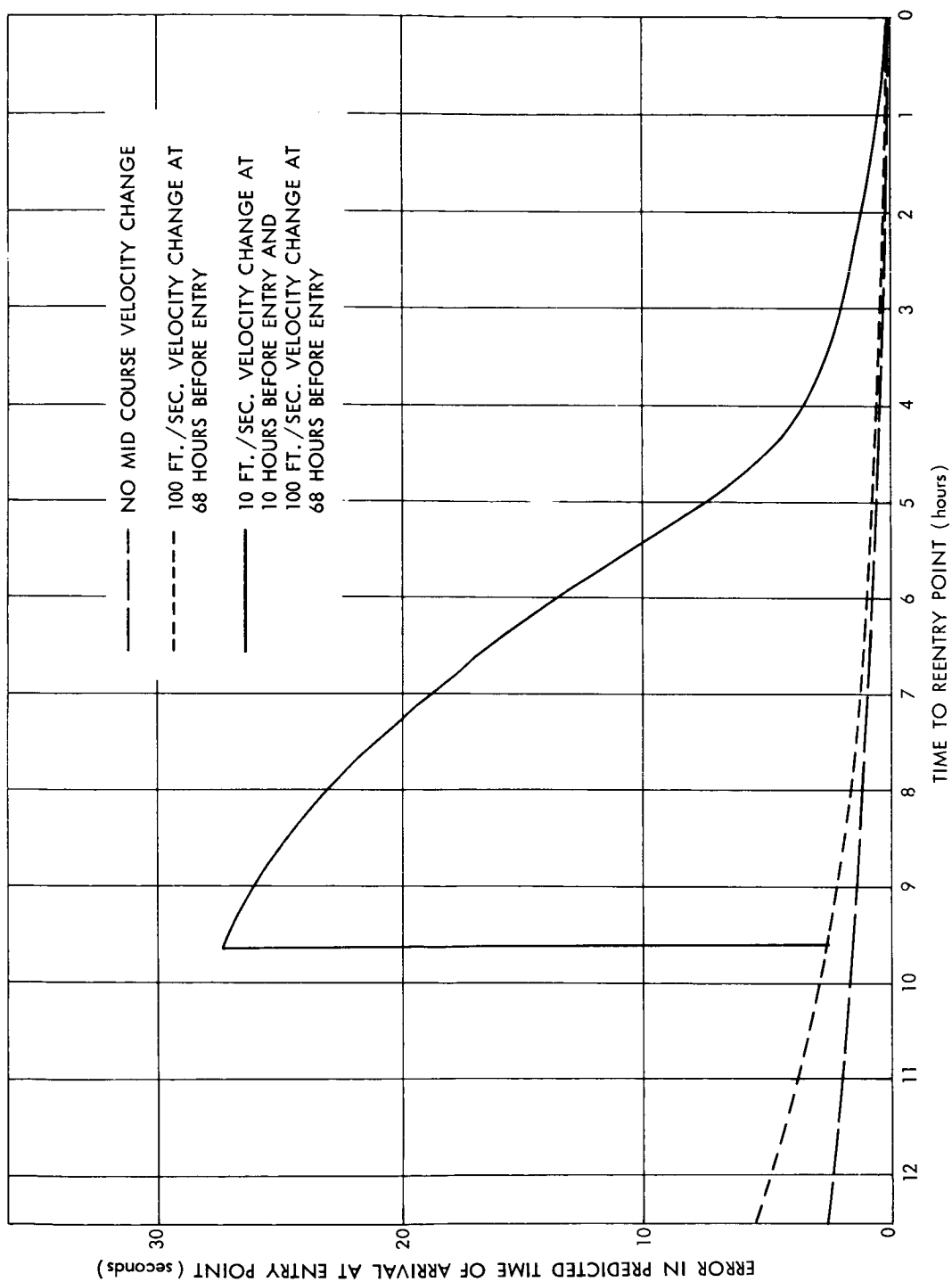
Figure 7a. Error in Time of Arrival at Predicted Entry Point

51
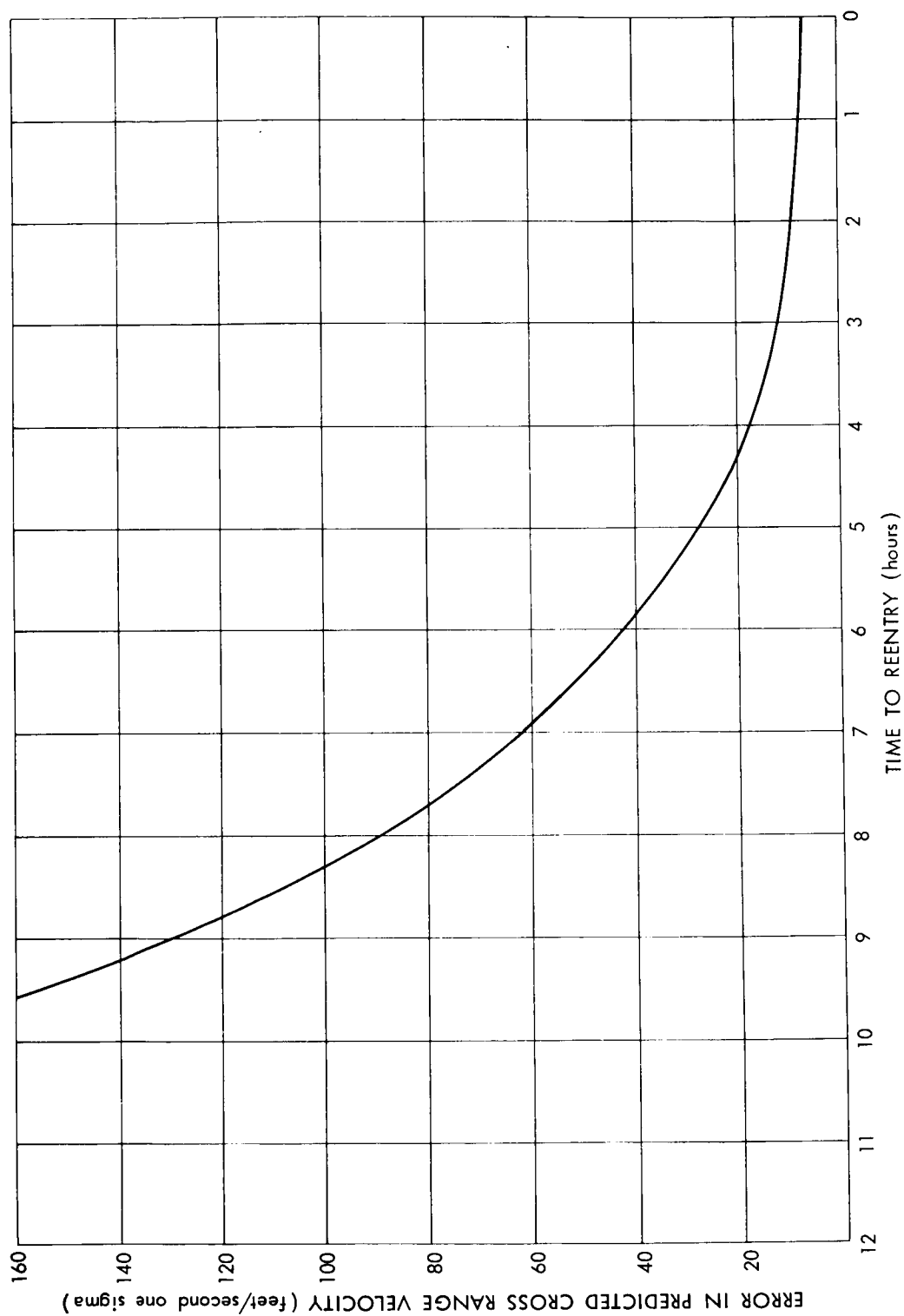
Figure 8. Error in Predicted Cross Range Velocity with 10 Feet Per Second Velocity Change at 10 Hours Before Entry and 100 Feet Per Second Velocity Change at 68 Hours Before Entry
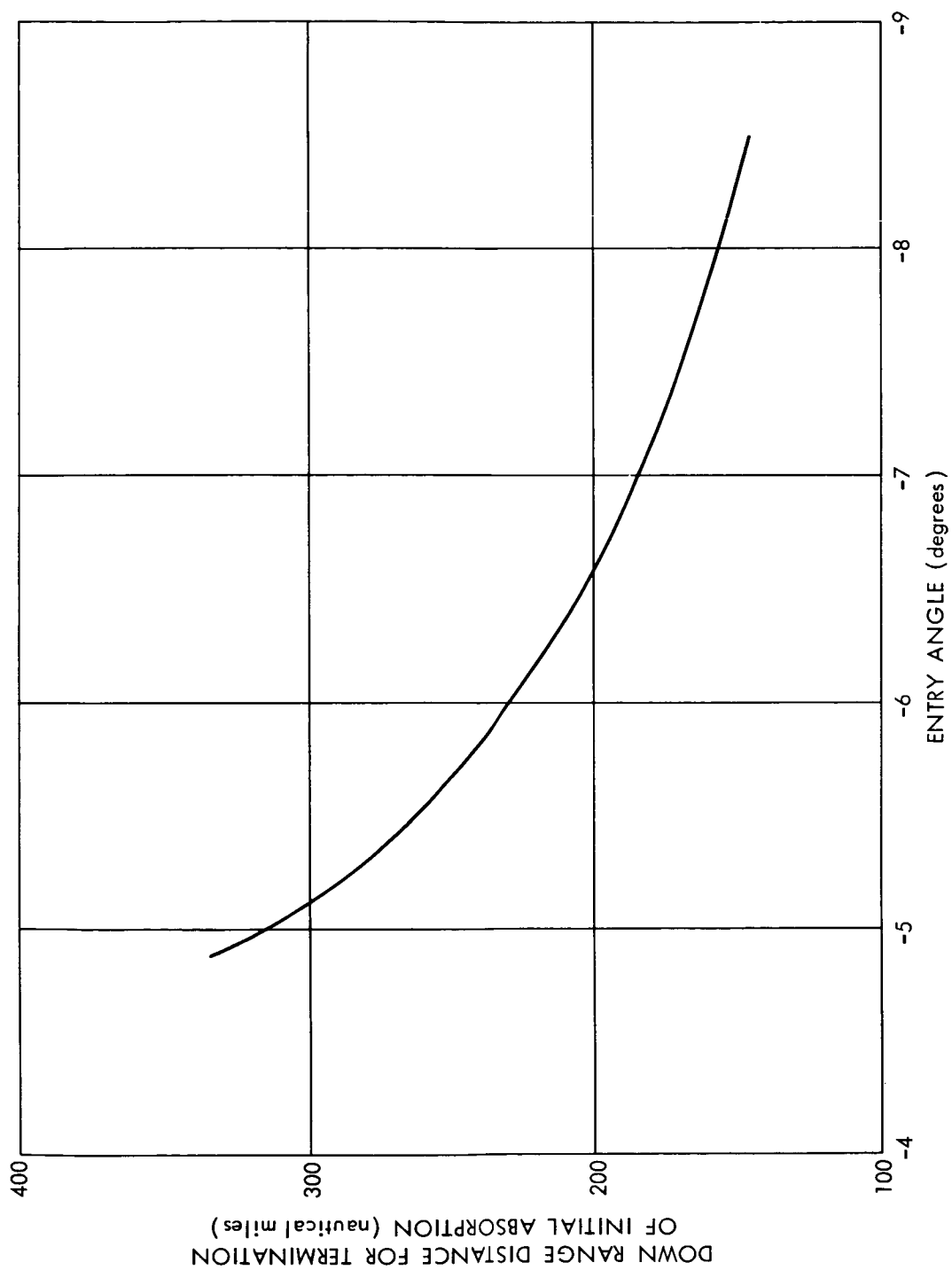
Figure 9. Down Range Distance to Termination of Initial Radio Absorption Area

53
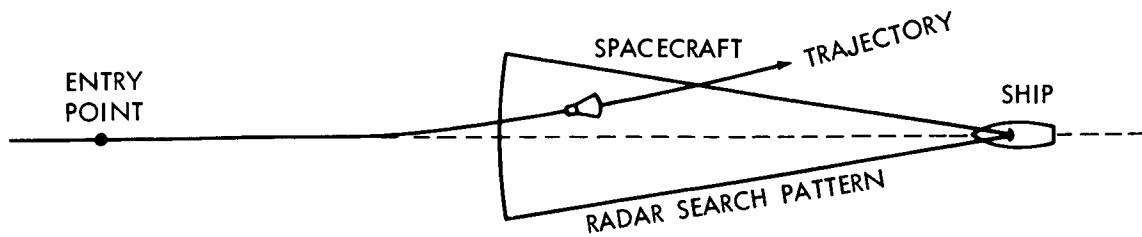
Figure 10. Horizontal Projection of Acquisition Deployment
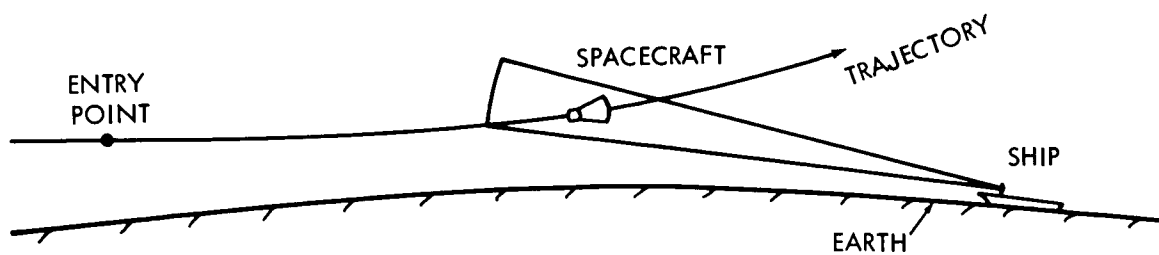
Figure 11. Vertical Projection of Acquisition Deployment
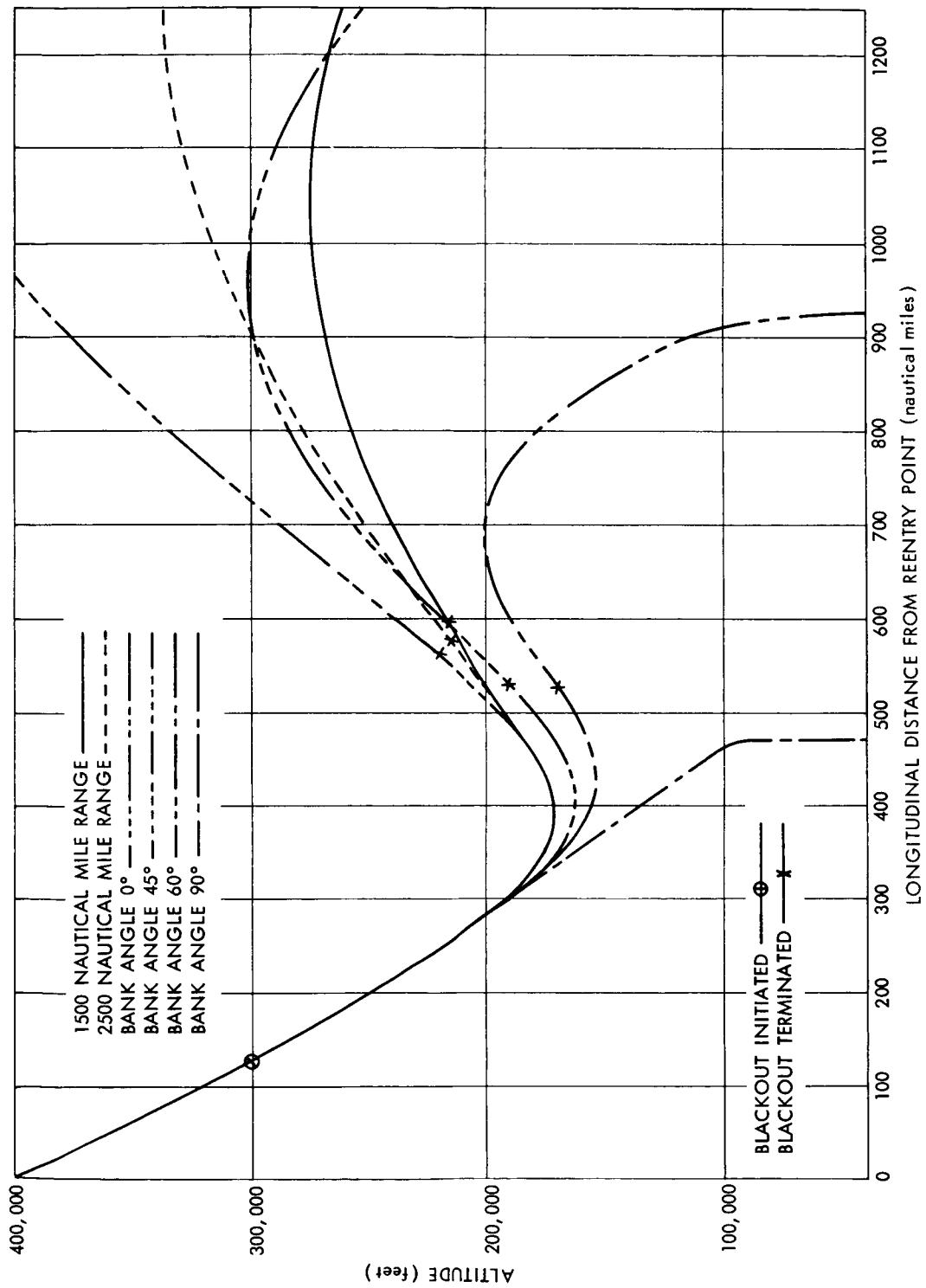
Figure 12. Elevation Projection of Reentry Trajectories Originating from −7.51° Entrance Angle

LONGITUDINAL DISTANCE FROM REENTRY POINT (nautical miles)

ALTITUDE (feet)

1500 NAUTICAL MILE RANGE
2500 NAUTICAL MILE RANGE
BANK ANGLE 0°
BANK ANGLE 45°
BANK ANGLE 60°
BANK ANGLE 90°

BLACKOUT INITIATED
BLACKOUT TERMINATED
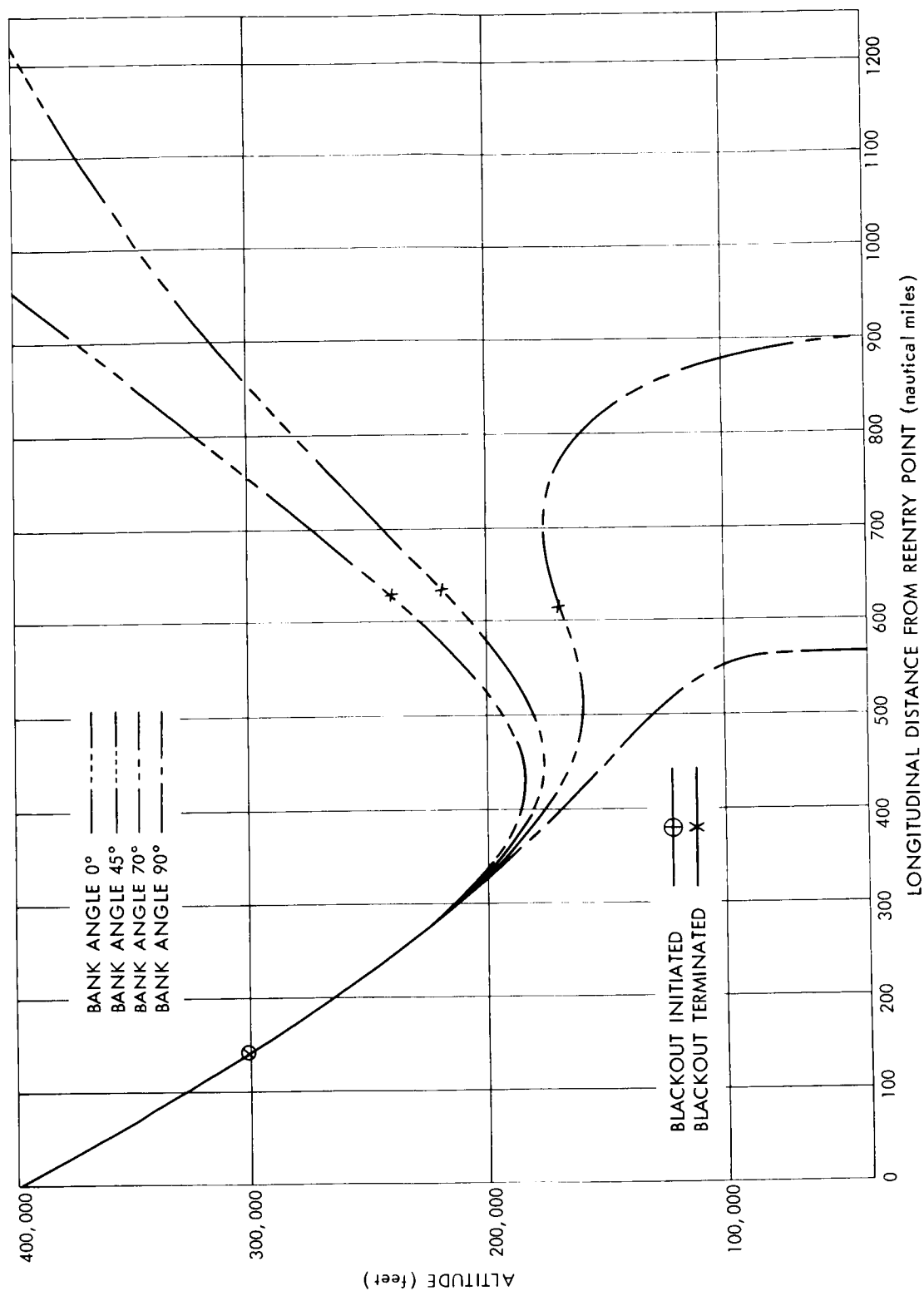
Figure 13. Elevation Projection of Reentry Trajectories Originating from -6.80° Entrance Angle

LONGITUDINAL DISTANCE FROM REENTRY POINT (nautical miles)

ALTITUDE (feet)

BANK ANGLE 0°
BANK ANGLE 45°
BANK ANGLE 70°
BANK ANGLE 90°

BLACKOUT INITIATED
BLACKOUT TERMINATED
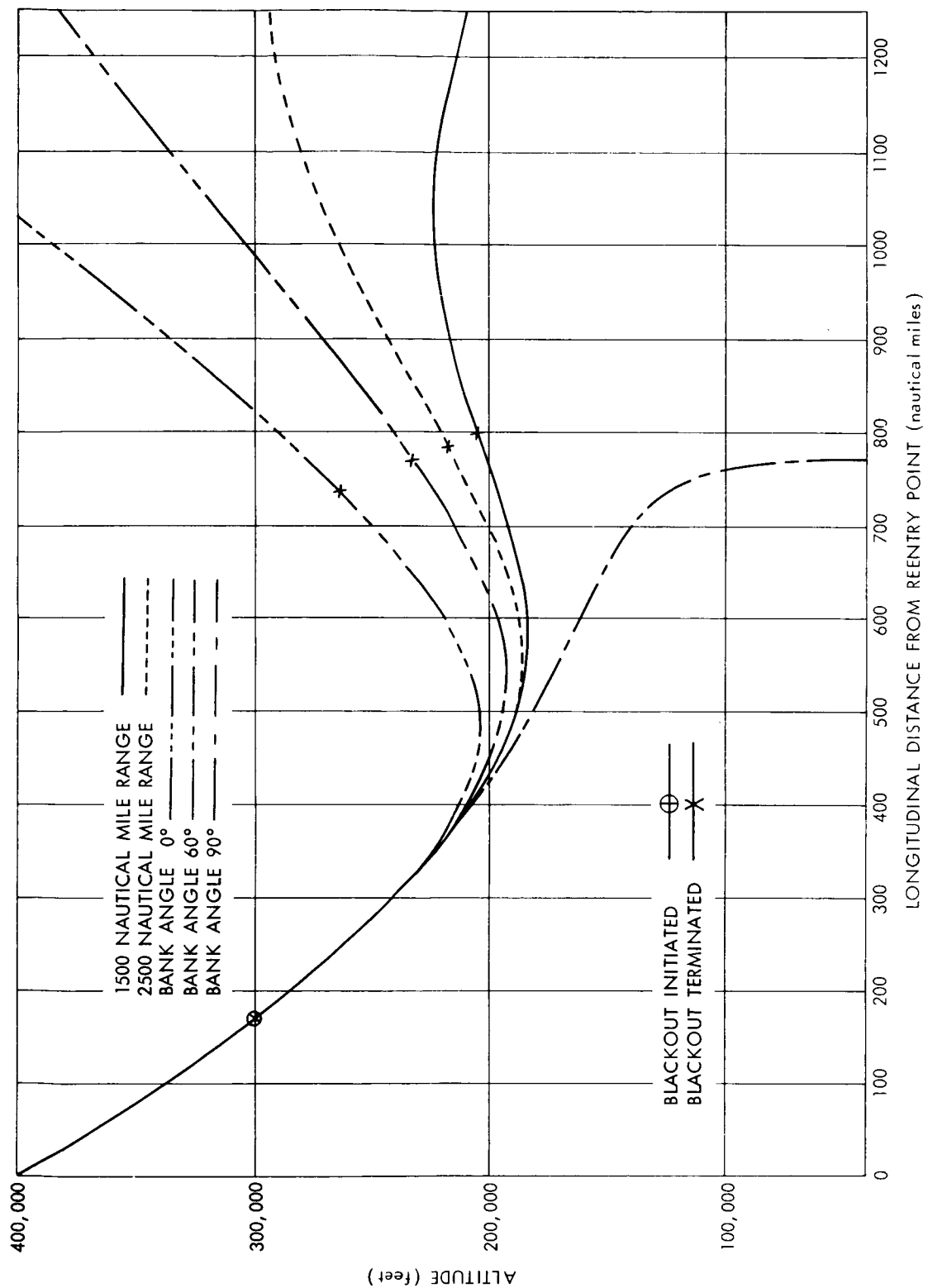
Figure 14. Elevation Projection of Reentry Trajectories Originating from –6.00° Entrance Angle

57
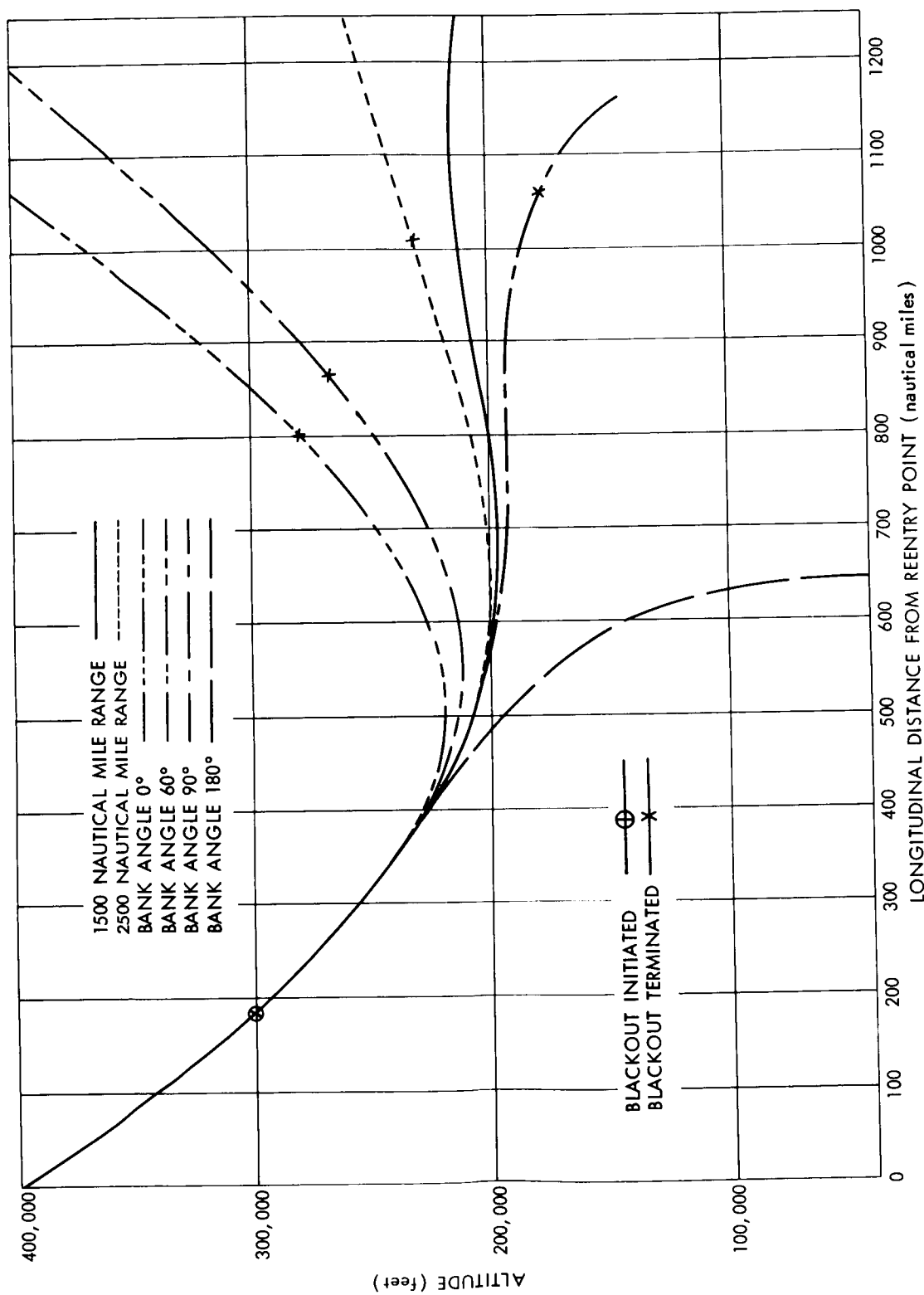
Figure 15. Elevation Projection of Reentry Trajectories Originating from –5.53° Entrance Angle

58
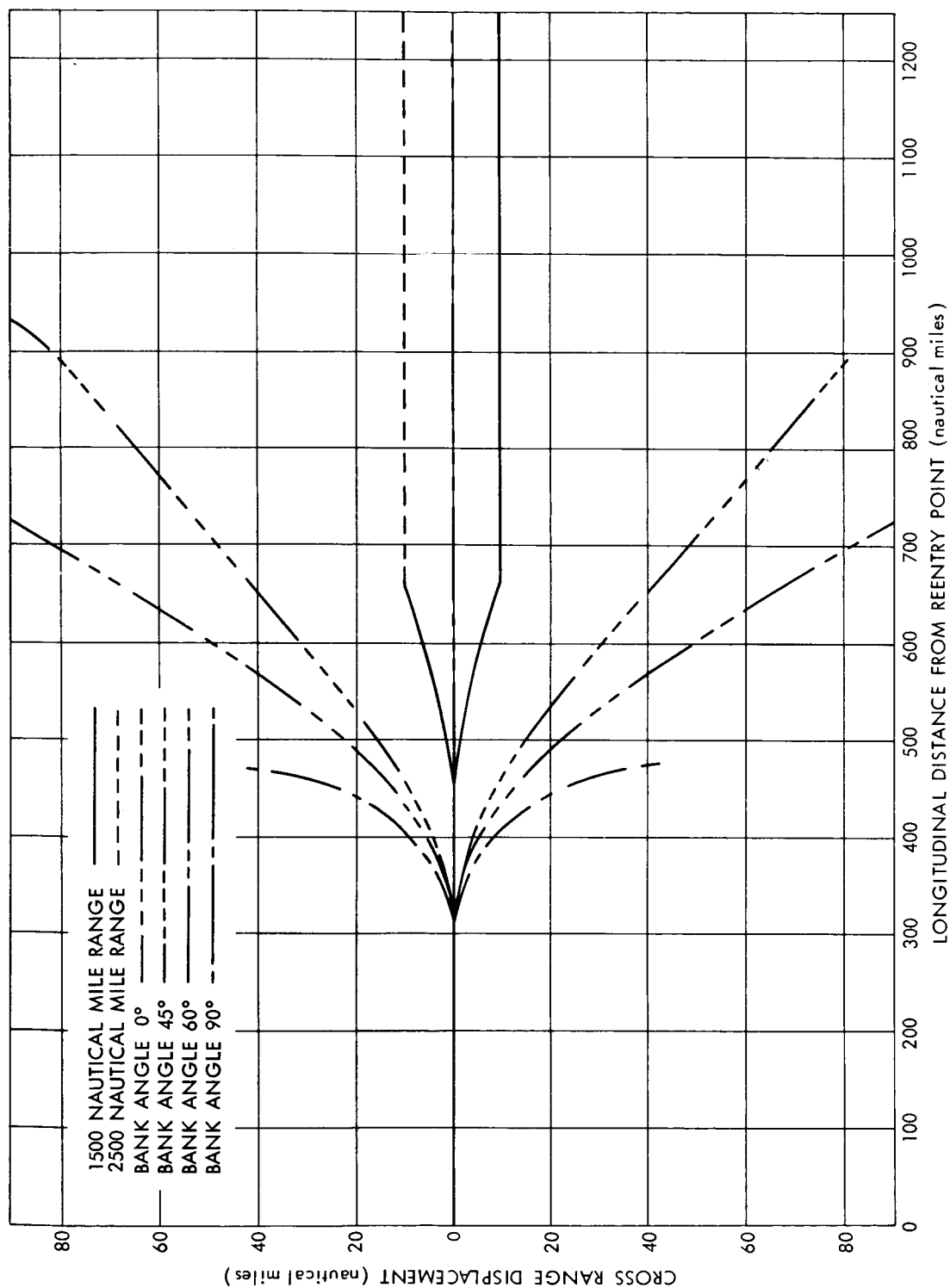
Figure 16. Horizontal Projection of Reentry Trajectories Originating from -7.50 Entrance Angle

59
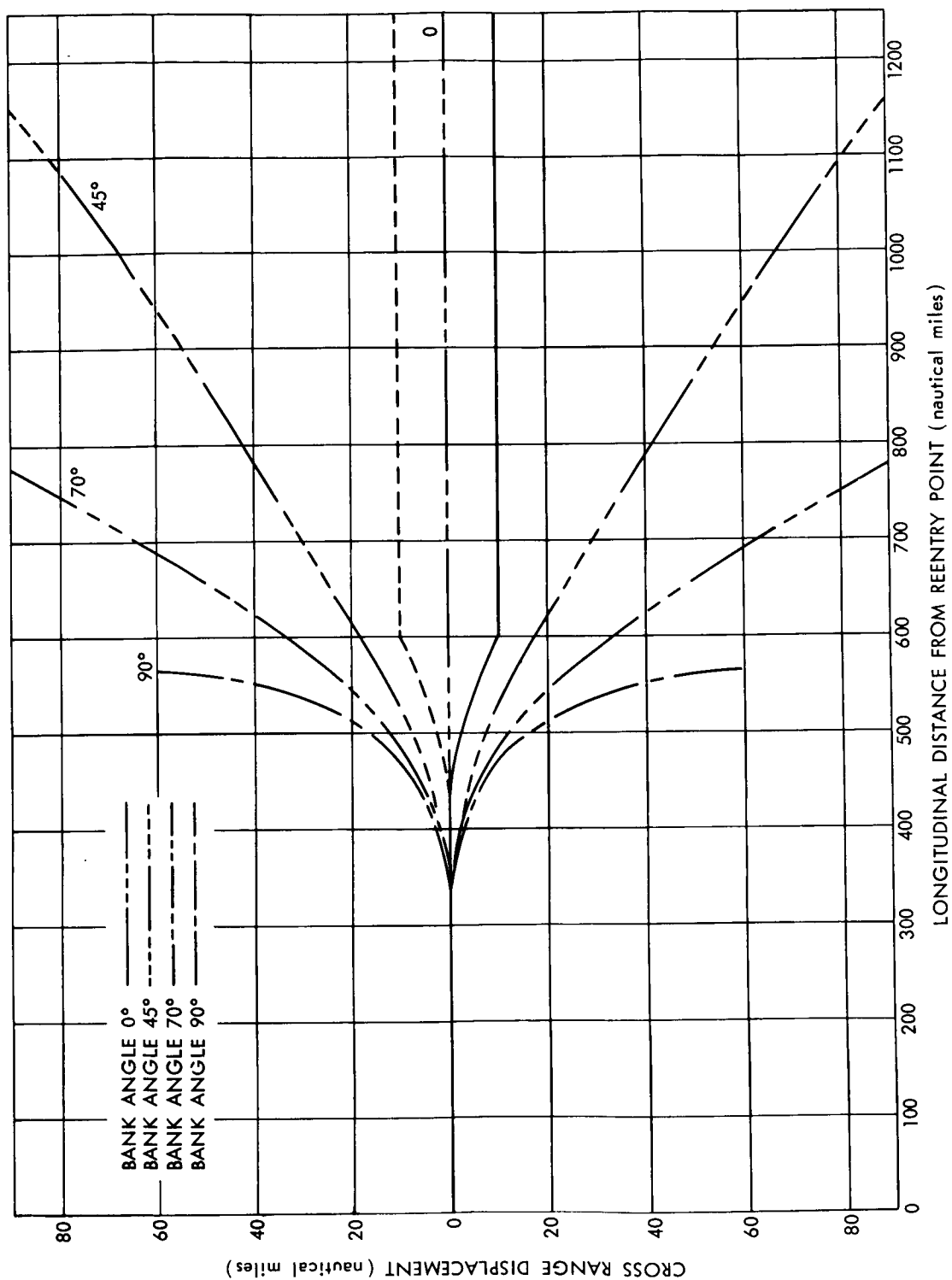
Figure 17. Horizontal Projection of Reentry Trajectories Originating from −6.80° Entrance Angle

60
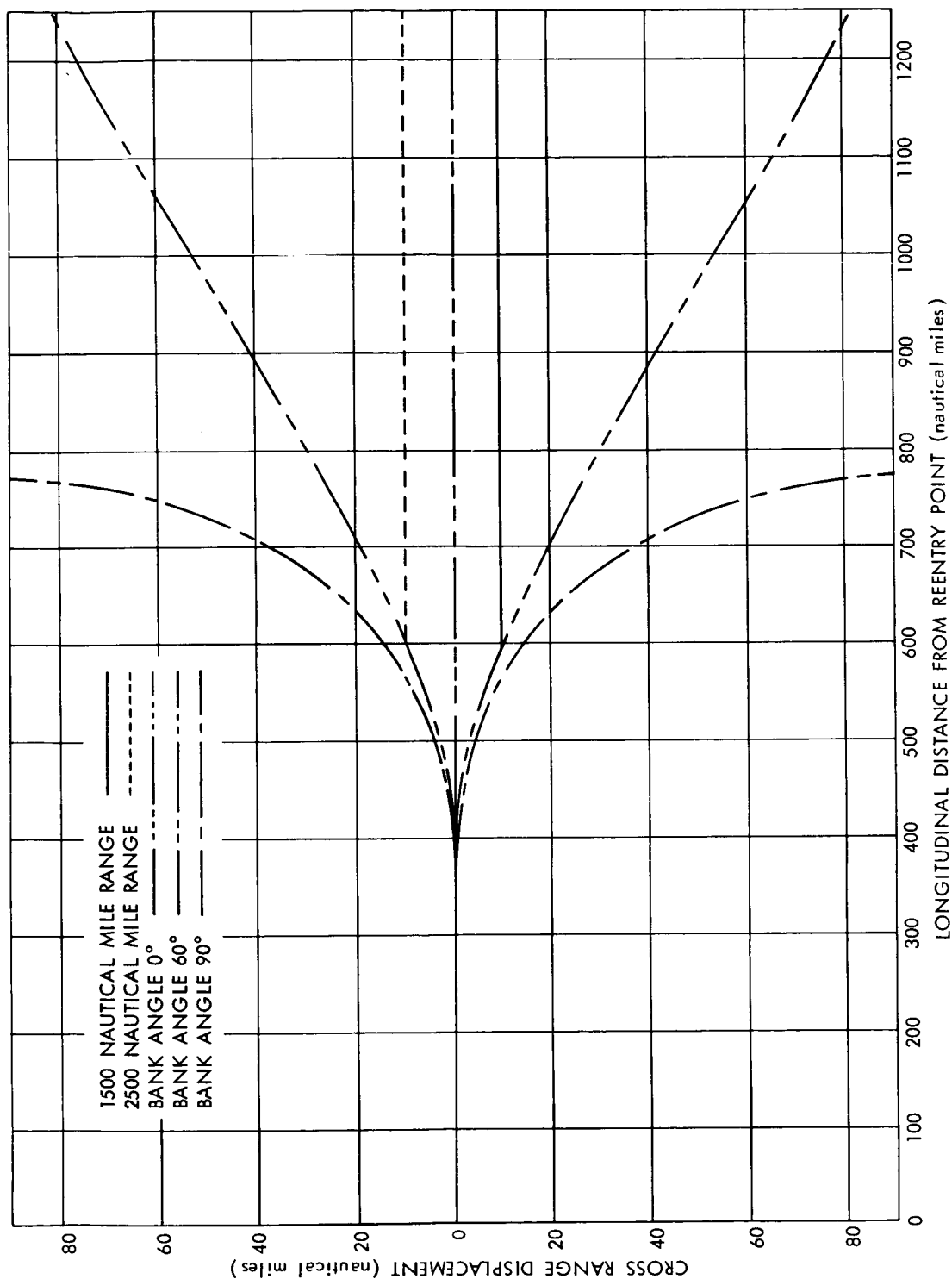
Figure 18. Horizontal Projection of Reentry Trajectories Originating from -6.00° Entrance Angle

61
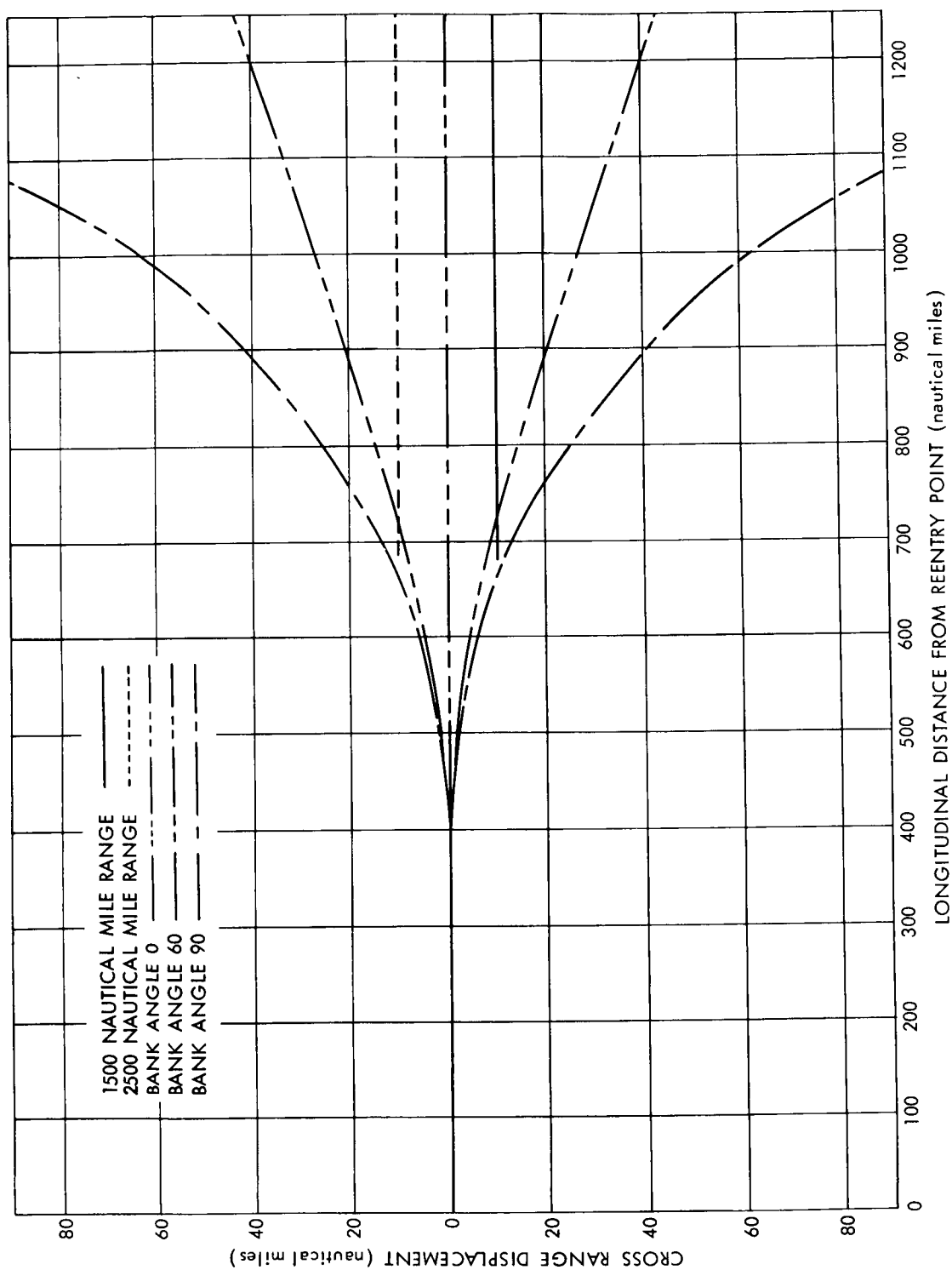
Figure 19. Horizontal Projection of Reentry Trajectories Originating from −5.53° Entrance Angle

62
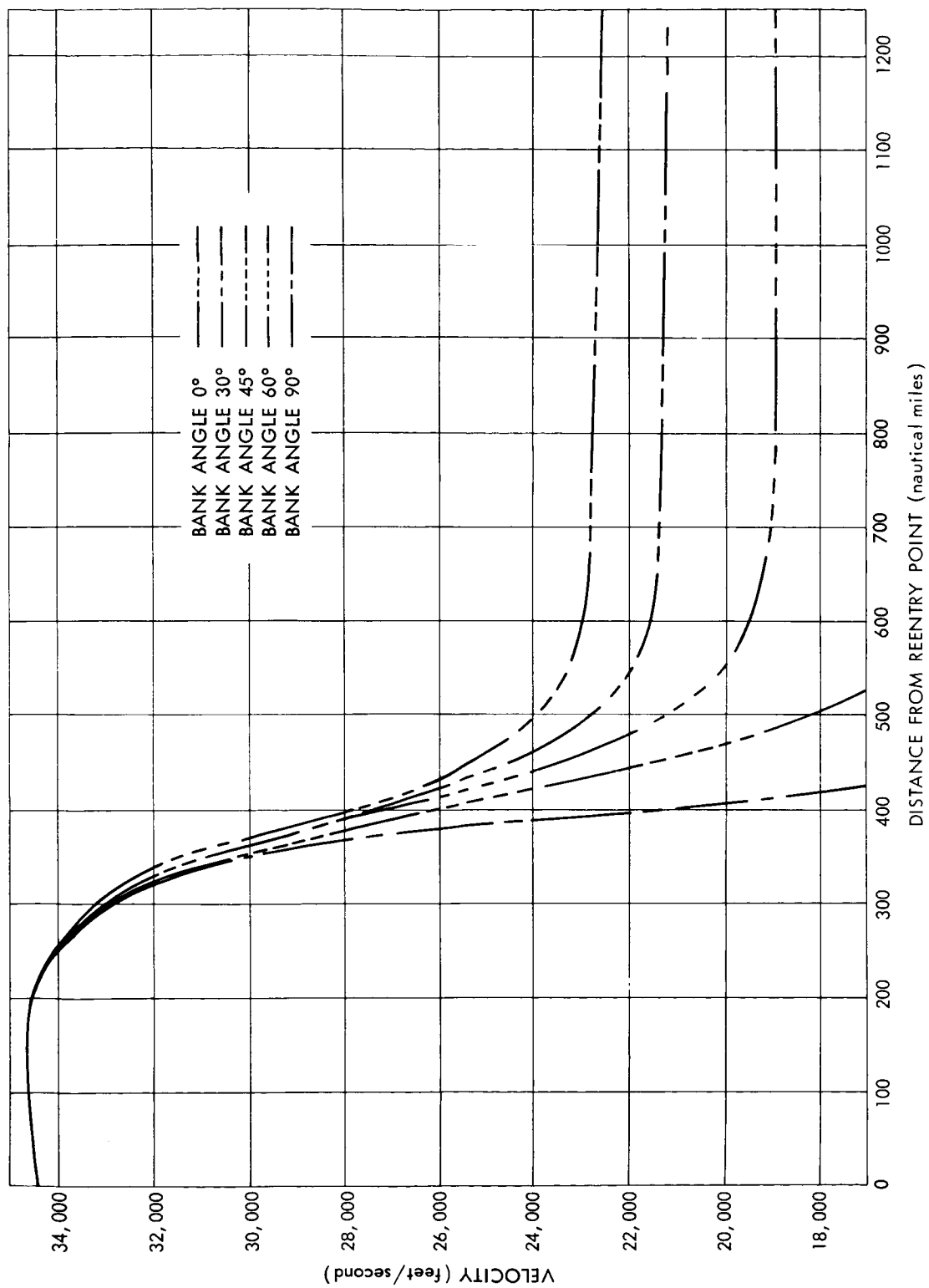
Figure 20. Velocity in Reentry Trajectories Originating from −7.51° Entrance Angle

VELOCITY (feet/second)

DISTANCE FROM REENTRY POINT (nautical miles)

BANK ANGLE 0°
BANK ANGLE 30°
BANK ANGLE 45°
BANK ANGLE 60°
BANK ANGLE 90°

63
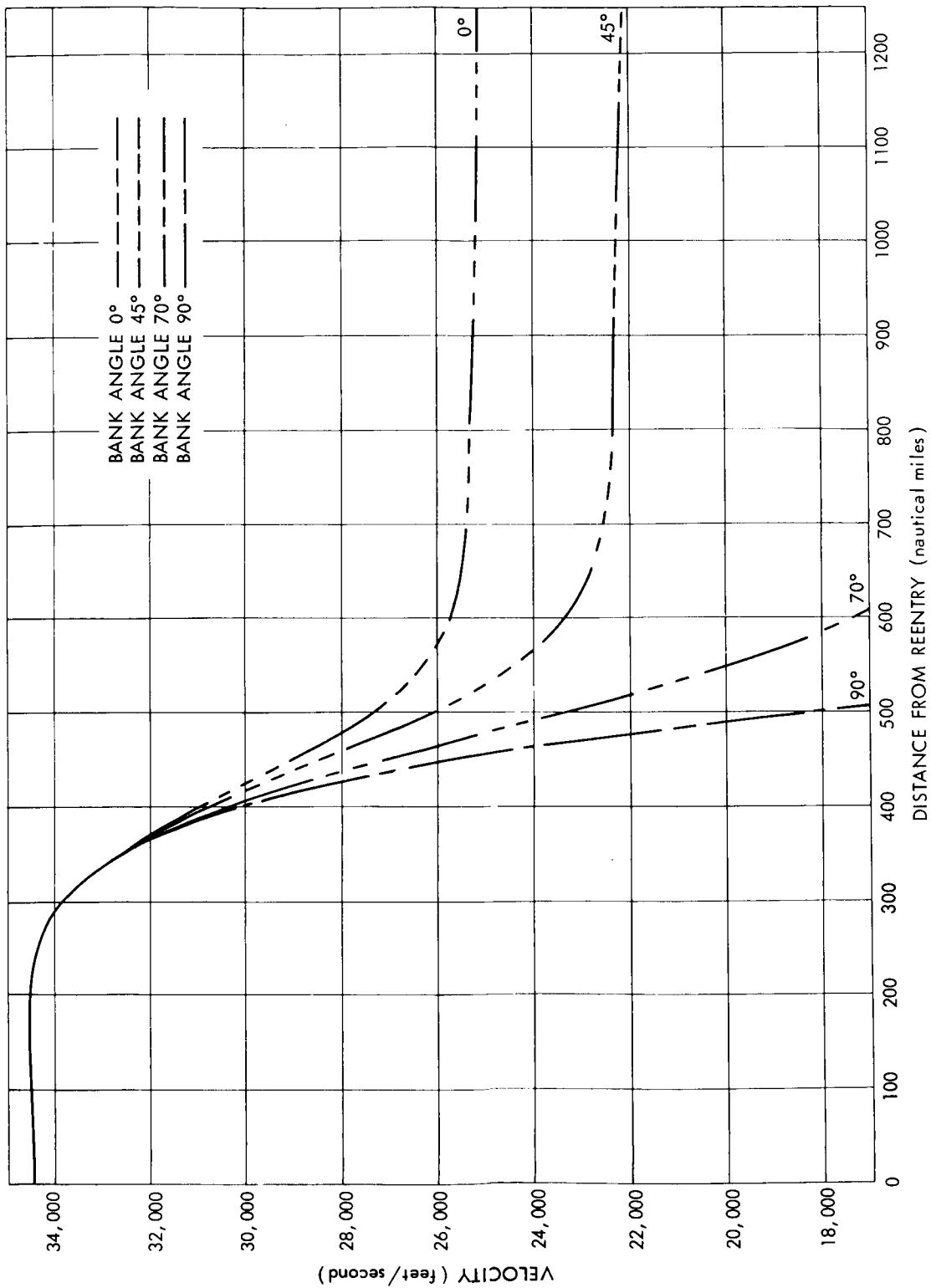
Figure 21. Velocity in Reentry Trajectories Originating from -6.80° Entrance Angle

64
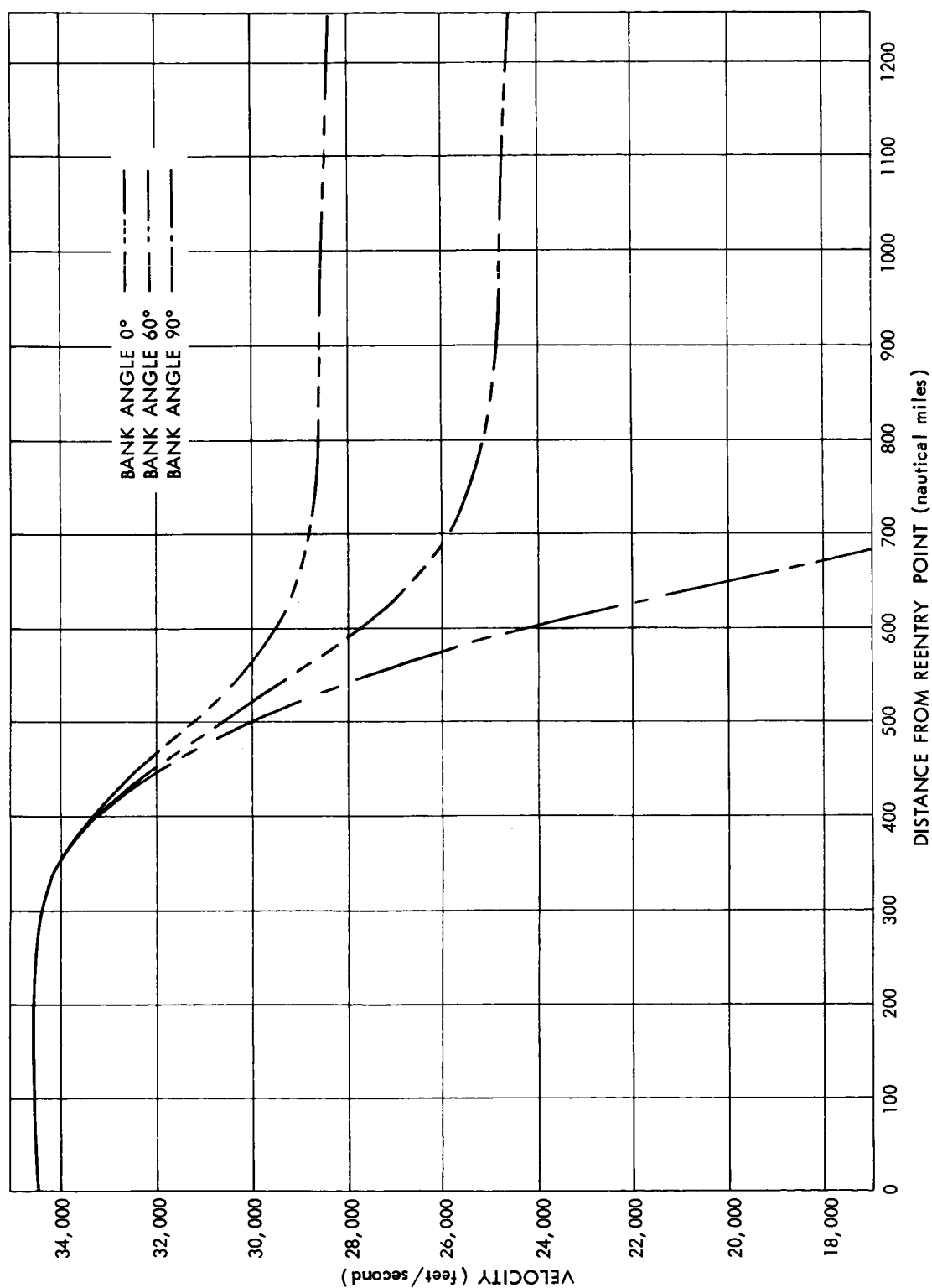
Figure 22. Velocity in Reentry Trajectories Originating from –6.00° Entrance Angle

65
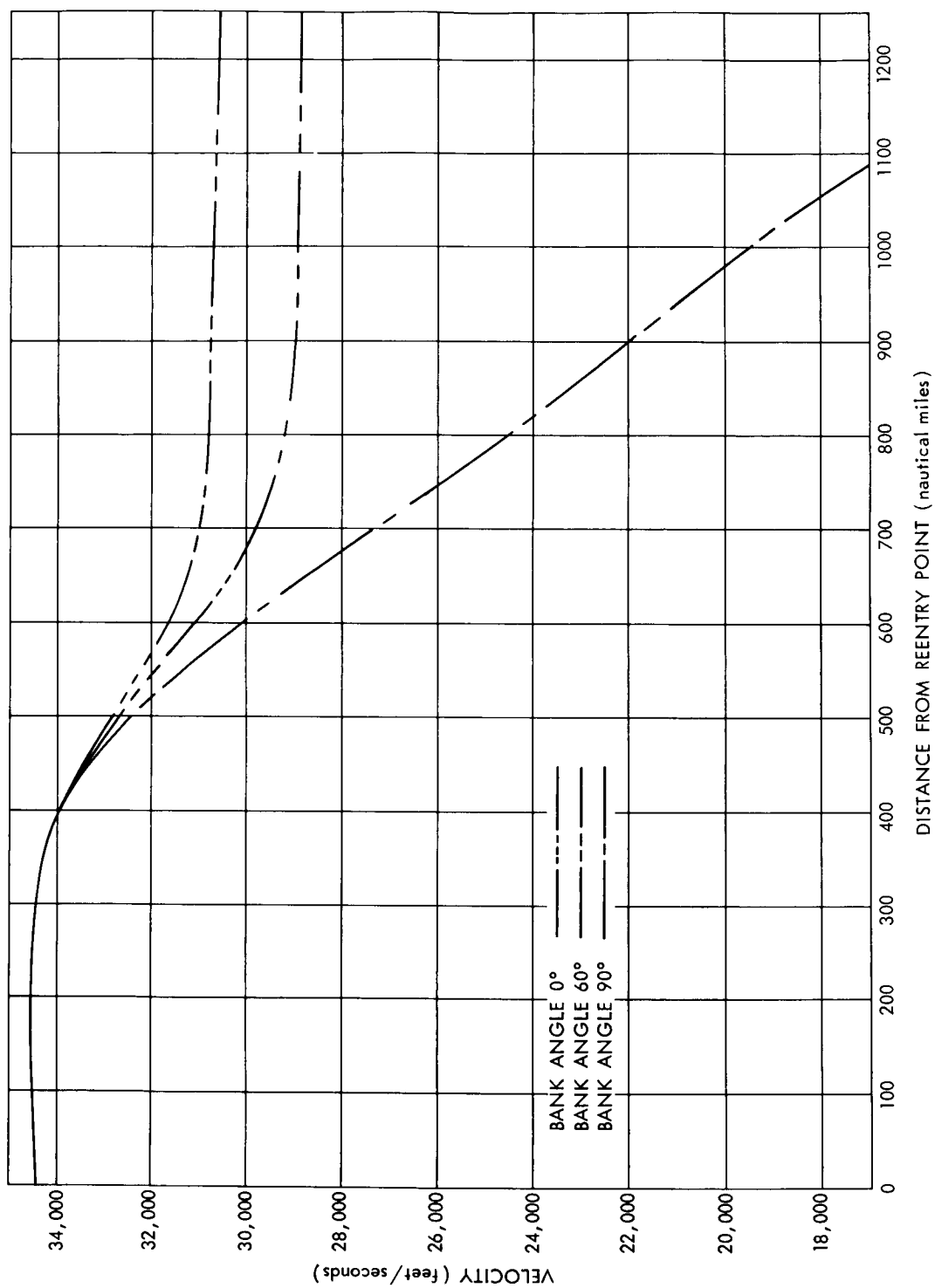
Figure 23. Velocity in Reentry Trajectories Originating from −5.53° Entrance Angle

66
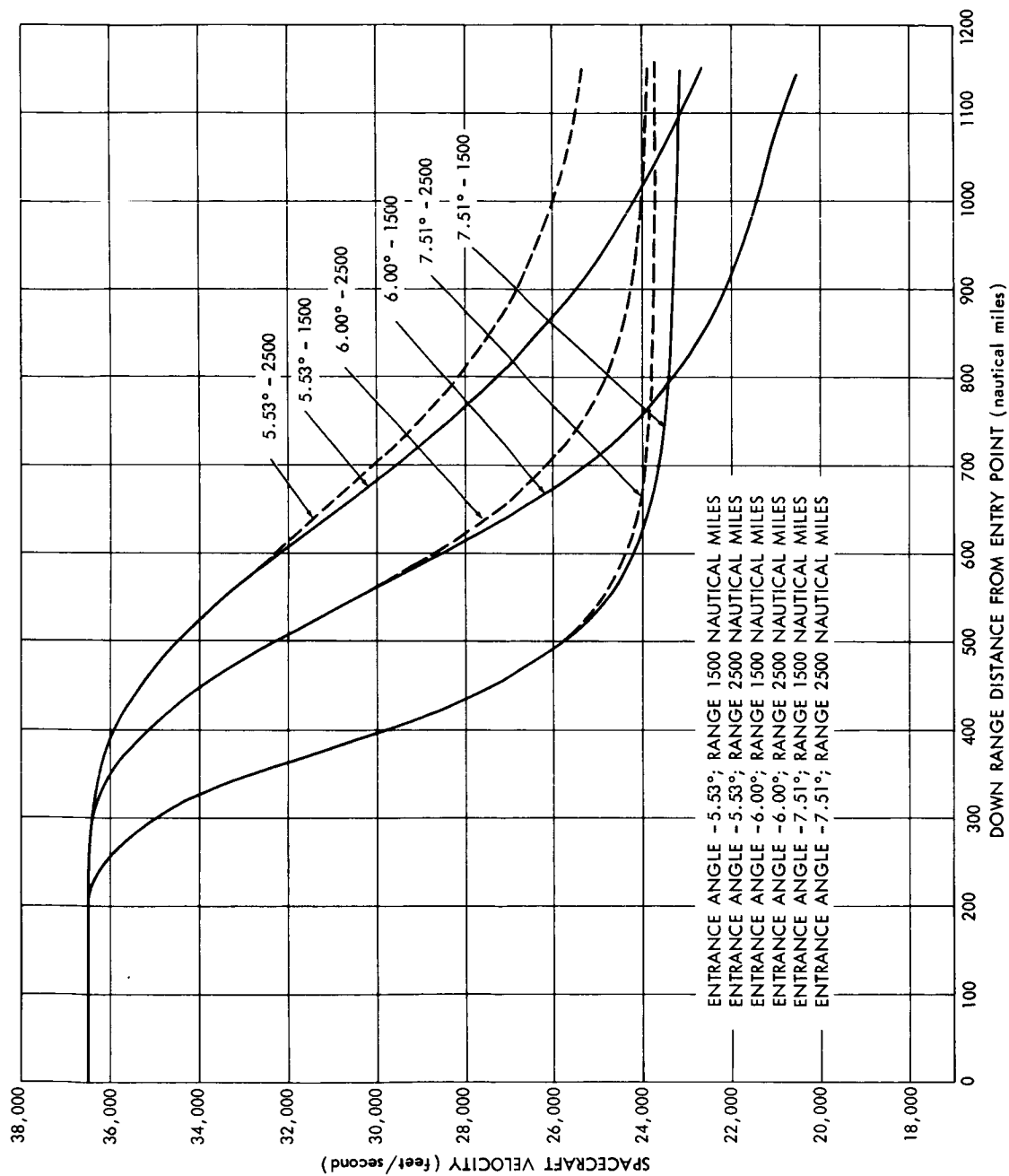
Figure 24. Velocity in Controlled Reentry Trajectories

ENTRANCE ANGLE −5.53°; RANGE 1500 NAUTICAL MILES
ENTRANCE ANGLE −5.53°; RANGE 2500 NAUTICAL MILES
ENTRANCE ANGLE −6.00°; RANGE 1500 NAUTICAL MILES
ENTRANCE ANGLE −6.00°; RANGE 2500 NAUTICAL MILES
ENTRANCE ANGLE −7.51°; RANGE 1500 NAUTICAL MILES
ENTRANCE ANGLE −7.51°; RANGE 2500 NAUTICAL MILES

5.53° − 2500
5.53° − 1500
6.00° − 2500
6.00° − 1500
7.51° − 2500
7.51° − 1500

SPACECRAFT VELOCITY (feet/second)

DOWN RANGE DISTANCE FROM ENTRY POINT (nautical miles)

67

Figure 25. Force Due to Deceleration, Entry Angle = -7.51°, Constant Bank Angle

68
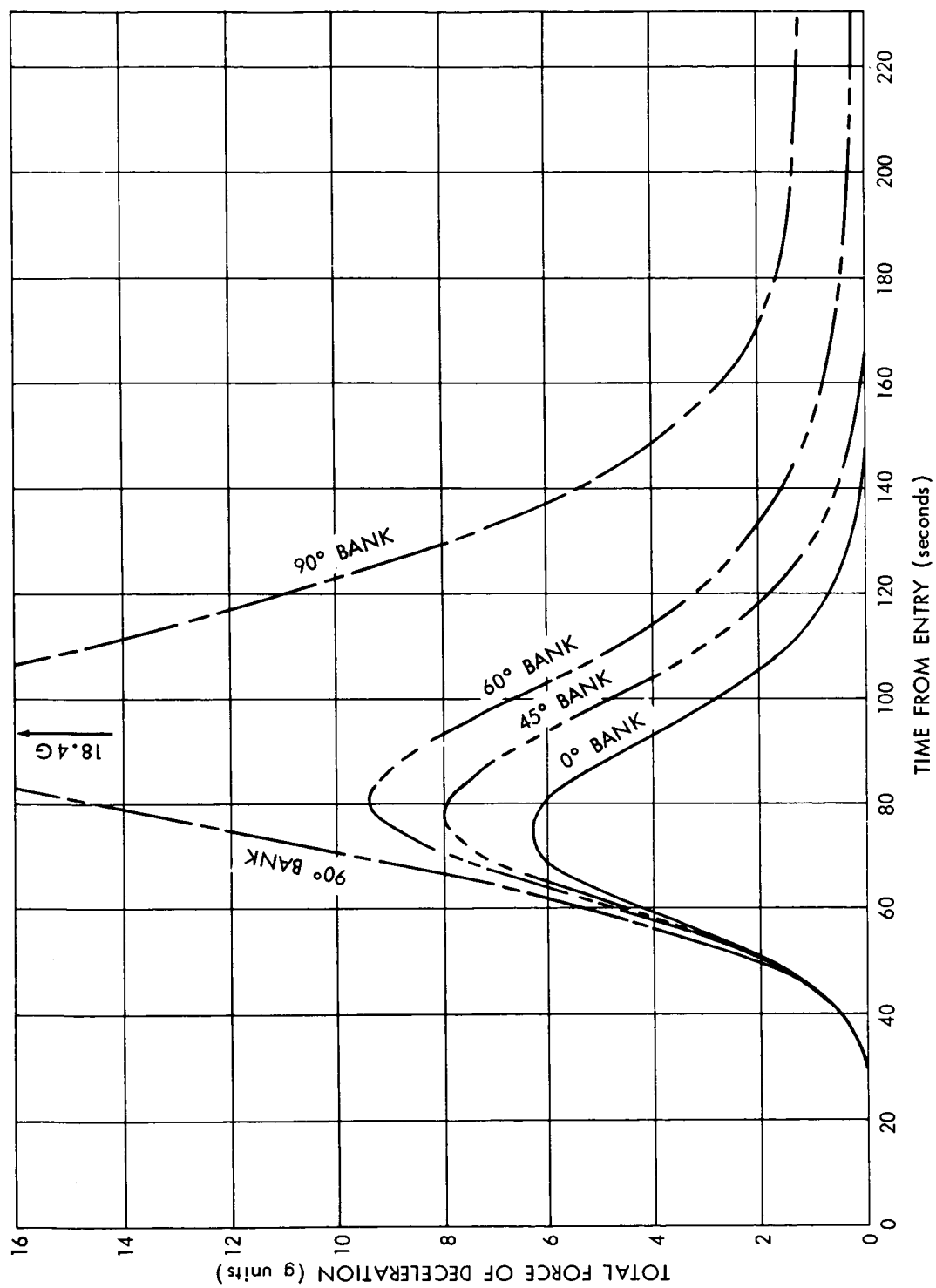
Figure 26. Force Due to Deceleration, Entry Angle = –6.80°, Constant Bank Angle

69
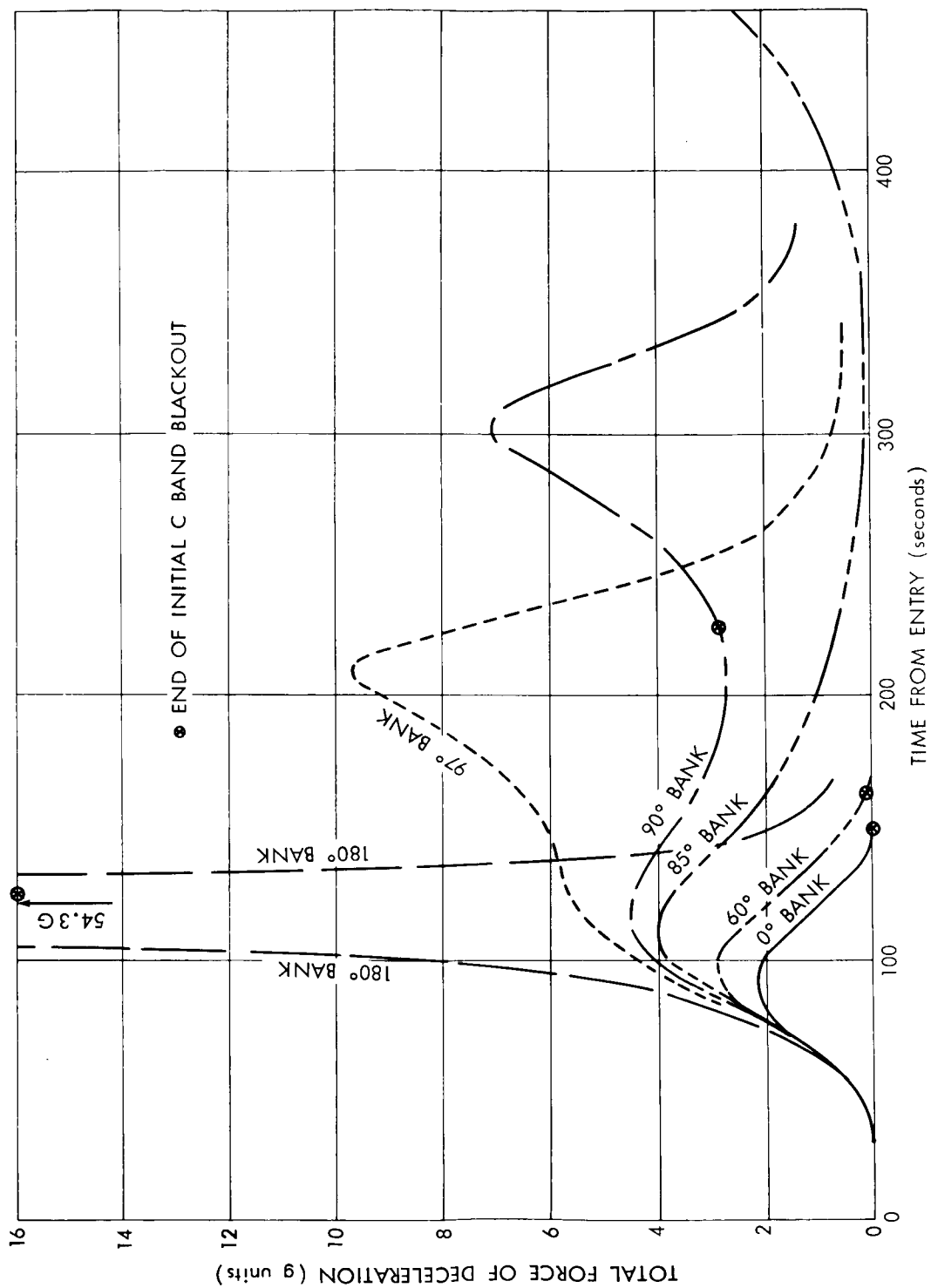
Figure 27. Force to Deceleration, Entry Angle = -5.53°, Constant Bank Angle

70
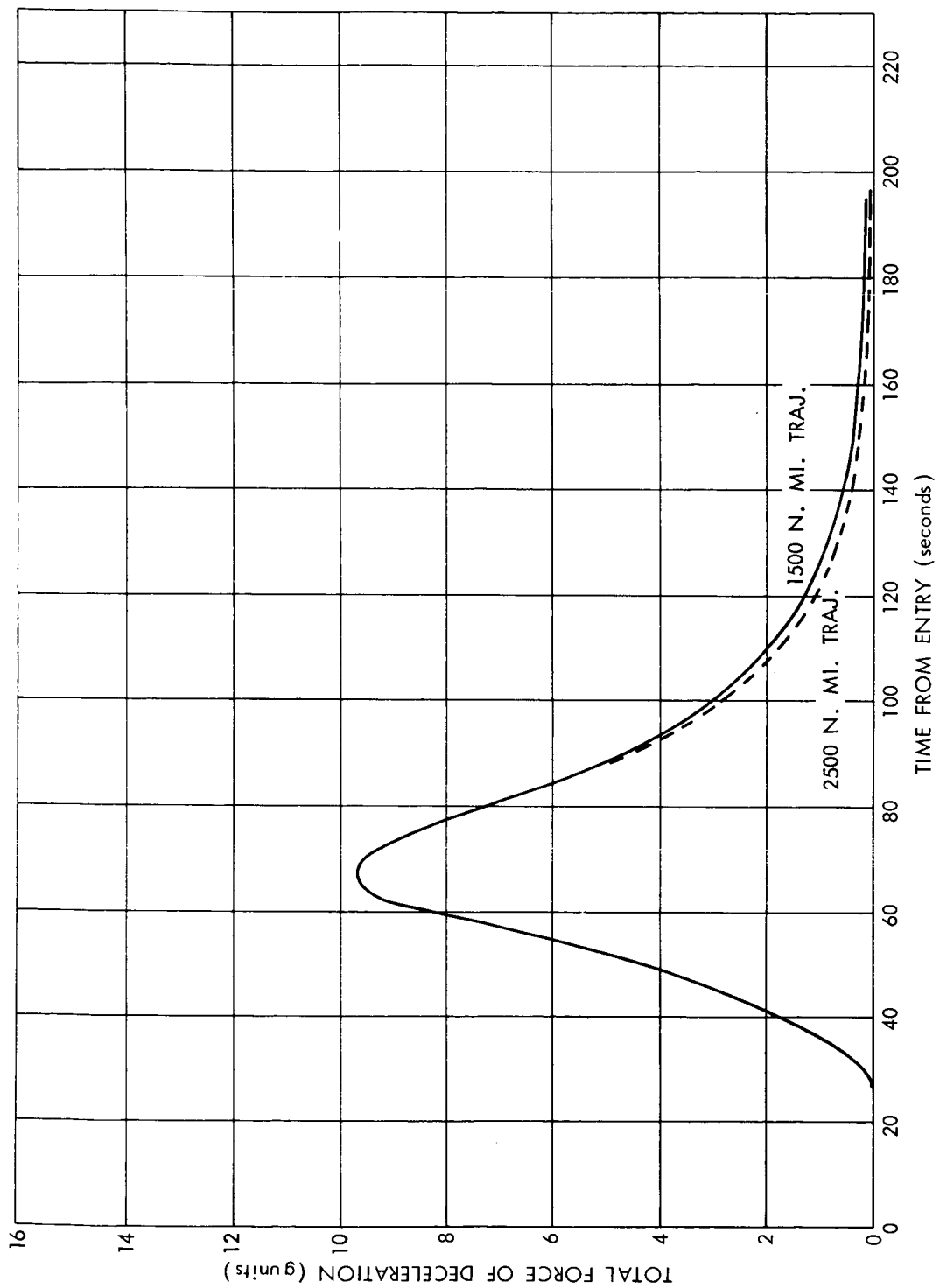
Figure 28. Force Due to Deceleration in Normal Reentry Trajectory

TOTAL FORCE OF DECELERATION (g units)

TIME FROM ENTRY (seconds)

1500 N. MI. TRAJ.

2500 N. MI. TRAJ.

71
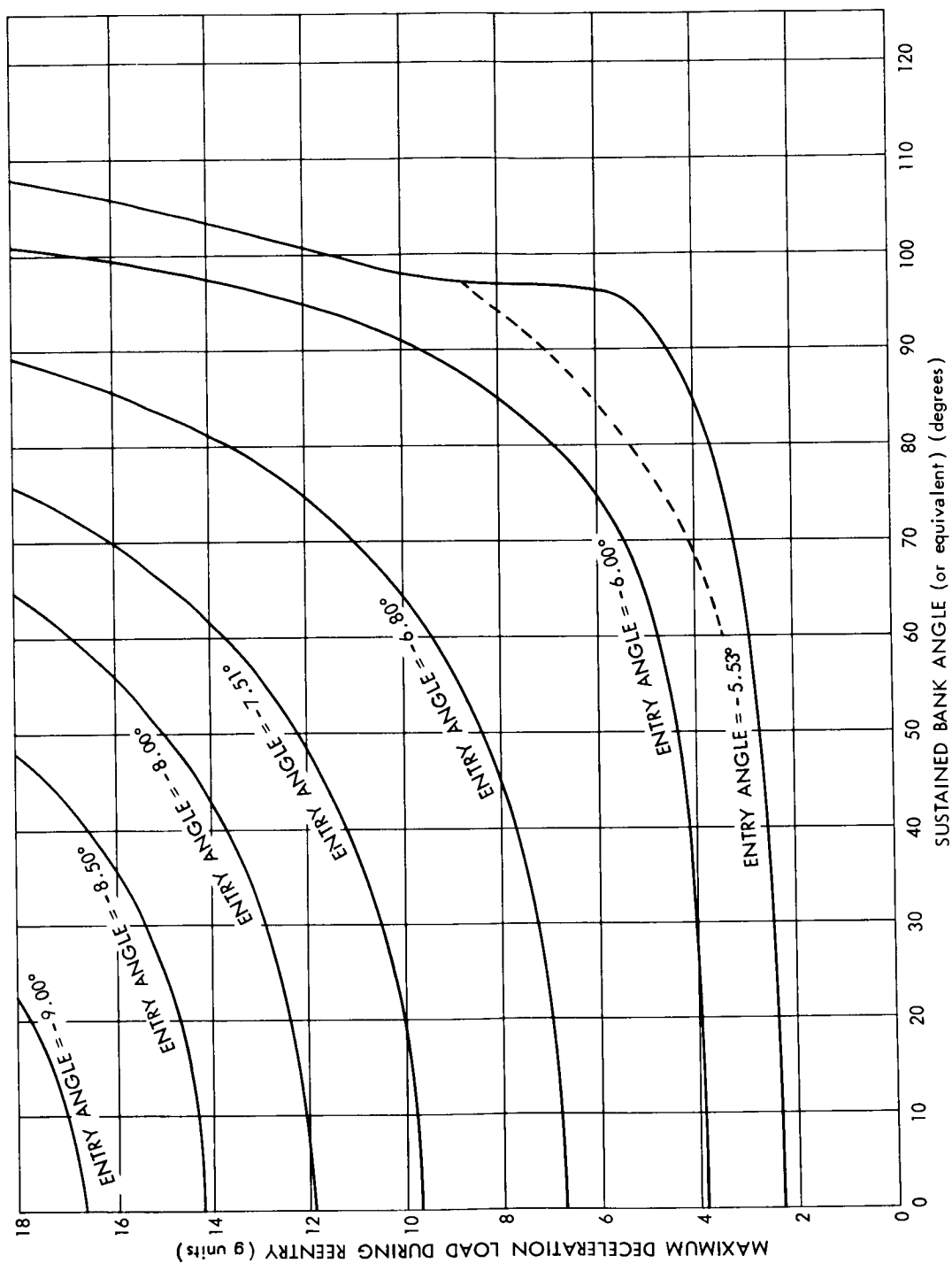
Figure 29. Maximum Deceleration Loading Experienced During Reentry of Apollo Command Module

72
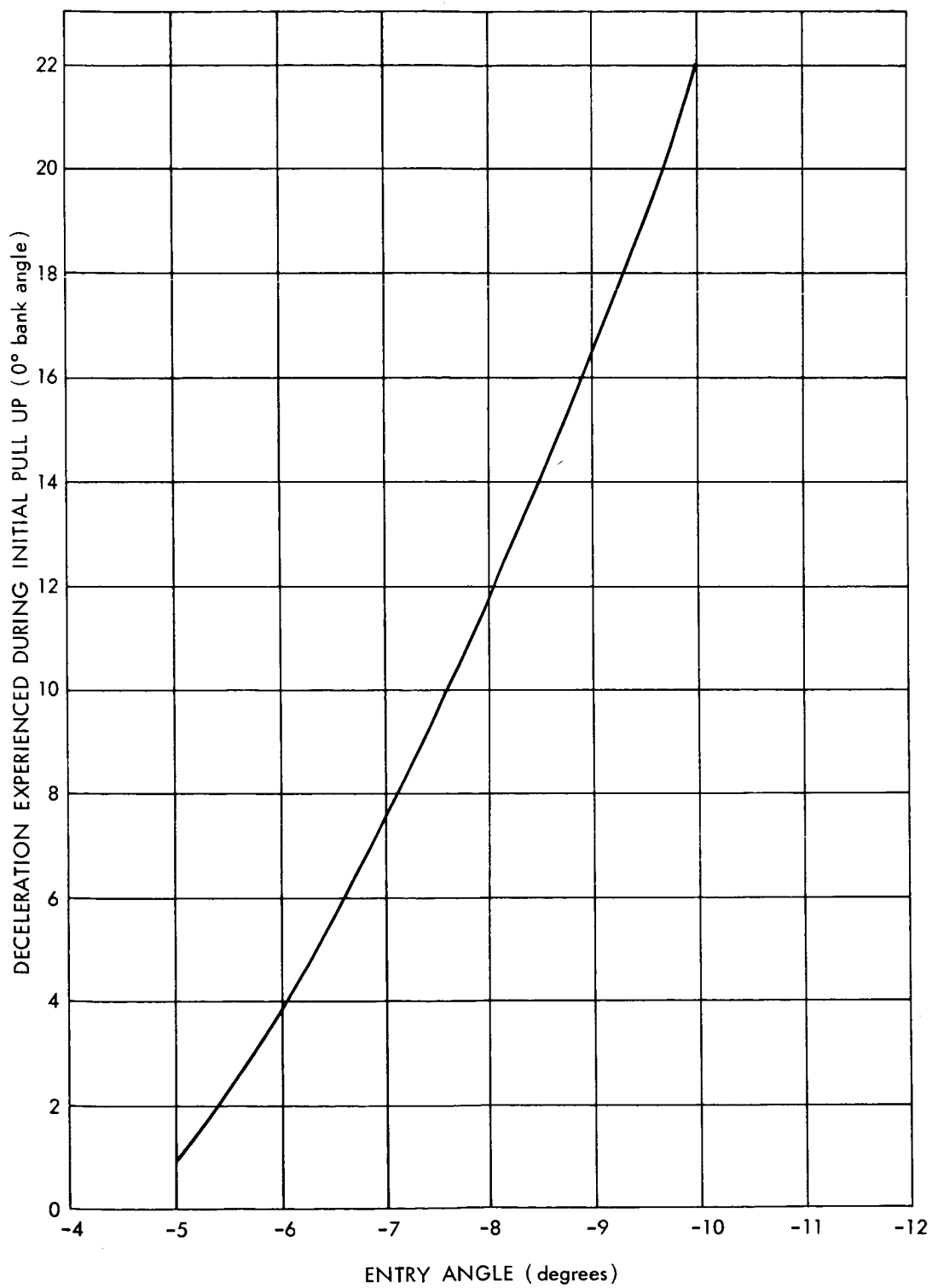
Figure 30. Deceleration Force Due to Initial Pull Up at Zero Bank Angle
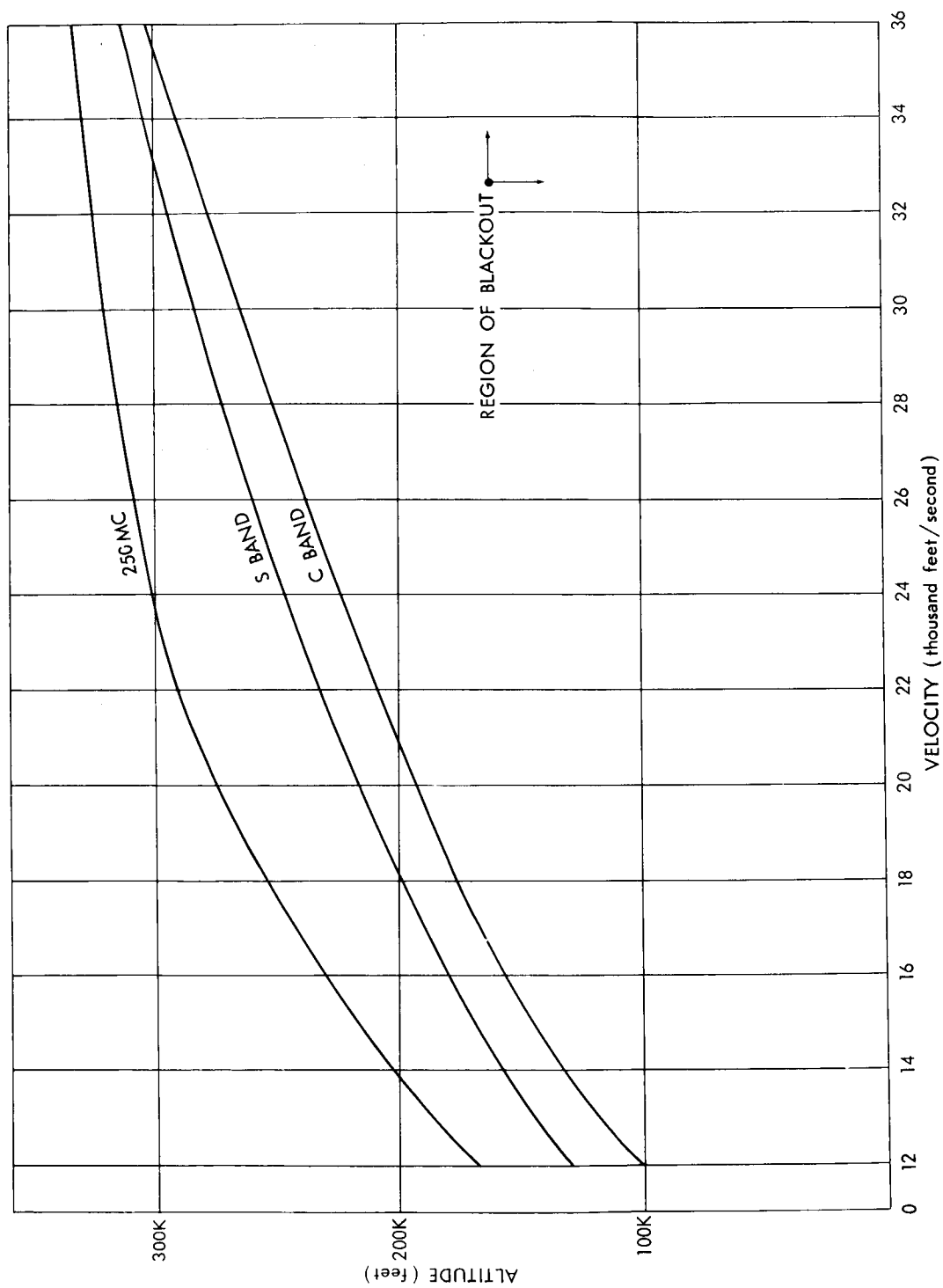
Figure 31. Blackout Region as Function of Altitude and Velocity

74
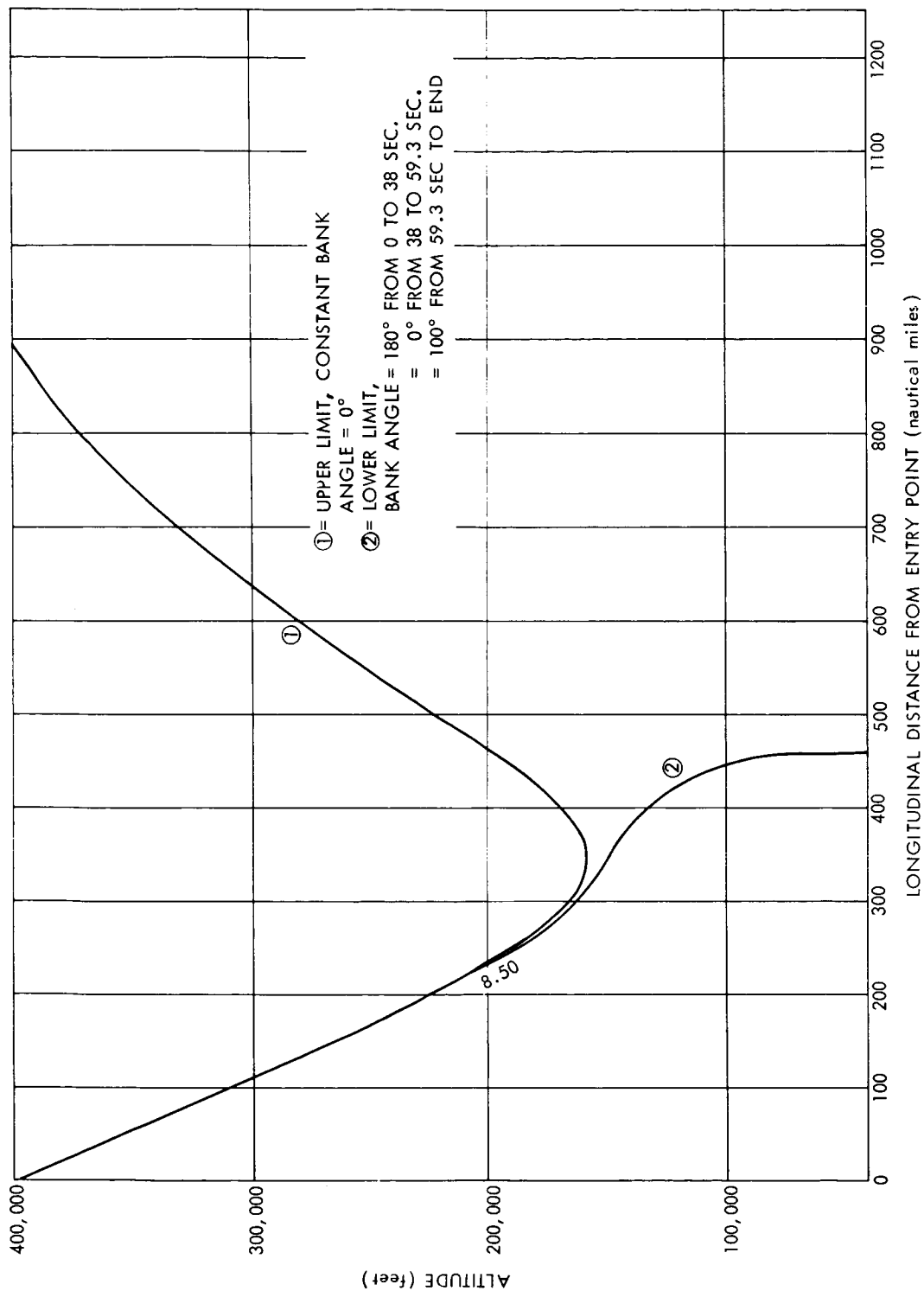
Figure 32. Upper & Lower Limit Trajectories, Entry Angle = -8.50°

①= UPPER LIMIT, CONSTANT BANK
    ANGLE = 0°
②= LOWER LIMIT,
    BANK ANGLE = 180° FROM 0 TO 38 SEC.
               = 0° FROM 38 TO 59.3 SEC.
               = 100° FROM 59.3 SEC TO END

LONGITUDINAL DISTANCE FROM ENTRY POINT (nautical miles)

ALTITUDE (feet)

8.50

75
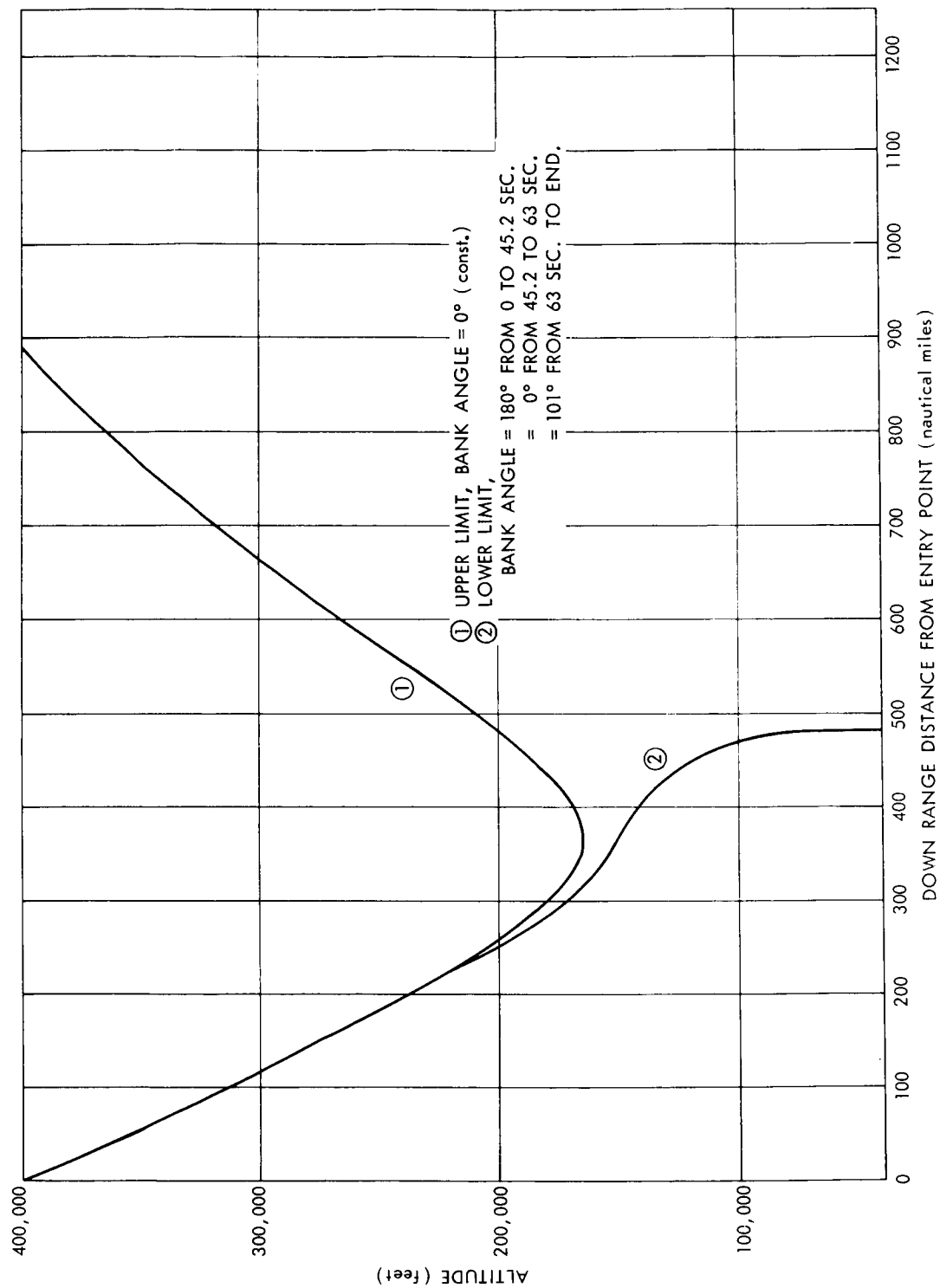
Figure 33. Upper & Lower Limit Trajectories, Entry Angle = -8.00°

① UPPER LIMIT, BANK ANGLE = 0° (const.)
② LOWER LIMIT,
   BANK ANGLE = 180° FROM 0 TO 45.2 SEC.
              = 0° FROM 45.2 TO 63 SEC.
              = 101° FROM 63 SEC. TO END.

DOWN RANGE DISTANCE FROM ENTRY POINT (nautical miles)

ALTITUDE (feet)

76
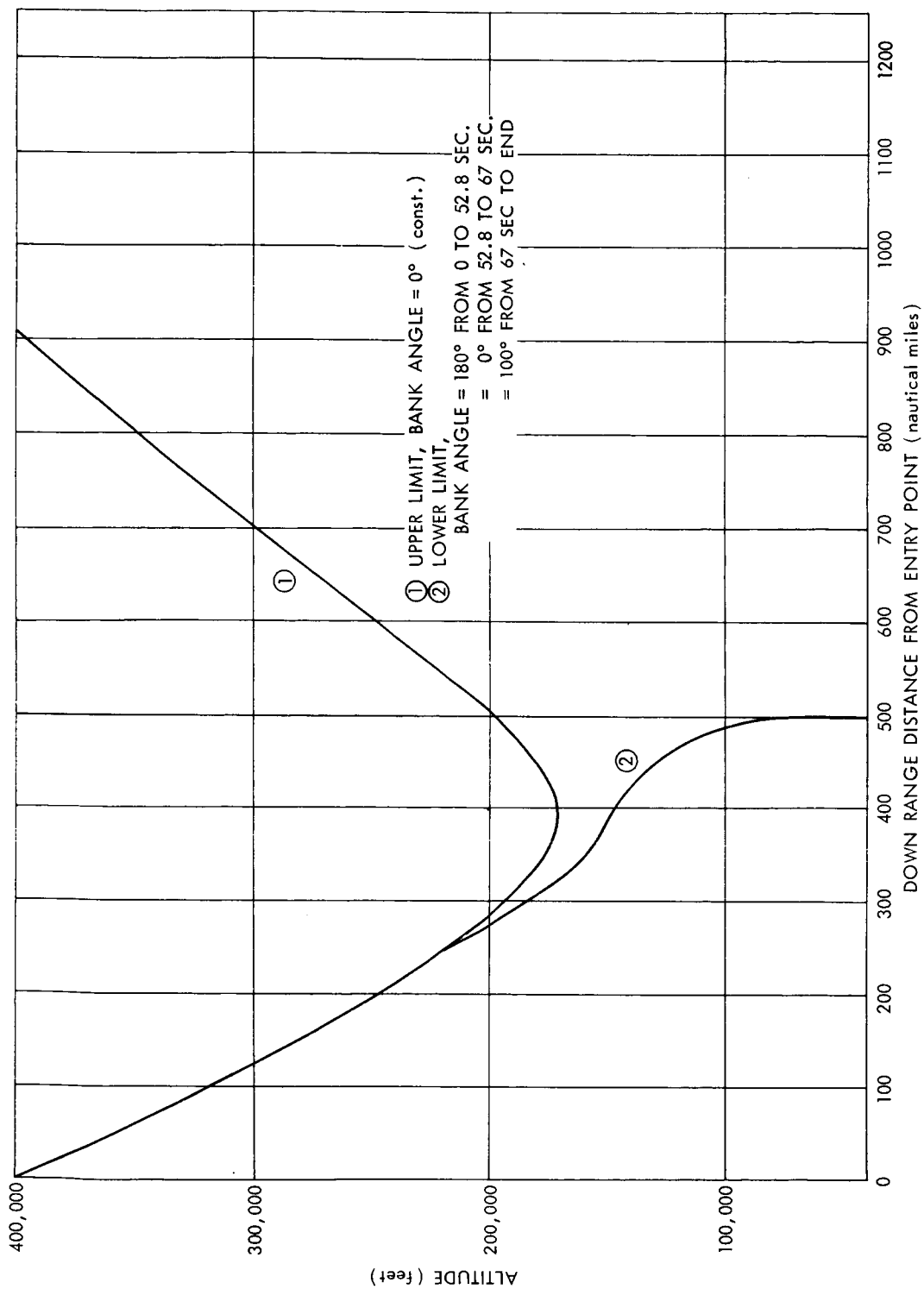
Figure 34. Upper & Lower Limit Trajectories, Entry Angle = -7.51°

77
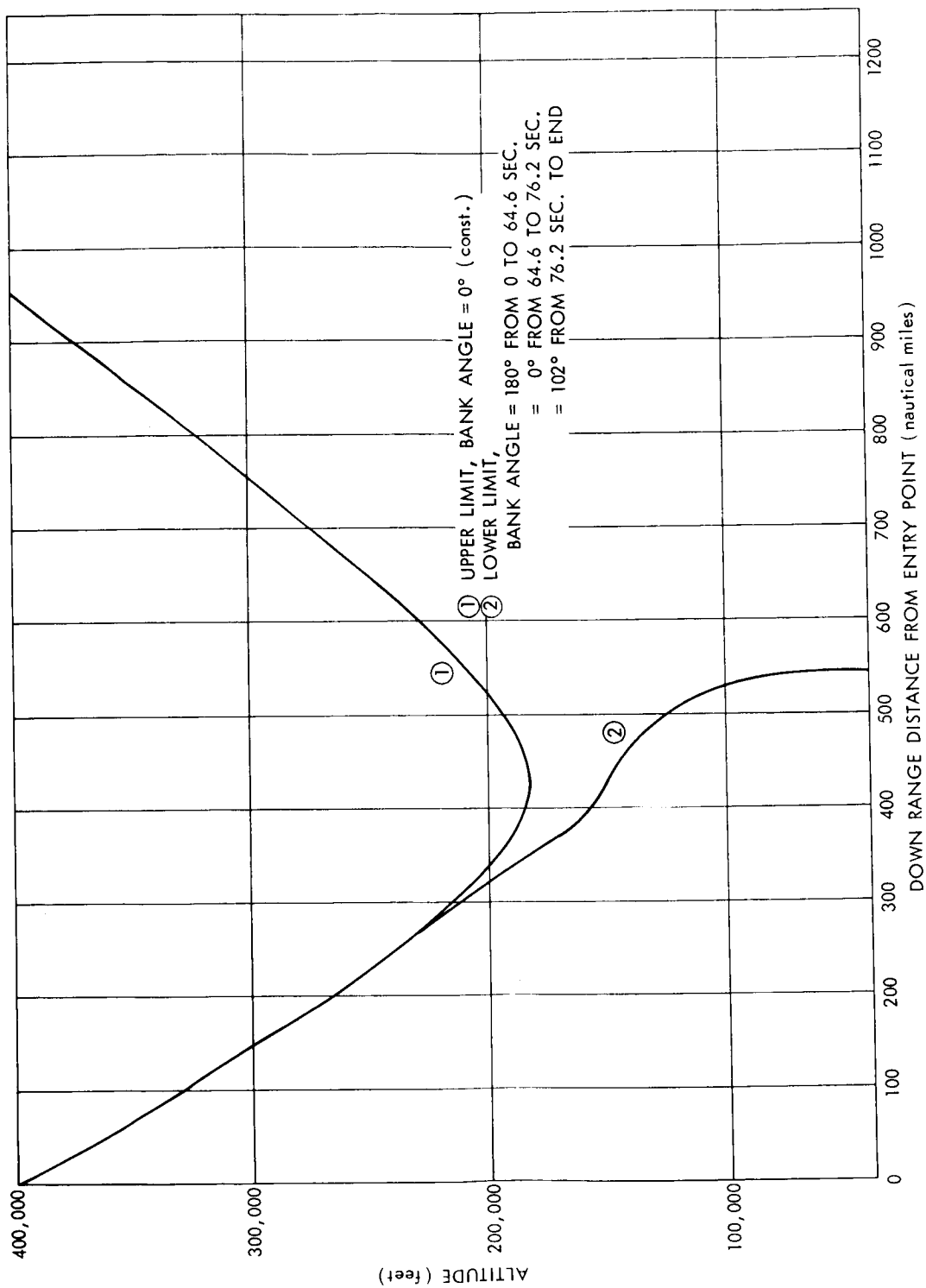
Figure 35. Upper & Lower Limit Trajectories, Entry Angle = -6.80°

① UPPER LIMIT, BANK ANGLE = 0° (const.)
② LOWER LIMIT,
   BANK ANGLE = 180° FROM 0 TO 64.6 SEC.
           = 0° FROM 64.6 TO 76.2 SEC.
           = 102° FROM 76.2 SEC. TO END

DOWN RANGE DISTANCE FROM ENTRY POINT (nautical miles)

ALTITUDE (feet)

78

Figure 36. Upper and Lower Limit Trajectories, Entry Angle = -6.00°

① UPPER LIMIT, BANK ANGLE = 0° (const.)
② LOWER LIMIT,
   BANK ANGLE = 180° FROM 0 TO 84.2 SEC.
             = 0° FROM 84.2 TO 93 SEC.
             = 100° FROM 93 SEC. TO END

DOWN RANGE DISTANCE FROM ENTRY POINT (nautical miles)

ALTITUDE (feet)

Figure 37. Upper and Lower Limit Trajectories, Entry Angle = −5.53°

80

Figure 38. Upper and Lower Limit Trajectories, Entry Angle = -5.00°

81
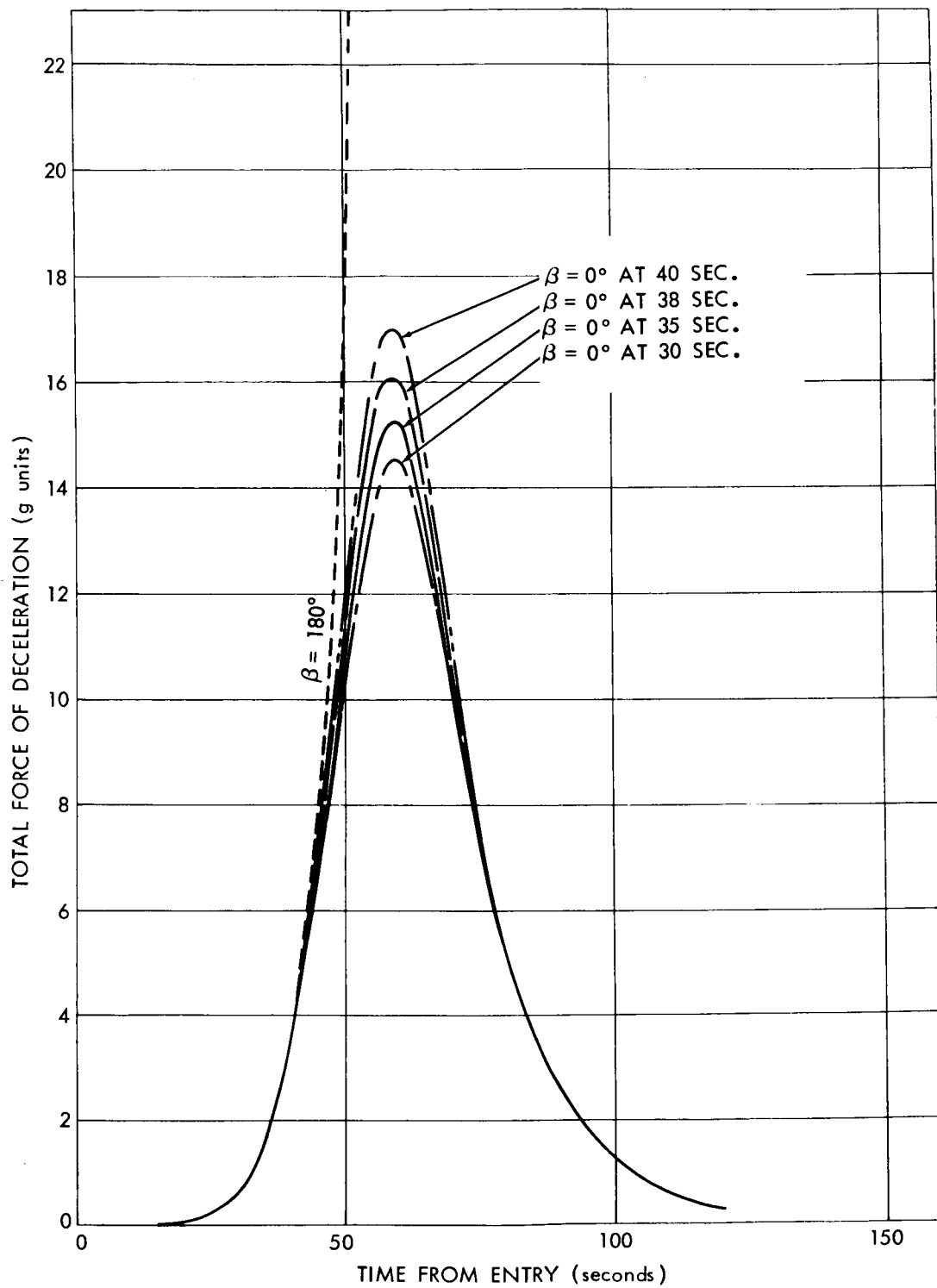
Figure 39. Change in Deceleration Effected by Rotation of
Bank Angle from 180° at Entry to 0° at T Seconds
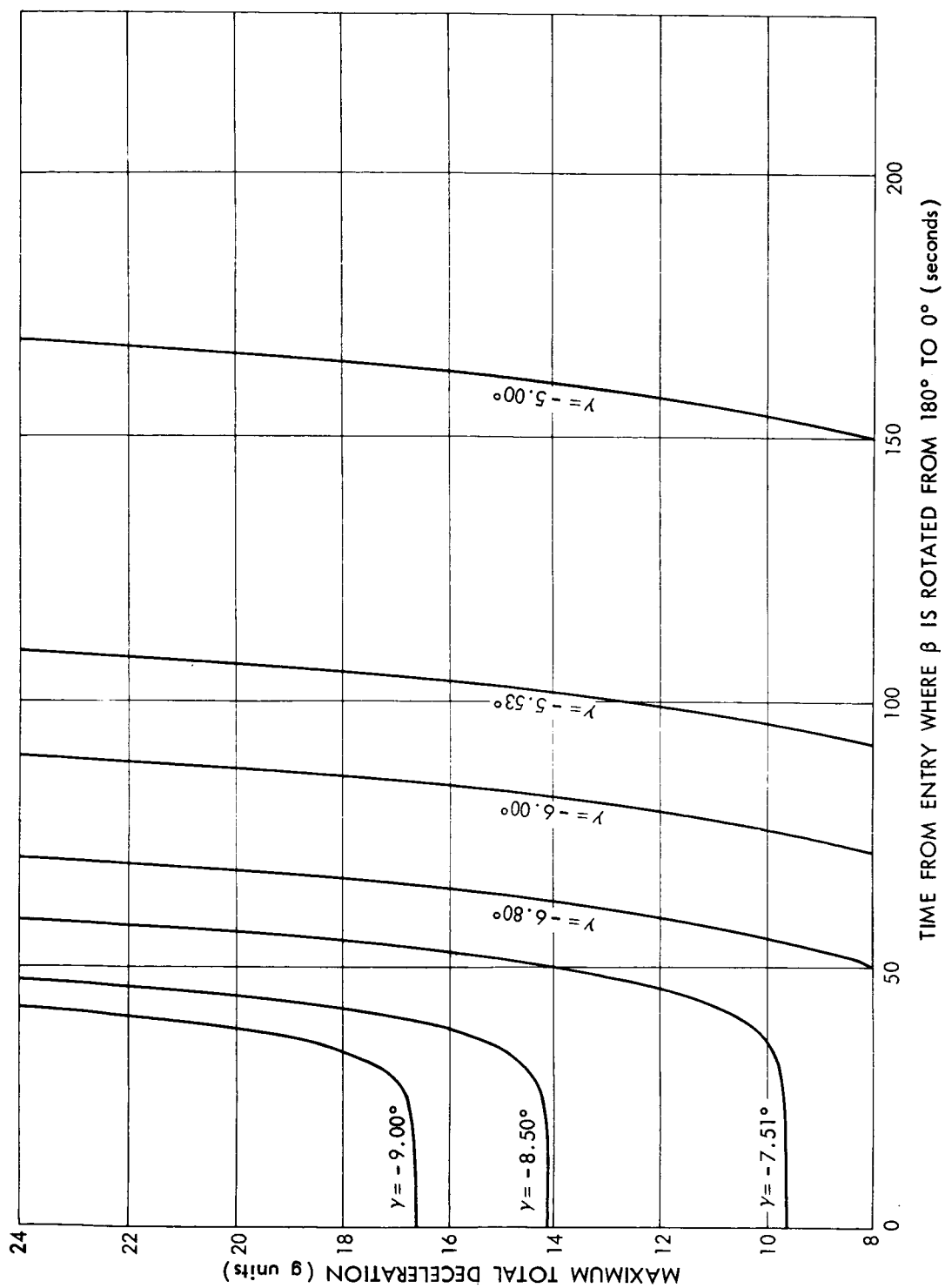
Figure 40. Peak Deceleration Force as Function of Time of Rotation of Bank Angle

83
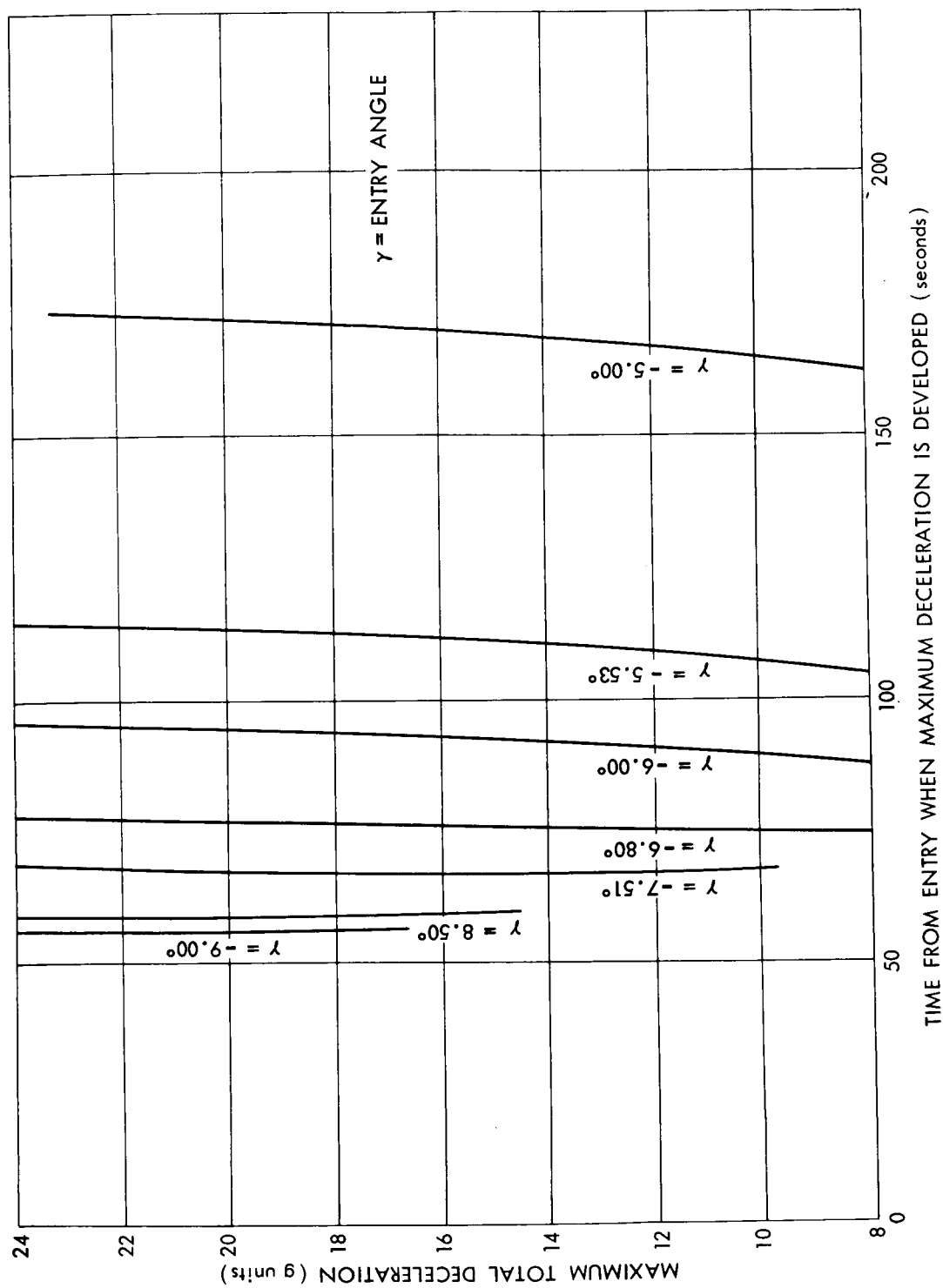
Figure 41. Time After Entry When Peak Force of Figure 40 is Attained

84
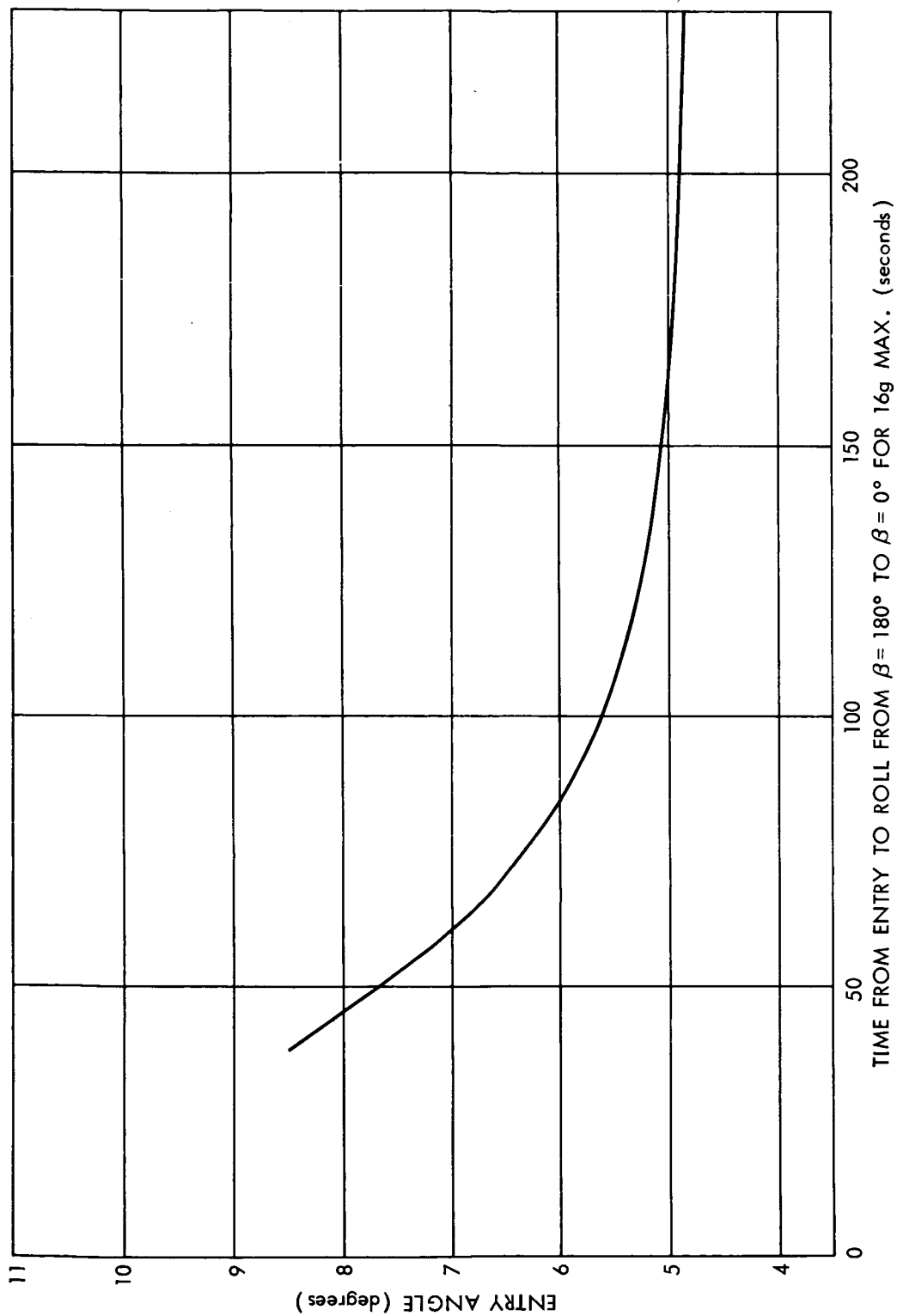
Figure 42. Time from Entry at Which Bank Angle Must Be Rotated from
180° to 0° to Attain Maximum Deceleration of 16g

85
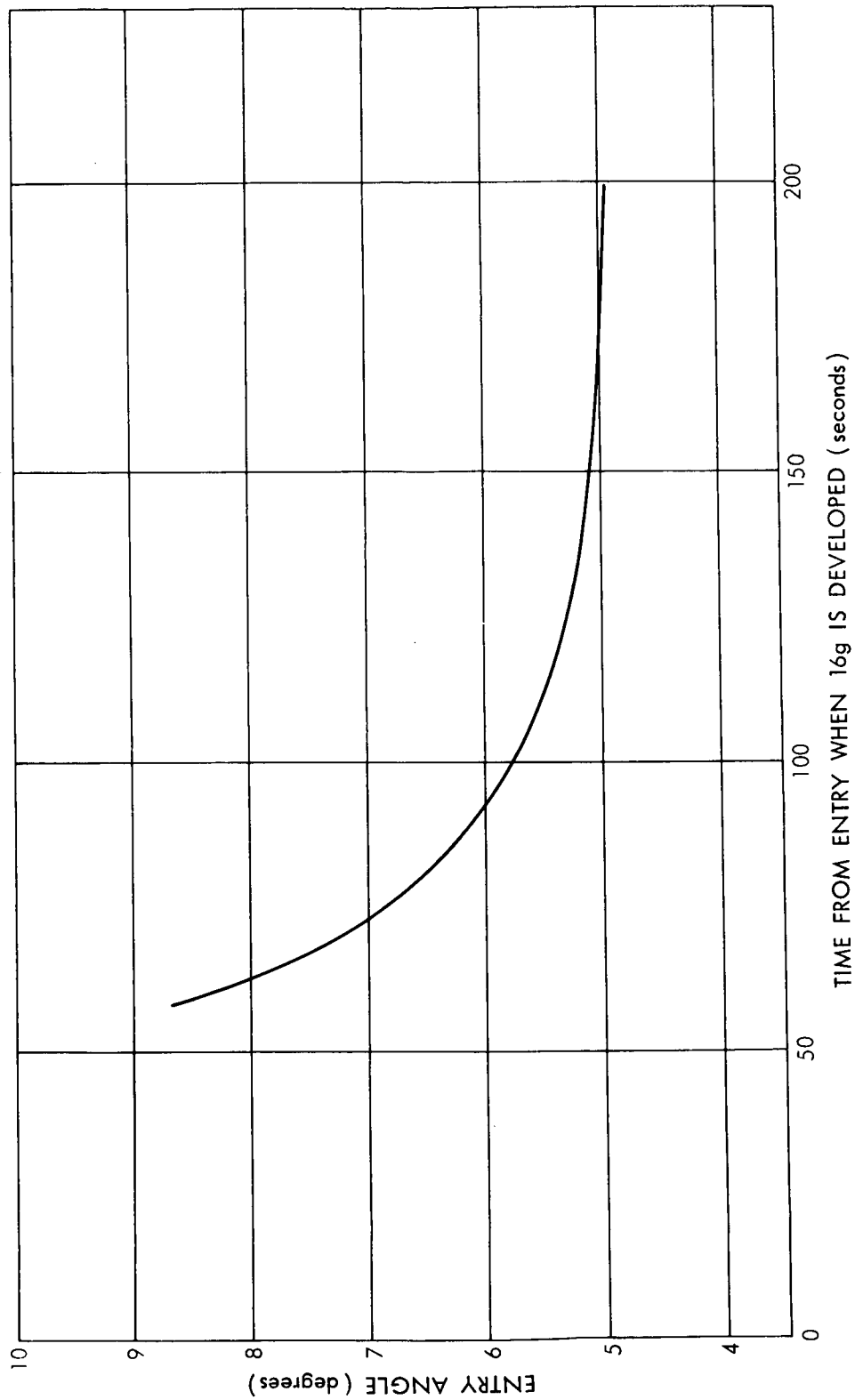
Figure 43. Time From Entry When 16g Deceleration id Developed by Entry at Bank Angle of 180° and Rotation to 0° As Specified in Figure 42
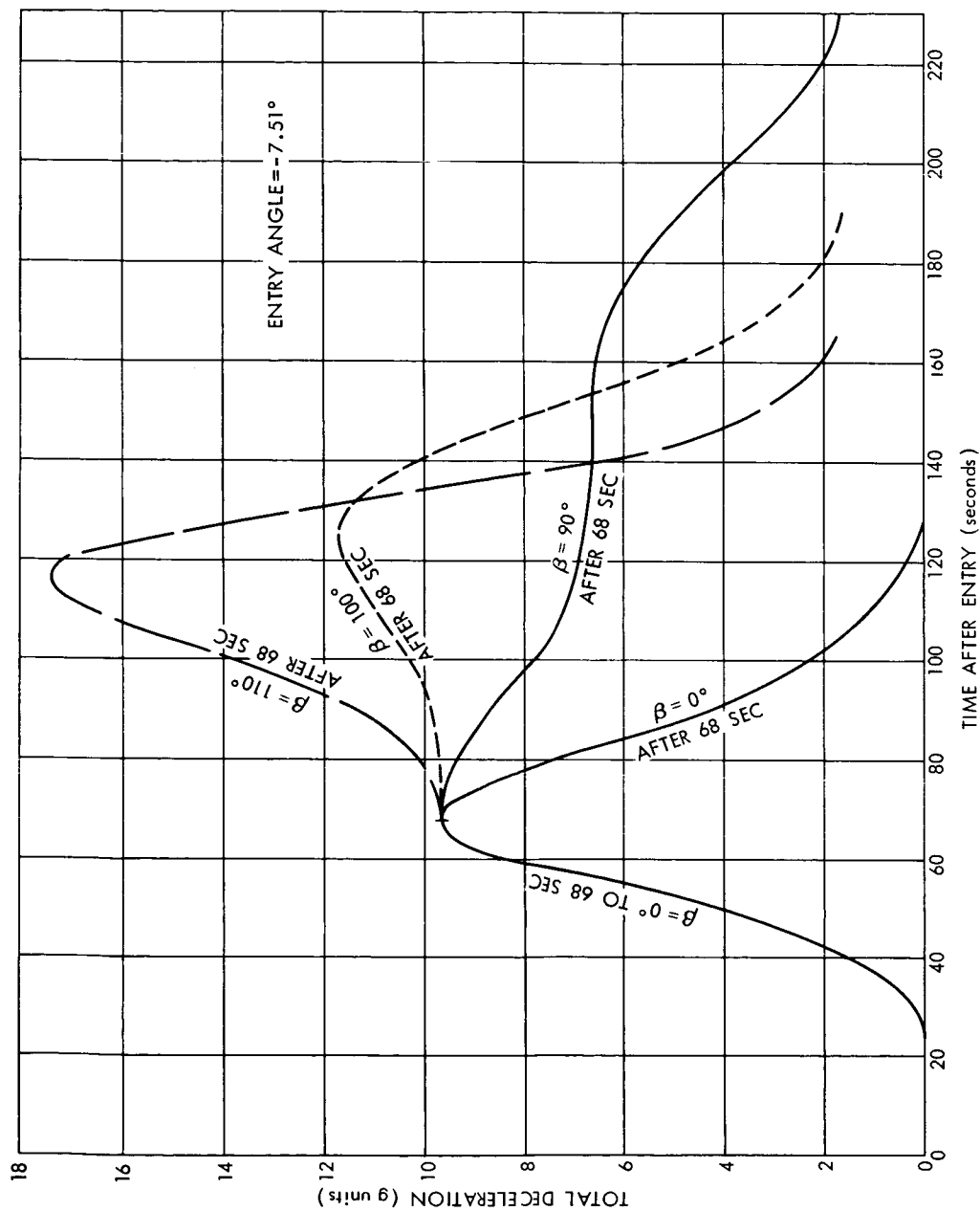
Figure 44. Effect of Bank Angle Value on Deceleration. Bank Angle Set After Reaching Peak Deceleration as Shown in Figure 39

87
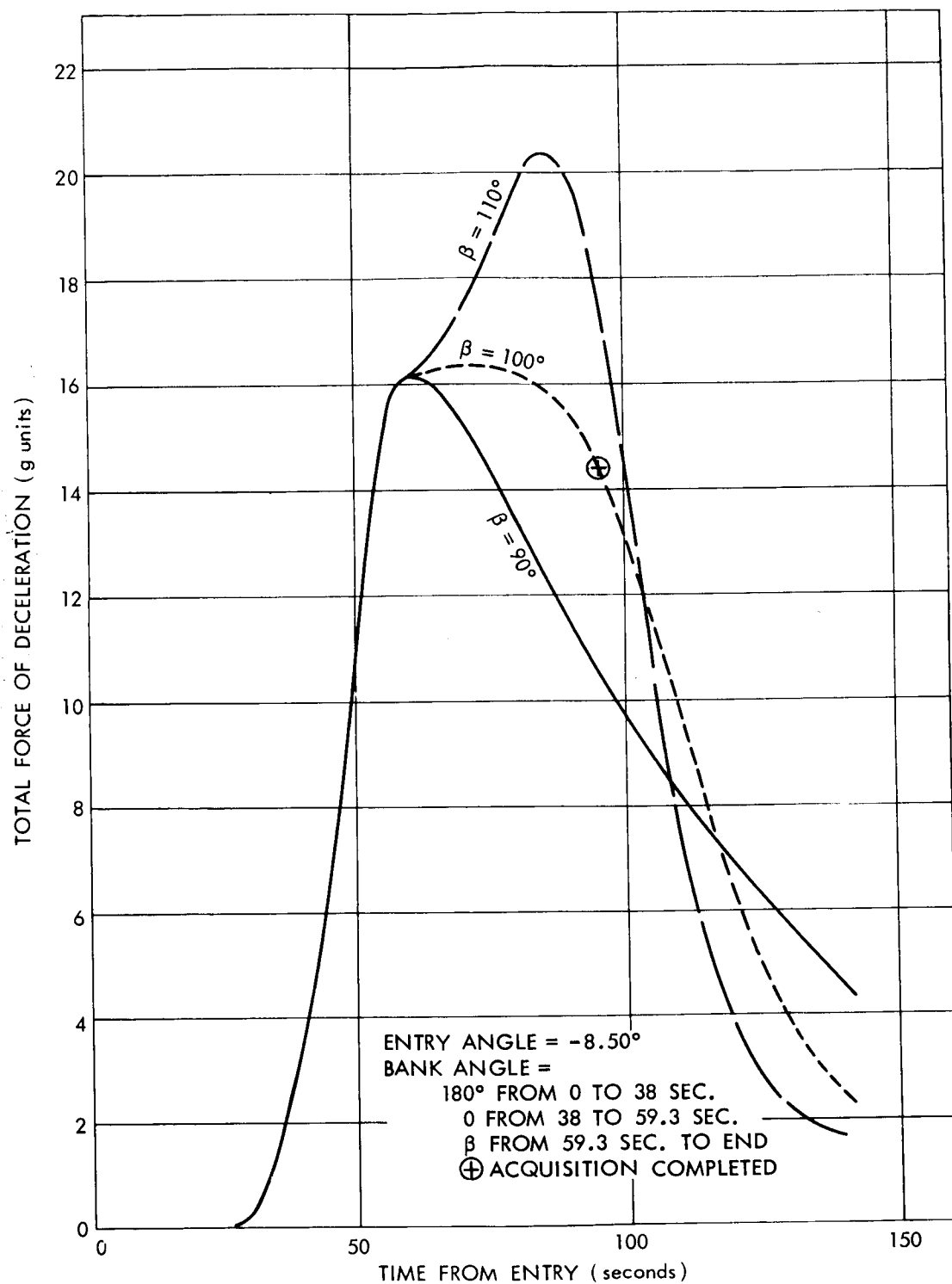
Figure 45. Development of Sustained Deceleration, Entry Angle = -8.50°
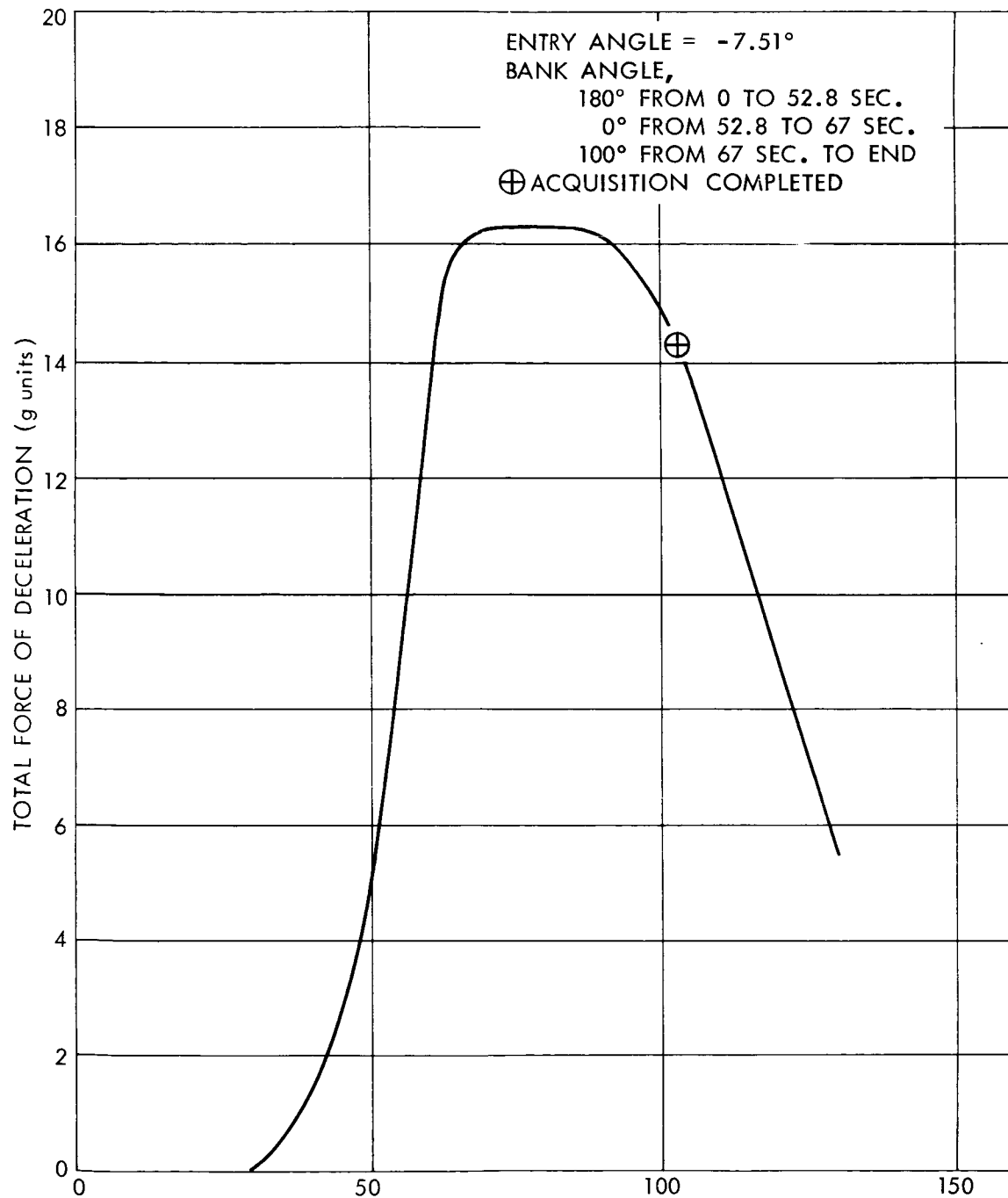
Figure 46. Development of Sustained Deceleration, Entry Angle = -7.51°
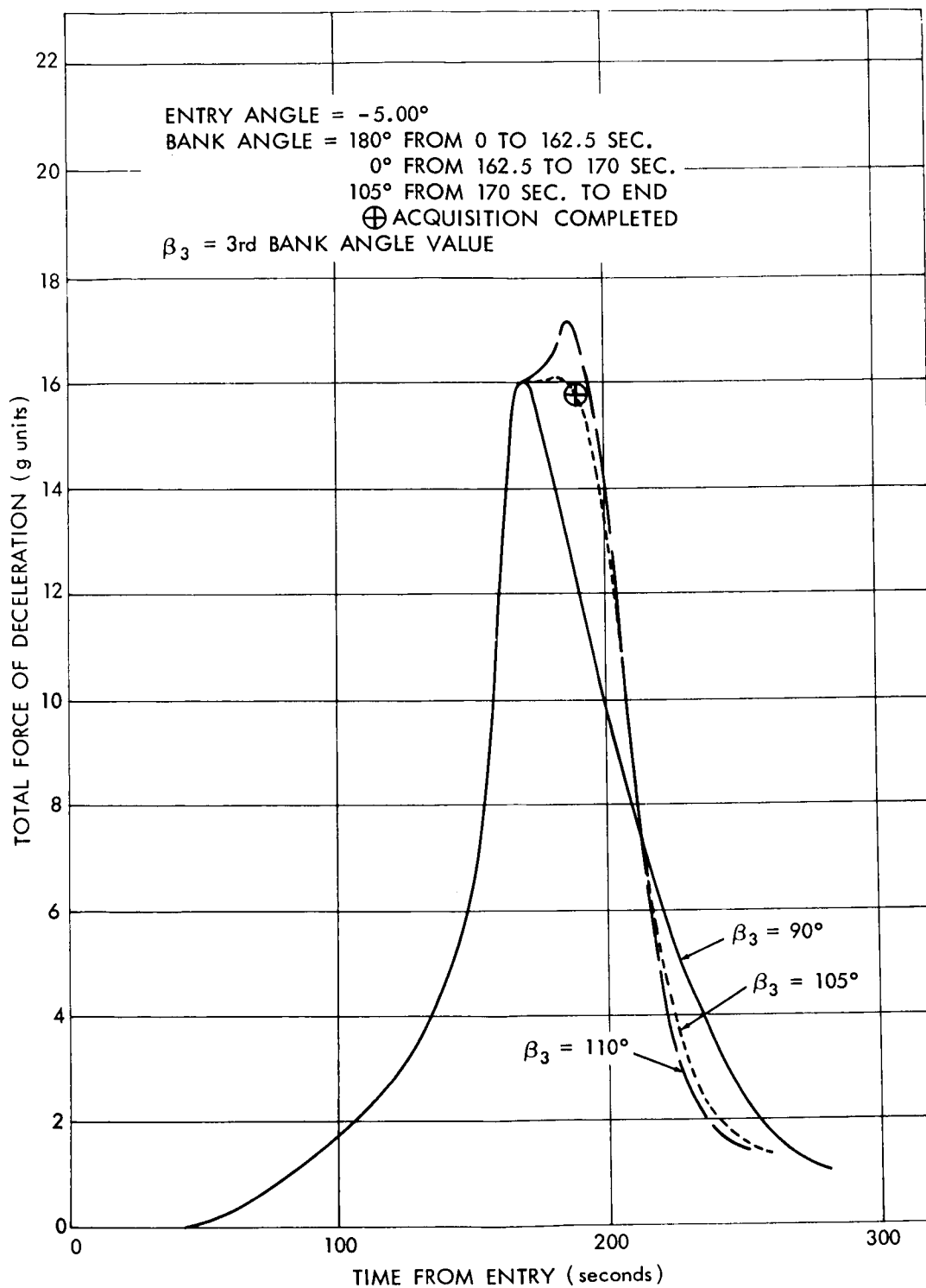
Figure 47. Development of Sustained Deceleration, Entry Angle = -5.00°
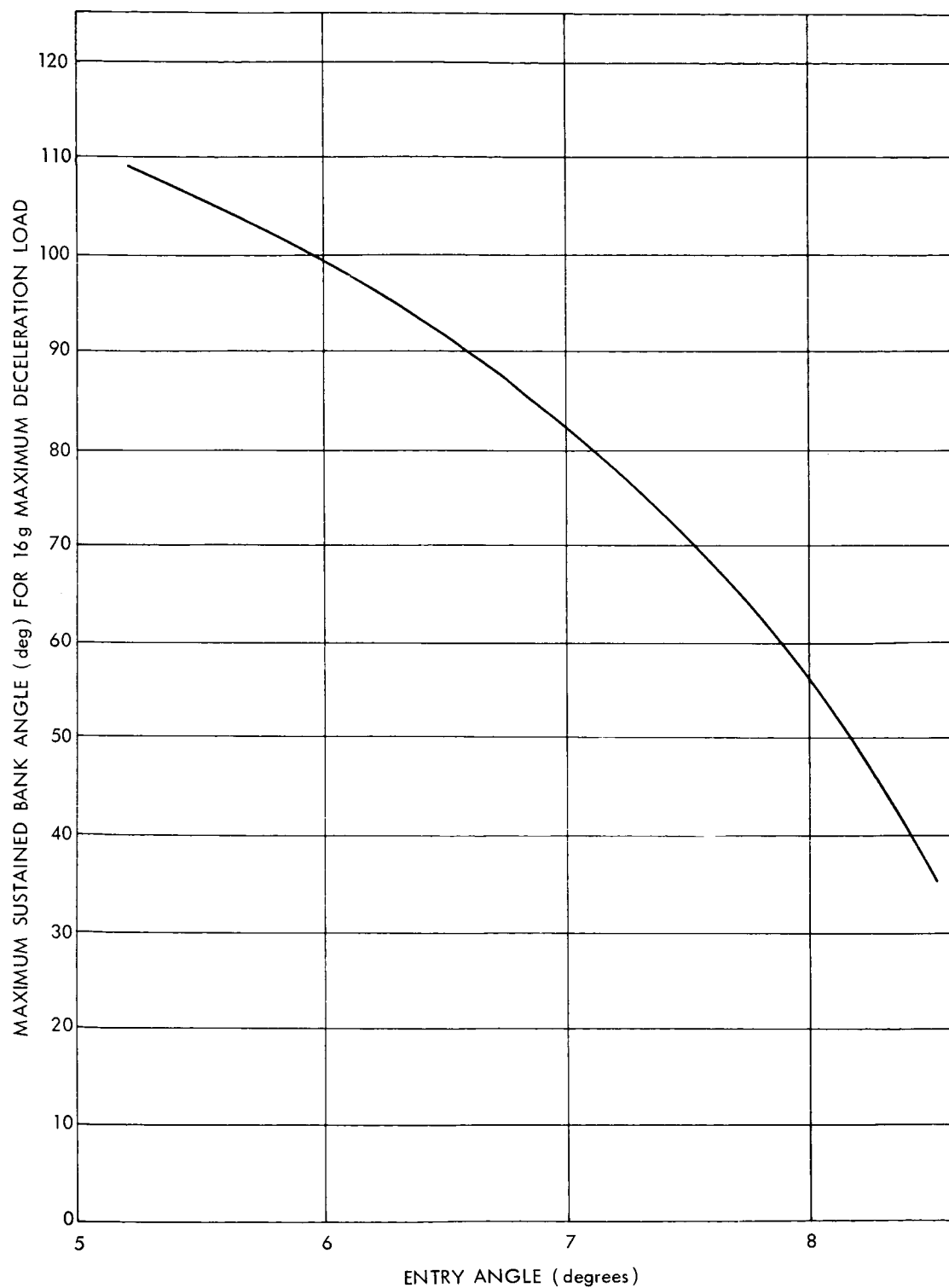
Figure 48.   Sustained Bank Angle Which Will Result in Maximum
Deceleration of 16g During Reentry

91
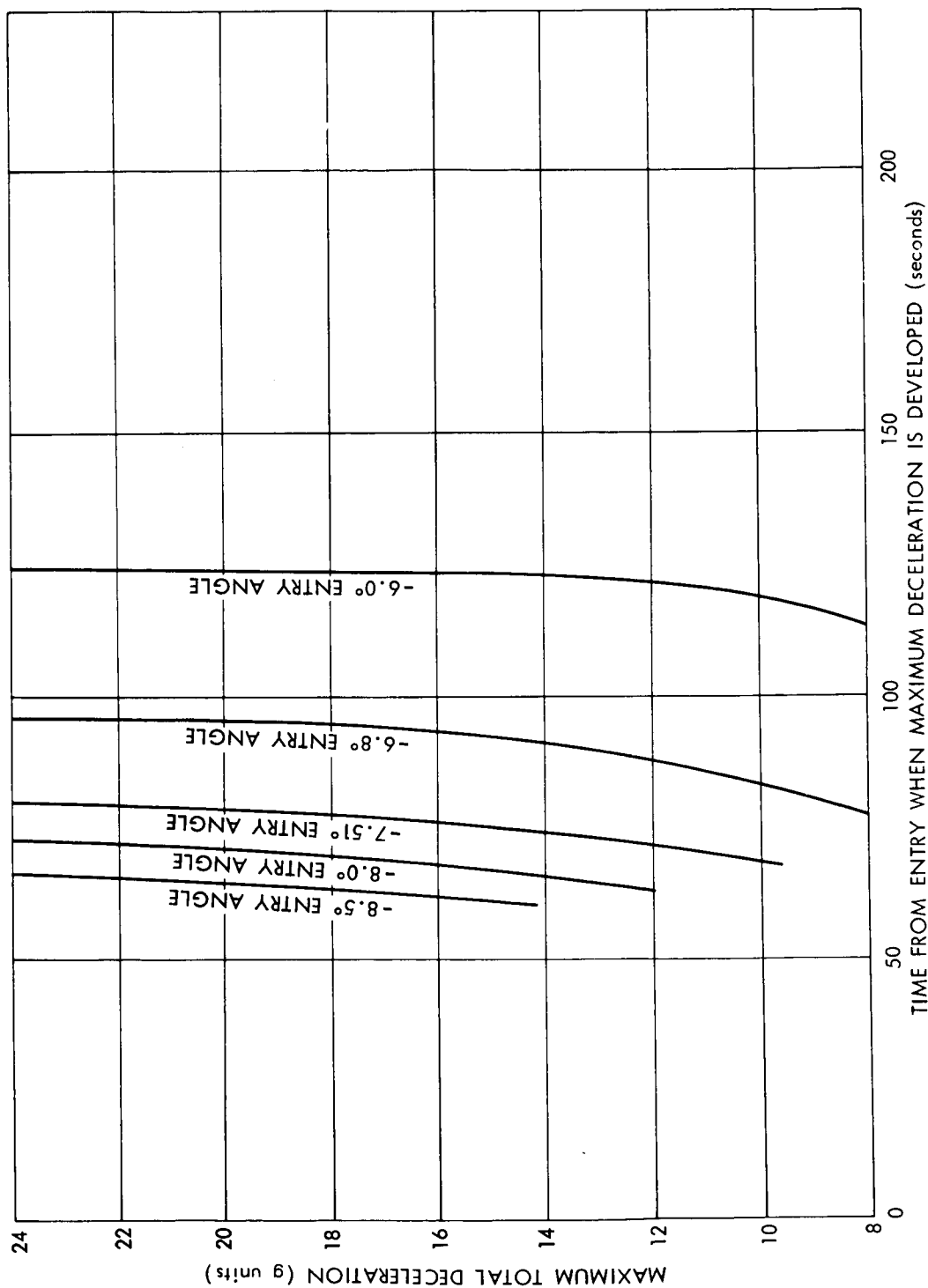
Figure 49. Time From Entry When Maximum Deceleration of 16g is Developed With Sustained Bank Angle of Figure 48

92
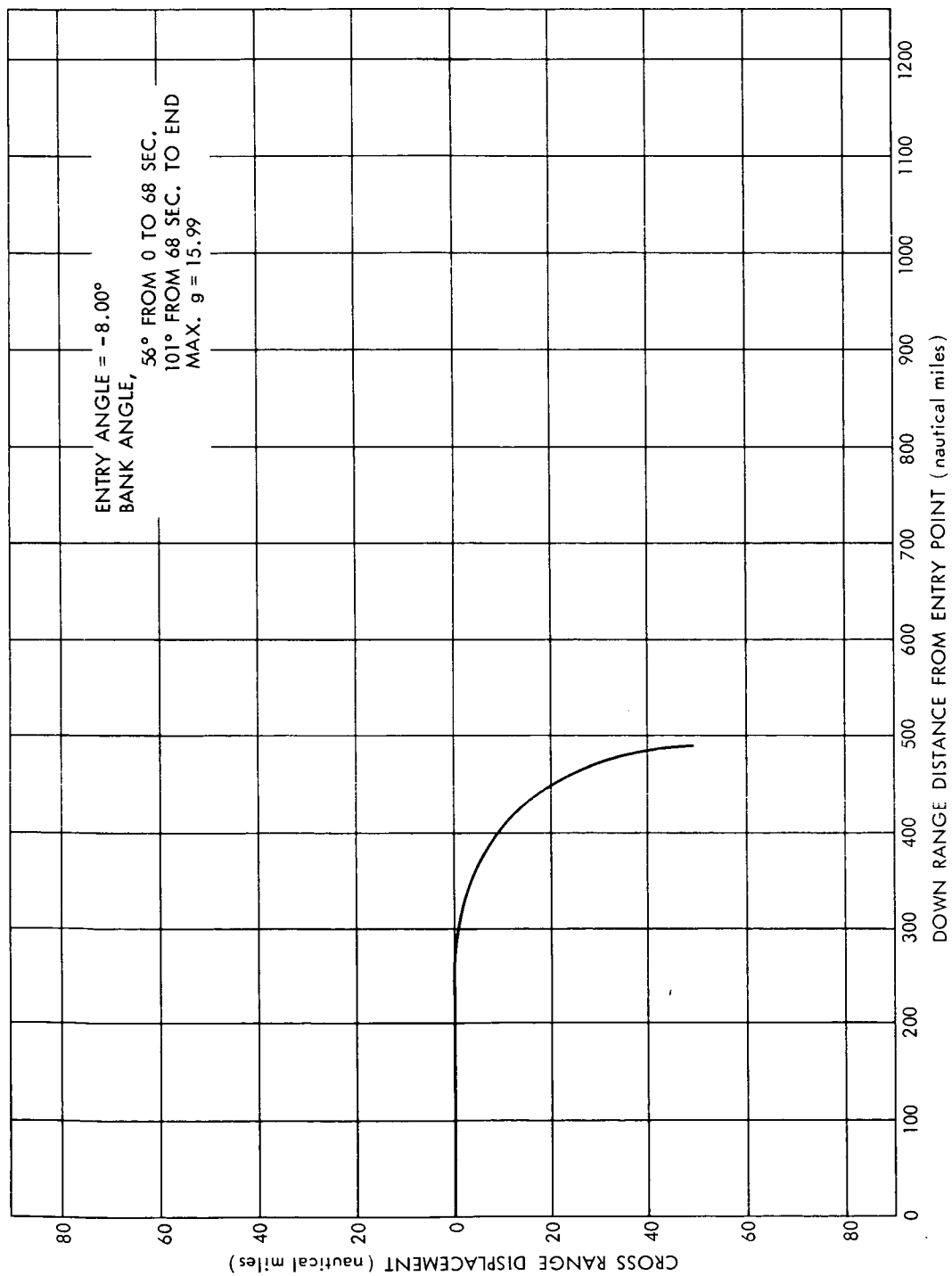
Figure 51. Horizontal Projection of Side Limit Trajectory, Entry Angle = -8.00°

ENTRY ANGLE = -8.00°
BANK ANGLE,

56° FROM 0 TO 68 SEC.
101° FROM 68 SEC. TO END
MAX. g = 15.99

DOWN RANGE DISTANCE FROM ENTRY POINT (nautical miles)

CROSS RANGE DISPLACEMENT (nautical miles)

ENTRY ANGLE = -8.50°
BANK ANGLE,
36° FROM 0 TO 61.6 SEC.
100° FROM 61.6 SEC. TO END
MAX. g = 15.91

DOWN RANGE DISTANCE FROM ENTRY POINT (nautical miles)

CROSS RANGE DISPLACEMENT (nautical miles)
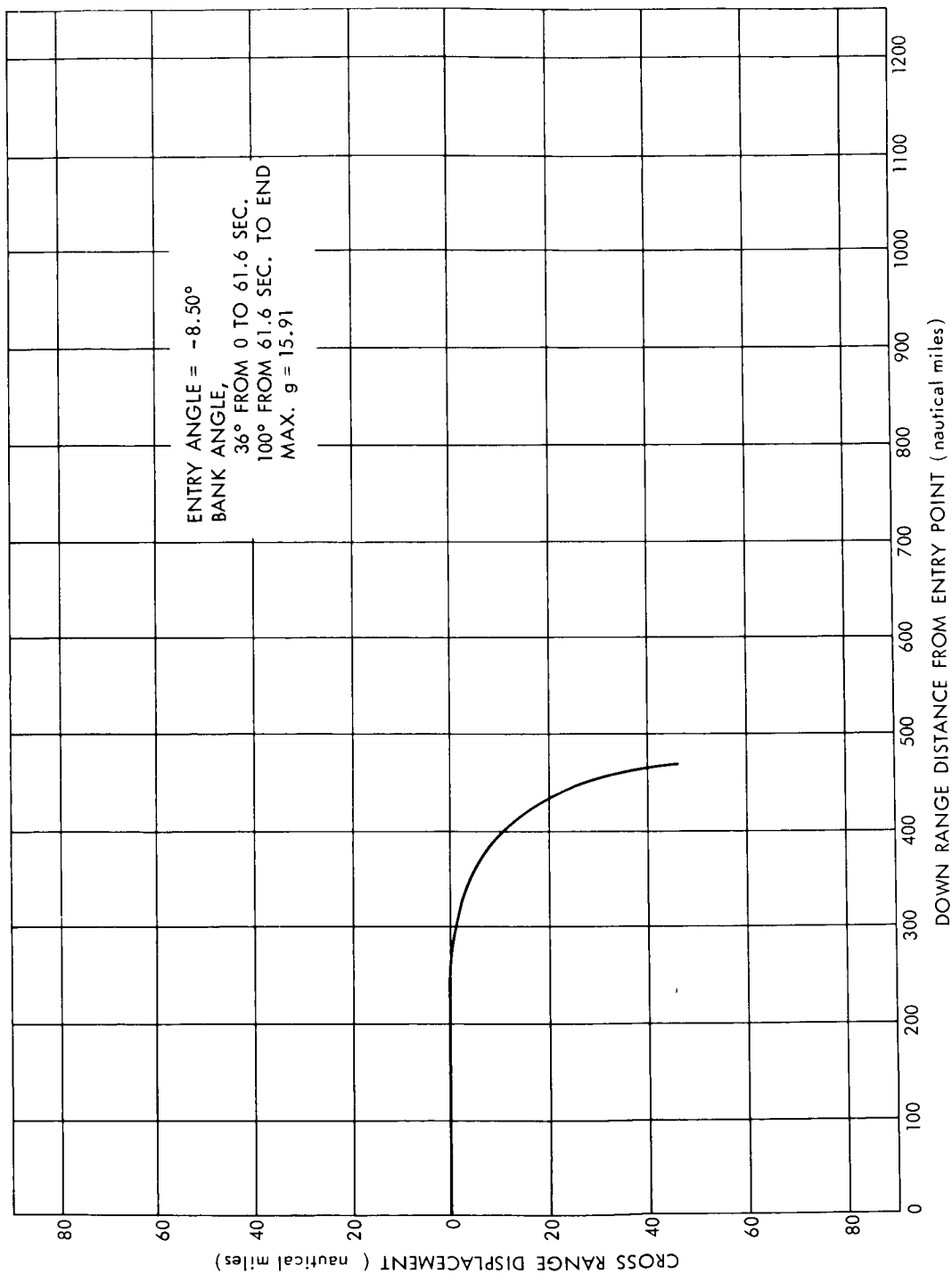
Figure 50. Horizontal Projection of Side Limit Trajectory, Entry Angle = -8.50°
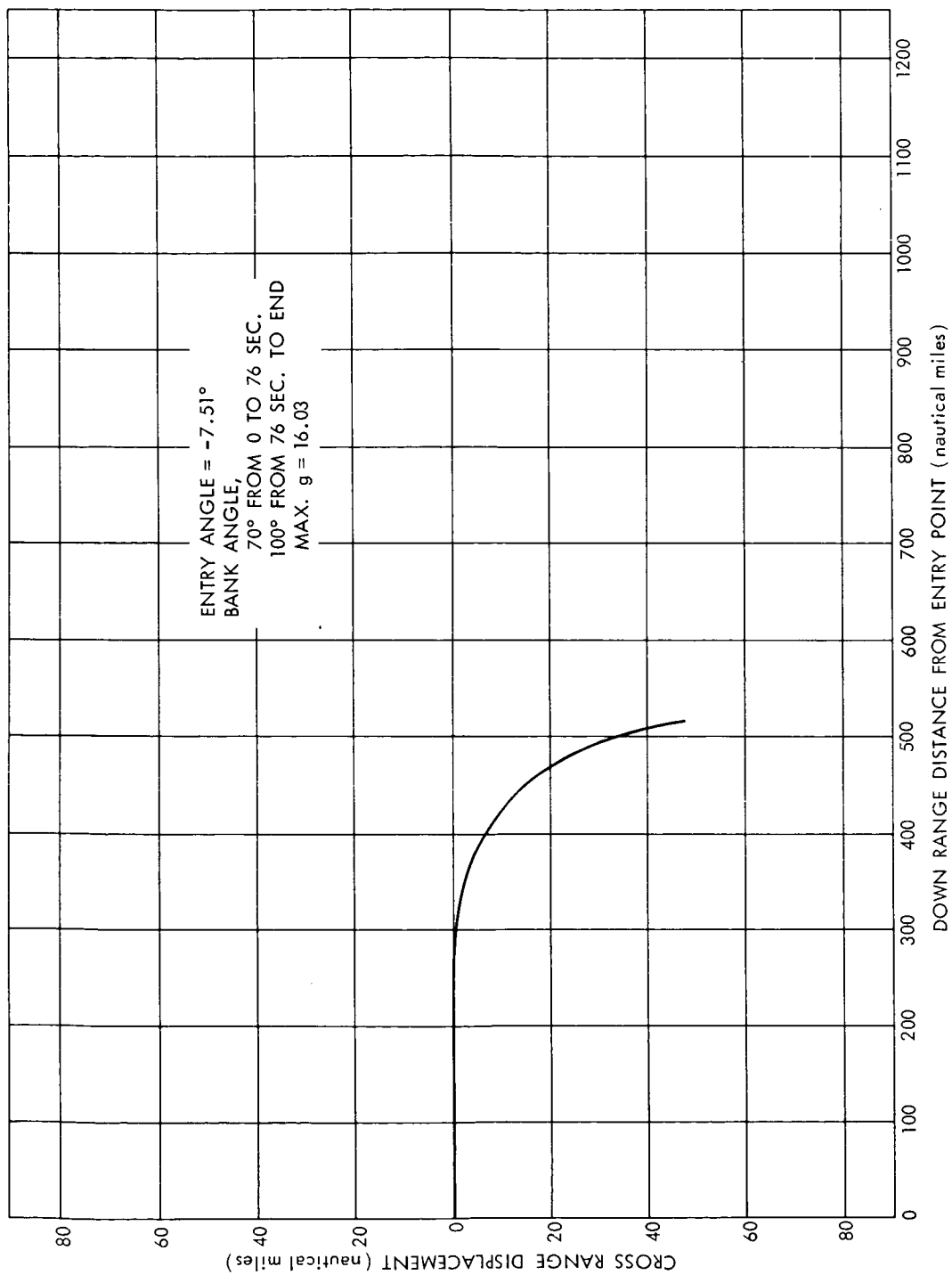
Figure 52. Horizontal Projection of Side Limit Trajectory, Entry Angle = -7.51°

ENTRY ANGLE = -7.51°
BANK ANGLE,
70° FROM 0 TO 76 SEC.
100° FROM 76 SEC. TO END
MAX. g = 16.03

DOWN RANGE DISTANCE FROM ENTRY POINT (nautical miles)

CROSS RANGE DISPLACEMENT (nautical miles)
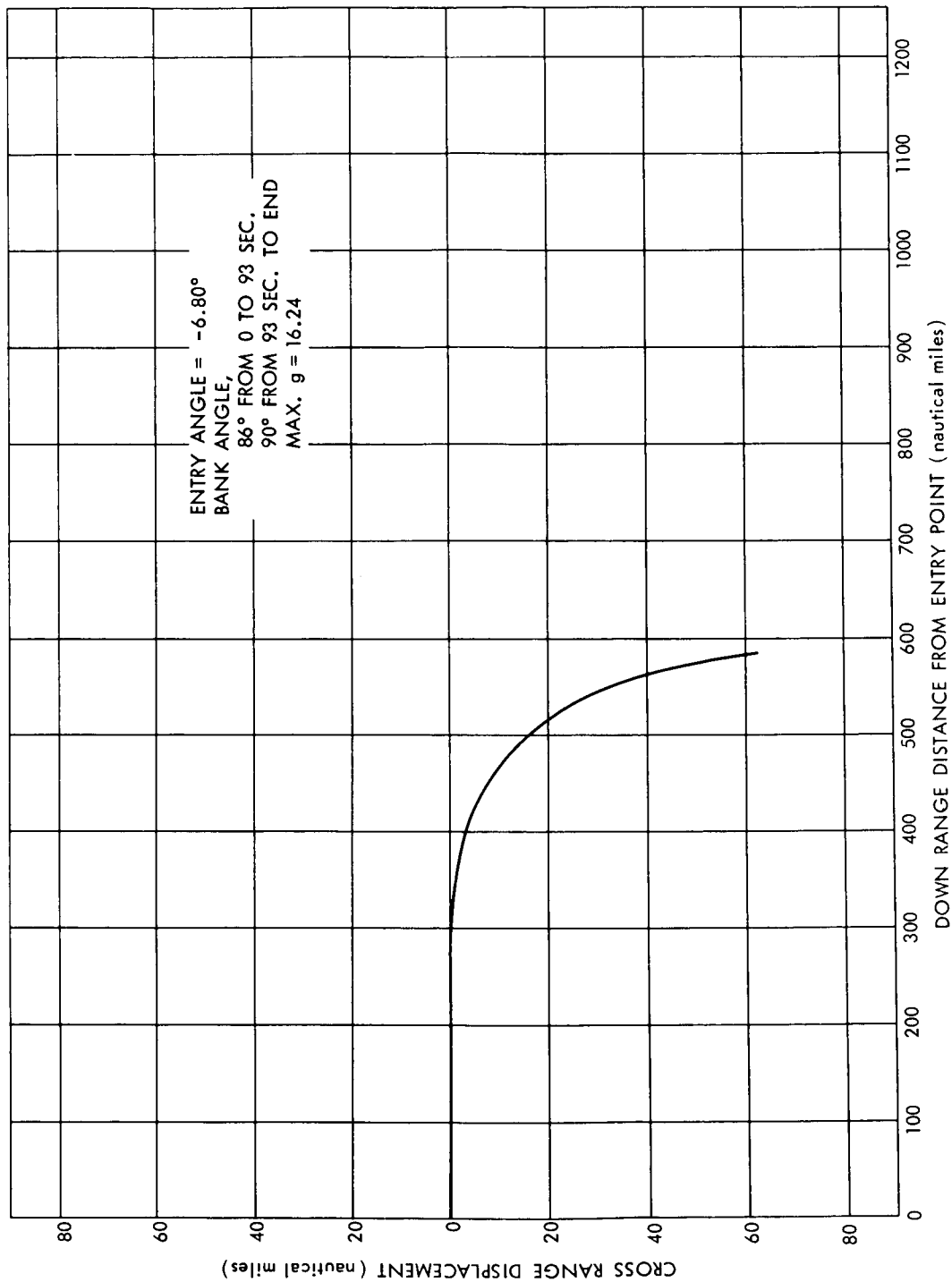
Figure 53. Horizontal Projection of Side Limit Trajectory, Entry Angle = –6.80°

96
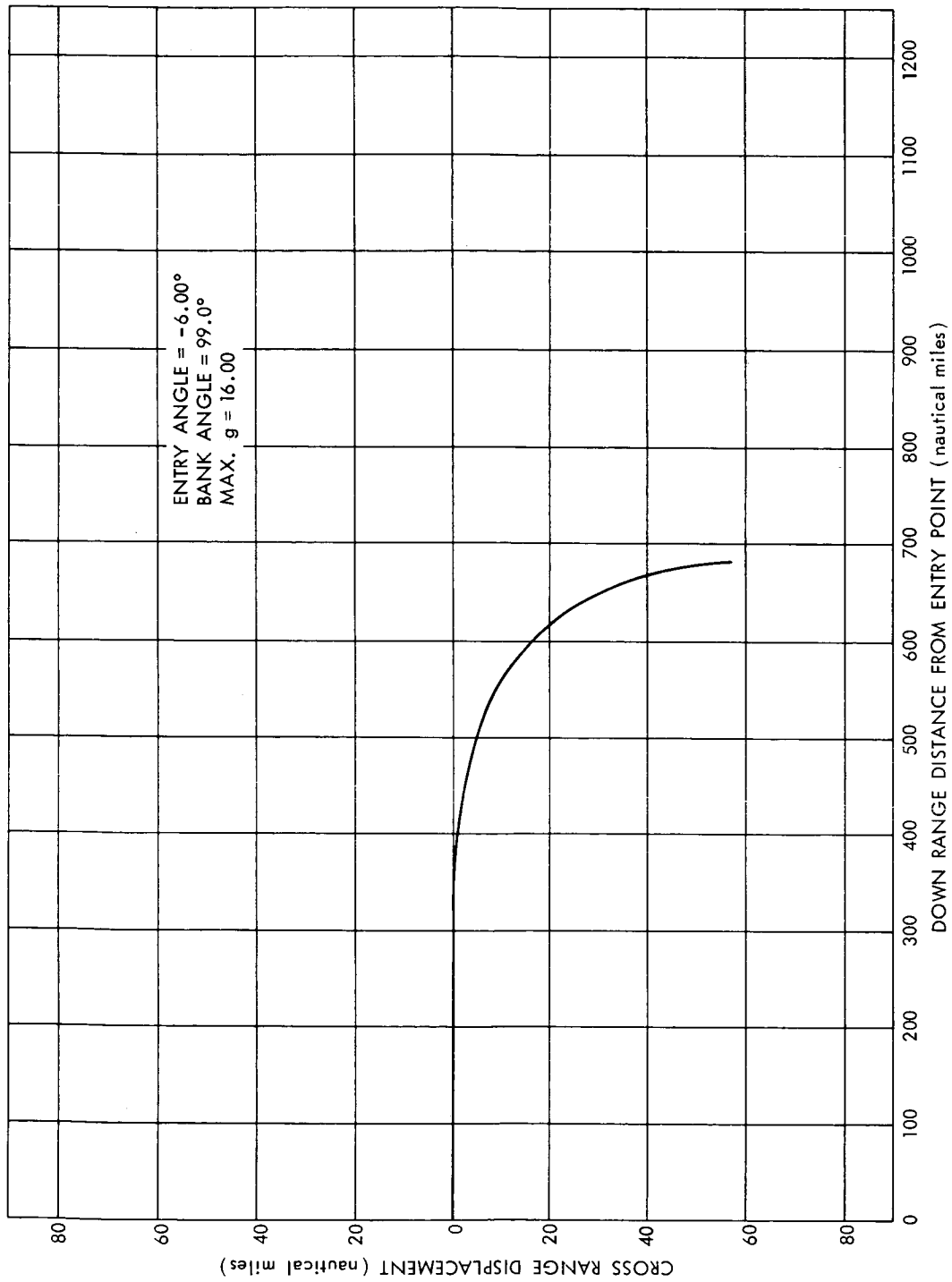
Figure 54. Horizontal Projection of Side Limit Trajectory, Entry Angle = -6.00°

ENTRY ANGLE = -6.00°
BANK ANGLE = 99.0°
MAX. g = 16.00

DOWN RANGE DISTANCE FROM ENTRY POINT (nautical miles)

CROSS RANGE DISPLACEMENT (nautical miles)

97
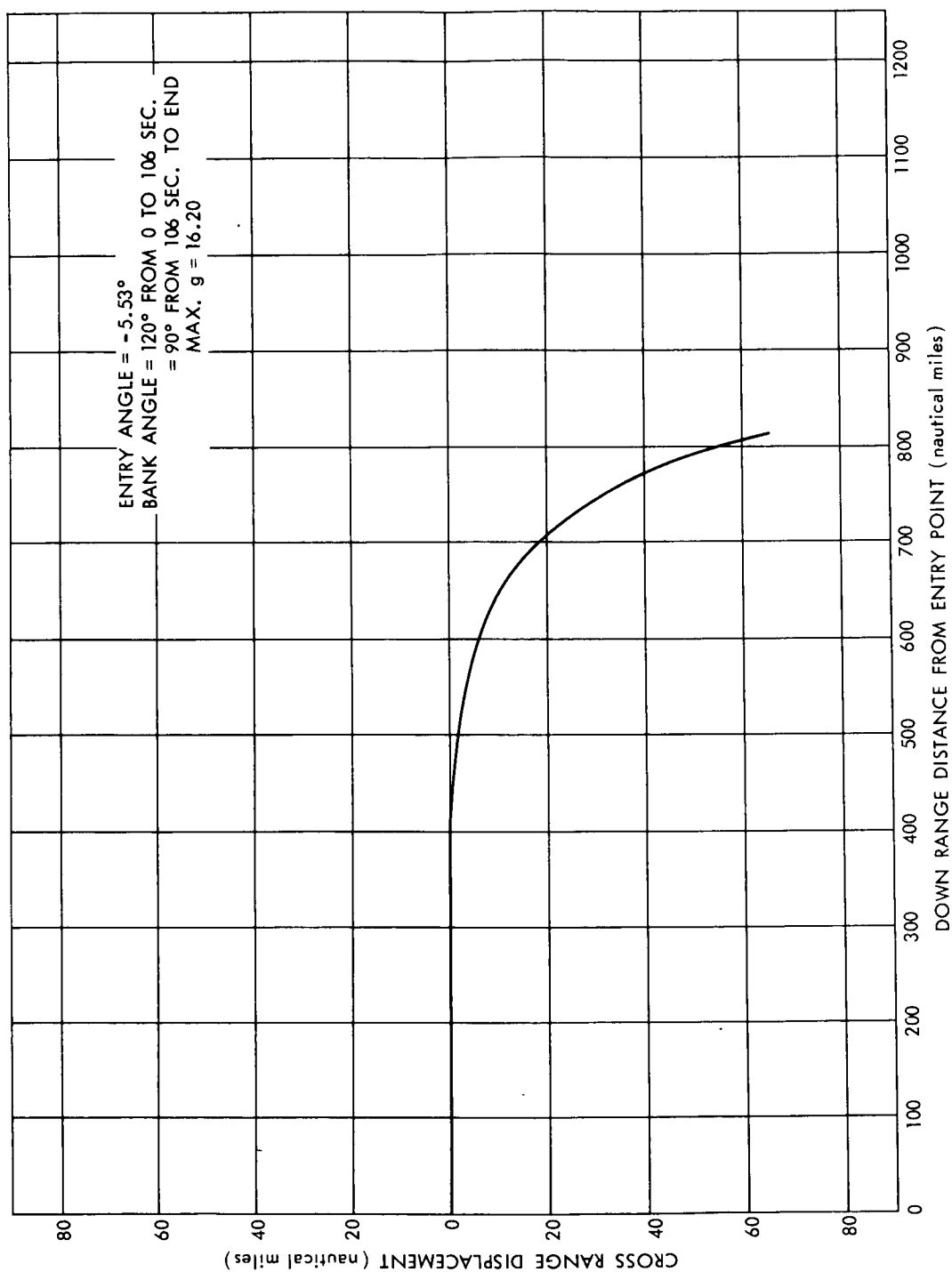
Figure 55. Horizontal Projection of Side Limit Trajectory, Entry Angle = -5.53°

ENTRY ANGLE = -5.53°
BANK ANGLE = 120° FROM 0 TO 106 SEC.
= 90° FROM 106 SEC. TO END
MAX. g = 16.20

DOWN RANGE DISTANCE FROM ENTRY POINT (nautical miles)

CROSS RANGE DISPLACEMENT (nautical miles)
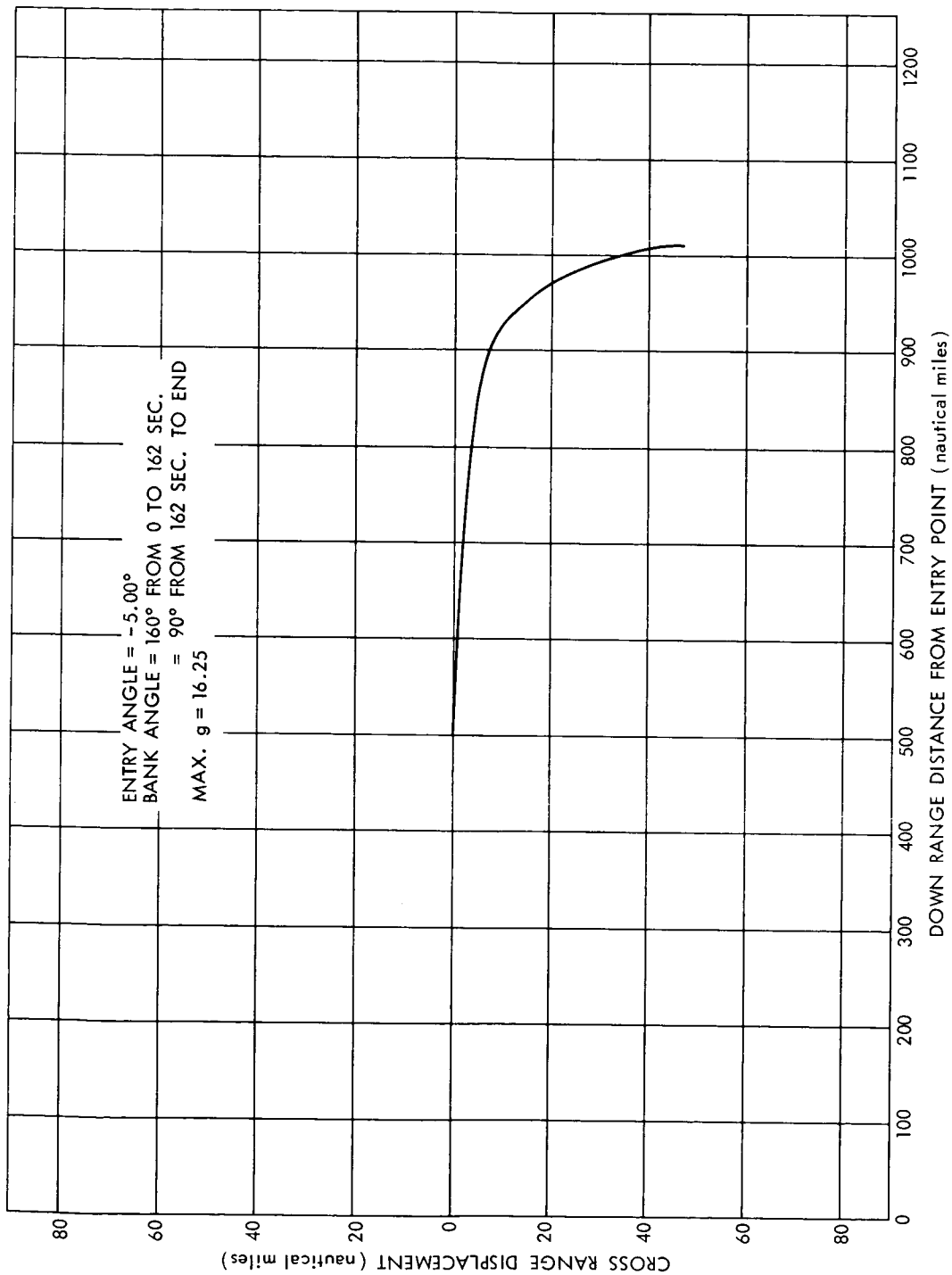
Figure 56. Horizontal Projection of Side Limit Trajectory, Entry Angle = -5.00°

99

106

100

108

2
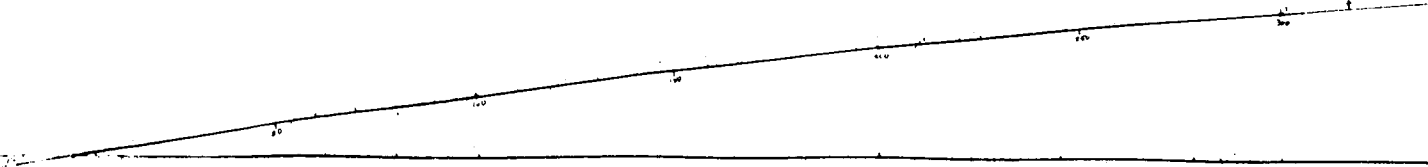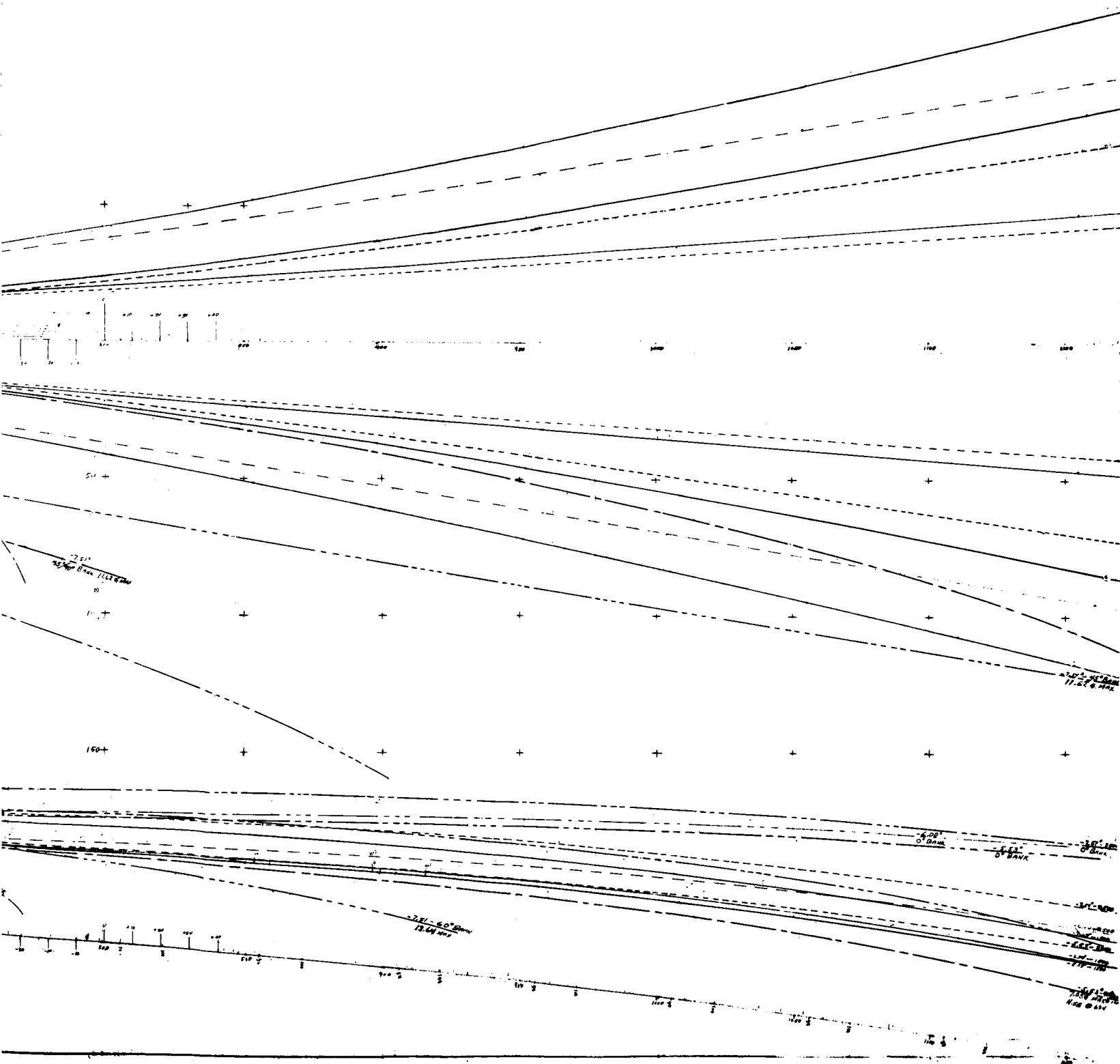
Figure 57. Picture of Plot Board
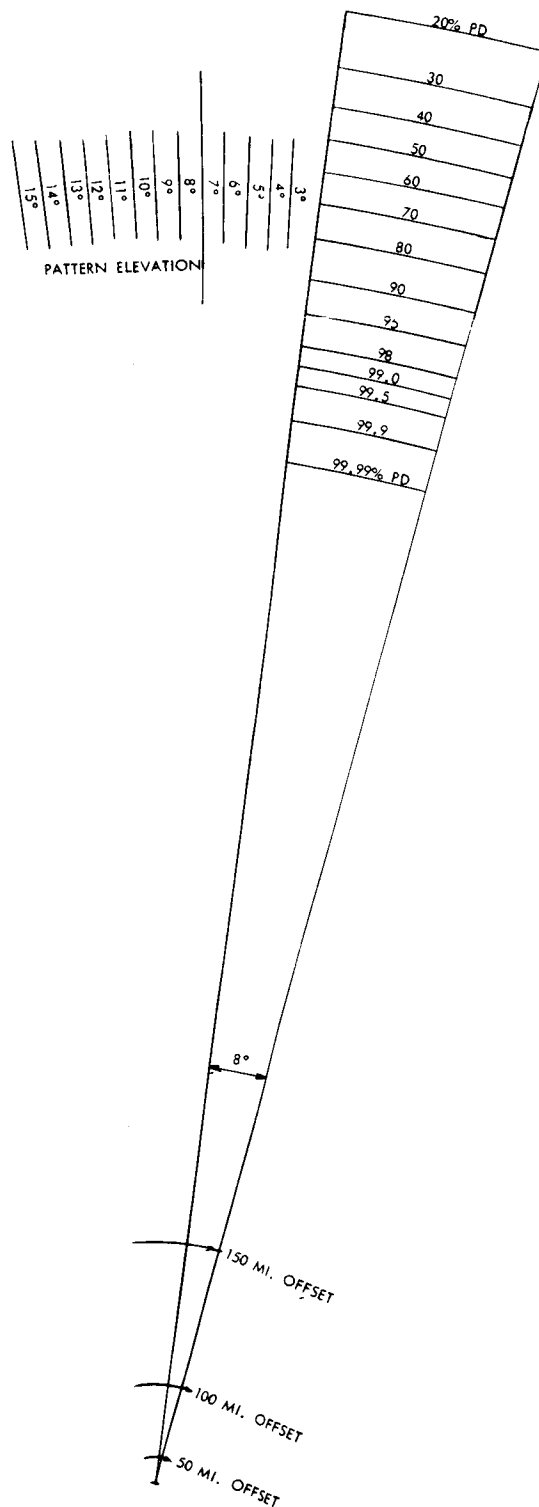
Figure 59. Picture of Vertical Overlay
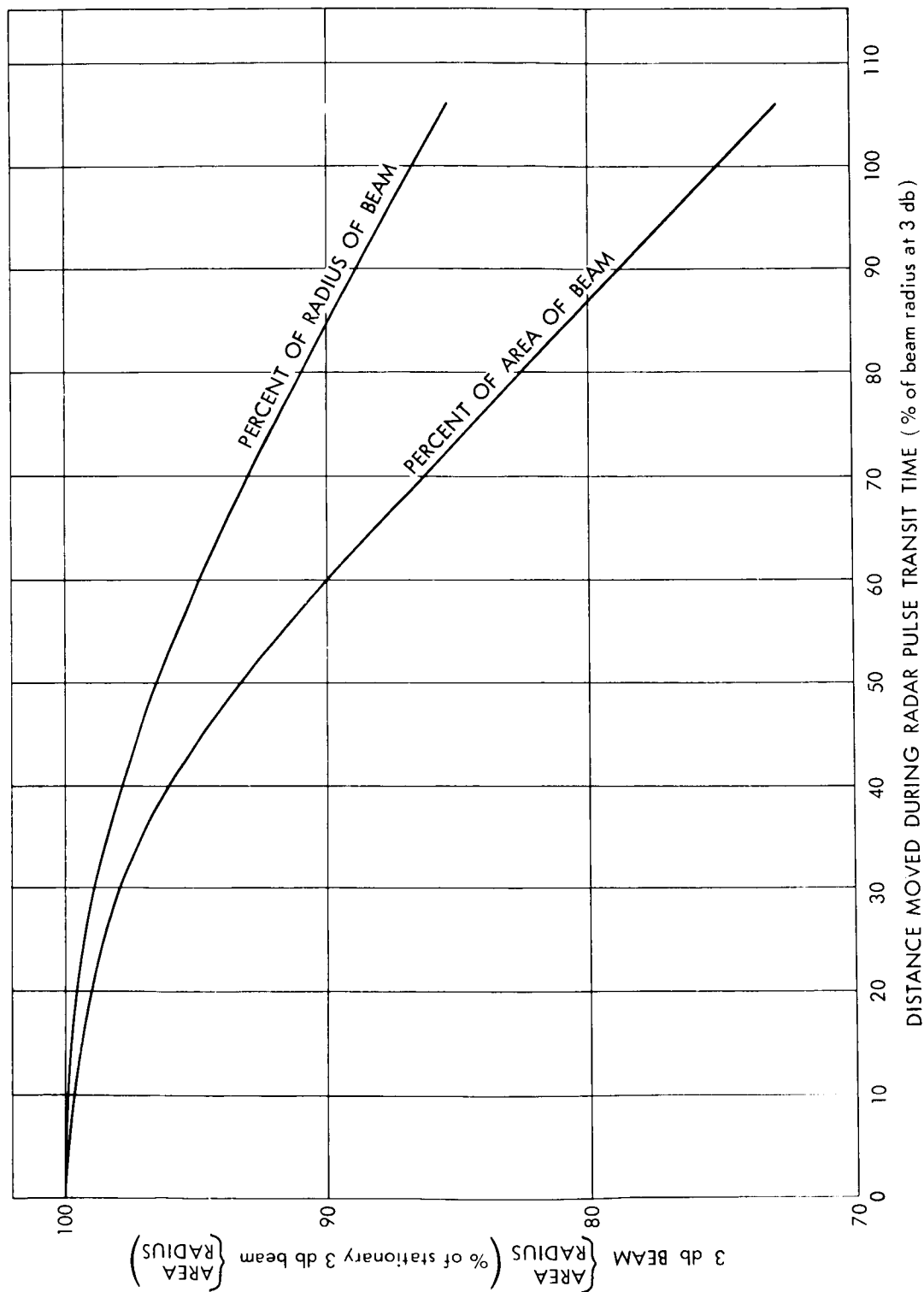
Figure 58. Shrinkage in Radar Beam Coverage Due to Motion of Beam
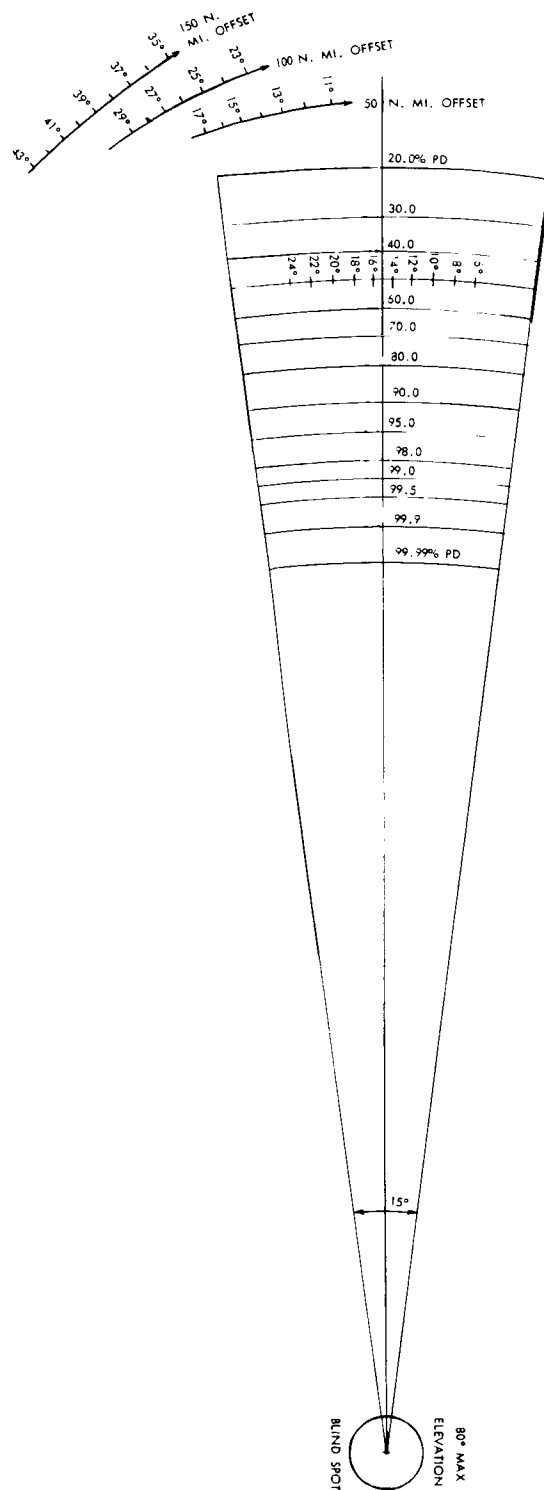
Figure 60. Picture of Horizontal Overlay

105
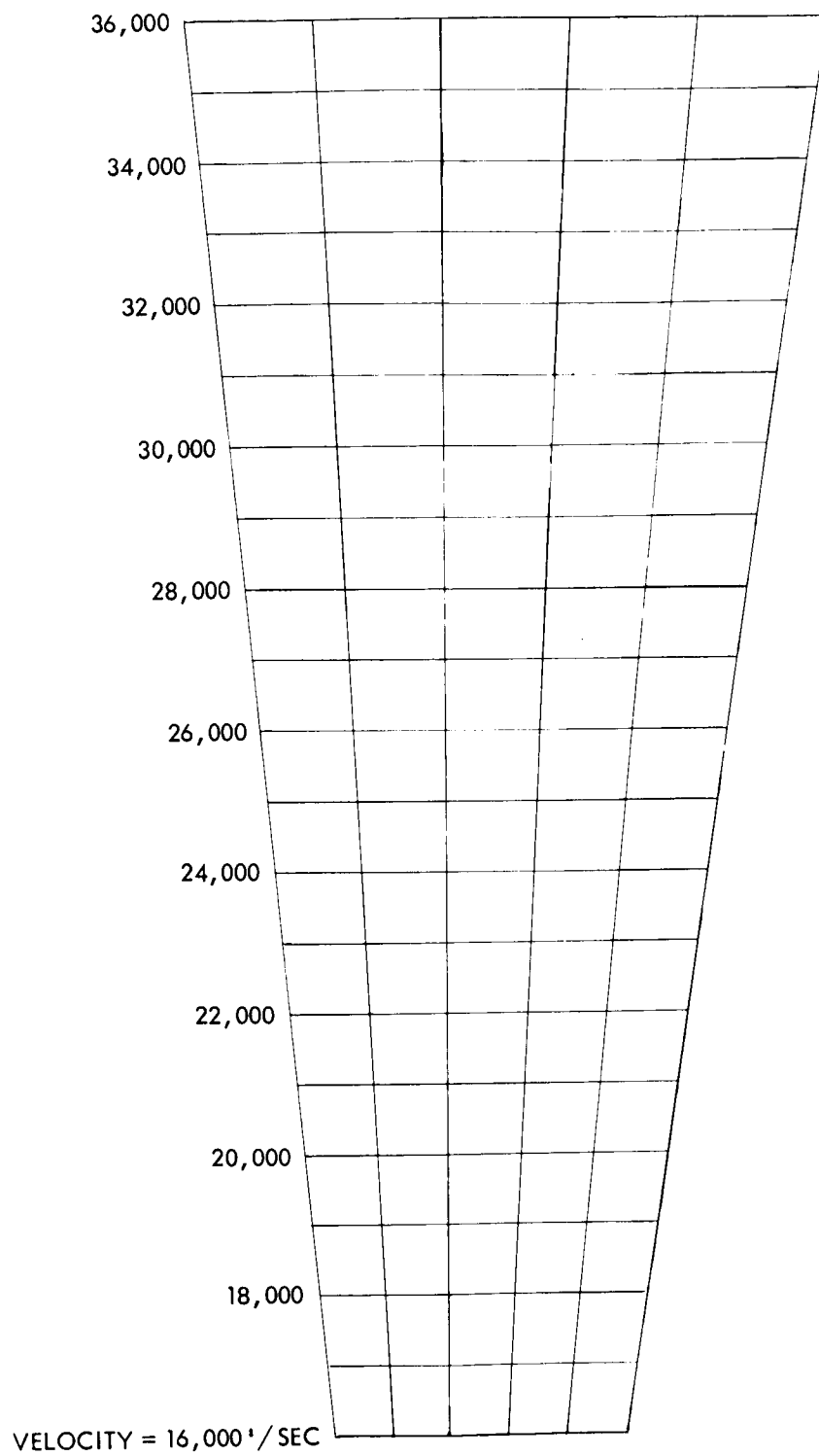
Figure 61. Picture of Overlay for Distance
Traveled in 5-Second Search Period

VERTICAL PROJECTION OF 8° × 15° RADAR
SEARCH PATTERN.
PATTERN ELEVATION = 7° AT CENTER

0° (horizon)

11° ABOVE HORIZON

281 NAUTICAL MILE RANGE

3° ABOVE HORIZON

SHIP POSITION
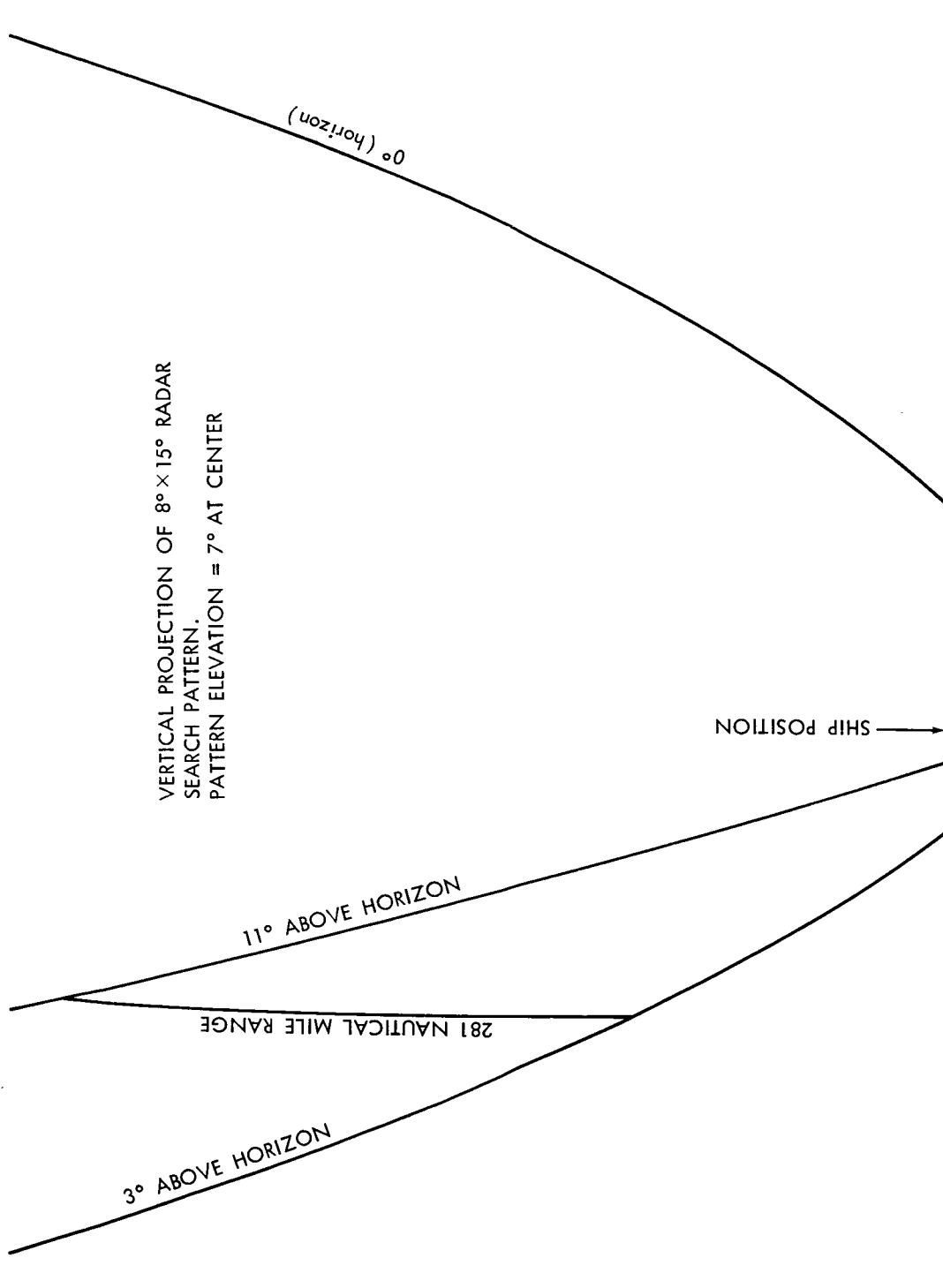
Figure 62.   Vertical Projection of 8° x 15° Radar Search Pattern Elevated 7°

VERTICAL PROJECTION OF 8° x 15° RADAR
SEARCH PATTERN
PATTERN ELEVATION = 8° AT CENTER.

0° HORIZON

12° ABOVE HORIZON

281 NAUTICAL MILE RANGE

4° ABOVE HORIZON

SHIP POSITION ⟶
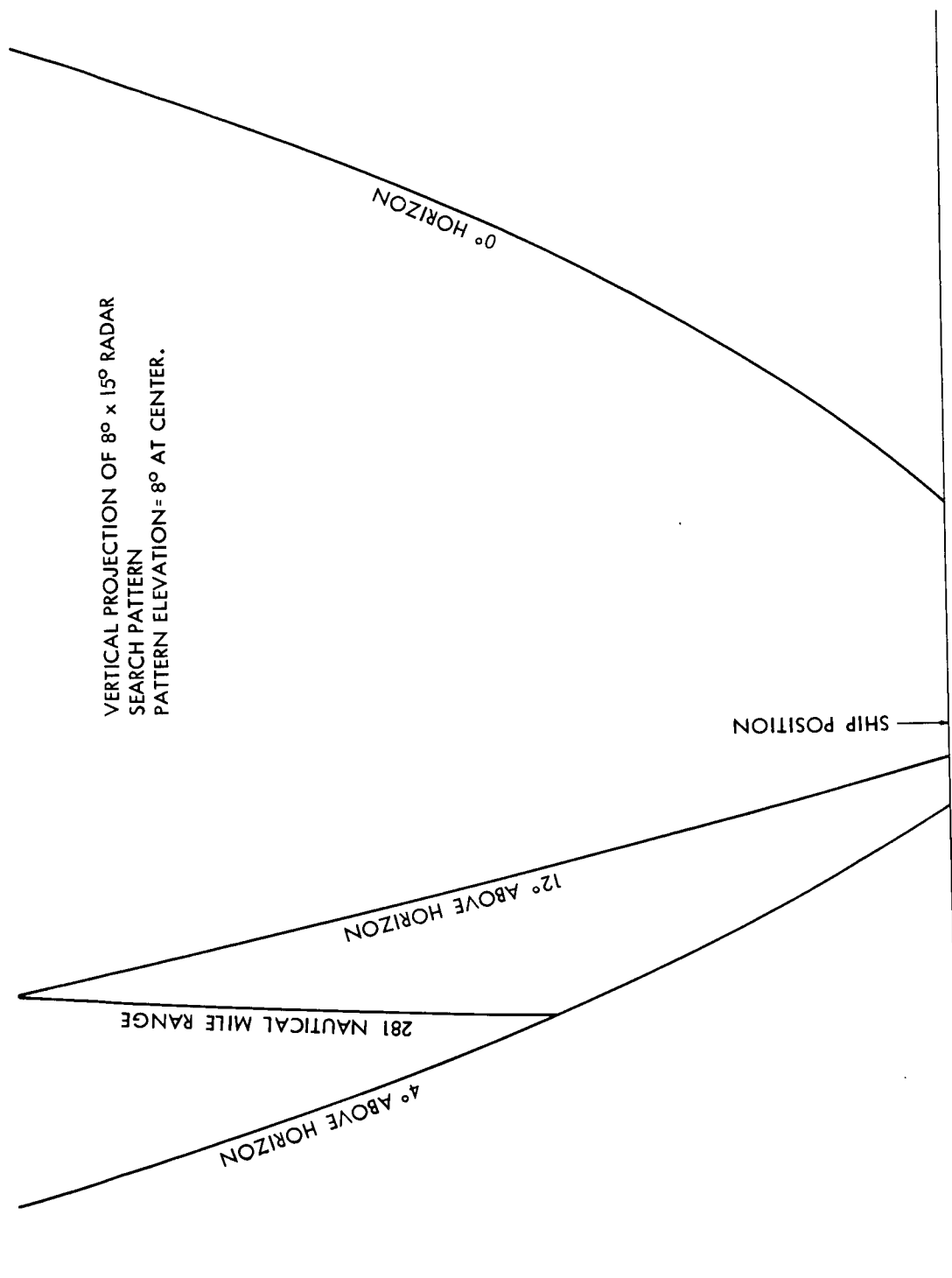
Figure 63.   Vertical Projection of 8° × 15° Radar Search Pattern Elevated 8°

108
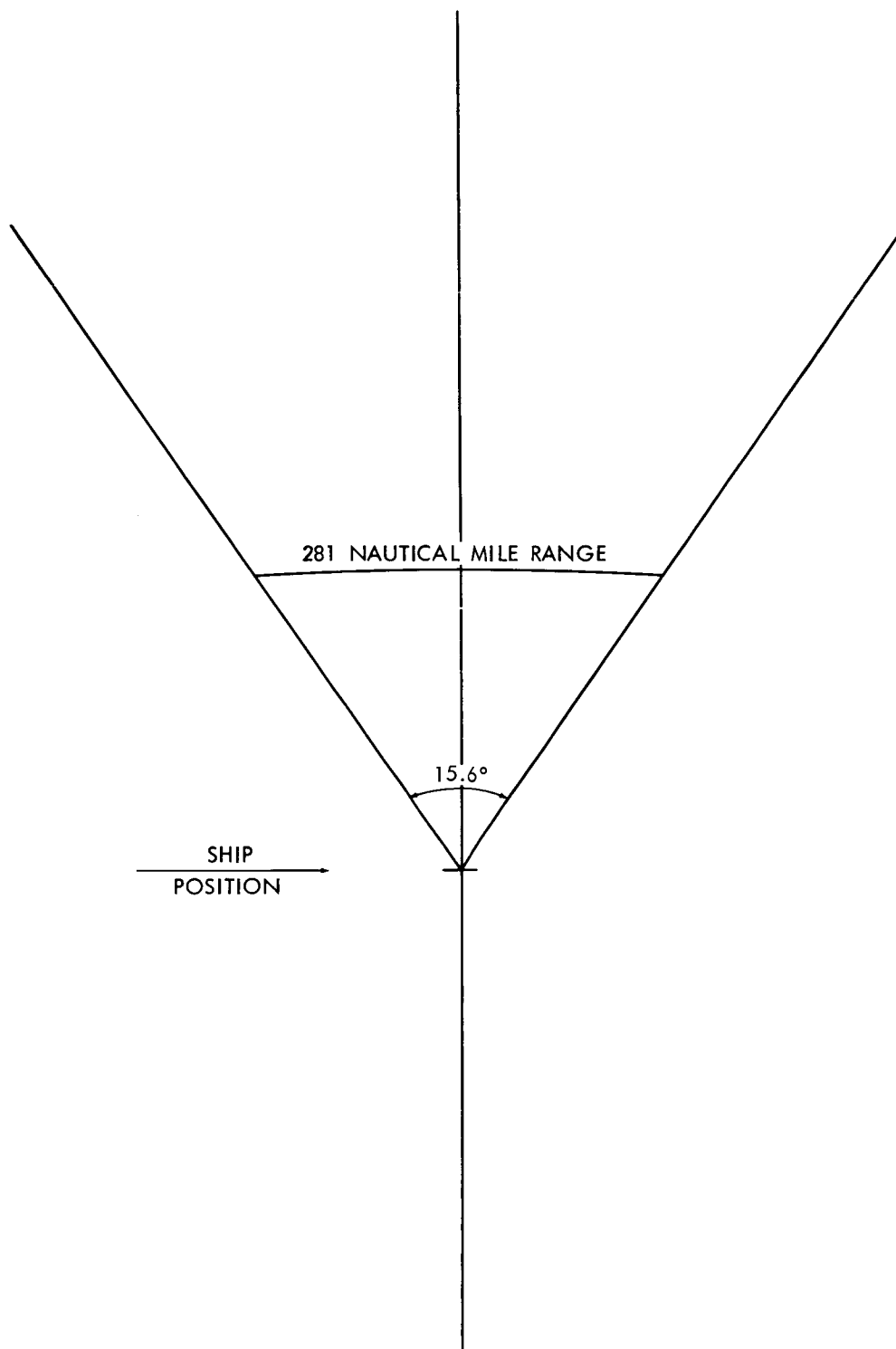
Figure 64.   Horizontal Projection of 8° × 15° Radar Search Pattern
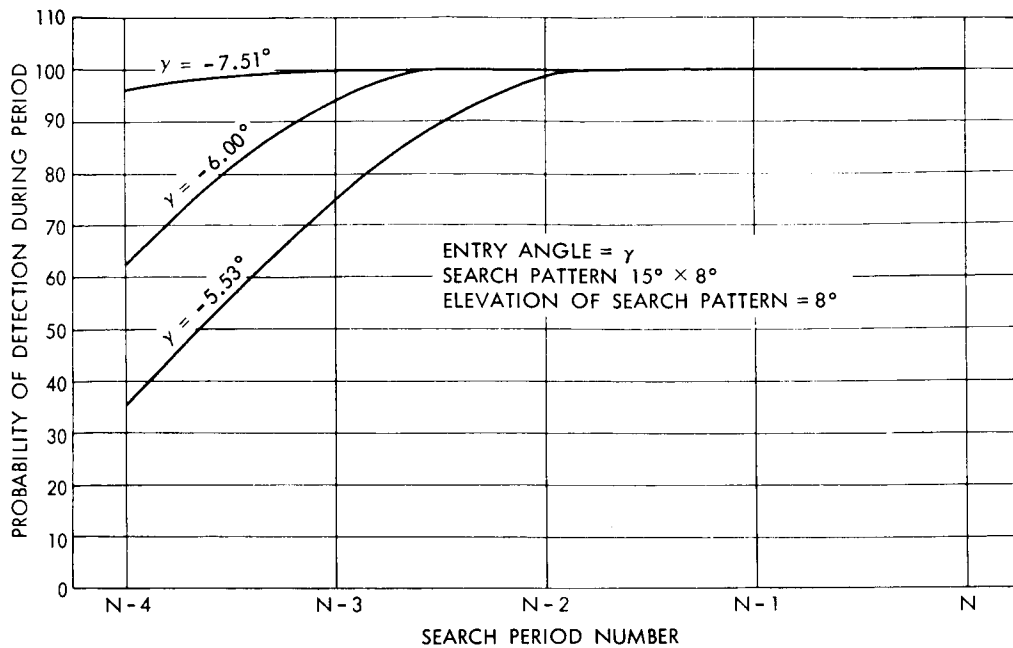
Figure 65.   Probability of Detection. Station on Projected Pre-Reentry
Ground Track, 600 Nautical Miles from Entry. Normal
Trajectory With Range of 2500 Nautical Miles.
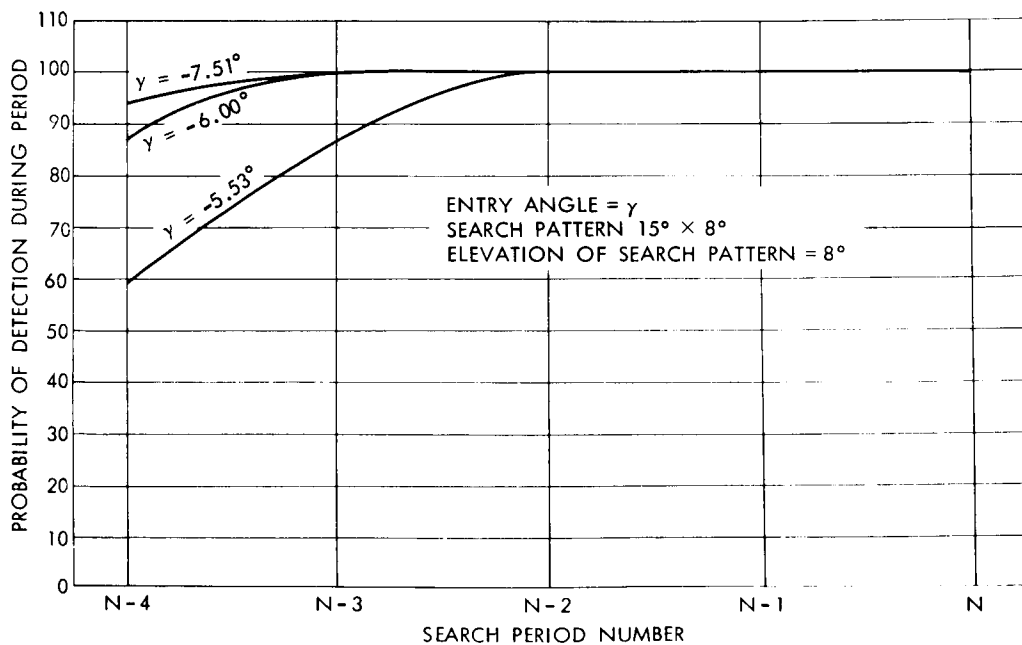
Figure 66.   Probability of Detection. Station on Projected Pre-Reentry
Ground Track, 700 Miles From Entry. Normal Trajectory
with Range of 2500 Nautical Miles

110
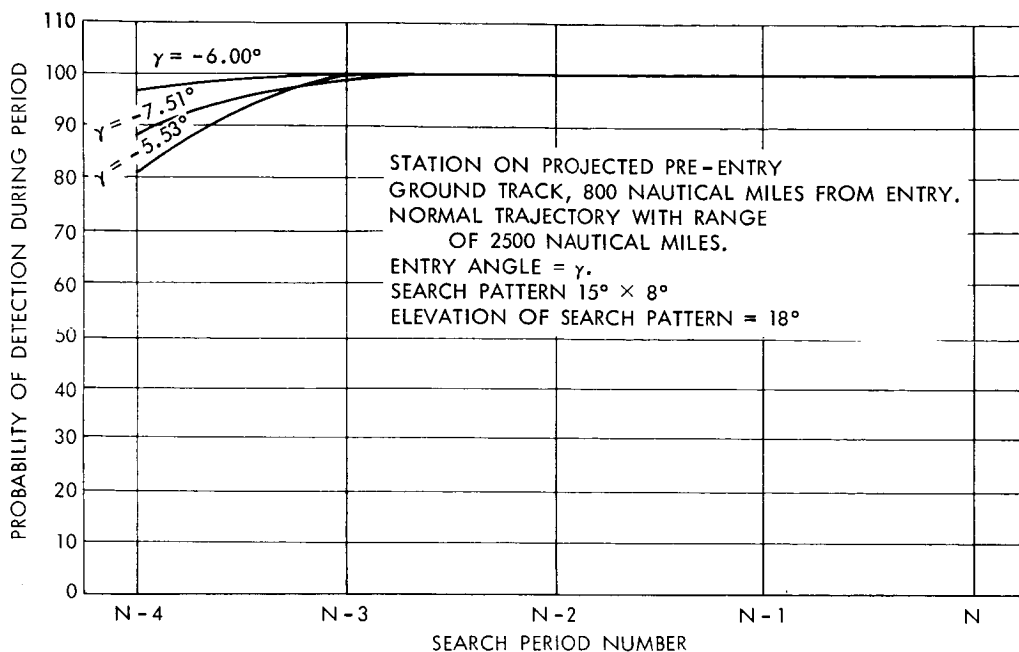
Figure 67. Probability of Detection. Station on Projected Pre-Reentry
Ground Track, 800 Nautical Miles From Entry. Normal
Trajectory With Range of 2500 Nautical Miles
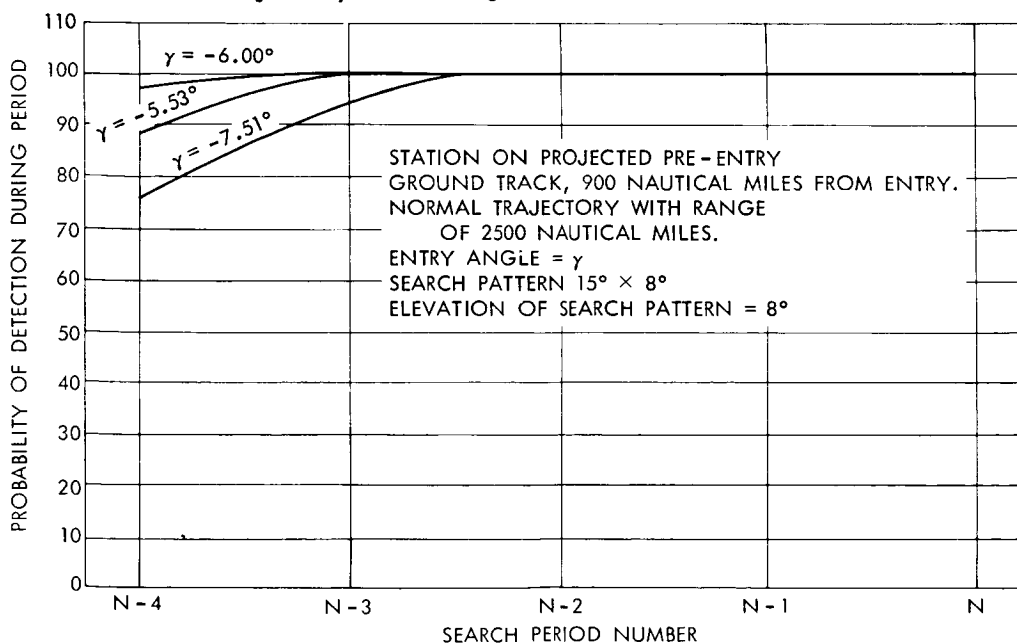
Figure 68. Probability of Detection. Station on Projected Pre-Reentry
Ground Track, 900 Nautical Miles From Entry. Normal
Trajectory with Range of 2500 Nautical Miles.

111
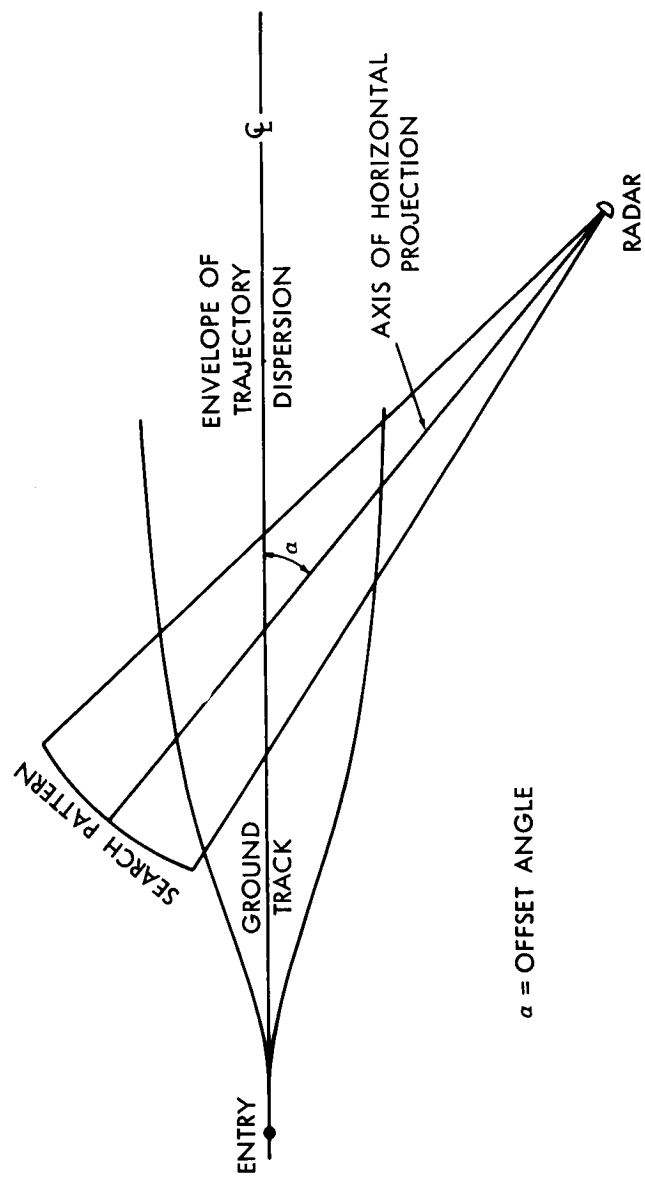
Figure 96. Definition of Offset Angle
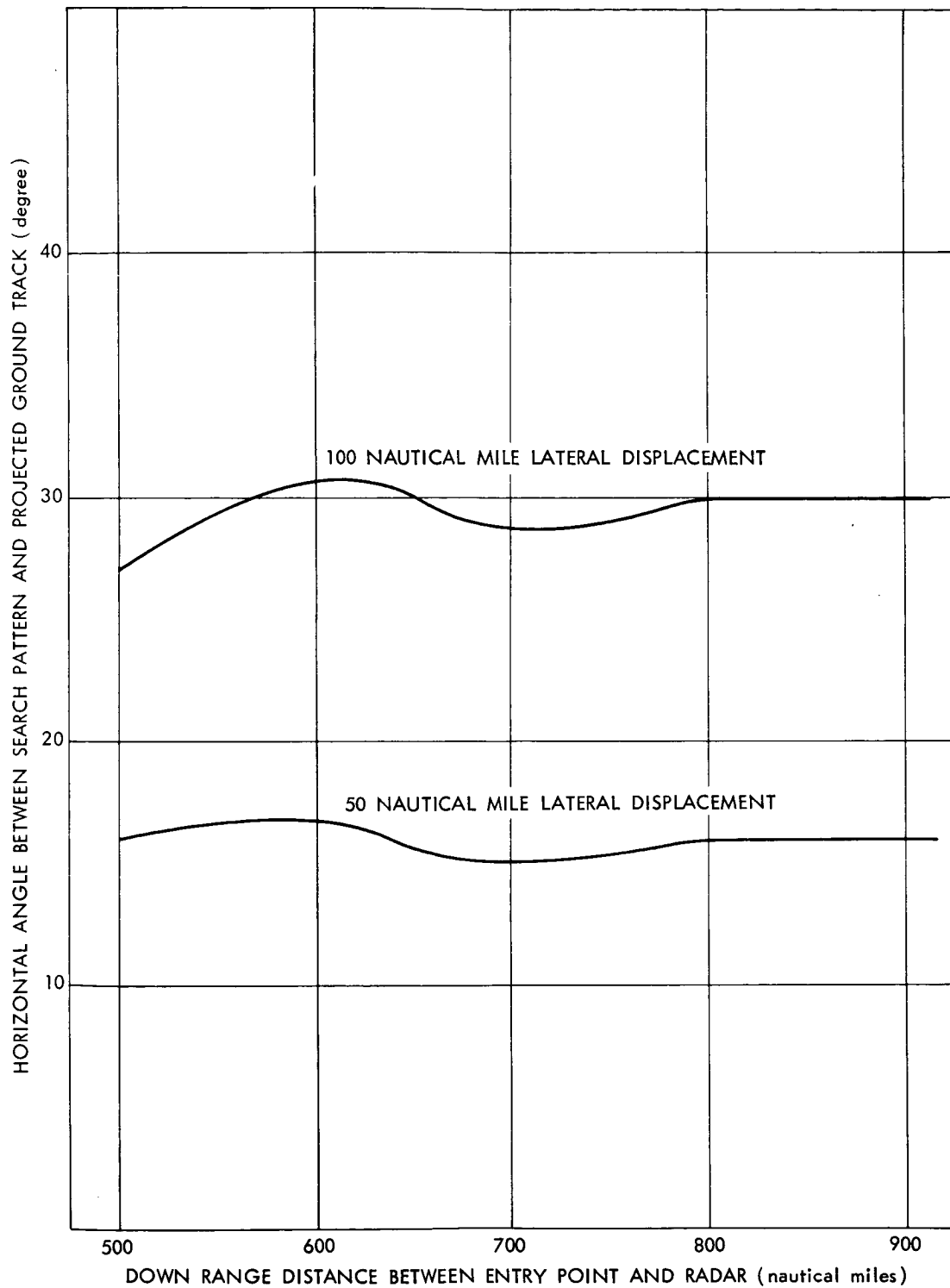
Figure 70. Optimum Offset Angle for Radar Location
from Projected Pre-Reentry Ground Track

113
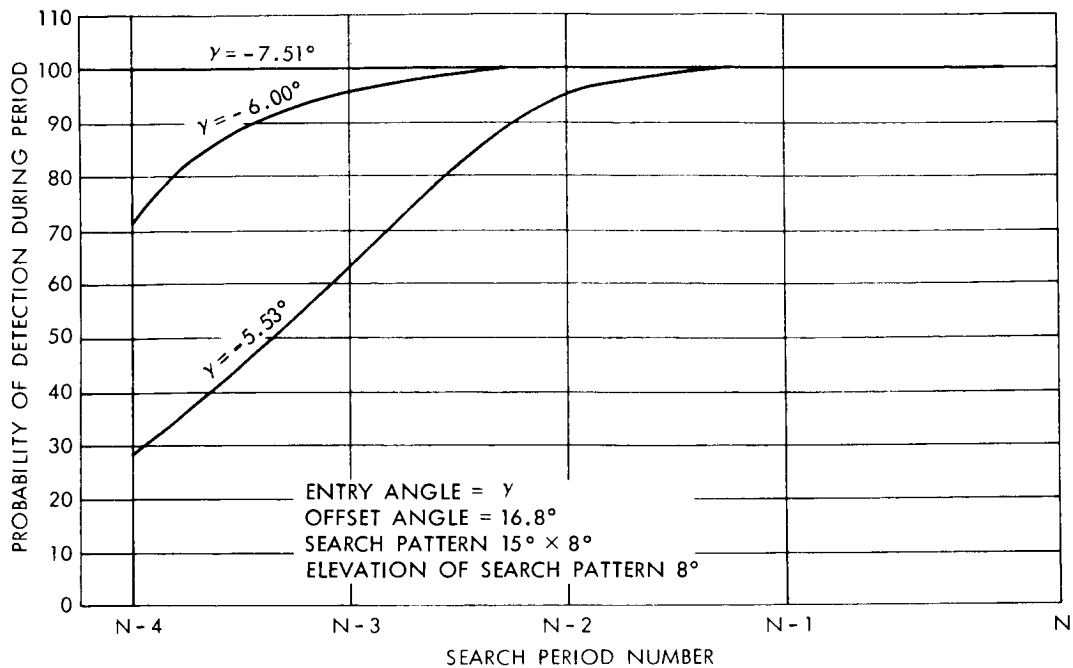
Figure 71. Probability of Detection. Station 600 Nautical Miles Down Range from Entry. Lateral Displacement 50 Nautical Miles From Projected Ground Track. Normal Trajectory with Range of 2500 Nautical Miles from Entry
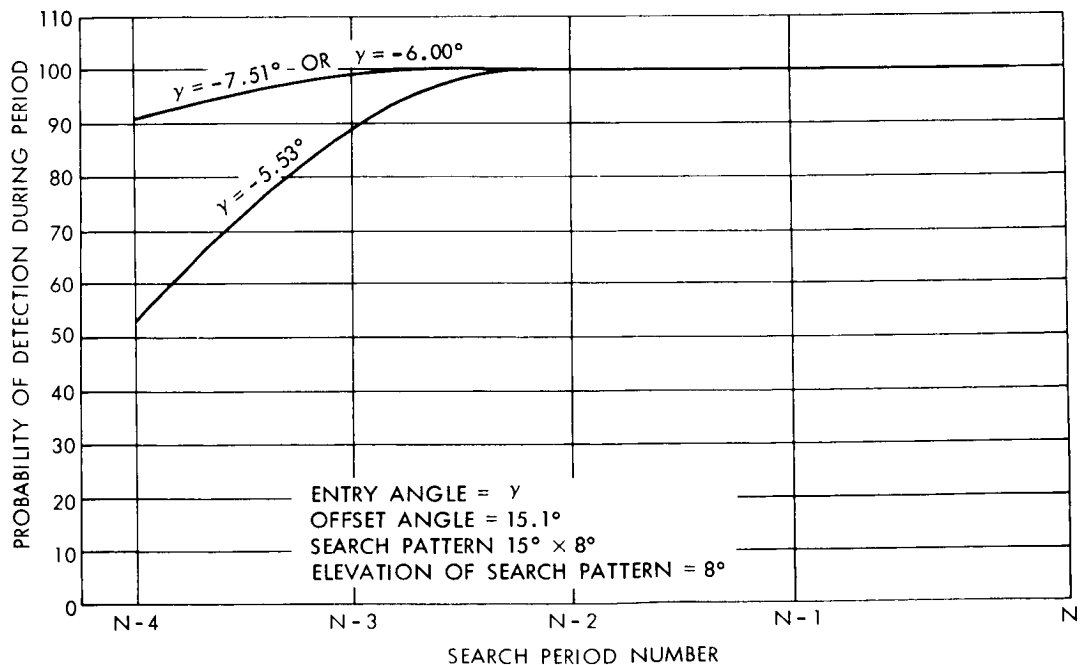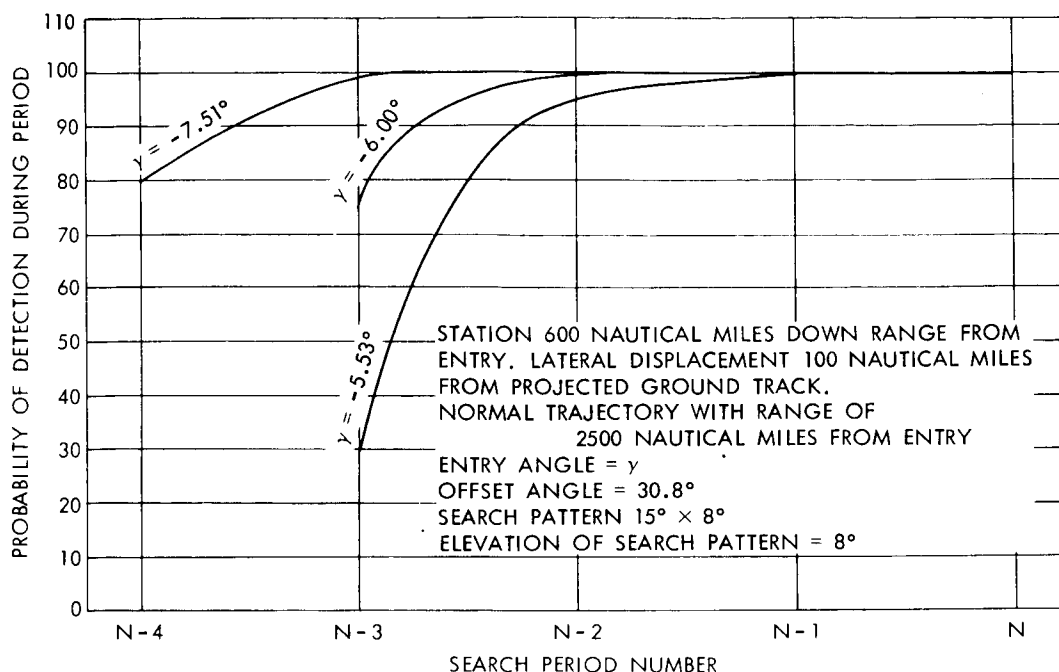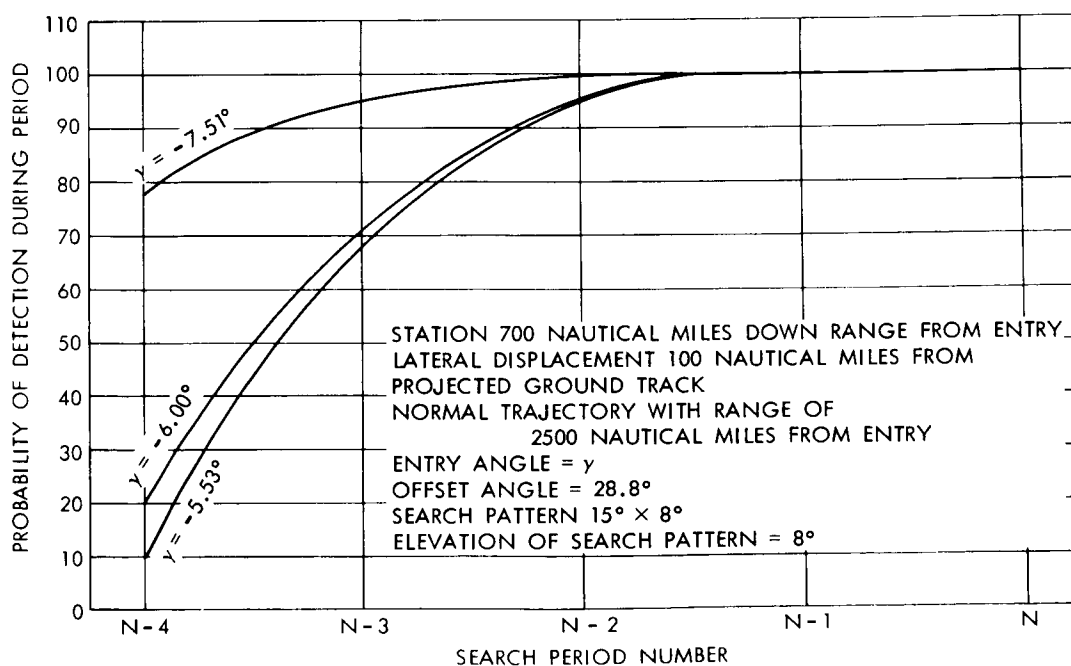

Figure 72. Probability of Detection. Station 700 Nautical Miles Down Range From Entry. Lateral Displacement 50 Nautical Miles from Projected Ground Track. Normal Trajectory with Range of 2500 Nautical Miles from Entry
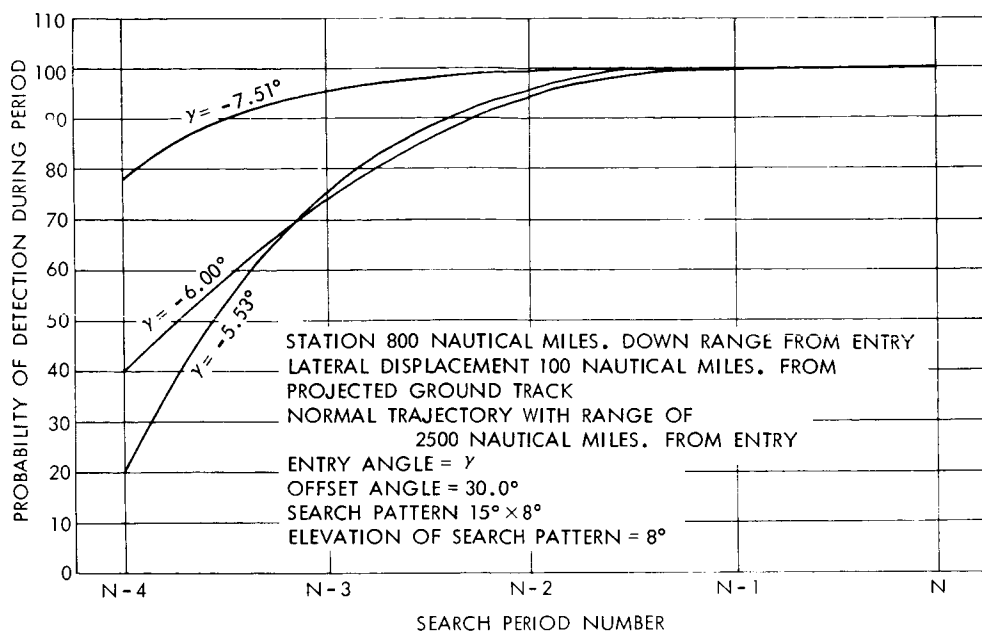
114
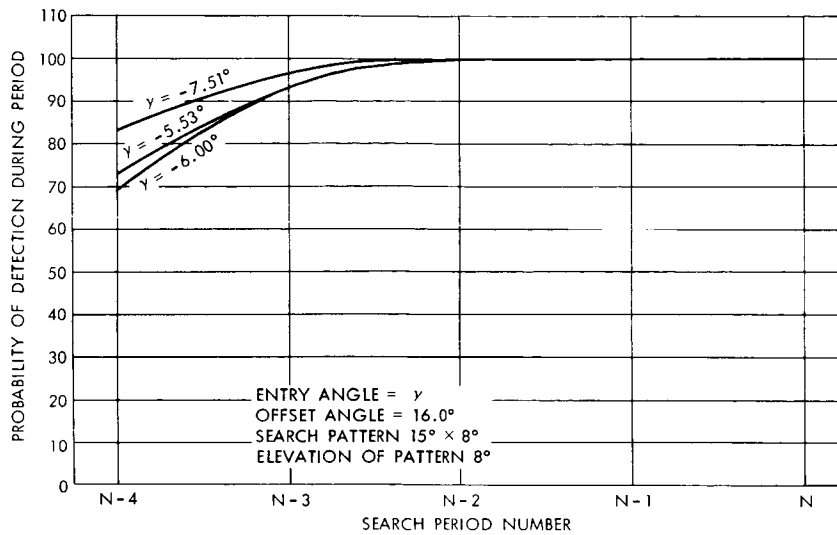
Figure 73. Probability of Detection. Station 800 Nautical Miles Down Range from Entry. Lateral Displacement 50 Nautical Miles From Projected Ground Track. Normal Trajectory with Range of 2500 Nautical Miles from Entry.
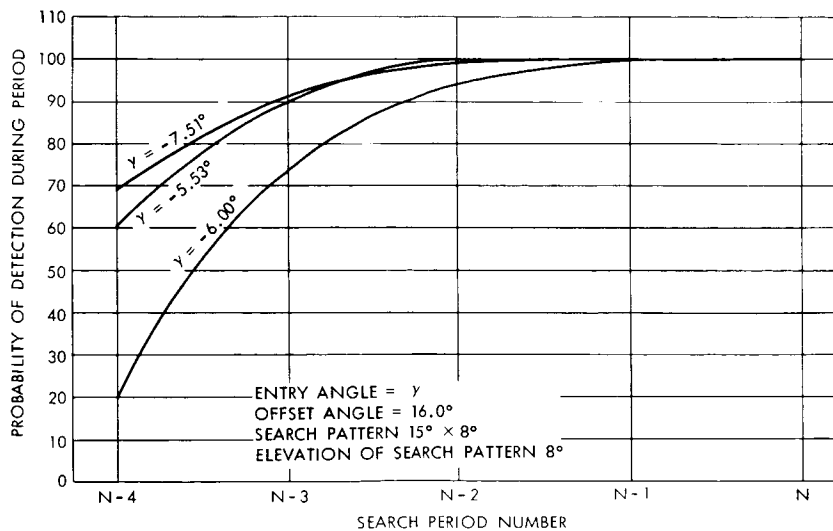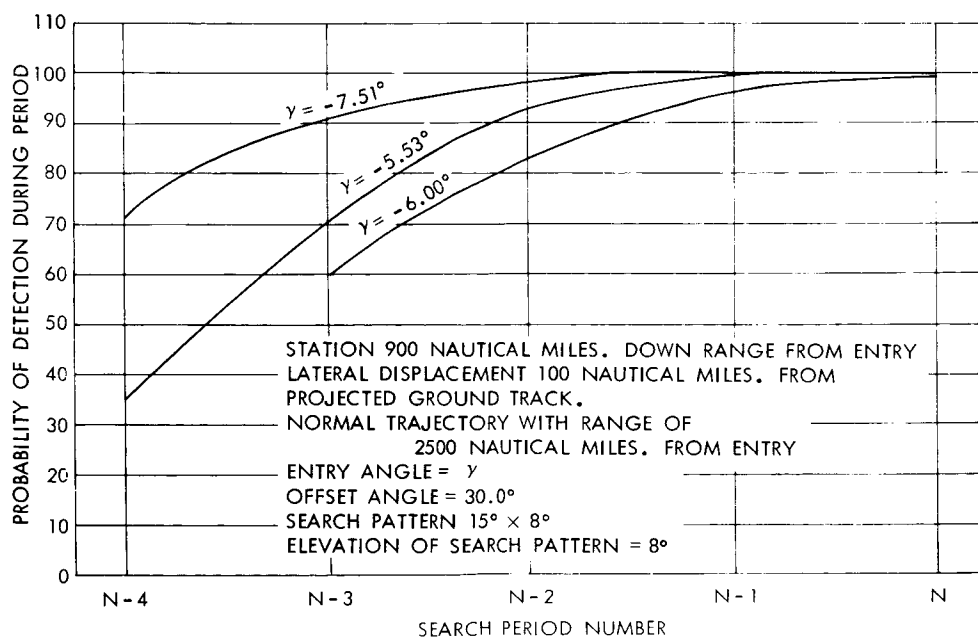

Figure 74. Probability of Detection. Station 900 Nautical Miles Down Range from Entry. Lateral Displacement 50 Nautical Miles From Projected Ground Track. Normal Trajectory with Range of 2500 Nautical Miles from Entry.

115

Figure 75. Probability of Detection. Station 600 Nautical Miles Down Range from Entry. Lateral Displacement 100 Nautical Miles from Projected Ground Track

Figure 76. Probability of Detection. Station 700 Nautical Miles Down Range from Entry. Lateral Displacement 100 Nautical Miles from Projected Ground Track. Normal Trajectory with Range of 2500 Nautical Miles from Entry.

116

Figure 77. Probability of Detection. Station 800 Nautical Miles Down Range from Entry. Lateral Displacement 100 Nautical Miles from Projected Ground Track. Normal Trajectory with Range of 2500 Nautical Miles from Entry

Figure 78. Probability of Detection. Station 900 Nautical Miles Down Range from Entry. Lateral Displacement 100 Nautical Miles from Projected Ground Track. Normal Trajectory with Range of 2500 Nautical Miles from Entry

117
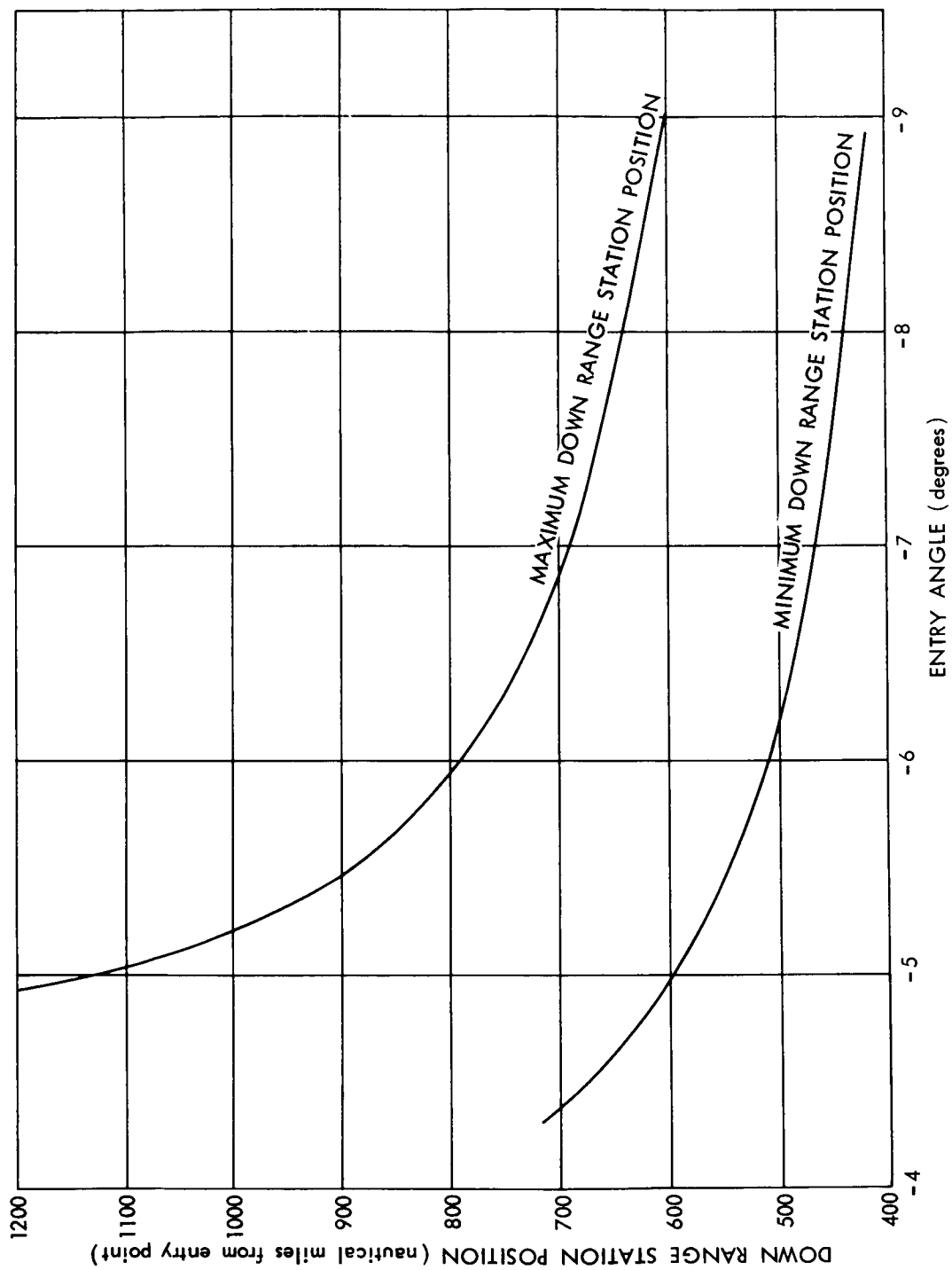
Figure 79. Maximum Down Range Station Location Based on Loss of Lower Limit 16g Trajectory. Minimum Down Range Station Location Which Will Avoid Initial Radar Absorption Area
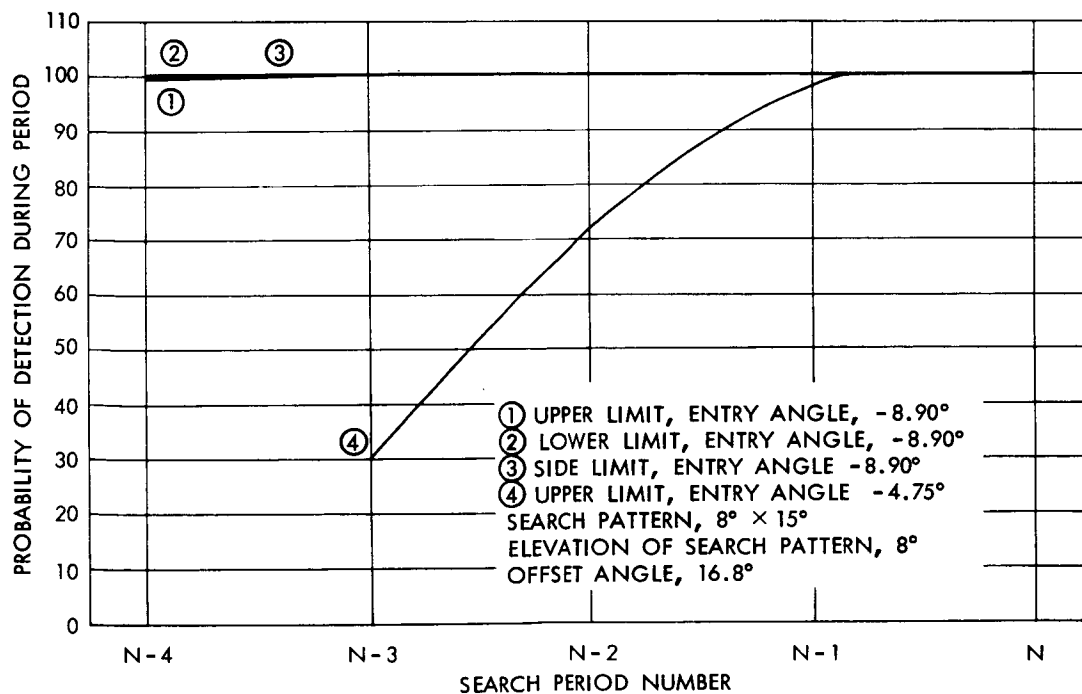
118
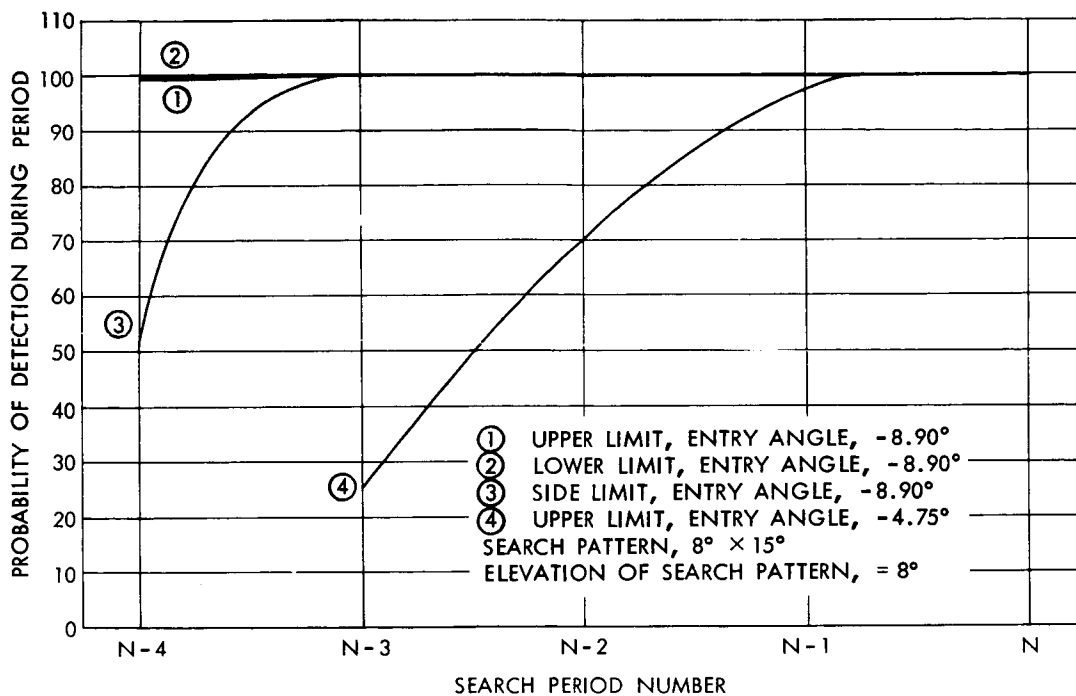
Figure 80. Probability of Detection, Station: 603 Nautical Miles Down Range, 0 Nautical Miles Cross Range

Figure 81. Probability of Detection, Station: 603 Nautical Miles Down Range, 50 Nautical Miles Cross Range
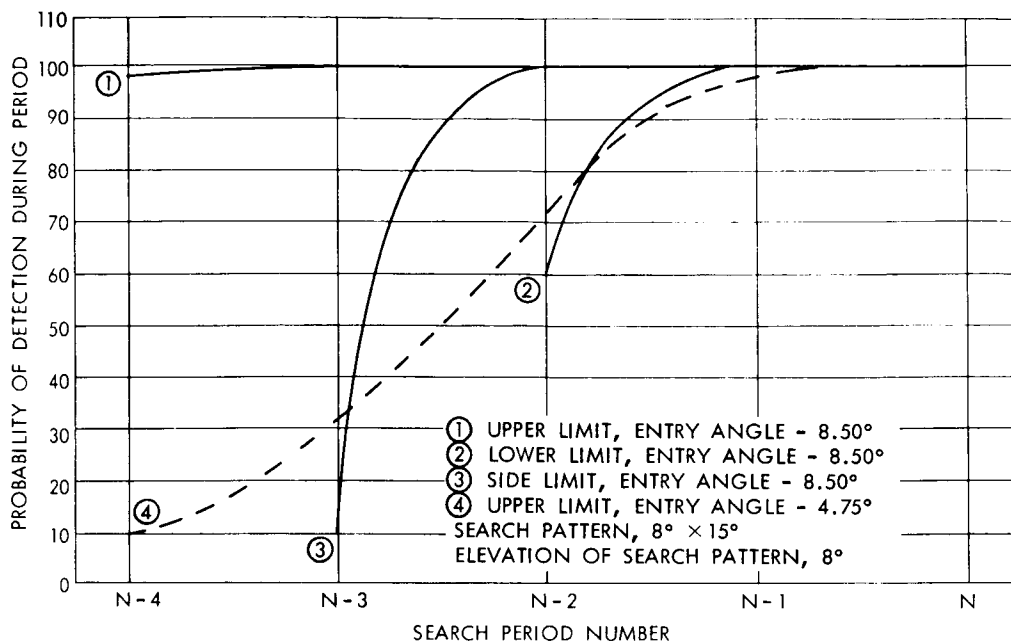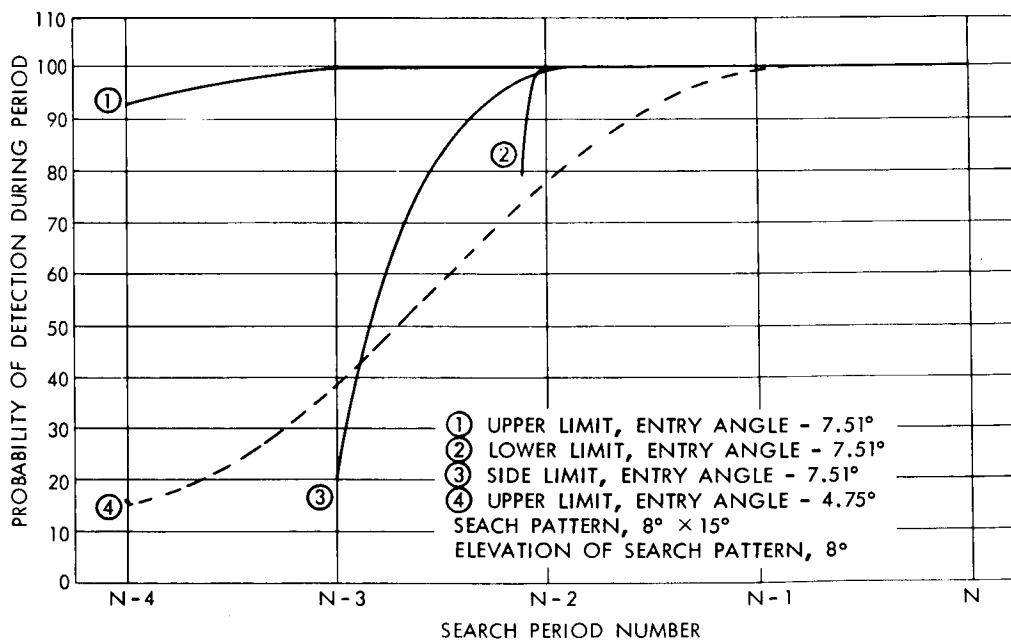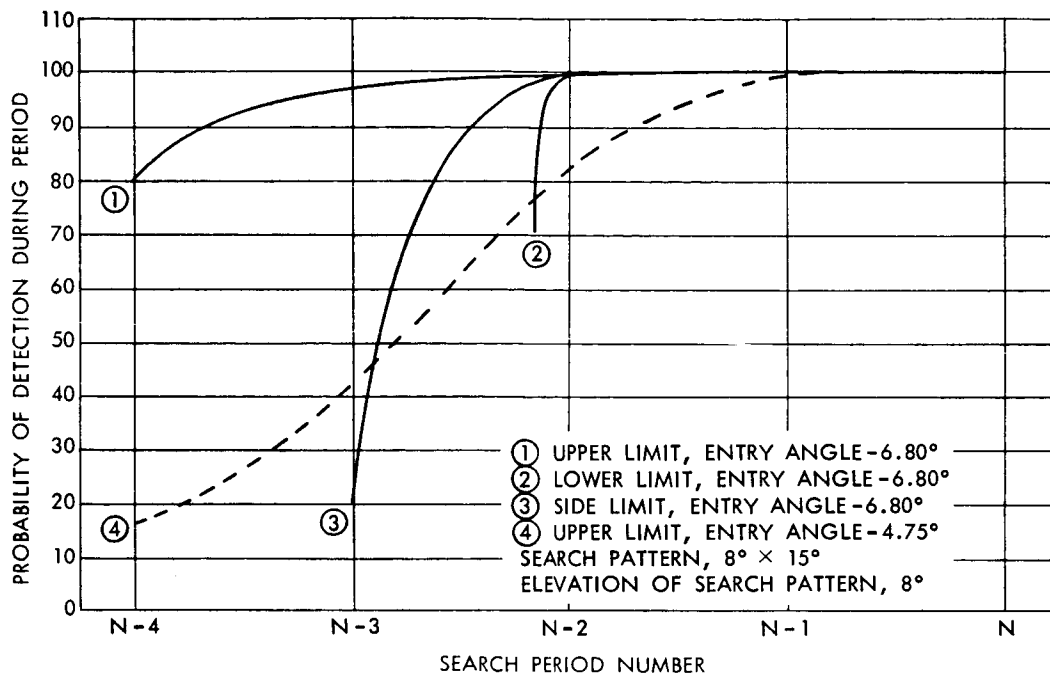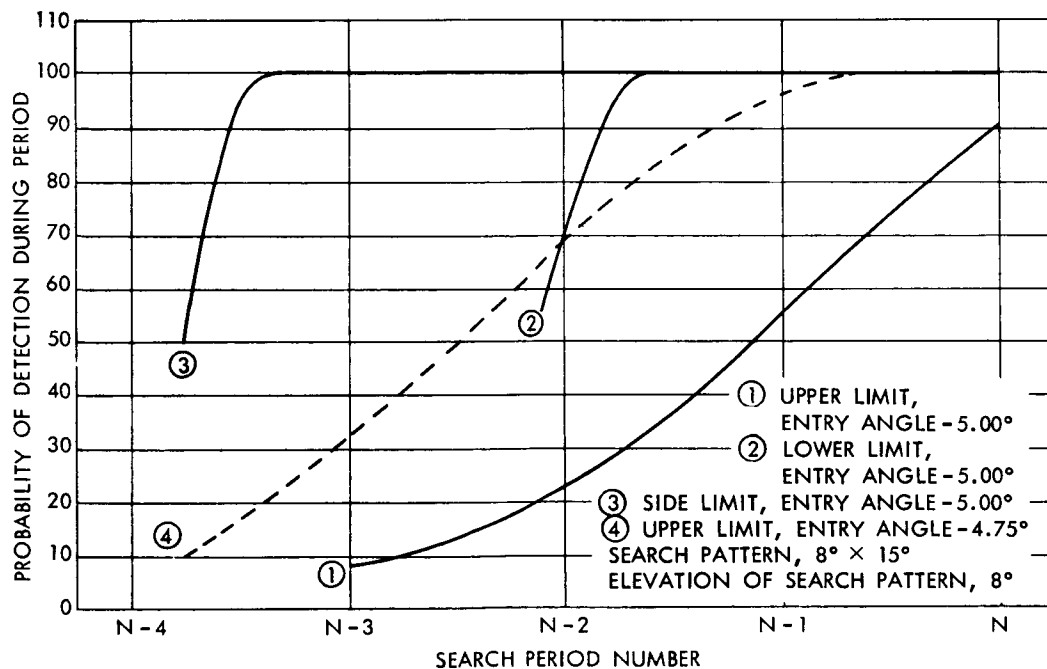
119

Figure 82. Probability of Detection, Station: 620 Nautical Miles
Down Range, 0 Nautical Miles Cross Range

The first figure contains:
- PROBABILITY OF DETECTION DURING PERIOD (y-axis, 0 to 110)
- SEARCH PERIOD NUMBER (x-axis: N-4, N-3, N-2, N-1, N)
- ① UPPER LIMIT, ENTRY ANGLE - 8.50°
- ② LOWER LIMIT, ENTRY ANGLE - 8.50°
- ③ SIDE LIMIT, ENTRY ANGLE - 8.50°
- ④ UPPER LIMIT, ENTRY ANGLE - 4.75°
- SEARCH PATTERN, 8° × 15°
- ELEVATION OF SEARCH PATTERN, 8°

Figure 83. Probability of Detection, Station: 662 Nautical Miles
Down Range, 0 Nautical Miles Cross Range

The second figure contains:
- PROBABILITY OF DETECTION DURING PERIOD (y-axis, 0 to 110)
- SEARCH PERIOD NUMBER (x-axis: N-4, N-3, N-2, N-1, N)
- ① UPPER LIMIT, ENTRY ANGLE - 7.51°
- ② LOWER LIMIT, ENTRY ANGLE - 7.51°
- ③ SIDE LIMIT, ENTRY ANGLE - 7.51°
- ④ UPPER LIMIT, ENTRY ANGLE - 4.75°
- SEACH PATTERN, 8° × 15°
- ELEVATION OF SEARCH PATTERN, 8°

120

Figure 84. Probability of Detection, Station: 705 Nautical Miles
Down Range, 0 Nautical Miles Cross Range

Figure 85. Probability of Detection, Station: 1138 Nautical Miles
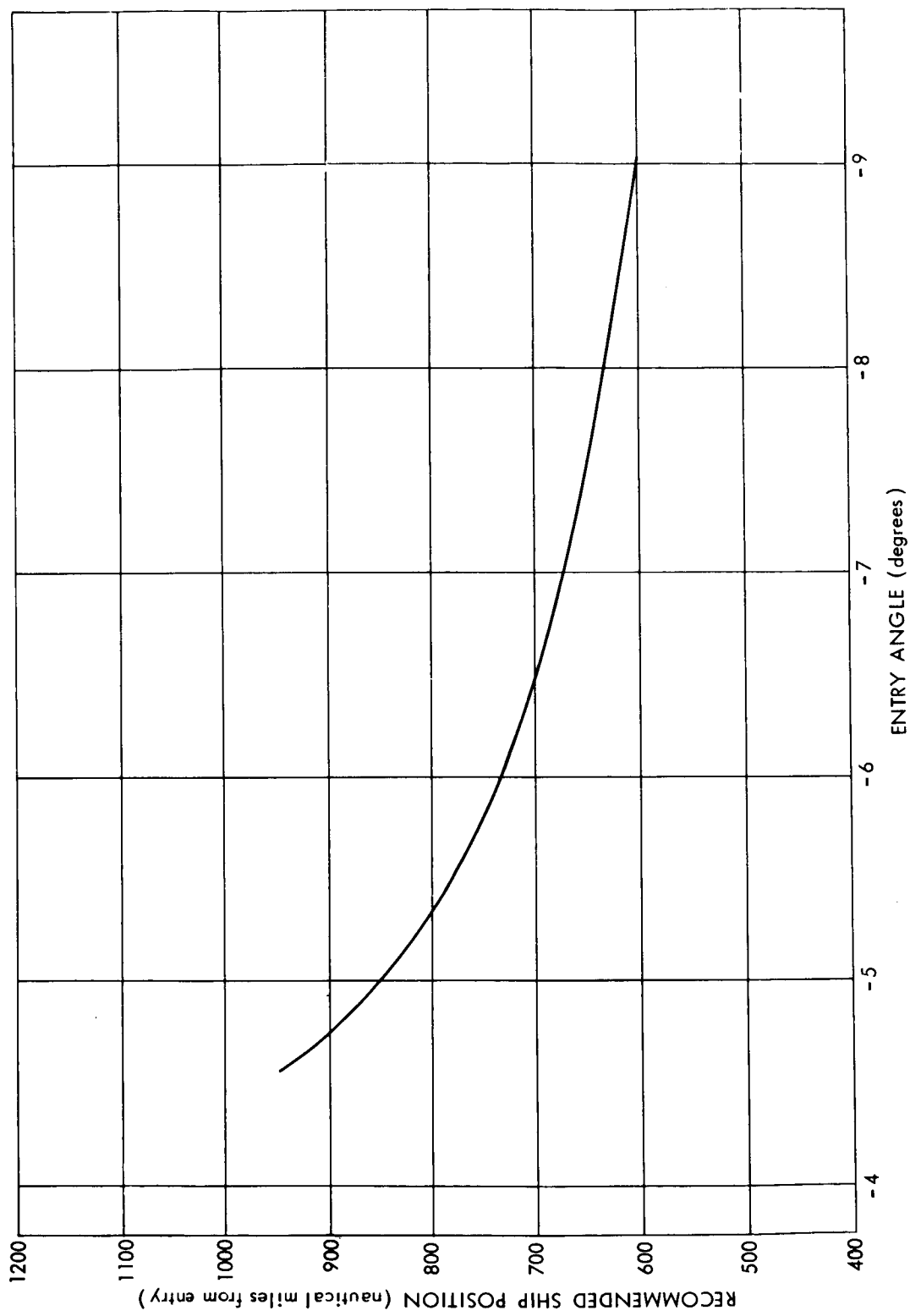Down Range, 0 Nautical Miles Cross Range

121

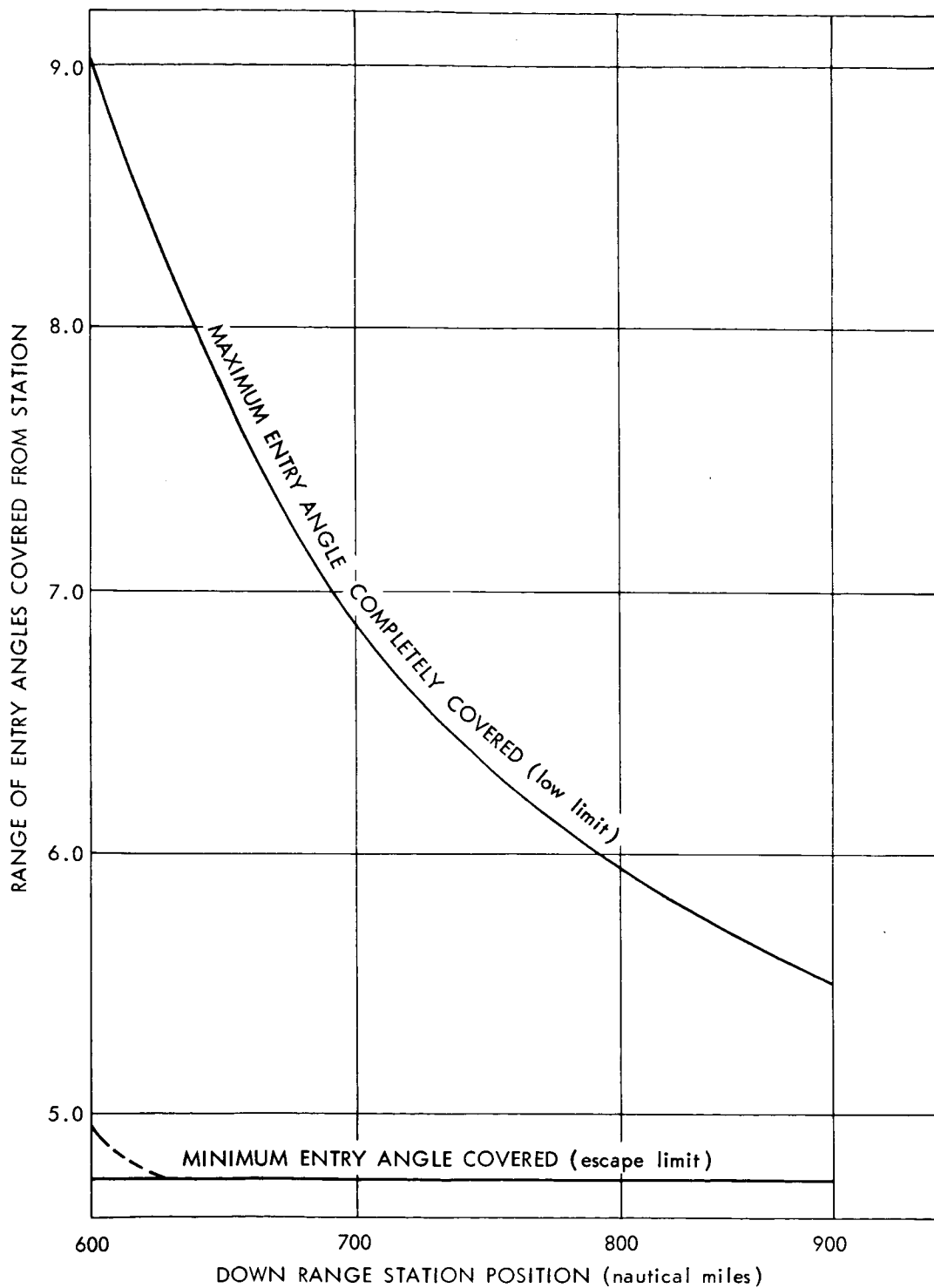Figure 86. Recommended Down Range Distance Between Entry Point and Radar Position

Figure 87. Range of Entry Angles Covered to Desired Probability of Detection
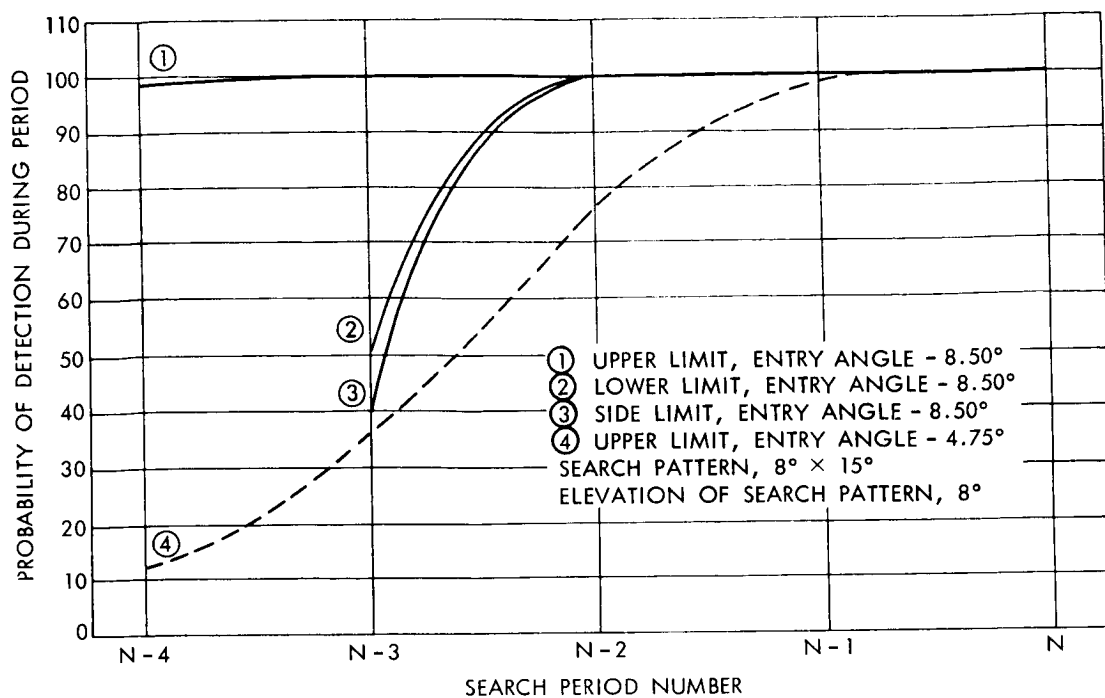Level By Radar Stationed According to Figure 86

Figure 88. Probability of Detection, Station: 618 Nautical Miles Down Range, 0 Nautical Miles Cross Range
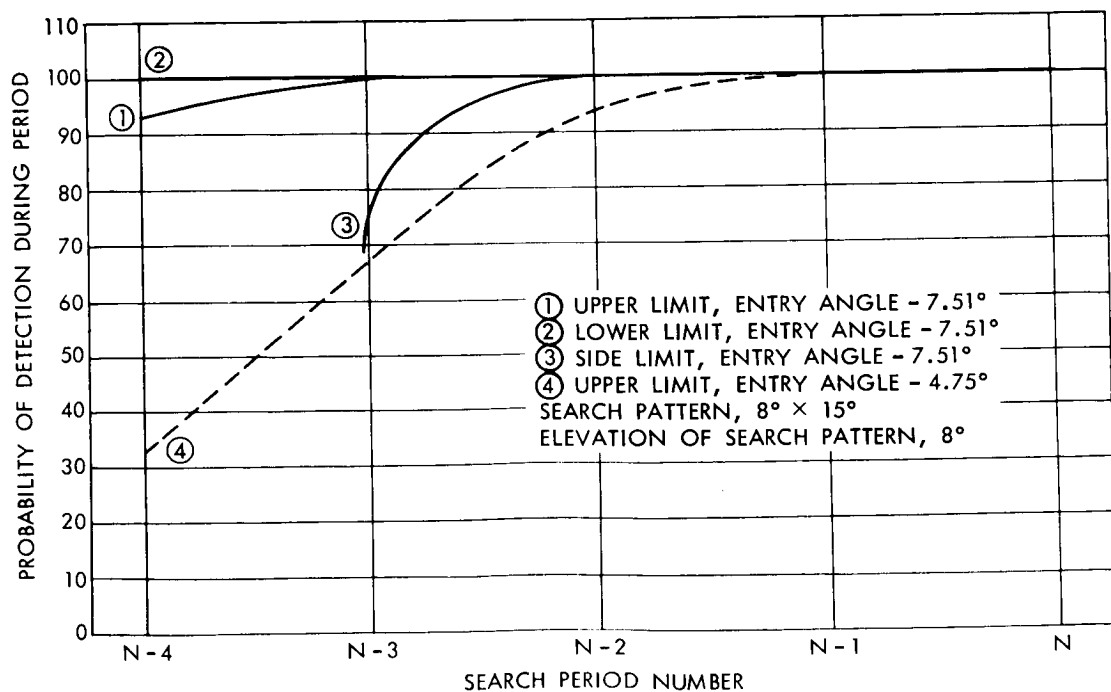

Figure 89. Probability of Detection, Station: 650 Nautical Miles Down Range, 0 Nautical Miles Cross Range
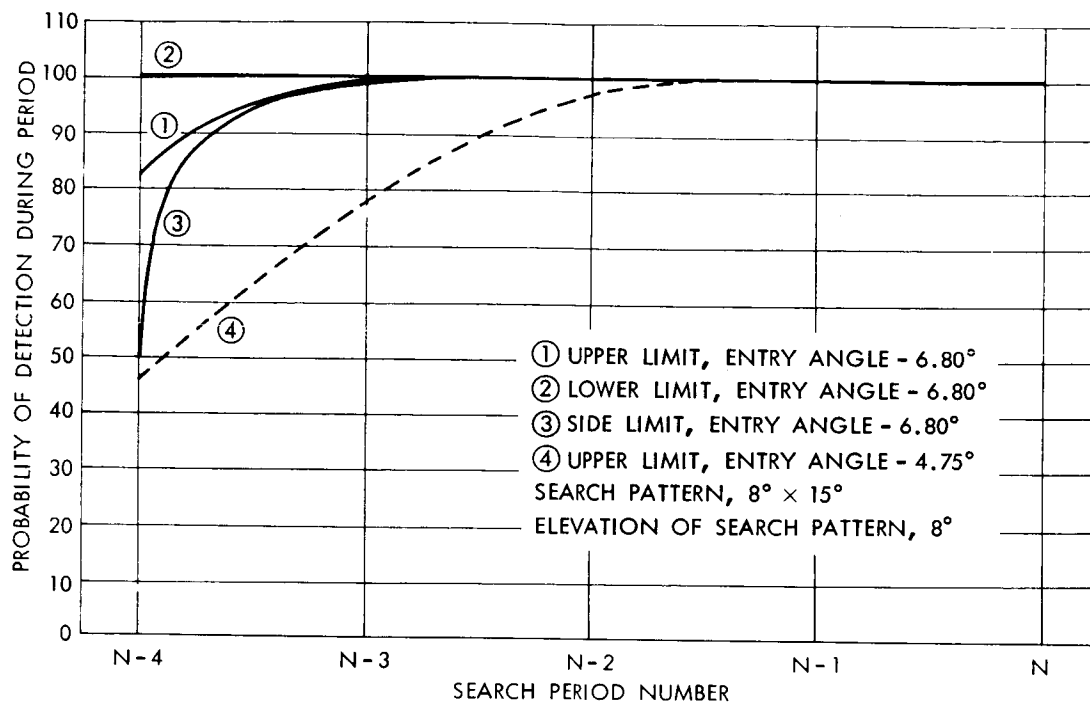
124

Figure 90. Probability of Detection, Station: 683 Nautical Miles
Down Range, 0 Nautical Miles Cross Range

Figure 91. Probability of Detection, Station: 852 Nautical Miles
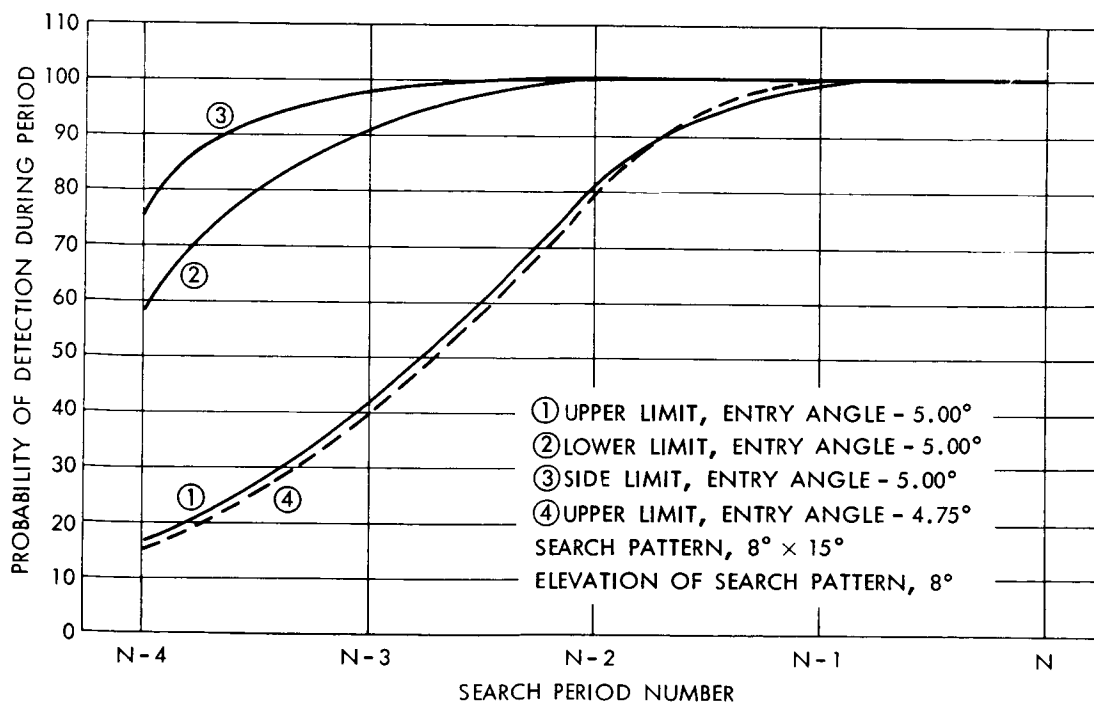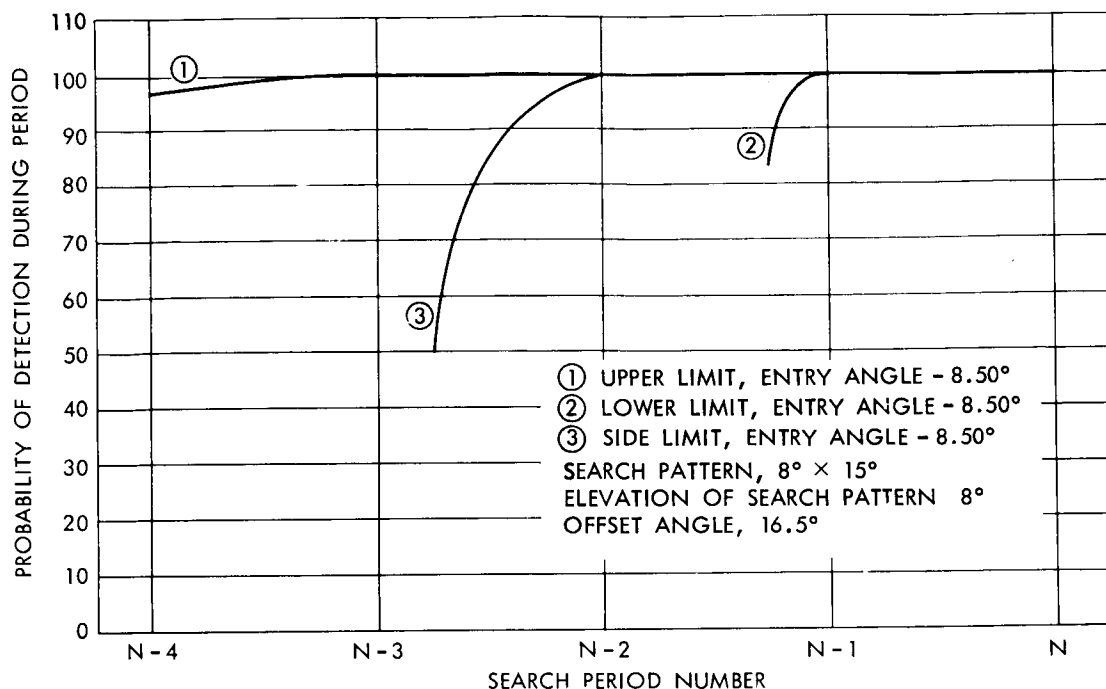Down Range, 0 Nautical Miles Cross Range

125

Figure 92. Probability of Detection, Station: 618 Nautical Miles Down Range, 50 Nautical Miles Cross Range

Figure 93. Probability of Detection, Station: 650 Nautical Miles Down Range, 50 Nautical Miles Cross Range
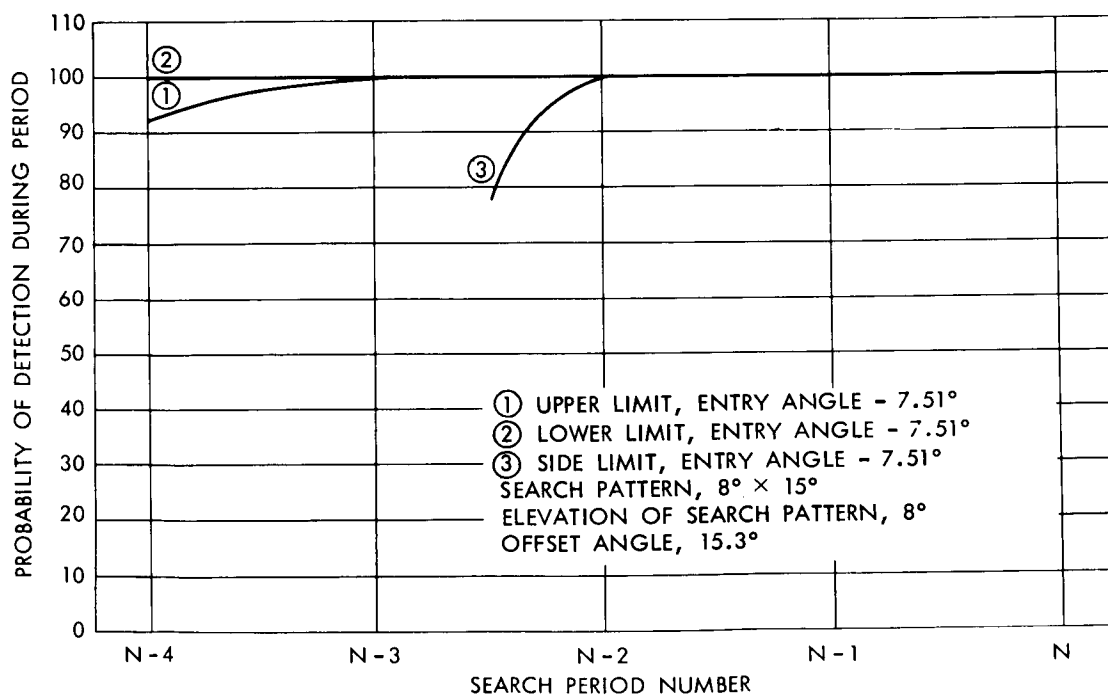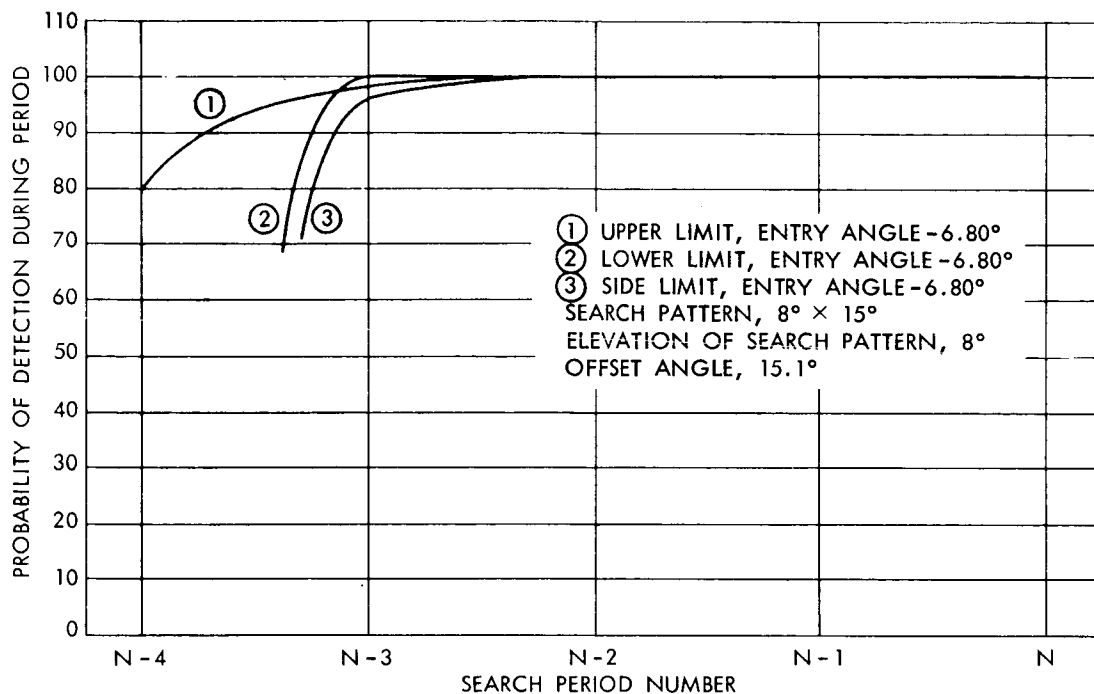
126

Figure 94. Probability of Detection, Station: 683 Nautical Miles
Down Range, 50 Nautical Miles Cross Range

Figure 95. Probability of Detection, Station: 850 Nautical Miles
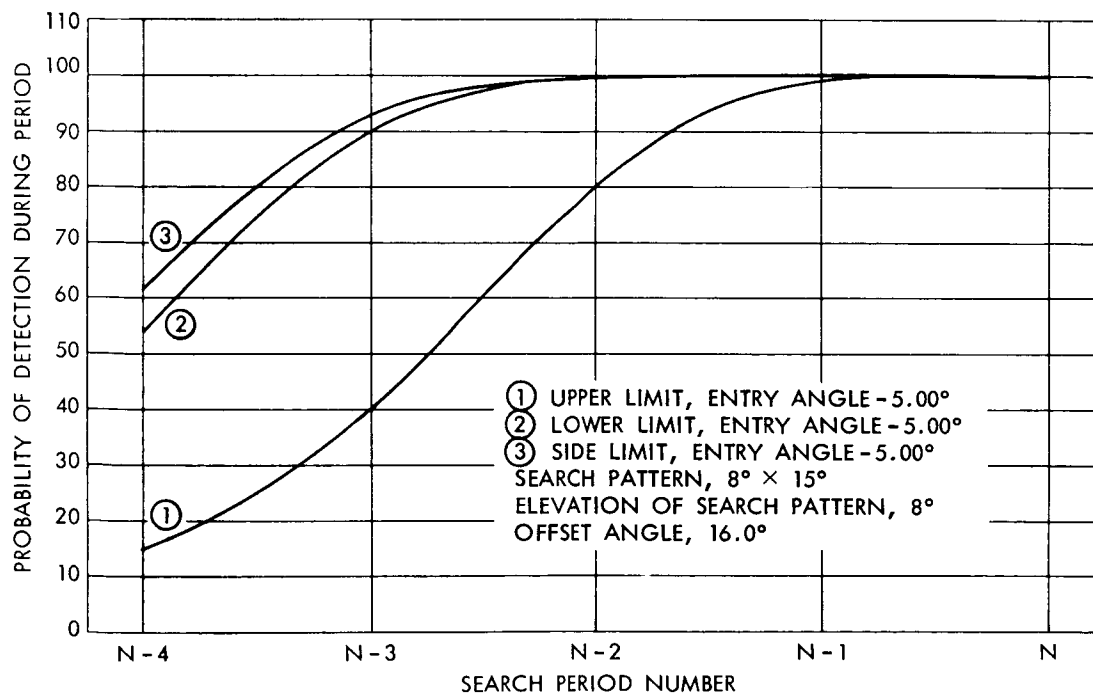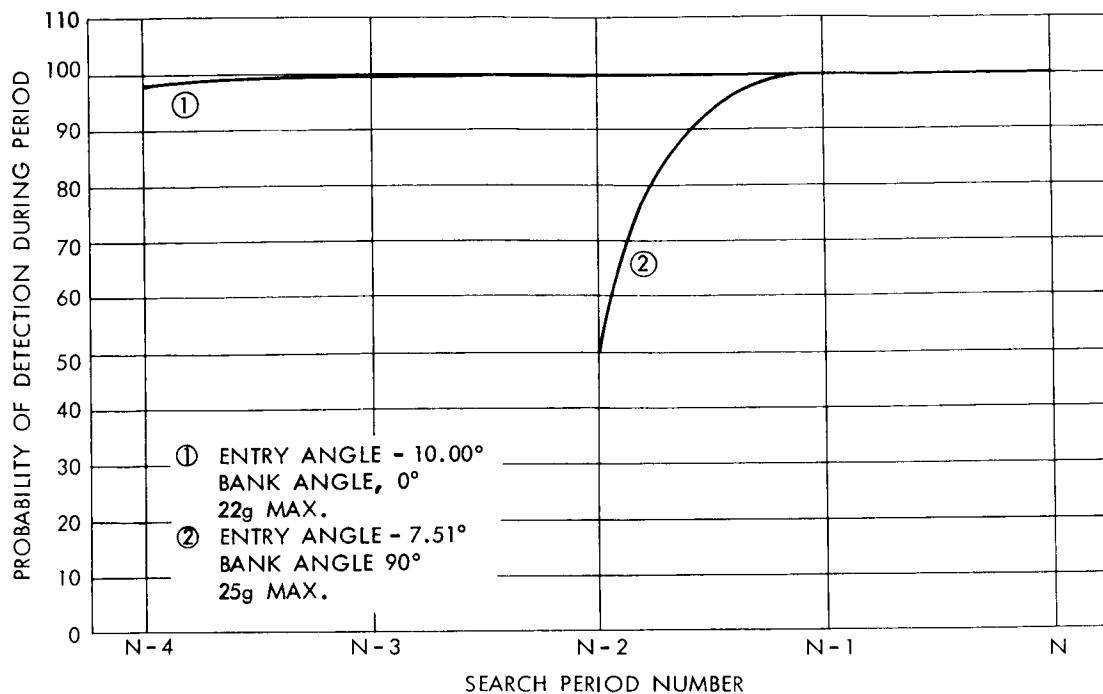Down Range, 50 Nautical Miles Cross Range

127

Figure 96. Probability of Detection, Example of High g Trajectories
Station: 618 Nautical Miles Down Range, 0 Nautical Miles Cross Range
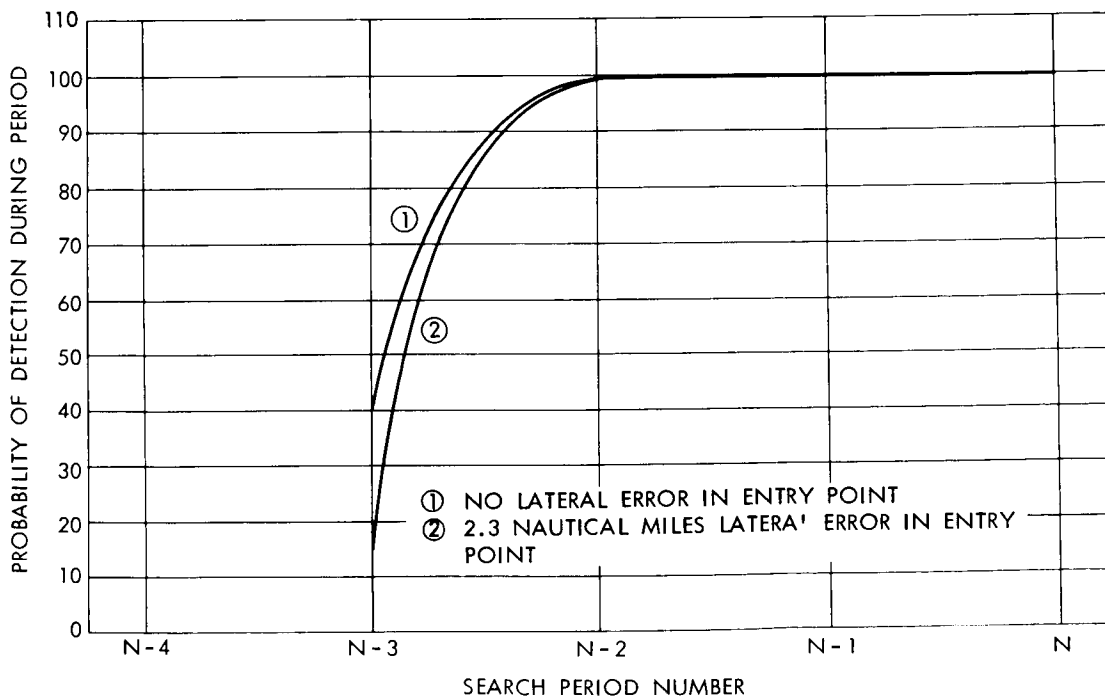

Figure 97. Probability of Detection, Lateral Error in Entry Point
Station: 618 Nautical Miles Down Range, 0 Nautical Miles Cross Range
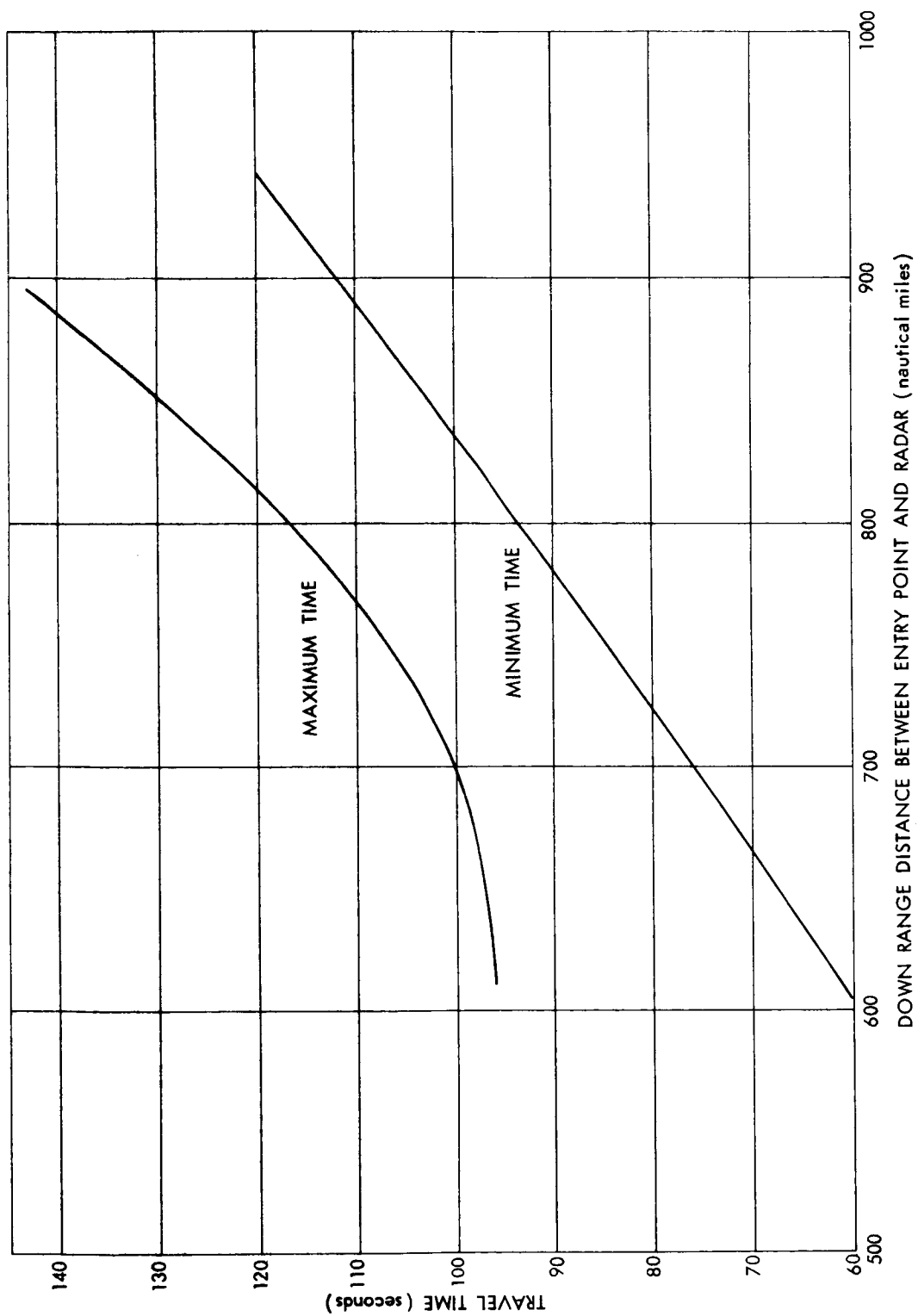
Figure 98. Variation in Time Required to Traverse Distance Between Entry Point and Radar Search Area

129
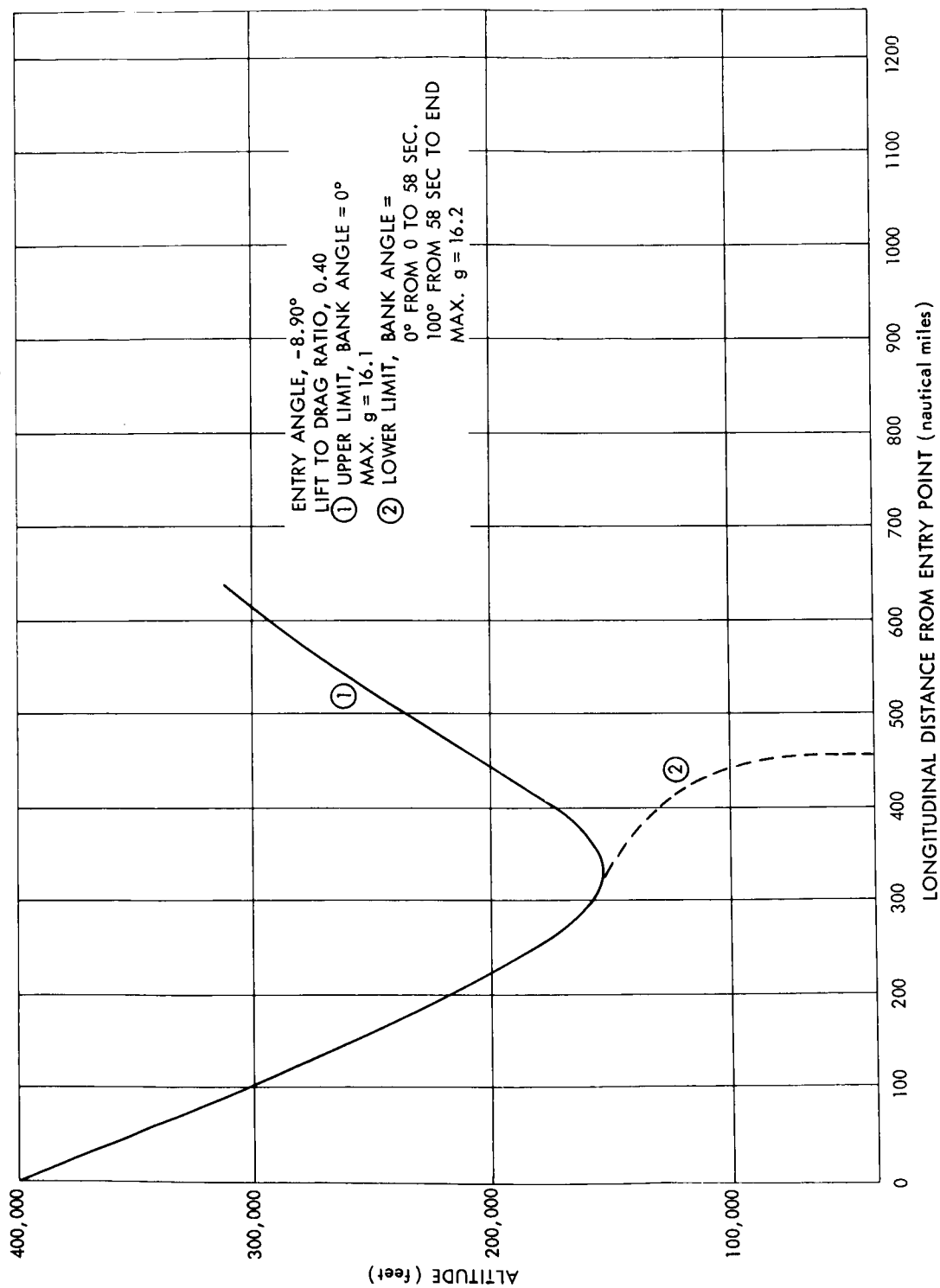
Figure 99. Horizontal Projection of Trajectories Entry Angle, –8.90° Lift to Drag Ratio, 0.40

ENTRY ANGLE, –8.90°
LIFT TO DRAG RATIO, 0.40
① UPPER LIMIT, BANK ANGLE = 0°
MAX. g = 16.1
② LOWER LIMIT, BANK ANGLE =
0° FROM 0 TO 58 SEC.
100° FROM 58 SEC TO END
MAX. g = 16.2

LONGITUDINAL DISTANCE FROM ENTRY POINT (nautical miles)

ALTITUDE (feet)
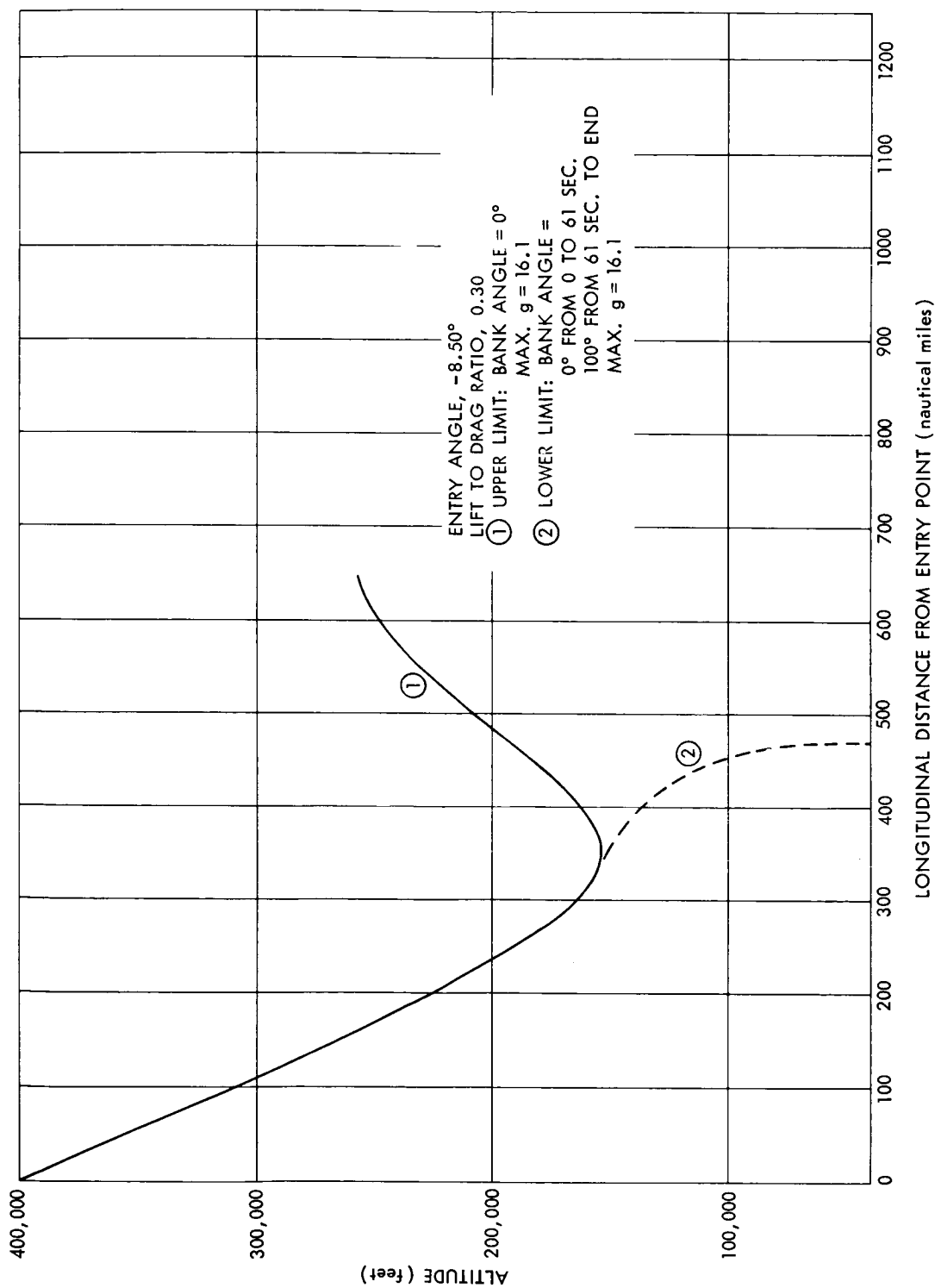
Figure 100. Horizontal Projection of Trajectories Entry Angle, -8.50° Lift to Drag Ratio, 0.30

131
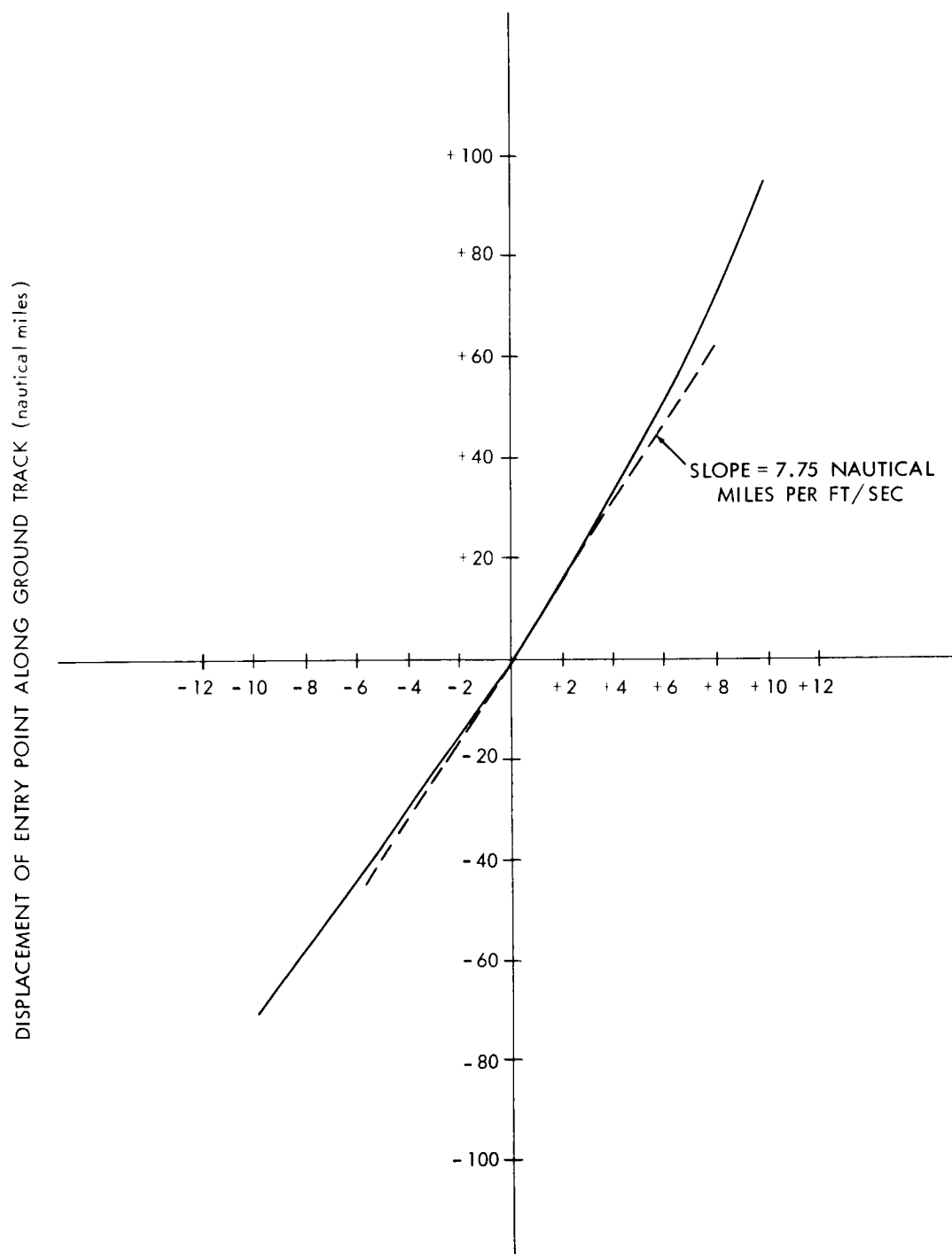
Figure 101. Down Range Displacement of Entry Point by Increment
in Velocity in Direction of Velocity Vector Applied 10 Hours Before Entry
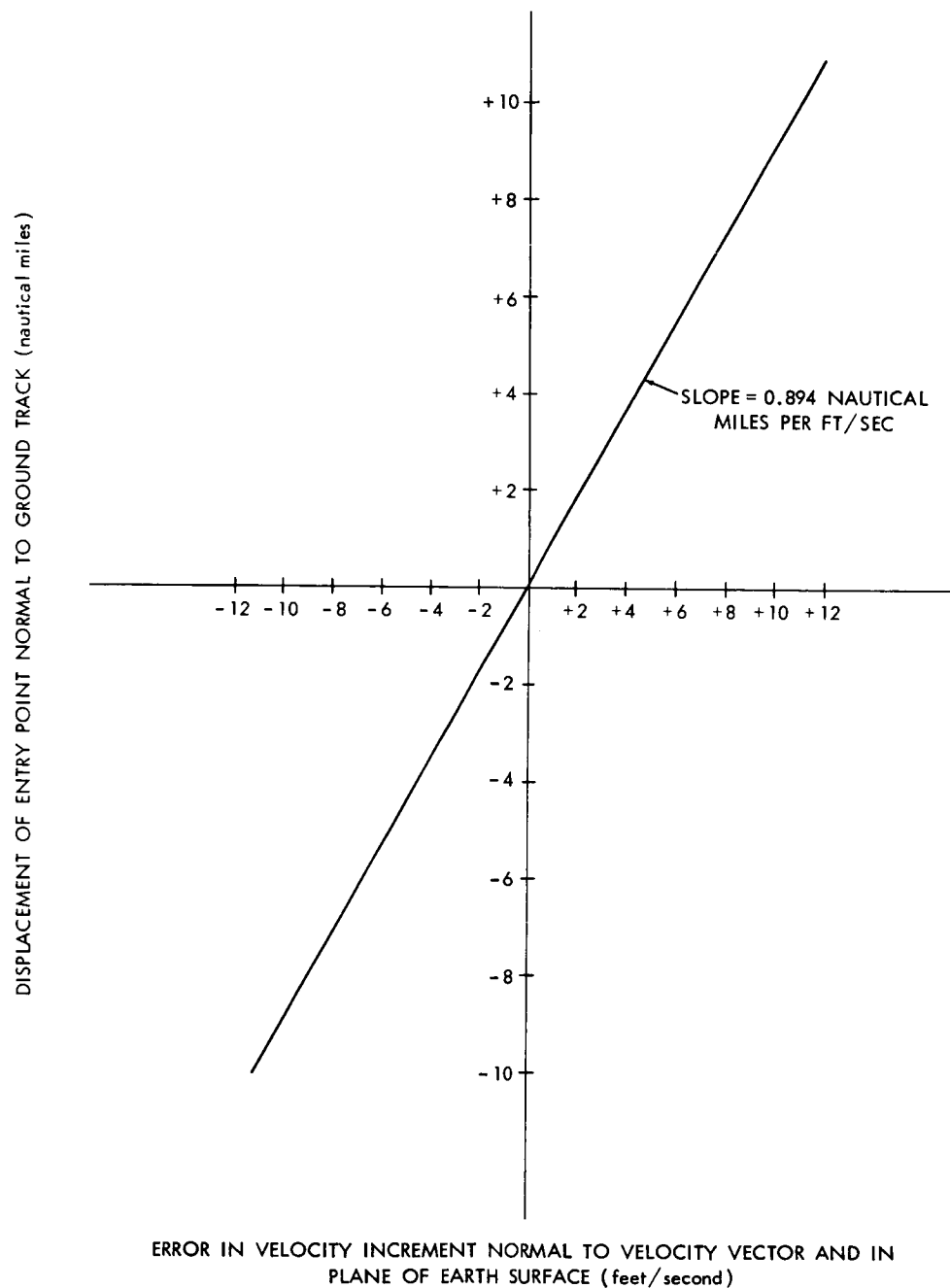
Figure 102. Cross Range Displacement of Entry Point by Increment in Velocity Normal to Velocity Vector and Normal to Earth Radius Vector, Applied 10 Hours Before Entry

133

Figure 103. Down Range Displacement of Entry Point By Increment in Velocity
Normal to Velocity Vector in Plane of Velocity Vector and Earth
Radius Vector. Increment Applied 10 Hours Before Entry

DISTANCE DOWN RANGE FROM DESIRED SHIP POSITION (nautical miles)
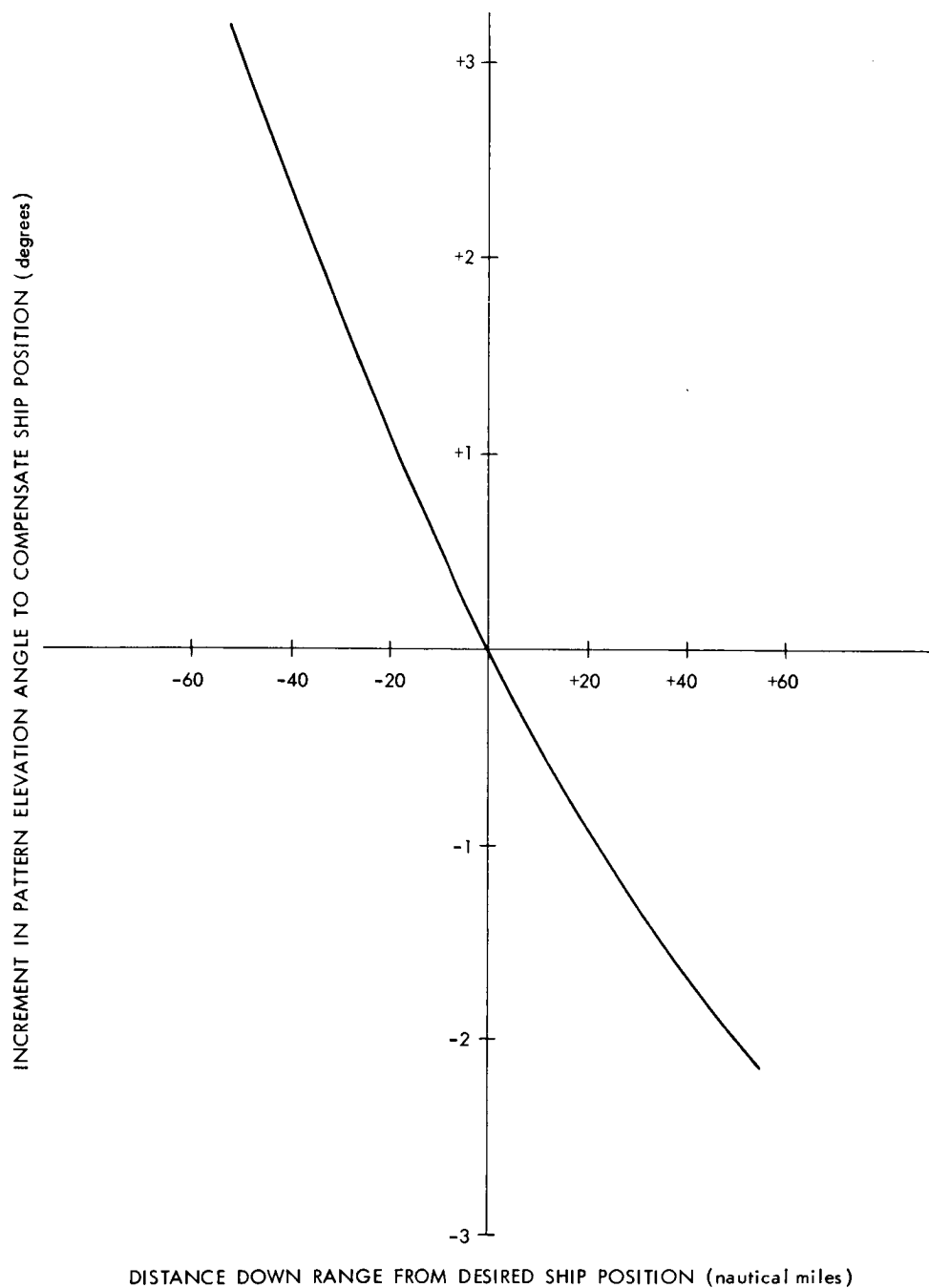
Figure 104. Increment in Pattern Elevation Angle to Compensate for Down
Range Displacement of Radar From Desired Position. To Be
Used Only On Low Limit or Near Low Limit Trajectories.

135

Figure 105. Increment in Azimuth Angle to Compensate for Cross Range
Displacement of Radar From Desired Position on Ground Track

APPENDIX A

COMPUTATION FOR 8° x 15° SEARCH PATTERN

The 8° high by 15° wide search pattern is composed of four 2° high horizontal passes, each 15.3° wide. The fourth pass terminates on the same side of the raster as the first pass originates, so that it is only necessary to lower the beam to the initial condition to start the second raster.
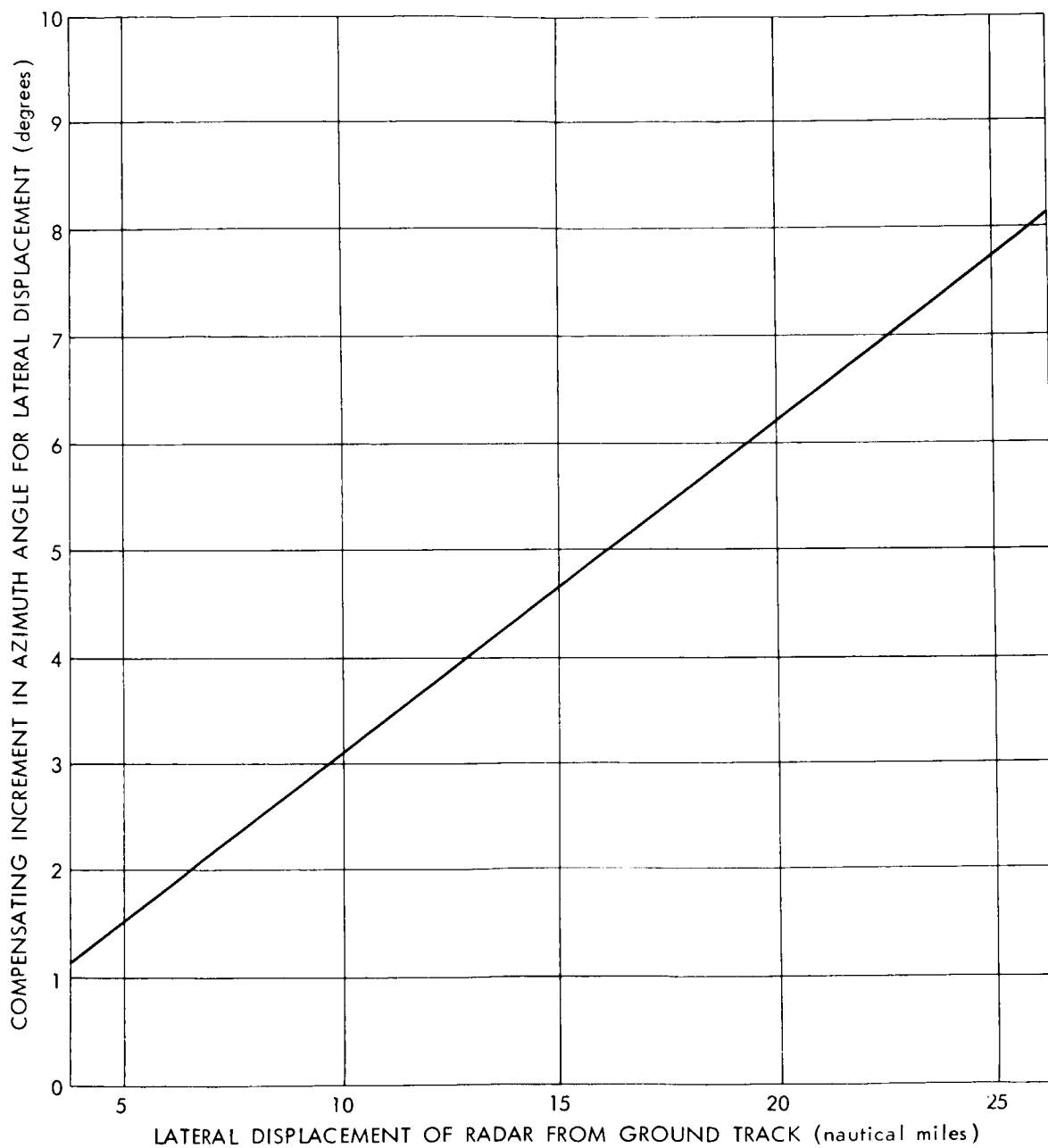
During the horizontal pass, the center line of the beam moves a distance of 14.958°. The added coverage is contracted by the width of nominal active width of the beam. (This is quite conservative since the range of travel in the end zone is so slow that the use of a full beam diameter would be justified.)

Vertical motion is started one degree before the end of the horizontal pass so that by the time the horizontal pass is completed, one half of the vertical motion, for a 2° vertical traverse, is completed. This results in a rounded corner on the raster, but the slow speed of the traverse increases the effective beam size so that the corner is essentially filled in.

Each complete pass will consist of a horizontal section with a quarter of a circle at each end. The upper pass has the quarter circles pointed downward and the lower pass has the terminal quarter circles pointed upward. The two interior passes have the circle section up at one end and down at the other end.

The return from the top trace to the bottow trace is accomplished by withholding the initiation of the first horizontal trace in the next raster until an additional vertical travel of four degrees is completed. This vertical motion is accomplished by continuing the downward vertical acceleration to the mid point in the raster and then applying an equal deceleration until the beam reaches the bottom of the raster. As may be expected, the horizontal trace is initiated one degree before this vertical motion is completed.

The time for each horizontal pass is computed as follows:

Time to accelerate to 18° per sec = 18.000 ÷ 52 = 0.346 sec

Distance traveled in this time = 0.346 x 18.000/2 = 3.115°

Distance traveled in deceleration = 3.115°

Distance traveled at constant velocity = 14.958 - (2 x 3.115) = 8.728°

A-1

Time for constant velocity = 8.728 ÷ 18 = 0.485 sec

Total time for pass = 0.485 + (2 x 0.346) = 1.177 sec

Time for normal 1° vertical = 2 x 1/52 = 0.196 sec

Time for return cycle = 2 x 3/52 = 0.340 sec

Additional time for vertical return = 2(0.340 - 0.196) = 0.288 sec

Total time for raster = (4 x 1.177) + 0.288 = 4.996 sec

It can be observed that the vertical return trace falls over an area which has already been search by the vertical pass between the two middle horizontal passes. This duplication may be avoided if the middle horizontal passes are shortened by 0.3° and the outer horizontal passes are extended during the constant velocity portion of the pass. The resultant raster is 8° high by 15.6° wide.

Figure 1-A is a plot of the path followed by the center of the radar beam in executing the search pattern.

The vertical progress of the beam in the search pattern must be from bottom to top, that is, the first horizontal sweep must be at the lowest elevation angle.
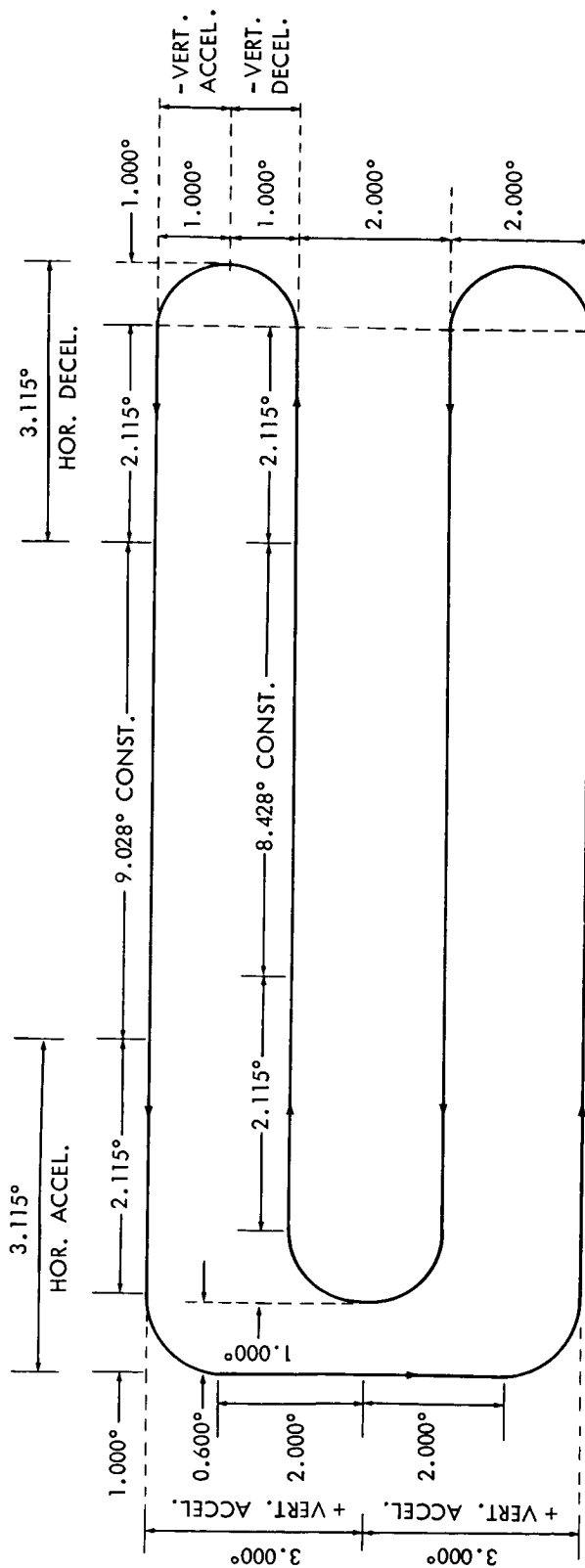
Figure A-1. Motion of Radar Beam for Development of 8° x 15° Search Pattern

APPENDIX B

Recommended procedure for completing acquisition after the initial detection.

An examination of the possible trajectory pattern shows that with the 5° x 15° pattern at an elevation of 8° the maximum angular velocity of the space-craft relative to the radar is different in the horizontal and vertical planes. In the vertical plane the angular velocity in the upward direction may be as much as 0.3° per second. In the downward direction the maximum angular velocity is less than 0.1° per second.

When the radar is stationed on the projected pre-reentry ground track, the angular velocity is the horizontal plane seldom exceeds 0.5° per second. How-ever, from an offset position of 50 nautical miles the azimuth angular velocity may be as high as ± 0.8° per second.

In preparing the following acquisition pattern, an azimuth angular velocity of 0.8° per second has been used. Offset distances in excess of 50 nautical miles will degrade the performance of the equipment against spacecraft in a trajectory which presented the maximum angular velocity in the horizontal plane.

Let it be assumed that the signal is observed when the radar is moving at a maximum horizontal velocity of 18° per second. Upon confirmation of the tar-get, the azimuth motion is arrested as quickly as possible. The deceleration is taken as 52° per second. This requires a time of 0.346 seconds and an angular distance of 3.11°.

During the initial horizontal deceleration period the elevation is changed so that the mid point between the middle and lower beam is at the level of the center of the beam in which the signal was observed. The maximum vertical movement required would be 1.5 vertical effective beam widths, or 1°, requiring 0.283 seconds.

The beam is accelerated to 11 degrees per second in the reverse direction, requiring 0.211 seconds and a distance of 1.160°.

The speed is now reduced to 4° per second in 0.135 seconds and 1.010° of angular distance.

At this point the beam center has moved forward 3.110° and returned 2.170° so that in azimuth the center of the beam is now 0.940 from the center

The total time since detection is 0.692 seconds, so that the spacecraft if it were in the extreme forward edge of the detecting beam, could now be 0.375 + (0.8 x 0.692) or 0.928 from the original center. Thus, the beam pattern has not reached the most advanced spacecraft position.

The beam is now moved at a constant velocity of 4° per second for 0.600 seconds or 2.400°. Motion is then stopped by constant deceleration in 0.077 seconds and 0.154° distance.

The beam has reached the most backward extent of the traverse. The center of the beam is -1.614° from the origin. The time elapsed from the initiation of the cycle is 1.369 seconds.

If it is assumed that the target were in the trailing edge of the beam at the start of the cycle it could now be -1.470° displaced from the origin in the horizontal direction. Thus, the three beam search pattern has passed over the entire horizontal area which may be occupied by the target, at a maximum speed of 4° per second.

To continue the cycle, the beam is accelerated to 4 degrees per second in the direction of the original sweep and maintained at that velocity for 3.760° or 0.940 seconds. At this point, the center of the beam is 2.300° from the origin at an elapsed time of 2.386 seconds.

If it is assumed that the target was in the leading edge of the beam at the initiation of the cycle, it could now be displaced 2.284° from the origin. Thus, the target area, in the horizontal direction, has again been searched at a maximum beam velocity of 4° per second.

In the vertical, the effective height of the search pattern above the origin is two effective beam width or 1.333°. The pattern extends one effective beam height or 0.667° below the origin.

The maximum upward excursion of the target, assuming the target were at the top edge of the original beam, is 1.091° during the search period of 2.386 seconds. The maximum passible downward excursion, assuming the target was in the lower edge of the original beam, is 0.614° in the same period. Thus, the target has remained in the effective vertical search pattern the entire search period.

In this acquisition cycle, the target has been subjected to two passes at a beam velocity of 4° per second. This is compared to a single pass at 18° per second in the five second search raster. Thus the illumination time in the

acquisition raster is nine times the illumination time in the search raster. Since the probability of detection has been specified as 50% in the search raster, the probability of detection in the acquisition raster should be 99.9% on the specified target size. (With signal integration, the 9 pulse period integration would yield far in excess of 99.99% probability of detection, or a three pulse period integration corresponding to a constant speed region of 12° per second instead of the recommended 4 degrees per second, would give a detection probability of 99.9%.) (References 13, 14).

The 4° per second beam velocity in the search area will allow the beam to be stopped within 0.154°, or approximately one fifth of a beam width. This should make transfer to tracking easy and positive.

Also, in case no target is detected, the beam may be accelerated to 18 degrees per second and adjusted to its original elevation for continuation in the search cycle. Acceleration to 18° per second would require 0.269 seconds and a travel distance of 2.959°. The total time in the cycle is 2.655 seconds, but an angular distance of 5.259° has been search beyond the starting point of the cycle. At 18° per second velocity this 5.259° would have taken 0.292 seconds, so that the time lost in the acquisition pattern, provided no signal is found, is 2.636 seconds.

It is quite important that the vertical motion in the standard five second search raster be from lower elevation to upper elevation. This reduces the relative vertical speed between the search beam and the target position, and makes escape by target motion during the raster virtually impossible.

The horizontal angular velocity of the radar beam during the acquisition cycle is shown in Figure B-1.

This acquisition cycle is recommended for use during re-acquisition when target angular velocities can be much higher than those in the initial search pattern.
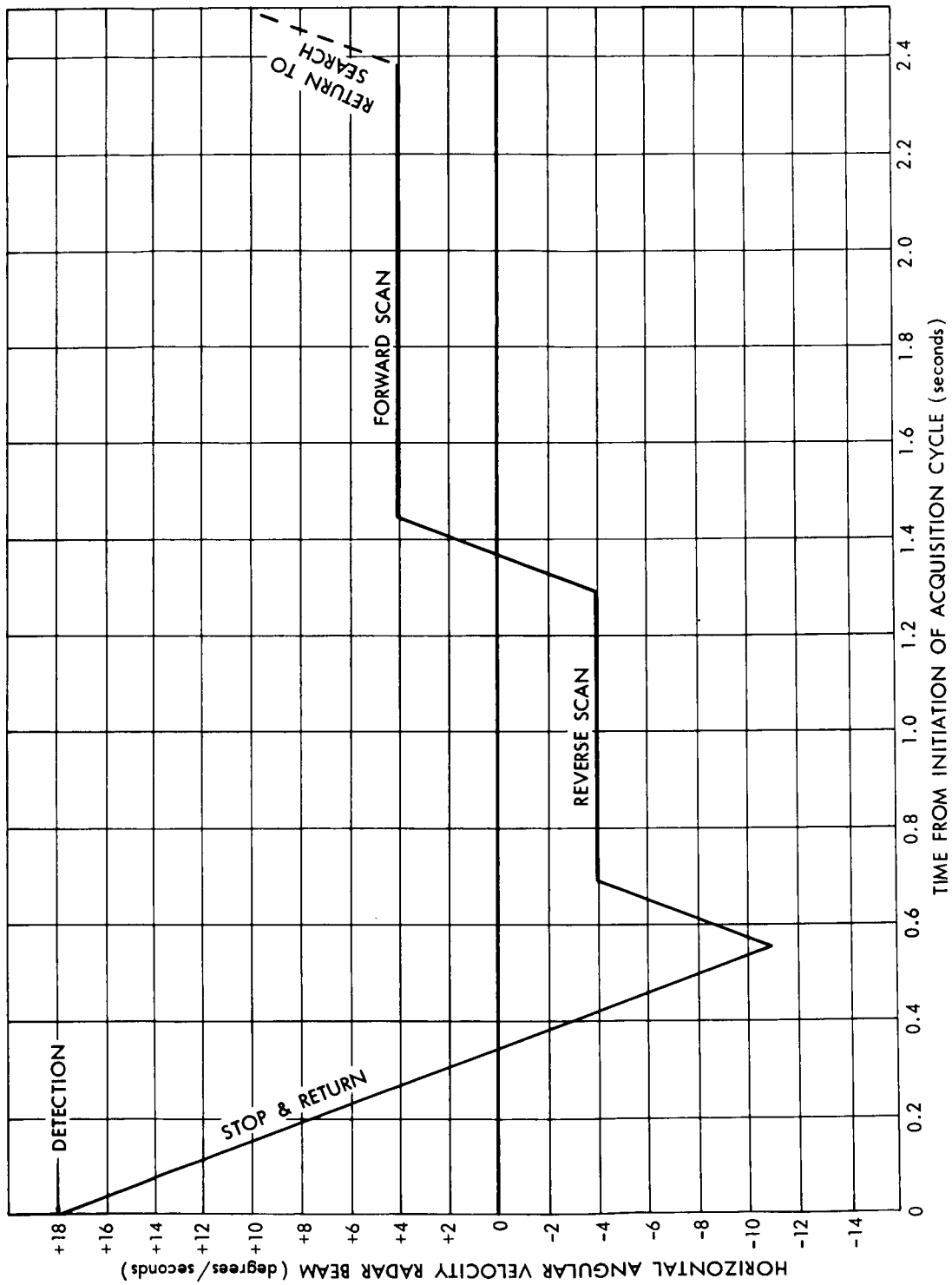
Figure B-1. Horizontal Angular Velocity of Radar Beam During Acquisition Cycle

B-4